
# MICROSCOPIC MODELING OF THE SELF ASSEMBLY OF SURFACTANTS: SHAPE TRANSITIONS AND CRITICAL MICELLE CONCENTRATIONS

**Asfaw Gezae Daful**

**ISBN:**
**Dipòsit Legal: T. 1024-2011**

UNIVERSITAT ROVIRA I VIRGILI
MICROSCOPIC MODELING OF THE SELF ASSEMBLY OF SURFACTANTS: SHAPE TRANSITIONS AND CRITICAL MICELLE CONCENTRATIONS
Asfaw Gezae Daful
ISBN:/DL:T. 1024-2011

Asfaw Gezae Daful

# Microscopic Modeling of the Self Assembly of Surfactants: Shape Transitions and Critical Micelle Concentrations

Doctoral Thesis

Department of Chemical Engineering
Universitat Rovira i Virgili

Tarragona
2011

UNIVERSITAT ROVIRA I VIRGILI
MICROSCOPIC MODELING OF THE SELF ASSEMBLY OF SURFACTANTS: SHAPE TRANSITIONS AND CRITICAL MICELLE CONCENTRATIONS
Asfaw Gezae Daful
ISBN:/DL:T. 1024-2011

UNIVERSITAT ROVIRA I VIRGILI
MICROSCOPIC MODELING OF THE SELF ASSEMBLY OF SURFACTANTS: SHAPE TRANSITIONS AND CRITICAL MICELLE CONCENTRATIONS
Asfaw Gezae Daful
ISBN:/DL:T. 1024-2011

UNIVERSITAT ROVIRA I VIRGILI
MICROSCOPIC MODELING OF THE SELF ASSEMBLY OF SURFACTANTS: SHAPE TRANSITIONS AND CRITICAL MICELLE CONCENTRATIONS
Asfaw Gezae Daful
ISBN:/DL:T. 1024-2011

UNIVERSITAT ROVIRA I VIRGILI
MICROSCOPIC MODELING OF THE SELF ASSEMBLY OF SURFACTANTS: SHAPE TRANSITIONS AND CRITICAL MICELLE CONCENTRATIONS
Asfaw Gezae Daful
ISBN:/DL:T. 1024-2011



# Microscopic Modeling of the Self Assembly of Surfactants: Shape Transitions and Critical Micelle Concentrations

Doctoral Thesis

**Asfaw Gezae Daful**
Departament d'Enginyeria Química
Escola Técnica Superior d'Enginyeria Química
Universitat Rovira i Virgili

Supervised By

**Dr. Allan Donald Mackie**

TARRAGONA, 2011

UNIVERSITAT ROVIRA I VIRGILI
MICROSCOPIC MODELING OF THE SELF ASSEMBLY OF SURFACTANTS: SHAPE TRANSITIONS AND CRITICAL MICELLE CONCENTRATIONS
Asfaw Gezae Daful
ISBN:/DL:T. 1024-2011

UNIVERSITAT ROVIRA I VIRGILI
MICROSCOPIC MODELING OF THE SELF ASSEMBLY OF SURFACTANTS: SHAPE TRANSITIONS AND CRITICAL MICELLE CONCENTRATIONS
Asfaw Gezae Daful
ISBN:/DL:T. 1024-2011



UNIVERSITAT ROVIRA I VIRGILI

Departament d'Enginyeria Química
Escola Técnica Superior d'Enginyeria Química
Universitat Rovira i Virgili
Av. Països Catalans 26
43007 Tarragona
España
Tel: + 34 977 55 96 74
Fax: + 34 977 55 96 67

**Dr. Allan Donald Mackie**, professor titular del Departament d'Enginyeria Química de la Universitat Rovira i Virgili,

Faig Constar:

Que el Sr. **Asfaw Gezae Daful**, presenta la seva tesi doctoral amb títol: **"Microscopic Modeling of the Self Assembly of Surfactants: Shape Transitions and Critical Micelle Concentrations"**, per optar al grau de Doctor amb Menció Europea.

Que tots els resultats presentats i la seva anàlisi són fruit de la investigació realitzada per l´esmentat doctorant, sota la meva direcció.

I perquè quediconstanàcia els efectes oportuns, signo el present faig constar.

Tarragona, 25 de gener de 2011

**Allan Donald Mackie**

UNIVERSITAT ROVIRA I VIRGILI
MICROSCOPIC MODELING OF THE SELF ASSEMBLY OF SURFACTANTS: SHAPE TRANSITIONS AND CRITICAL MICELLE CONCENTRATIONS
Asfaw Gezae Daful
ISBN:/DL:T. 1024-2011

UNIVERSITAT ROVIRA I VIRGILI
MICROSCOPIC MODELING OF THE SELF ASSEMBLY OF SURFACTANTS: SHAPE TRANSITIONS AND CRITICAL MICELLE CONCENTRATIONS
Asfaw Gezae Daful
ISBN:/DL:T. 1024-2011



UNIVERSITAT ROVIRA I VIRGILI

Departament d'Enginyeria Química
Escola Técnica Superior d'Enginyeria Química
Universitat Rovira i Virgili
Av. Països Catalans 26
43007 Tarragona
España
Tel: + 34 977 55 96 74
Fax: + 34 977 55 96 67

I STATE that the present study, entitled:

**Microscopic Modeling of the Self Assembly of Surfactants: Shape Transitions and Critical Micelle Concentrations**

presented by **Asfaw Gezae Daful** for the award of the degree of Doctor, has been carried out under my supervision at the Department of Chemical Engineering of Universitat Rovira i Virgili, and that it fulfils all the requirements to obtain the European Doctorate Award.

Tarragona, January 25 2011

Doctoral Thesis Supervisor

**Allan Donald Mackie**
Professor Titular de
Departament d'Enginyeria Química
Universitat Rovira i Virgili

UNIVERSITAT ROVIRA I VIRGILI
MICROSCOPIC MODELING OF THE SELF ASSEMBLY OF SURFACTANTS: SHAPE TRANSITIONS AND CRITICAL MICELLE CONCENTRATIONS
Asfaw Gezae Daful
ISBN:/DL:T. 1024-2011

UNIVERSITAT ROVIRA I VIRGILI
MICROSCOPIC MODELING OF THE SELF ASSEMBLY OF SURFACTANTS: SHAPE TRANSITIONS AND CRITICAL MICELLE CONCENTRATIONS
Asfaw Gezae Daful
ISBN:/DL:T. 1024-2011

# Abstract

Surfactants are chemicals exhibiting amphiphilic behavior towards a solvent. That is, they have two distinctly different characteristics, a polar hydrophilic head and non polar hydrophobic tail in different parts of the same molecule. At low concentrations, surfactants form a dilute homogeneous solution of individual amphiphilic molecules while beyond a threshold surfactant concentration, the amphiphilic molecules, spontaneously self-assemble into aggregates or microstructures known as micelles, with their hydrophilic groups exposed to the solvent, forming a corona of the micelle, and their hydrophobic groups shielded in the micellar interior. The onset of this aggregation into micelles usually occurs within a narrow range of surfactant concentrations, and is quantified by a single concentration value, the critical micelle concentration. Normally, at low concentrations close to the critical micelle concentration, small spherical micelles are formed; however, changes in the solution conditions such as surfactant concentration, temperature and other physicochemical parameters can cause changes in the micellar morphology, which is termed as a shape transition of micelles. At higher surfactant concentrations, the spherical micelles undergo one-dimensional growth into cylindrical micelles, or two-dimensional growth into discoidal micelles. This work is divided into (i) study of the shape transitions of micelles and (ii) CMC calculations

1. A Single Chain Mean-Field Theory (SCMFT) and Monte Carlo simulation simulations are used in a lattice model to study the micelle formation and shape transitions of micelles as well as to predict structural and thermodynamic properties of micelles of model nonionic surfactants of the type $\mathrm{H}_x\mathrm{T}_y$. A microscopic model of micellization is applied with no pre-assumed geometric shape of the micelle, able to calculate the standard chemical potential differences of micelles of any size and shape. The equilibrium shape and energy of the micelle is determined by functional minimization of the total

UNIVERSITAT ROVIRA I VIRGILI
MICROSCOPIC MODELING OF THE SELF ASSEMBLY OF SURFACTANTS: SHAPE TRANSITIONS AND CRITICAL MICELLE CONCENTRATIONS
Asfaw Gezae Daful
ISBN:/DL:T. 1024-2011



free energy. The size of the spherical micelle, formed at low aggregation numbers, increases with concentration and reaches an optimum aggregation number, a stable spherical micelle, where the chemical potential difference is minimum. Increasing concentration, increases the size of the micelle and forces the micelle to undergo morphological transformations, into geometric shapes compatible with the new thermodynamic conditions and packing parameters. The micelle elongates into prolate spheroid, and then gradually changes into croquette like structure that finally transforms into a finite size cylindrical micelle with two spherical end caps. Further increase of aggregation number increases the length of cylindrical part of the micelle. We also explore an alternate path way of the shape transition via our SCMFT, the spherical micelles change into oblate micelles which in turn transforms into disk micelle and then to toroidal or donut micelles. The variation of standard chemical potential difference with concentration as well as with micelles of different geometric shape is analyzed. Though the energy barriers for the sphere to disk transition is lower than that of the sphere to cylinder, the finite size cylindrical micelles have lower standard chemical potential differences, thus more stable than the disk micelles. Similarly, our Monte Carlo simulations show that the sphere to cylinder shape transition occurs through a region where spherical and cylindrical micelles coexist, i.e., at low concentration only spherical micelles are obtained, as the concentration increases the coexistence of both spherical and cylindrical micelles is observed. Further increase of surfactant concentration leads to predominantly long cylindrical micelles.

2. A Single Chain Mean Field Theory is used in a continuous space to quantitatively describe the micellization process of the nonionic surfactants of polyethylene oxide alkyl ether, abbreviated as CnEm. The main objective was to develop an explicit but simple microscopic model within our SCMFT simulation methodology in order to capture the micellization process. In particular, three interaction parameters ($\chi_{TW}$, $\chi_{TH}$ and $\chi_{HW}$ : where T and H denote the tail and head of the surfactant and W denotes water) in a continuous space model have been chosen. This model is shown to be able to reproduce and predict with high accuracy the critical micelle concentrations of a wide range of head and tail surfactant lengths. In addition, the aggregation numbers of the micelles are studied, and the effect of the number of the hydrophobic and hydrophilic segments on the CMC and aggregation number of the micelles is discussed. The temperature dependence of the CMC and aggregation numbers is also analyzed.

UNIVERSITAT ROVIRA I VIRGILI
MICROSCOPIC MODELING OF THE SELF ASSEMBLY OF SURFACTANTS: SHAPE TRANSITIONS AND CRITICAL MICELLE CONCENTRATIONS
Asfaw Gezae Daful
ISBN:/DL:T. 1024-2011

# Resumen

Los surfactantes son moléculas anfifílicas, con una cabeza hidrofílica y una cola hidrófoba. En concentraciones bajas, los surfactantes forman una solución homogénea y diluida de moléculas anfifílicas individuales mientras más allá de la concentración crítica de surfactantes, las moléculas anfifílicas, se auto ensamblen espontáneamente en conjuntos o micro-estructuras conocidas como micelas, con sus grupos hidrofílicos expuestos al solvente, formando la corona de la micela, y sus grupos hidrófobos protegidos en el interior de la micela. A esta concentración, a la cual se dá este cambio, se le llama concentración micelar crítica (CMC). Normalmente, a bajas concentraciones cerca de la CMC, se forman pequeñas micelas esféricas ; sin embargo, cambios de condiciones de la solución, como la concentración de surfactantes, temperatura y otros parámetros fisico-químicos pueden causar cambios de la morfología de las micelas, por ejemplo a cilindros o discos, que se puede llamar como transición de forma de las micelas.

Este trabajo está dividido en dos partes (i) estudio de las transiciones de formas de las micelas (ii) cálculo de la CMC

1. En este trabajo, hemos utilizando una teoría conocida como "Single Chain Mean Field Theory, (SCMFT)" y simulaciones de Monte Carlo en una red para estudiar la formación de las micelas y las transiciones de forma de las micelas así como predecir propiedades estructurales y termodinámicas de las micelas de modelo surfactantes no iónicos del tipo $H_xT_y$. Se aplica un modelo microscópico de micelizacón sin una forma geométrica preasumida de la micela, capaz de calcular las diferencias potenciales químicas estándares de las micelas de cualquier tamaño y forma. Se determina la forma de equilibrio y la energía de la micela por la minimización funcional de la energa libre total. A bajas concentraciones, se forman micelas esféricas. Al aumentar la

UNIVERSITAT ROVIRA I VIRGILI
MICROSCOPIC MODELING OF THE SELF ASSEMBLY OF SURFACTANTS: SHAPE TRANSITIONS AND CRITICAL MICELLE CONCENTRATIONS
Asfaw Gezae Daful
ISBN:/DL:T. 1024-2011



concentración, el tamaño de la micela cambia y obliga la micela a someterse a transformaciones morfológicas, en formas geométricas compatibles con las nuevas condiciones termodinámicas y sus "packing" parámetros. Al aumentar la concentración de los surfactantes, la micela alarga en un esferoide protardío y entonces gradualmente cambian a una estructura que parece como una croqueta. Esta estructura, al añadir más surfactantes, se transforma finalmente a una micela cilndrica con un tamaño finito y con dos tapas esféricas a las dos partes finales de la parte cilíndrica de la micela. El aumento adicional del número de agregación, o la concentración de los surfactantes, aumenta la longitud de la parte cilíndrica de la micela cilíndrica. Exploramos también un camino alternativo vía SCMFT, el cambio de la micela esfírica a una forma esferoide de oblata que por su parte transforma a una micela de forma disco y luego a micelas donut o toroidales. Se analiza la variación de la diferencia en potencial qumica estándar con la concentración así como con diferentes formas geométricas de las micelas. Aunque las barreras de energía para la transición de esfera a disco sean más bajas que aquella de la esfera al cilindro, las micelas cilíndricas tiene las diferencias potenciales químicas estándares inferiores, y son más estables que las micelas discoidales. Del mismo modo, nuestra simulaciónes de Monte Carlo muestra que la transición de forma esférica a cilindro ocurre por una región donde micelas esféricas y cilíndricas coexisten, es decir, a concentraciones bajas sólo micelas esféricas son obtenidas cuando la concentración aumenta la coexistencia tanto de micelas esféricas como de cilíndricas es observada. El aumento adicional de la concentración de los surfactantes lleva predominantemente a micelas cilíndricas largas.

2. Se usa la teoría "Single Chain Mean Field Theory, (SCMFT)" en espacio continuo para describir cuantitativamente el proceso de la formación de las micelas de los surfactantes no iónicos de clase del óxido de polietileno alquil éter, abreviado como $C_nE_m$. El objetivo principal era desarrollar un modelo microscópico explícito pero simple dentro de nuestra metodología de simulación SCMFT a fin de capturar el proceso de la formación de las micelas. En particular, un modelo de tres parámetros de interacción ($\chi_{TW}$, $\chi_{TH}$ y $\chi_{HW}$ : T y H se refieren a una cola hidrófoba y a una cabeza hidrofílica de los surfactantes y W denota el agua) en espaco continuo ha sido elegido. Se muestra que este modelo es capaz de reproducir con una exactitud alta las concentraciones micelar críticas de una amplia variedad de longitudes de las cabezas y colas de las surfactantes. Además, hemos podido calcular los números de agregación de las micelas, así como el efecto del número de segmentos hidrófobos y hidrofílicos en la CMC. Se ha mostrado que el modelo y

UNIVERSITAT ROVIRA I VIRGILI
MICROSCOPIC MODELING OF THE SELF ASSEMBLY OF SURFACTANTS: SHAPE TRANSITIONS AND CRITICAL MICELLE CONCENTRATIONS
Asfaw Gezae Daful
ISBN:/DL:T. 1024-2011



predice las CMC con gran precisión. Además, se estudian los números de la agregación de las micelas. Se analizan el efecto del número de los segmentos hidrofóbicos e hidrofílicos en la CMC y el número de agregación. Se analizan la dependencia de la temperatura del CMC y también los números de la agregación.

UNIVERSITAT ROVIRA I VIRGILI
MICROSCOPIC MODELING OF THE SELF ASSEMBLY OF SURFACTANTS: SHAPE TRANSITIONS AND CRITICAL MICELLE CONCENTRATIONS
Asfaw Gezae Daful
ISBN:/DL:T. 1024-2011

UNIVERSITAT ROVIRA I VIRGILI
MICROSCOPIC MODELING OF THE SELF ASSEMBLY OF SURFACTANTS: SHAPE TRANSITIONS AND CRITICAL MICELLE CONCENTRATIONS
Asfaw Gezae Daful
ISBN:/DL:T. 1024-2011

# Acknowledgements

First, I thank my advisor Dr. Allan D. Mackie, for his continuous support through out this work. He was always there to listen and to give advice. I express my deepest gratefulness to him for his helpful advises, guidance. I would like to thank Dr. Josep Bonet i Avalos for is valuable discussions and his technical supports on solving problems, for which I am very grateful. My sincere thanks go to Dr. Vladimir A. Baulin, for his kind support and invaluable assistance on solving problems. I am also grateful to Dr. Edgar M. Blokhuis from Leiden University for giving me the opportunity to work in his research group for three months, and for his supervision and financial supports during my stay.

Special thanks goes to Teresa Mármol, for her being at a *click* distance for any help during my stay in Tarragona. I would like to thank to all, former and current colleagues from our group for providing a good working atmosphere and specially Alessandro, Henery, and Javier I appreciate their assistance when I started my work. Special thanks to all Ethiopian students in URV for their support, and all staff members of the department of chemical engineering, university of Rovira i Virgili, for their unique help and support. I would like to thank URV for the financial support.

Finally, I am grateful for the support of my family and friends. I would especially like to thank my wonderful partner, Ariadna, for her love and understandings. I am also indebted to my mother.

UNIVERSITAT ROVIRA I VIRGILI
MICROSCOPIC MODELING OF THE SELF ASSEMBLY OF SURFACTANTS: SHAPE TRANSITIONS AND CRITICAL MICELLE CONCENTRATIONS
Asfaw Gezae Daful
ISBN:/DL:T. 1024-2011

UNIVERSITAT ROVIRA I VIRGILI
MICROSCOPIC MODELING OF THE SELF ASSEMBLY OF SURFACTANTS: SHAPE TRANSITIONS AND CRITICAL MICELLE CONCENTRATIONS
Asfaw Gezae Daful
ISBN:/DL:T. 1024-2011

# Contents

**Abstract** **xi**

**Resumen** **xiii**

**Acknowledgements** **xvi**

**List of Figures** **xxiii**

**List of Tables** **xxxi**

**1 Introduction** **1**

1.1 Background . . . . . 1

1.2 Objectives . . . . . 3

1.3 Thesis outline . . . . . 3

**2 Surfactant Behavior** **5**

2.1 Introduction . . . . . 5

2.1.1 Types of Surfactants . . . . . 8

2.1.2 Applications of Surfactants . . . . . 9

2.2 Micelle Formation by Surfactants . . . . . 11

UNIVERSITAT ROVIRA I VIRGILI
MICROSCOPIC MODELING OF THE SELF ASSEMBLY OF SURFACTANTS: SHAPE TRANSITIONS AND CRITICAL MICELLE CONCENTRATIONS
Asfaw Gezae Daful
ISBN:/DL:T. 1024-2011



**3 Theory of Self-Assembly** **15**
3.1 Introduction . . . 15
3.2 Equilibrium Ensembles . . . 16
3.3 The Boltzmann Distribution . . . 17
3.4 Free Energy, Entropy and Chemical Potential . . . 18
3.5 Partition Function of the Micellar Aggregate . . . 22
3.6 Thermodynamics of Self Assembly of Nonionic Surfactants . . . 23
3.6.1 Mass Action Model . . . 24
3.7 Simulation Techniques . . . 28
3.7.1 Periodic Boundary Conditions . . . 30
3.7.2 Monte Carlo Simulations . . . 30
3.7.3 Molecular Dynamics . . . 34
3.7.4 Mean Field Theory . . . 34
3.7.5 Self-Avoiding Random Walk . . . 35
3.8 Micellar Structure and Shape . . . 37
3.8.1 The Packing Parameter . . . 37
3.8.1.1 Optimal Head group Area . . . 38
3.8.1.2 Packing Characteristics . . . 38

**4 Single Chain Mean Field Theory and Monte Carlo Simulation** **41**
4.1 Introduction . . . 41
4.2 Lattice Model Description . . . 41
4.3 Single Chain Mean Field Theory . . . 45
4.3.1 SCMFT in Lattice Space . . . 46
4.3.2 SCMFT in Continuous Space . . . 51
4.4 Lattice Monte Carlo Simulation . . . 55
4.4.1 Introduction . . . 55
4.4.2 Metropolis Monte Carlo algorithm . . . 55

UNIVERSITAT ROVIRA I VIRGILI
MICROSCOPIC MODELING OF THE SELF ASSEMBLY OF SURFACTANTS: SHAPE TRANSITIONS AND CRITICAL MICELLE CONCENTRATIONS
Asfaw Gezae Daful
ISBN:/DL:T. 1024-2011



4.4.3 Monte Carlo Moves . . . 56
4.4.3.1 Chain Reptation . . . 57
4.4.3.2 Configurational Bias Monte Carlo Move . . . 57
4.4.3.3 Cluster Move . . . 58
4.5 Principal Moments of Inertia and Radius of Gyration Tensor . . . 60
4.5.1 Principal Moments of Inertia . . . 60
4.5.2 Radius of Gyration Tensor . . . 61

**5 Shape Transitions of Micelles 65**
5.1 Introduction . . . 65
5.2 Simulation Methodology . . . 72
5.2.1 1D SCMFT . . . 72
5.2.2 2D SCMFT . . . 73
5.2.3 Monte Carlo . . . 74
5.3 Results and Discussions . . . 75
5.3.1 1D Spherical and Infinite Cylindrical Micelles . . . 75
5.3.1.1 $H_3T_6$ . . . 76
5.3.1.2 $H_2T_6$ . . . 78
5.3.1.3 $H_4T_4$ . . . 79
5.3.1.4 $H_3T_3$, $H_4T_5$, $H_4T_6$ and $H_4T_{16}$ . . . 83
5.3.2 2D Spherical and Finite Size Cylindrical Micelles . . . 89
5.3.2.1 Micelle Shape and Size: Volume Fraction Profiles 96
5.3.2.2 Principal Moments of Inertia . . . 103
5.3.2.3 Standard Chemical Potential Differences . . . 104
5.3.3 Disk and Donut like Micelles . . . 108
5.3.4 Monte Carlo Simulation . . . 109
5.4 Conclusions . . . 125

UNIVERSITAT ROVIRA I VIRGILI
MICROSCOPIC MODELING OF THE SELF ASSEMBLY OF SURFACTANTS: SHAPE TRANSITIONS AND CRITICAL MICELLE CONCENTRATIONS
Asfaw Gezae Daful
ISBN:/DL:T. 1024-2011



**6 Accurate Critical Micelle Concentrations from a SCMFT** **127**

6.1 Introduction . . . . . 127

6.1.1 Calculation of the CMC . . . . . 130

6.2 Model of the $C_nE_m$ Surfactant . . . . . 131

6.2.1 Interaction Parameters . . . . . 134

6.3 Results and Discussion . . . . . 135

6.4 Conclusions . . . . . 150

**Bibliography** **152**

UNIVERSITAT ROVIRA I VIRGILI
MICROSCOPIC MODELING OF THE SELF ASSEMBLY OF SURFACTANTS: SHAPE TRANSITIONS AND CRITICAL MICELLE CONCENTRATIONS
Asfaw Gezae Daful
ISBN:/DL:T. 1024-2011

# List of Figures

2.1 Schematic representation of the hydrophilic and hydrophobic parts of an amphiphilic molecule . . . . . 6

2.2 Aggregation and orientation of surfactants, to reduce the the hydrophobic tail-water contact . . . . . 7

2.3 Schematic representation of the concentration dependence of some physical properties for solutions of micelle-forming surfactants. . . 12

3.1 Schematic representation of self-assembly of amphiphiles into aggregates of different sizes and shapes . . . . . 25

3.2 Schematic illustration of periodic boundary conditions. A surfactant molecule that leaves to the right of the simulation box (center) is replaced by an identical one, moving by the same amount out of a periodic image of the original box . . . . . 31

3.3 Growth of a self-avoiding random walk . . . . . 36

3.4 Schematic representation of surfactant geometry . . . . . 39

4.1 Discretization of the mean field into $N_c$ concentric circular shells of radius $r$ and $Z_l$ layers or slices in a 2D cylindrical fields. Lattice sites in the corners of the box are included with those of the last shell. 47

4.2 One dimensional discretization of the mean field into (a) concentric spherical shells and (b) concentric cylindrical shells of radius $r$. . . 52

4.3 Equilibrated energy, in $k_BT$ . . . . . 56

UNIVERSITAT ROVIRA I VIRGILI
MICROSCOPIC MODELING OF THE SELF ASSEMBLY OF SURFACTANTS: SHAPE TRANSITIONS AND CRITICAL MICELLE CONCENTRATIONS
Asfaw Gezae Daful
ISBN:/DL:T. 1024-2011



4.4 Schematic representation of different geometric shape of micelles as a function of the ratios of the radii of gyration tensors, $\alpha$ and $\beta$; $(a)$. if $\alpha \approx \beta \approx 0$ that is $R_1 >> R_2 \approx R_3$ then the aggregate is finite size cylindrical micelle $(b)$. if $\alpha \approx \beta \approx 1$ that is $R_1 \approx R_2 \approx R_3$ then the aggregate is spherical micelle $(c)$. if $\alpha \neq \beta$ (or $\alpha$ close to 1 and $\beta$ close to 0) that is $R_1 \approx R_2 > R_3$ the aggregate is can be of disk micelle $(d)$. for $0 \ll \alpha \approx \beta \ll 1$, spherical and finite size cylindrical micelles exist together with micelles of intermediate shapes in the system, indicating the shape transition of spherical micelles into finite size cylindrical micelles. . . . . 63

5.1 The standard chemical potential difference $(\mu_N^o - \mu_1^o)/k_BT$, of $H_3T_6$ versus micellar aggregation number $N$ of the spherical micelle (square) and the infinite cylindrical micelle (circles), at $T^* = 9.5$. In the case of the infinite cylindrical geometry, the *x-axis* gives the number of surfactants for a 19 lattice site section of the infinite cylinder. . . . 76

5.2 Radial variation of volume fraction profiles of tail $\phi_T(r)$, head $\phi_H(r)$, and solvent $\phi_S(r)$, versus radius $r$, of the spherical micelle (dash dot dot lines with opened symbols) and infinite cylindrical micelle (solid lines with filled symbols) for $H_3T_6$ . . . . . 77

5.3 Standard chemical potential differences, $(\mu_N^o - \mu_1^o)/k_BT$, of $H_3T_6$ versus micellar aggregation number $N_m$ of the spherical micelles at $T^* = 9.5$ for different simulation box sizes . . . . . 78

5.4 Free surfactant mole fraction $(X_1)$ as a function of the total surfactant concentration $(X_N)$ for $H_3T_6$, at $T^* = 9.5$. CMC$\approx 7.0 \times 10^{-4}$ in mole fraction . . . . . 79

5.5 Standard chemical potential differences, $(\mu_N^o - \mu_1^o)/k_BT$, of $H_2T_6$, versus micellar aggregation number $N$ of the micelle at $T^* = 9.5$. Spherical micelle (squares)and infinite cylindrical micelle(circles). In the case of the infinite cylindrical geometry, the *x-axis* gives the number of surfactants for a 19 lattice site section of the infinite cylinder. The inset shows the standard chemical potential differences plot for the range of $N = 40$ to $N = 80$ for the spherical micelle . . 80

5.6 Radial variation of volume fraction profile of tail $\phi_T(r)$, head $\phi_H(r)$, and solvent $\phi_S(r)$, versus radius $r$, of the spherical micelle (dash dot dot lines with opened symbols) and infinite cylindrical micelle (solid lines with filled symbols) for $H_2T_6$ at $T^* = 9.5$ . . . . . 80

UNIVERSITAT ROVIRA I VIRGILI
MICROSCOPIC MODELING OF THE SELF ASSEMBLY OF SURFACTANTS: SHAPE TRANSITIONS AND CRITICAL MICELLE CONCENTRATIONS
Asfaw Gezae Daful
ISBN:/DL:T. 1024-2011



5.7 Free surfactant mole fraction ($X_1$) as a function of the total surfactant concentration ($X_N$) for $H_2T_6$. CMC$\approx 4.90 \times 10^{-4}$ in mole fraction . . . . . 81

5.8 Standard chemical potential difference, $(\mu_N^o - \mu_1^o)/k_BT$, of spherical micelles of $H_4T_4$ versus micelles aggregation number, $N$, for dimensionless temperatures $T^* = 7.25$, $T^* = 7$ and $T^* = 6.5$, in a simulation box of size $19^3$ . . . . . 82

5.9 Standard chemical potential difference, $(\mu_N^o - \mu_1^o)/k_BT$, for spherical micelle (squares) and for infinite cylindrical micelle (circles), of $H_4T_4$, at dimensionless temperature $T^* = 6.5$. In the case of the infinite cylindrical geometry, the *x-axis* gives the number of surfactants for a 19 lattice site section of the infinite cylinder. . . . 82

5.10 Radial variation of volume fraction profile of tail $\phi_T(r)$, head $\phi_H(r)$, and solvent $\phi_S(r)$, versus radius $r$, of the spherical micelle (dash dot dot lines with opened symbols) and infinite cylindrical micelle (solid lines with filled symbols) for $H_4T_4$ . . . . . 83

5.11 Free surfactant volume fraction $\phi_1$ versus the total surfactant volume fraction $\phi_t$ for $H_4T_4$ at dimensionless temperatures, $T^*$ of 6.5, 7.0 and 7.25 . . . . . 84

5.12 Standard chemical potential difference of $H_3T_3$ versus micelles aggregation number, $N$ (left); radial variation of volume fraction profile of tail, $\phi_T(r)$ head $\phi_H(r)$, and solvent $\phi_S(r)$, versus radius $r$, of the spherical micelle ($N = 67$) (right); for dimensionless temperature $T^* = 7.0$, box size $19^3$ . . . . . 85

5.13 Standard chemical potential difference of $H_4T_5$ versus micelles aggregation number, $N$ (left); radial variation of volume fraction profile of tail, $\phi_T(r)$ head $\phi_H(r)$, and solvent $\phi_S(r)$, versus radius $r$, of the spherical micelle ($N = 70$) (right); for dimensionless temperature $T^* = 9.5$, box size $19^3$ . . . . . 86

5.14 Standard chemical potential difference of $H_4T_6$ versus micelles aggregation number, $N$ (left); radial variation of volume fraction profile of tail, $\phi_T(r)$ head $\phi_H(r)$, and solvent $\phi_S(r)$, versus radius $r$, of the spherical micelle ($N = 50$) (right); for dimensionless temperature $T^* = 9.5$, box size $19^3$ . . . . . 87

UNIVERSITAT ROVIRA I VIRGILI
MICROSCOPIC MODELING OF THE SELF ASSEMBLY OF SURFACTANTS: SHAPE TRANSITIONS AND CRITICAL MICELLE CONCENTRATIONS
Asfaw Gezae Daful
ISBN:/DL:T. 1024-2011



5.15 Standard chemical potential difference of $H_4T_{16}$ versus micelles aggregation number, $N$ (left); radial variation of volume fraction profile of tail, $\phi_T(r)$ head $\phi_H(r)$, and solvent $\phi_S(r)$, versus radius $r$, of the spherical micelle ($N = 70$) (right); for dimensionless temperature $T^* = 16.0$, box size $35^3$ . . . . . 88

5.16 Standard chemical potential differences, $(\mu_N^o - \mu_1^o)/k_BT$, vs. $N$, from 1D-SCMFT (circles) and 2D-SCMFT (triangles) for $H_4T_4$ at $T^* = 7.0$ . . . . . 90

5.17 Standard chemical potential differences, $(\mu_N^o - \mu_1^o)/k_BT$, vs. $N$, from 1D-SCMFT (circles) and 2D-SCMFT (triangles) for $H_3T_6$ at $T^* = 9.5$ . . . . . 90

5.18 Standard chemical potential differences, $(\mu_N^o - \mu_1^o)/k_BT$, vs. $N$, for spherical micelles of $H_4T_4$ at $T^* = 7.0$, from 2D-SCMFT simulation, $N_{bulk} \approx 10$ . . . . . 91

5.19 Volume fraction profile of the solvent ($\phi_S$), hydrophobic tail ($\phi_T$), and hydrophilic head ($\phi_H$) from top to bottom. 2D contour plots (left) and 3D surface plots (right) of spherical micelle of $N = 60$, in a cubic box of $V = 17^3$. For the linear surfactant $H_4T_4$ at $T^* = 7.0$. $N_{bulk} \approx 10$ . . . . . 92

5.20 Volume fraction profile of the hydrophobic tails ($\phi_T$), showing that the spherical micelle of $H_4T_4$ surfactant keeps on growing without changing its spherical shape. These micelles are presented for selected systems with total number of surfactants, $N$, from a simulation box of volume, $V = 17^3$. For linear surfactant $H_4T_4$ at $T^* = 7.0$. . 93

5.21 The 3D-*isosurface* plots of the hydrophobic core of micelles of different aggregation number, $N$. The *isosurfaces* correspond to the layer (surface) of the core of the micelle where $\phi_T(r, z) \approx \phi_T^{bulk}$. For linear surfactant $H_4T_4$ at $T^* = 7.0$ . . . . . 94

5.22 Contour plots of the distribution function $PD(\alpha, \beta)$ (sec. 4.5.2), plotted as a function of $\alpha$ and $\beta$, for systems with volume fraction, $\phi$ of 0.008, 0.016, 0.024, and 0.032,(containing 1000, 2000, 3000, and 4000 surfactants) in a simulation box of volume $V = 100^3$ for $H_4T_4$ at $T^* = 6.5$ . . . . . 95

5.23 Micellar size distribution for systems with volume fractions 0.016, 0.024, and 0.032 in a simulation box of volume $100^3$, for $H_4T_4$ at $T^* = 6.5$. . . . . 95

UNIVERSITAT ROVIRA I VIRGILI
MICROSCOPIC MODELING OF THE SELF ASSEMBLY OF SURFACTANTS: SHAPE TRANSITIONS AND CRITICAL MICELLE CONCENTRATIONS
Asfaw Gezae Daful
ISBN:/DL:T. 1024-2011



5.24 Volume fraction profile of the solvent, hydrophobic tail, and hydrophilic head from top to bottom. 2D contour plots (left) and 3D surface plots (right); of spherical micelle of $N = 60$ (above) and a prolate spheroid micelle of $N = 130$ (below), in a simulation box of $V = 27^3$ for the linear surfactant $H_3T_6$ at $T^* = 9.5$, $N_{bulk} \approx 22$ in both cases. . . . . 97

5.25 Volume fraction profile of the solvent, hydrophobic tail, and hydrophilic head from top to bottom. 2D contour plots (left) and 3D surface plots (right); for a finite size cylindrical micelle of $N = 240$, in a simulation box of $V = 35^3$ (above) and an infinitely long cylindrical micelle of $N = 90$ in a simulation box of $V = 19^3$ (below) for a linear surfactant $H_3T_6$ at $T^* = 9.5$, $N_{bulk} \approx 52$ . . . . . 98

5.26 Volume fraction profile of the hydrophobic tails, showing the shape transition of micelles. Spherical, ellipsoidal, prolate spheroids and croquette like micelles are presented for systems of selected number of surfactants, $N$, from simulations in a cubic box of volume, $V = 27^3$. For linear surfactant $H_3T_6$ at $T^* = 9.5$. . . . . 99

5.27 Volume fraction profile of the hydrophobic tails, showing the shape transition of micelles. Ellipsoidal, prolate spheroids, croquette like micelles and finite size cylindrical micelles are presented for selected systems with $N$ surfactants, from simulations in a cubic box of volume $V = 35^3$. For linear surfactant $H_3T_6$ at $T^* = 9.5$. . . . . 101

5.28 The 3D-*isosurface* plots of the hydrophobic core of micelles of different $N$. The *isosurfaces* correspond to the layer (surface) of the core of the micelle where $\phi_T(r, z) \approx \phi_T^{bulk}$. For linear surfactant $H_3T_6$ at $T^* = 9.5$ . . . . . 102

5.29 Variation of the ratio of the principal moments of inertia, $I_{xx}/I_{zz}$, with the total number of surfactants in the system, $N$, for simulation boxes of volume sizes $V = 27^3$ (squares) and $V = 35^3$ (circles) . . . 103

5.30 Standard chemical potential differences $(\mu_N^o - \mu_1^o)/k_BT$ versus the total number of surfactants in the system, $N$, at dimensionless temperature, $T^* = 9.5$; for simulation boxs of $27^3$ (squares) and $35^3$ (circles) . . . . . 105

5.31 Standard chemical potential differences $(\mu_N^o - \mu_1^o)/k_BT$ versus the micellar aggregation number of the micelle, $N_m$, from simulations of $27^3$ and $35^3$. . . . . 106

UNIVERSITAT ROVIRA I VIRGILI
MICROSCOPIC MODELING OF THE SELF ASSEMBLY OF SURFACTANTS: SHAPE TRANSITIONS AND CRITICAL MICELLE CONCENTRATIONS
Asfaw Gezae Daful
ISBN:/DL:T. 1024-2011



5.32 Micellar shape transition along with the standard chemical potential differences $(\mu_N^o - \mu_1^o)/k_BT$ versus the micellar aggregation number of the micelle, $N_m$, for $N_m = 40$, $N_m = 80$, $N_m = 110$, $N_m = 125$, $N_m = 140$ and $N_m = 200$ . . . . . 107

5.33 Variation of the number of free surfactants in the bulk solution, $N_{bulk}$, versus the total number of surfactants in the system, $N$, in simulation boxes of $V = 27^3$ (left) and $V = 35^3$ (right), along with their respective standard chemical potential difference, $(\mu_N^o - \mu_1^o)/k_BT$ 109

5.34 Volume fraction profiles of the hydrophobic tail are presented for selected systems of $N$ surfactants showing the sphere to disk transition of micelles of $H_3T_6$ at $T^* = 9.5$, in a cubic box of $V = 25^3$ . 110

5.35 The 3D-*isosurface* plots of the hydrophobic core of micelles for different, $N$, to show the sphere to disk shape transition. The *isosurfaces* correspond to the layer (surface) of the core of the micelle where $\phi_T(r, z) \approx \phi_T^{bulk}$. . . . . 111

5.36 Volume fraction profile of the solvent, hydrophobic tail, and hydrophilic head from top to bottom. 2D contour plots (left) and 3D surface plots (right) of donut micelle of $N = 230$, in a cubic box of $V = 25^3$. For linear surfactant $H_3T_6$ at $T^* = 9.5$. . . . . 112

5.37 Standard chemical potential differences, $(\mu_N^o - \mu_1^o)/k_BT$, vs. $N$, of disk micelle, for $H_3T_6$ . . . . . 112

5.38 Standard chemical potential differences, $(\mu_N^o - \mu_1^o)/k_BT$, vs. $N_m$, of disk micelles(squares) and finite size cylindrical micelles(circles). 113

5.39 Contour plots of the distribution function $PD(\alpha, \beta)$ (sec. 4.5.2), plotted as a function of $\alpha$ and $\beta$, for systems with volume fractions ($\phi$) 0.00675, 0.009, 0.0135, 0.018, 0.0225, 0.027, 0.0333 and 0.036 (containing 750, 1000, 1500, 2000, 2500, 3000, 3700, 4000 surfactants) in a simulation box of volume $100^3$ . . . . . 114

5.40 Micellar size distribution for systems containing with volume fractions 0.009, 0.0135, 0.018, 0.0225, 0.027, 0.0333 and 0.036 in a simulation box of volume $100^3$, for $H_3T_6$ at $T^* = 9.5$ . . . . . 115

5.41 Snapshots of aggregate morphologies of $H_3T_6$ for $N = 1000$, $N = 2000$, $N = 3000$ and $N = 4000$ surfactants in the solution; starting from top left and proceeding clockwise . . . . . 116

UNIVERSITAT ROVIRA I VIRGILI
MICROSCOPIC MODELING OF THE SELF ASSEMBLY OF SURFACTANTS: SHAPE TRANSITIONS AND CRITICAL MICELLE CONCENTRATIONS
Asfaw Gezae Daful
ISBN:/DL:T. 1024-2011



5.42 Snapshots obtained from Monte Carlo simulations illustrate the spherical micelles of aggregation numbers $N = 91$ (above) and $N = 89$ (below) . . . . . 117

5.43 Snapshots of ellipsoidal micelles obtained from Monte Carlo simulations for aggregation numbers $N = 73$, $N = 75$, $N = 110$ and $N = 87$ starting from top left and proceeding clockwise . . . . . 118

5.44 Snapshots of short cylindrical micelle (croquette like micelle) and long cylindrical micelles with spherical end caps of larger diameters than the cylindrical body, obtained from Monte Carlo simulations for aggregation numbers $N = 88$, $N = 94$, $N = 130$ and $N = 150$. . 119

5.45 Snapshots of long cylindrical micelles with spherical end caps of larger diameters than the cylindrical body, obtained from Monte Carlo simulations for aggregation numbers $N = 170$, $N = 209$, $N = 160$ and $N = 350$. . . . . 120

5.46 Snapshots of long cylindrical micelles with spherical end caps of larger diameters than the cylindrical body, obtained from Monte Carlo simulations for aggregation numbers $N = 212$, (above) and $N = 170$ (below) . . . . . 121

5.47 Snapshots of disk micelles, obtained from Monte Carlo simulations for aggregation numbers $N = 121$, presented with top and side views 122

5.48 Snapshots of disk micelles, obtained from Monte Carlo simulations for aggregation numbers $N = 124$, presented with top and side views 123

5.49 Snapshots of disk micelles, obtained from Monte Carlo simulations for aggregation numbers $N = 107$ , presented with top and side views 124

6.1 a) Coarse-grained model of the $C_8E_3$ surfactant and the resulting mean-field "snapshot" (plot of most probable conformations) of a spherical micelle comprising of $N = 382$ surfactants, b) perspective view and c) cross-section view. The hydrophobic part is shown as red and the hydrophilic part as light blue. The chain is completely rigid within each Kuhn segment. . . . . 132

6.2 Standard chemical potential differences $\frac{\mu_N^o - \mu_1^o}{k_B T}$ versus the total number of surfactants in the system, $N$, for surfactants $C_6E_3$, $C_6E_6$, $C_{14}E_3$, $C_{12}E_{25}$, $C_{16}E_6$, and $C_8E_4$ starting from top left and proceeding clockwise . . . . . 137

UNIVERSITAT ROVIRA I VIRGILI
MICROSCOPIC MODELING OF THE SELF ASSEMBLY OF SURFACTANTS: SHAPE TRANSITIONS AND CRITICAL MICELLE CONCENTRATIONS
Asfaw Gezae Daful
ISBN:/DL:T. 1024-2011



6.3 Critical micelle concentration in [mol/L] versus the length of the hydrophobic tail group $n$ for surfactants $C_nE_3$, $C_nE_4$, $C_nE_5$, $C_nE_6$, $C_nE_7$, $C_nE_8$, and $C_nE_9$. Open circles are experimental data from the literature, while filled squares are values calculated from the SCMF theory values, lines are included to help guide the eye. . . . 140

6.4 Critical micelle concentration in [mol/L] versus the length of the head group, $m$ for $C_nE_m$ surfactants for given tail lengths, $n$ ($n$=6, 8, 10, 12, 14, and 16 from top to bottom). Open circles are experimental values from the literature, while filled squares are values calculated from the SCMF theory, lines are included to help guide the eye. . . . 141

6.5 Variation of the free surfactant concentration $X_1$ as a function of the total concentration $X_t$ for $C_nE_3$. . . . 143

6.6 Micellar concentration, $X_N$, versus aggregation number $N$ for selected surfactants . . . 144

6.7 Effect of the number of oxyethylene monomers, $m$, on the aggregation number for the polyoxyethylene alkyl ether surfactants of hydrophobic length 12, $C_{12}E_m$, in a log-linear plot. Open circles represent literature experimental values while filled squares represent SCMFT simulation values from this work. . . . 145

6.8 Radial distribution of volume fraction profiles for the $C_{16}E_3$ surfactant for a micelle of size $N = 100$: tail (circles), head (triangles) and solvent(squares) . . . 147

6.9 Radial distribution of volume fraction profile for the $C_{16}E_3$ surfactant for a micelle of size $N = 1000$: tail (circles), head (triangles) and solvent(squares) . . . 147

6.10 CMC of $C_8E_6$ as a function of temperature: experimental value (circles), simulation value (squares) . . . 148

6.11 Aggregation number of as a function of temperature:experimental value (circles), simulation value (squares) . . . 149

6.12 CMC values of $C_{12}E_4$ as a function of temperature: experimental value (circles), simulation value (squares). The inset shows its aggregation number, $N$, of as a function of temperature from the the SCMFT calculations . . . 150

UNIVERSITAT ROVIRA I VIRGILI
MICROSCOPIC MODELING OF THE SELF ASSEMBLY OF SURFACTANTS: SHAPE TRANSITIONS AND CRITICAL MICELLE CONCENTRATIONS
Asfaw Gezae Daful
ISBN:/DL:T. 1024-2011

# List of Tables

3.1 Geometric relations for Sphere, Cylinder and Bilayer types of aggregates . . . . . 40

4.1 Approximate representations of variations of shapes of aggregates with $\alpha$ and $\beta$ . . . . . 63

5.1 Configurations $\alpha$ for different simulation boxes of volume $V$ . . . . 78

5.2 CMC values of model nonlinear surfactants in mole fraction ($X$) and volume fraction ($\phi$) . . . . . 89

6.1 Calculated and experimental critical micelle concentrations and micelle aggregation numbers of polyoxyethylene alkyl ether surfactants, $C_nE_m$, at $25°C$. . . . . 138

6.2 Constants for relating a and b in Eq. (6.4), for surfactants $C_nE_m$ . 142

UNIVERSITAT ROVIRA I VIRGILI
MICROSCOPIC MODELING OF THE SELF ASSEMBLY OF SURFACTANTS: SHAPE TRANSITIONS AND CRITICAL MICELLE CONCENTRATIONS
Asfaw Gezae Daful
ISBN:/DL:T. 1024-2011

UNIVERSITAT ROVIRA I VIRGILI
MICROSCOPIC MODELING OF THE SELF ASSEMBLY OF SURFACTANTS: SHAPE TRANSITIONS AND CRITICAL MICELLE CONCENTRATIONS
Asfaw Gezae Daful
ISBN:/DL:T. 1024-2011

# Chapter 1

# Introduction

## 1.1 Background

Surfactants are chemicals exhibiting amphiphilic behavior towards a solvent. That is, they have two distinctly different characteristics, polar hydrophilic (water-loving) and non polar hydrophobic (water-hating) in different parts of the same molecule. At low concentrations, surfactants form a dilute homogeneous solution of individual amphiphilic molecules while beyond a threshold surfactant concentration, the amphiphilic molecules, spontaneously self-assemble into aggregates or microstructures known as micelles[1–4], with their hydrophilic groups exposed to solvent, forming corona of the micelle, and their hydrophobic groups shielded in the micellar interior. The onset of this aggregation into micelles usually occurs within a narrow range of surfactant concentration, and is quantified by a single concentration value, the critical micelle concentration[1]. Above the critical micelle concentration, amphiphilic molecules in aqueous solutions spontaneously self-assemble to form micelles. Normally, at low concentrations close to the critical micelle concentration, small spherical micelles are formed; however changes in the solution conditions such as surfactant concentration, temperature and other physicochemical parameters can cause changes in the micellar morphology, which is termed as a shape transition of the micelles[1–6].

The self-assembly phenomenon of surfactant solutions plays an important role in biological, pharmaceutical and industrial processes such as in drug loading and delivery, catalysis, cosmetics, separation processes in engineering and environmental science and technology because of their unique solution properties [1–4, 6, 7].

UNIVERSITAT ROVIRA I VIRGILI
MICROSCOPIC MODELING OF THE SELF ASSEMBLY OF SURFACTANTS: SHAPE TRANSITIONS AND CRITICAL MICELLE CONCENTRATIONS
Asfaw Gezae Daful
ISBN:/DL:T. 1024-2011



Furthermore, such self-assembled aggregates can serve as models to study special features of biological objects such as cell wall, liposomes and red blood cells.

A number of experimental studies [8–27] have revealed the rich diversity of micellar morphologies displayed by amphiphilic systems. Interestingly, all these applications depend on the capability to tune and control the shape and size of the aggregates that surfactants form in solution. The size, shape, and structure of micelles in surfactant solutions are thus important characteristics in determining their main properties and areas of application.

Because micellization is such a broadly applicable phenomenon, gaining a fundamental understanding of the factors that affect it, is of great academic as well as practical relevance. To understand surfactant self-assembly in such complex solutions, it is desirable to establish theoretical models that realistically account for the major *intermolecular* and *intramolecular* interactions in the surfactant solution. Frequently, a highly specific set of micellar solution characteristics is required for a given application. These characteristics typically include the critical micelle concentration and the shape and size of the micellar aggregates that form in solution.

Despite the large amount of work experimentally [10–30], theoretically [31–36], and simulations [37–55], devoted to the self assembly of surfactants into micelles and the shape transition of micelles, a comprehensive microscopic understanding of the concentration induced shape transition is still missing. Micelles of different geometric shapes have drawn a considerable interest over the past few decades, both from a theoretical viewpoint as well as for industrial and technological applications, the range of which keeps expanding. Understanding how micellar structure is connected to the chemical composition and geometry of the surfactant, and in turn, how the structural features of the aggregates can be tuned by specific control parameters, and how these dictate the bulk properties, offers a considerable challenge.

The development of more realistic models that explicitly incorporate the actual surfactant chemical structure as well as the molecular details of micellization will be paramount importance. For instance, it would significantly reduce the time and cost associated with experiments aimed at designing and optimizing new surfactant formulations, which are currently conducted through tedious and time consuming experimentations. In many cases, theoretical predictions of the Critical Micelle Concentration, CMC, the micellar shape, and the micellar size can also be correlated with practically relevant surfactant performance characteristics. For example, researchers have reported correlations between the geometry of micelles and micellar solution viscosity[2, 56]. With these challenges and opportunities in

UNIVERSITAT ROVIRA I VIRGILI
MICROSCOPIC MODELING OF THE SELF ASSEMBLY OF SURFACTANTS: SHAPE TRANSITIONS AND CRITICAL MICELLE CONCENTRATIONS
Asfaw Gezae Daful
ISBN:/DL:T. 1024-2011



mind, apart describing microscopically, the micellization process by itself, this thesis focuses on two areas that are particularly relevant to the practical application of surfactant science, namely CMC calculations and study of the shape transitions of micelles.

## 1.2 Objectives

1. to study the micellization process and stability analysis for spherical and finite cylindrical micelles of model surfactants, $H_xT_y$. In this work we focus on the Shape Transition of Micelles, namely investigating how a spherical micelle formed at low surfactant concentration, undergoes a one-dimensional growth into a finite size cylindrical micelle or a two-dimensional growth into discoidal micelle. How the gradual morphological transformation takes place and how the energy barriers between aggregates of different geometric shapes affect the shape transition will be presented using a two dimensional Single Chain Mean Field Theory (2D-SCMFT) in conjunction with Molecular Simulation.
2. to develop a microscopic model of micellization using off lattice Single Chain Mean Field Theory for the determination of the Critical Micelle Concentration and micelle size distributions for nonionic polyethylene oxide alkyl ether, $C_nE_m$ surfactants and compare with experimental results. In addition, obtain key thermodynamic properties of micellar solutions such as the micelle size distribution.

## 1.3 Thesis outline

The remainder of the thesis is organized as follows. Surfactant self assembly behavior is reviewed in chapter 2 including their applications. A review of statistical thermodynamics and, in particular the thermodynamics of micelle formation along with the application of the mass action law for the micellization process is given in chapter 3. A brief introduction of simulation techniques will also be given followed by descriptions of micellar structures and shapes. In chapter 4, we will show the Lattice model description for model surfactants systems. The Single Chain Mean Field Theory will be presented for Lattice model and for continuous space followed by a description of the Monte Carlo simulations.

In chapter 5, we present the micelle formation and stability analysis of micelles of model surfactants $H_xT_y$. We continue with analyzing micellar shape transitions

UNIVERSITAT ROVIRA I VIRGILI
MICROSCOPIC MODELING OF THE SELF ASSEMBLY OF SURFACTANTS: SHAPE TRANSITIONS AND CRITICAL MICELLE CONCENTRATIONS
Asfaw Gezae Daful
ISBN:/DL:T. 1024-2011



of the model nonionic surfactants and address question like, how the shape of the micelle changes from spherical to finite size cylindrical micelles, and from spherical to disk or donut like micelles by increasing the surfactant concentration. Important results from 1D-SCMFT, 2D-SCMFT, and Monte Carlo simulations, that show the micellar shape transitions will be discussed. The chapter summarizes the concentration induced shape transitions of micelles.

The application of Single Chain Mean Field Theory, SCMFT, in continuous space to study the micellization problem will be presented in chapter 6. And we show how the SCMFT together with an explicit microscopic model for surfactant molecule can be used to *quantitatively* model the micellization process of surfactants. A large amount of simulation results are presented for nonionic surfactants particularly a family of polyoxyethylene alkyl ethers, $C_nE_m$, and compared with experimental data available in the literature. The dependence of CMC and micellar sizes on the hydrophobic chain length as well as on the hydrophilic chain length will be discussed.

UNIVERSITAT ROVIRA I VIRGILI
MICROSCOPIC MODELING OF THE SELF ASSEMBLY OF SURFACTANTS: SHAPE TRANSITIONS AND CRITICAL MICELLE CONCENTRATIONS
Asfaw Gezae Daful
ISBN:/DL:T. 1024-2011

# Chapter 2

# Surfactant Behavior

## 2.1 Introduction

Surfactants are an important class of chemicals consisting of two moieties that interact very differently with a solvent[2–4, 6, 57, 58], water is the solvent of interest in this thesis. One moiety, the hydrophilic head of surfactant, interacts favorably with the solvent. The other moiety, the hydrophobic tail, interacts unfavorably with the solvent. The term **surfactant** is a contraction of the phrase **surf**ace **act**ive **a**ge**nt**. Surfactants molecules are present in everyday life playing a crucial role in many areas including such diverse fields as detergency, food, paint, pharmaceutical products, cosmetics and industrial as well as biological processes [2–4, 6, 46, 57, 58]. Chemically, surfactants are amphiphilic molecules consisting of two distinctly different characteristics: a polar hydrophilic head and an apolar hydrophobic tail in different parts of the same molecule. Symbolically, a surfactant molecule can be represented as having a polar *head* and a non-polar *tail* as shown in Fig. 2.1.

The amphiphilic, dual nature of surfactants towards water leads to the segregation of hydrophobic tails from water and to the exposure of the hydrophilic heads to water, which results in two interesting and useful phenomena in aqueous solution[2–4, 6, 46, 57, 58]: (1) their preferential adsorption at interfaces (e.g. oil/water) and at surfaces (e.g. air/water) (2) their ability to spontaneously self-assemble in water into a variety of microstructures, known as micelles, as shown in Fig. 2.2.

The word *amphiphile*[2] comes from two Greek roots. First the prefix *amphi*

UNIVERSITAT ROVIRA I VIRGILI
MICROSCOPIC MODELING OF THE SELF ASSEMBLY OF SURFACTANTS: SHAPE TRANSITIONS AND CRITICAL MICELLE CONCENTRATIONS
Asfaw Gezae Daful
ISBN:/DL:T. 1024-2011



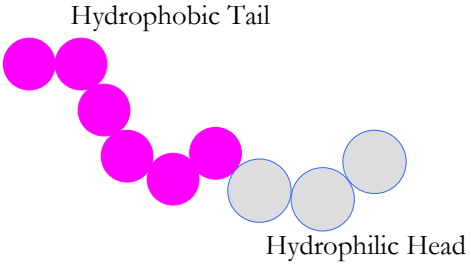


**Figure 2.1:** Schematic representation of the hydrophilic and hydrophobic parts of an amphiphilic molecule

which means double, "from both sides", "around". Then the root *philos* which expresses friendship or affinity, as in "hydrophilic" (compatible with water). Thus, an amphiphilic substance exhibits a double affinity, which can be defined from the physico-chemical point of view as a polar-apolar duality. The polar (hydrophilic head) group of the surfactant can be charged or uncharged, which contains heteroatoms such as O, S, P, or N, included in functional groups such as alcohol, thiol, ether, ester, acid, sulfate, sulfonate, phosphate, amine, amide etc. On the other hand, an essentially apolar group which is usually a saturated or partially unsaturated alkane chain. The hydrophobic group in a surfactant for use in aqueous medium is usually a hydrocarbon chain (-$CH_2$-) but may also be a fluorocarbon or siloxane ($R_2SiO$) chain of appropriate length. In addition, aromatic groups, such as benzene rings may be present in the surfactant tail. The polar portion exhibits an strong affinity for polar solvents, particularly water, and it is often called hydrophilic part or hydrophile. The apolar part is called hydrophobe or lipophile, from Greek roots phobos (fear) and lipos (grease)[2]. The unusual properties of aqueous surfactant solutions can be ascribed to the presence of a hydrophilic head group and a hydrophobic tail group in the molecule. The presence of these type of molecules in aqueous solution has a profound effect on the properties of interfaces and surfaces. Apart from interfacial effects, surfactants present in the aqueous phase show a wide range of phase behavior of which the formation of micelles or bilayers are well known examples.

Since surfactant molecules have both hydrophilic and hydrophobic parts, the most attractive place for them in water is at the surface where the forces of both attraction and repulsion to water can be satisfied. Most importantly, surfactant molecules aggregate in water, above a threshold concentration, forming micelles to minimize the contact between the hydrophobic group of the surfactant and the

UNIVERSITAT ROVIRA I VIRGILI
MICROSCOPIC MODELING OF THE SELF ASSEMBLY OF SURFACTANTS: SHAPE TRANSITIONS AND CRITICAL MICELLE CONCENTRATIONS
Asfaw Gezae Daful
ISBN:/DL:T. 1024-2011



water. Two factors are involved in the spontaneous formation of micelles. First, the hydrophobic effect causes the nonpolar portion of the molecule to be separated from water and sequestered in the interior of the structure. Second, interactions between the head groups determine how closely the molecules may be packed. The self assembly of surfactant molecules in water into, spherical micelle is illustrated schematically in Fig. 2.2. Micelles consist of hydrophobic interior regions, where hydrophobic tails interact with one another. These hydrophobic regions are surrounded by the hydrophilic regions where the heads of the surfactant molecules interact with water. Micelles form a variety of geometric shapes, including spheres, cylinders, disks, etc., and always in a manner that reduces the contacts of the hydrophobic tails with water, while maintaining the favorable contacts of the hydrophilic heads with water.

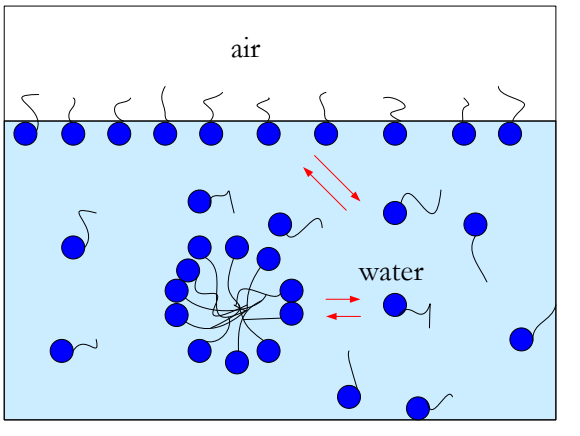


**Figure 2.2:** Aggregation and orientation of surfactants, to reduce the the hydrophobic tail-water contact

At very low concentrations, surfactant molecules occur as free individual molecules. As the total concentration of surfactant in water increases and exceeds a threshold concentration, the surfactant molecules begin to spontaneously self-assemble into microstructures known as, micelles, that coexists with singly dispersed surfactant molecules. The concentration at which micelles form is called the critical micelle concentration (CMC). Micelles form in a variety of shapes like spheres, cylinders, disks etc., and always in such a way that reduces the contacts of the hydrophobic tails with water, while keeping the favorable contacts of the hydrophilic heads with water. The CMC and other micellar properties including the shape and size as well as concentration (micellar size distribution) are of practical

UNIVERSITAT ROVIRA I VIRGILI
MICROSCOPIC MODELING OF THE SELF ASSEMBLY OF SURFACTANTS: SHAPE TRANSITIONS AND CRITICAL MICELLE CONCENTRATIONS
Asfaw Gezae Daful
ISBN:/DL:T. 1024-2011



interest, see section 2.1.2.

The widespread use of surfactant solutions in practical surfactant applications motivates the need for a comprehensive predictive theory that will improve our fundamental understanding of the behavior of these complex systems and facilitate the design and optimization of new surfactant applications.

Understanding the physics of self-assembly of amphiphiles is extremely challenging and also important because the underlying ideas have profound connections to other fundamental areas, such as shape transition of micelles. Furthermore, syntheses of novel nano-structured and meso-structured materials have been achieved by a surfactant-directed templating route, to produce ordered hexagonal arrays of cylindrical structures, disordered worm-like structures, and sponge-like porous structures. Synthesis of a wide variety of structures using short di-block and tri-block co-polymers has also gained considerable attention in designing and fabricating intricate patterns spanning many length scales[2, 45, 59, 60].

### 2.1.1 Types of Surfactants

Surfactants can be classified according to their physicals properties or functionalities. The following is the most common classification and it is based on the nature of the hydrophilic group[2, 3, 45, 57].

1. **Anionic Surfactants**: the hydrophilic group of the surfactant molecule bears a negative charge, for example, $RCOO^-Na^+$ (soap or Carboxylic acid salts), $RC_6H_4SO_3^-Na^+$ (alkylbenzene sulfonate)

2. **Cationic Surfactants**: have a positively charged hydrophilic group. For instance $RNH_3^+Cl^-$ (salt of long chain amine), $RN(CH_3)_3^+Cl^-$ (quaternary ammonium chloride)

3. **Nonionic Surfactants**: are composed of uncharged polar head groups. The most common nonionic surfactants are those based on polyethylene oxide, referred to as ethoxylated surfactants. Several classes can be distinguished: such as alcohol ethoxylates, alkyl phenol ethoxylates, fatty acid ethoxylates, monoalkaolamide ethoxylates, sorbitan ester ethoxylates, fatty amine ethoxylates and ethylene oxide propylene oxide copolymers (sometimes referred to as polymeric surfactants).

4. **Zwitterionic**: both positive and negative charges may be present in the hydrophilic group, for example, $RN^+H_2(CH_2)COO^-$, (long-chain amino acid), (sulfobetaine) $RN^+(CH_3)_2CH_2CH_2SO_3^-$.

UNIVERSITAT ROVIRA I VIRGILI
MICROSCOPIC MODELING OF THE SELF ASSEMBLY OF SURFACTANTS: SHAPE TRANSITIONS AND CRITICAL MICELLE CONCENTRATIONS
Asfaw Gezae Daful
ISBN:/DL:T. 1024-2011



### 2.1.2 Applications of Surfactants

Surfactants have found a wide range of applications in both academia and industry. The main action of surfactants is to lower the surface tension between two phases, usually oil and water. The most common surfactant application is detergency. The ability of surfactants to aid in the mixing of hydrophobic and hydrophilic molecules is used extensively in the chemical industry in applications such as removal of oily materials from a substrate, which is known as detergency. A rich variety of industrial, environmental, pharmaceutical and biological processes make use of surfactants. In environmental applications, surfactant micelles can be used to solubilize and separate toxic ingredients in waste water for water purification[61, 62].

Surfactants are also used in oil recovery from petroleum reservoirs [6, 63]. Several hundred meters below the ground, oil is found in tightly packed sand in the presence of water and natural gas. By injecting water, around 35% of the available crude oil is recovered in the primary and secondary recovery processes. The remaining 65% is trapped because of the high interfacial tension ($20 - 25\ mN/m$) between the oil and the aqueous phase inside the reservoir. Only when this surface tension can be reduced to $\sim 10^{-3}\ mN/m$ (for instance by injecting surfactants), one can mobilize the residual oil in the porous environment in which it is trapped. Once mobilized, all oil must coalesce to form a continuous oil bank. The oil droplet coalescence is enhanced by the very low viscosity in the system. By injecting a surfactant mixture in the porous media, a microemulsion is formed that is in equilibrium with the reservoir aqueous phase and the oil phase. This microphase is propagated through the reservoir leading to an oil rich region that is eventually recovered by production wells[6].

Surfactants are involved in the production of many common food items and can be found in the extraction of cholesterol, solubilization of oil, emulsification, prevention of component separation and solubilization of essential nutrients. However, the choice of edible surfactants is very limited and their concentration in foods should be low so that it does not impart taste or odor on the food [3, 4, 6, 63].

Liquid carbon dioxide $CO_2$ is a cheap, and nontoxic solvent. At $31.1\ ^{\circ}C$ and $73.8\ bar$, the critical point is accessible and variation of density with temperature and pressure makes liquid $CO_2$ a very flexible solvent. Many low molecular weight molecules are soluble in $CO_2$. This, for example, makes the decaffeination of coffee possible. The weak intermolecular interactions in $CO_2$, however, result in a low solubility of polar molecules. The formation of water-in-$CO_2$ (w/c) emulsions is one of the approaches to overcome this problem: polar molecules can be dissolved in the water droplets and nonpolar molecules in the $CO_2$ phase. The most com-

UNIVERSITAT ROVIRA I VIRGILI
MICROSCOPIC MODELING OF THE SELF ASSEMBLY OF SURFACTANTS: SHAPE TRANSITIONS AND CRITICAL MICELLE CONCENTRATIONS
Asfaw Gezae Daful
ISBN:/DL:T. 1024-2011



monly used surfactant types used here are fluorinated hydrocarbon surfactants or fluorinated polyether-based amphiphiles [4, 6, 63].

Several reactions in organic chemistry need contact between nonpolar reactants and inorganic salts that serve as the catalyst. Examples are alkaline hydrolysis, oxidative cleavage of olefins and addition of hydrogen sulfite to olefins. If the organic component is a large nonpolar molecule, it is difficult for the polar catalyst to reach this molecule. This poor phase contact in organic synthesis can be overcome by performing the reaction in a mixture of two immiscible solvents and adding surfactants to increase the contact area between the two phases [4, 6, 63].

Surfactants are also used to stabilize suspensions of Ag colloids that have hydrophobic surfaces[2–4, 6, 63]. In addition, they can stabilize foams such as fire-fighting foams. These foams smother fires, preventing air from mixing with flamable vapors, separating flames from the fuel surface and cooling the fuel and its surface.

Surfactants have medicinal applications as well. Micelles made up from amphiphilic block copolymers can be used as "drug vehicles". These drug vehicles contain hydrophobic drug molecules. For example, anti-cancer drugs are designed to be highly cytotoxic, i.e. they cause cell death, not only to cancerous tissue but unfortunately to almost all types of living cells. When incorporated into micelles, healthy human body tissue is protected from these toxic compounds. Cancerous tissue is more permeable than healthy tissue, allowing for the diffusion of the administered mesoscale drug vehicles to the desired location. The accumulation of micelles in the diseased tissue in due time leads to micelle breakup and release of the anti-cancer medicine [2, 3, 6, 63].

Surfactants are common in every day household use and are considered to be safe. This may seem so for human beings, however, surfactants are highly toxic to aquatic organisms, so the occurrence of large amounts of surfactants in the environment is undesirable. Fortunately, under aerobic condition, surfactants are readily degradable.

Surfactants are also used in the pharmaceutical industry to encapsulate water insoluble drugs in aqueous vehicles for oral or intravenous delivery into a patient's body[64].

These important applications have encouraged researchers to systhesize, tune, and optimize new, more complex surfactants in order to attain improved performance characteristics.

UNIVERSITAT ROVIRA I VIRGILI
MICROSCOPIC MODELING OF THE SELF ASSEMBLY OF SURFACTANTS: SHAPE TRANSITIONS AND CRITICAL MICELLE CONCENTRATIONS
Asfaw Gezae Daful
ISBN:/DL:T. 1024-2011



## 2.2 Micelle Formation by Surfactants

We now turn our attention to a micelle formation by surfactants, micellization process. In an aqueous solution, surfactants spontaneously self-assemble into a wide variety of microstructures referred to as micelles. Micelles are the main type of structure formed by the association of amphiphiles. They consist of a core of hydrophobic chains shielded from contact with water by hydrophilic head groups. The hydrophilic units of surfactants form a micellar corona. Micelles can either be spherical or extended into an ellipsoidal, cylindrical or discoidal shape [1–4, 57].

Many researchers have carried out theoretical investigations of surfactant micellization in aqueous solution in order to predict micellar solution properties as well as the microstructure of the micellar aggregates. In particular, Tanford did groundbreaking work to develop a phenomenological theory of micellization, which provides significant insight into the physical process of micelle formation[65]. Israelachvili developed a geometric packing theory to model micellization, which allows predictions of micelle shape based on the surfactant geometry[1]. This depends on the packing of the molecules, as will be discussed in Chapter 5 on page 65.

The basic driving force behind the self-assembly process is the need to minimize the standard Gibbs free energy of formation, by minimizing the degree of mixing between the hydrophobic tails of the amphiphile with water, while keeping the hydrophilic head groups in contact with water. The standard Gibbs free energy of formation is defined as the change of Gibbs free energy that accompanies the formation of 1 mole of that substance from its component elements at their standard state. Here in micellization, we consider the standard Gibbs free energy of formation or free energy of micellization associated with transferring a surfactant molecule from the bulk solution into a micelle. Solubilization In measuring different physicochemical properties of an aqueous solution of a surfactant up to a relatively high concentration, we will encounter many peculiarities, as exemplified in, Fig. 2.3. One notable observation is the surface tension which decreases rapidly with surfactant concentration. At some higher concentration, which is different for different surfactants, unusual changes are recorded. For example the surface tension, as well as the osmotic pressure, take an approximately constant value, while solubilization starts to increase and self diffusion starts to decrease [2]. This is due to the fact that, surfactants exist as singly dispersed molecules in water up to a given threshold concentration (dependent on temperature and ionic strength), beyond which they are no longer soluble in water as monomeric units but form aggregates. The free surfactant concentration beyond which added surfactant forms micelles is called the critical micelle concentration (CMC). Experimentally, this CMC is determined by plotting measurements of some phy-

UNIVERSITAT ROVIRA I VIRGILI
MICROSCOPIC MODELING OF THE SELF ASSEMBLY OF SURFACTANTS: SHAPE TRANSITIONS AND CRITICAL MICELLE CONCENTRATIONS
Asfaw Gezae Daful
ISBN:/DL:T. 1024-2011



sical or spectroscopic properties that changes markedly with micelle formation as a function of surfactant concentration, e.g. Fig. 2.3. (CMC values of polyoxyethylene alkyl ether surfactants are parented via Single Chain Mean Field Theory simulations, see chapter 6 on page 127).

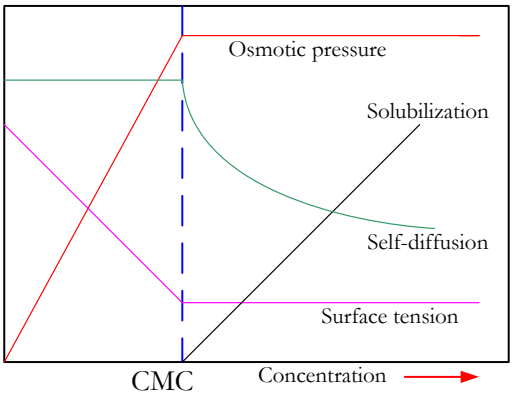


**Figure 2.3:** Schematic representation of the concentration dependence of some physical properties for solutions of micelle-forming surfactants.

Any understanding of effects produced in aqueous solution by the presence of micelles must be preceded by a consideration of the driving forces for molecular organization in this type of aggregate. Two principal factors govern such organization: (1) tail-tail interactions, in which the hydrophobic effect causes the non polar entities to coalesce; (2) head-head and head-water interactions which oppose the total separation of surfactant into a non polar phase. The interplay of these two factors determines the concentration onset of micelle formation, the micelle size distribution, and subsequent physical and chemical properties.

## The Hydrophobic Effect

The thermodynamic properties of amphiphiles in solution are controlled by the tendency for the hydrophobic tail to avoid contact with the water, which has been termed as, the hydrophobic effect. This leads to the spontaneous self-assembly of the surfactant molecules into micelles. These micelles can be of different geometric shape in which the hydrophobic inner core is shielded from the water by the hydrophilic ends of the surfactant, forming a surrounding corona. The formation

UNIVERSITAT ROVIRA I VIRGILI
MICROSCOPIC MODELING OF THE SELF ASSEMBLY OF SURFACTANTS: SHAPE TRANSITIONS AND CRITICAL MICELLE CONCENTRATIONS
Asfaw Gezae Daful
ISBN:/DL:T. 1024-2011



of micelles is an entropic and enthalpic effect, as can be seen from the contributions of the enthalpy and entropy to the Gibbs free energy of micellization. The enthalpic contribution results partly from the energetically favorable interactions between the hydrophobic tails. The entropic contribution arises from the local structuring of water due to hydrogen bonding. Simply stated, the hydrogen-bonded structure of bulk water must be distorted to accommodate hydrocarbon molecules. $H_2O$ forms an ordered, cage[66] like structure around the non polar solutes (an effect known as hydrophobic hydration) in an effort to give up as few H-bonds as possible. This constraint therefore leads to significantly restricted mobility of $H_2O$ in the hydration layer. Thus hydrophobic tails of free surfactants break up the hydrogen bond between water molecules and impose a locally more ordered structure that is entropically unfavorable. As this disruption of water structure is reduced when micelles are formed, they are entropically favorable compared to free surfactants[4, 65–67].

### Electrostatic Interactions

The counter balancing influence to the hydrophobic character for a charged surfactant is the polar head group, which exhibits several features contributing to micelle character. While the head groups provide water solubility to an otherwise insoluble entity, their localization in the surface region of the micelle introduces large charge-charge repulsions that limit the number of surfactant monomers that may come together[2–4, 57, 65–67].

UNIVERSITAT ROVIRA I VIRGILI
MICROSCOPIC MODELING OF THE SELF ASSEMBLY OF SURFACTANTS: SHAPE TRANSITIONS AND CRITICAL MICELLE CONCENTRATIONS
Asfaw Gezae Daful
ISBN:/DL:T. 1024-2011

UNIVERSITAT ROVIRA I VIRGILI
MICROSCOPIC MODELING OF THE SELF ASSEMBLY OF SURFACTANTS: SHAPE TRANSITIONS AND CRITICAL MICELLE CONCENTRATIONS
Asfaw Gezae Daful
ISBN:/DL:T. 1024-2011

# Chapter 3

# Theory of Self-Assembly

## 3.1 Introduction

Above a threshold concentration, surfactants self-assemble into aggregates, driven by the hydrophobicity of the tails and the hydrophilic nature of the head groups of the surfactant. In this chapter we will describe the self-assembly process of surfactants into micelles. This chapter continues with a review of statistical thermodynamics and, in particular the thermodynamics of micelle formation along with the application of mass action law for the micellization process. A brief introduction of simulation techniques will be given followed by a description of micellar structures and shape.

Self-assembly is the assembly of molecules without guidance or management from an outside source. The term *self-assembly* is rather broad and applies to spontaneous aggregation and order formation of constituents when they exist in correct proportions under appropriate conditions[1, 68, 69]. The process is reversible and represents thermodynamic equilibrium. Self-assembly can occur spontaneously in nature, for example, in cells such as the self-assembly of the lipid bilayer membrane. The self-assembly process plays an important role in a number of widely varying contexts. When amphiphilic molecules are dispersed in a single solvent, such as water, the hydrophobic interactions of the hydrocarbon chains drive the molecules to self-assemble into microstructures called micelles, where the hydrophobic tails are shielded from unfavourable interactions with the polar solvent by the hydrophilic, polar head groups. These microstructures typically have characteristic size and shape. These structures are not covalently bonded, but rather stabilized by

UNIVERSITAT ROVIRA I VIRGILI
MICROSCOPIC MODELING OF THE SELF ASSEMBLY OF SURFACTANTS: SHAPE TRANSITIONS AND CRITICAL MICELLE CONCENTRATIONS
Asfaw Gezae Daful
ISBN:/DL:T. 1024-2011



the weaker hydrophobic interactions; the sizes and shapes can change as a function of temperature, surfactant concentration[69]

## 3.2 Equilibrium Ensembles

It is of paramount importance to derive the laws of macroscopic thermodynamics from a fundamental set of postulates governing the microscopic state of the system. Most important for this work, is the form of the expressions for thermodynamic quantities and obtaining the observable quantities from nothing more than molecular interactions. Besides these macroscopic quantities, we can also obtain important microscopic details such as molecular organization, motion, and structure. A central concept is the equilibrium ensemble[1]. An equilibrium ensemble describes the equilibrium probability density distribution in phase space of a system subject to given external constraints. Different ensembles correspond to systems having different constraints. Depending on the system, one of several different ensembles may lend itself to the types of properties to be calculated.

Before introducing the various ensembles, we state two postulates which we will use.

**Postulate 1:** Given enough time, a system will sample all microstates consistent with the constraints imposed. This postulate states that the time-averaged properties of a thermodynamic system, the properties manifested by the collection of molecules as they proceed through their natural dynamics, are equal to the properties obtained by weighted averaging over all microstates in the ensemble. That is, time averages are equivalent to ensemble averages. Mathematically, we have

$$\langle x \rangle = \frac{\sum_i x_i \rho_i}{\sum_i \rho_i} = \lim_{t \to \infty} \frac{1}{t} \sum_i x_i \Delta t_i \tag{3.1}$$

where $\rho_i$, is the probability density of state $i$, $x$ is a thermodynamic property and $t$ is time. The angle brackets $\langle ... \rangle$ indicate the ensemble average of a property.

**Postulate 2:** Equal *a priori* probabilities: All microstates having the same energy are equally probable. We use this postulate to construct distribution functions based solely on energies of the ensembles, which can mathematically written as,

[1] An ensemble is a collection of microstates of system of molecules, all having in common one or more extensive properties. Additionally, an ensemble defines a probability distribution accords a weight to each element of the ensemble.

UNIVERSITAT ROVIRA I VIRGILI
MICROSCOPIC MODELING OF THE SELF ASSEMBLY OF SURFACTANTS: SHAPE TRANSITIONS AND CRITICAL MICELLE CONCENTRATIONS
Asfaw Gezae Daful
ISBN:/DL:T. 1024-2011



$$\rho_i = \rho_i(E_i) \tag{3.2}$$

Statistical mechanics groups many-body systems into ensembles. An ensemble in statistical mechanics consists of a very large, theoretically infinite, number of copies of a system, all characterized by the macroscopic variables. The four commonly used ensembles are, micro-canonical ensemble, canonical ensemble, grand-canonical ensemble and isothermal-isobaric ensemble.

1. The *micro-canonical ensemble* is a group of systems characterized by a fixed number of particles $\mathcal{N}$ and total energy $E$ and volume $V$. This ensemble is often denoted as the $\mathcal{N}VE$ ensemble and consists of copies of an isolated system.

2. The *canonical ensemble* consists of many-body systems with equal number of particles $\mathcal{N}$, which are at thermal equilibrium with a heat bath at temperature $T$, and volume $V$. This ensemble exchanges energy with the heat bath and is denoted as the $\mathcal{N}TV$ ensemble.

3. The *grand-canonical ensemble* is a collection of identical systems at equilibrium with an external reservoir with which they exchange both energy and particles. This ensemble is referred to as the $\mu VT$ ensemble, where $\mu$ is the chemical potential controlling the average in the number of particles.

4. In the *isothermal-isobaric ensemble*, all the systems have the same number of particles $\mathcal{N}$ and maintain the same temperature $T$ and pressure $P$. It is referred to as the $\mathcal{N}PT$ ensemble and it plays an important role in chemistry as many chemical systems are prepared and studied under conditions of constant temperature and pressure.

## 3.3 The Boltzmann Distribution

The Boltzmann distribution[70] law says that if the energy associated with some state or condition of a system is $\epsilon$, then the frequency with which that state or condition occurs, or the probability of its occurrence, is proportional to

$$e^{-\epsilon/k_B T} \tag{3.3}$$

where $T$, is the system's absolute temperature and $k_B$ is the Boltzmann constant, $k_B = 1.38 \times 10^{-23} J/K = 1.38 \times 10^{-16} erg/K$ [70, 71]. If there are $\mathbf{m}$ states, then

UNIVERSITAT ROVIRA I VIRGILI
MICROSCOPIC MODELING OF THE SELF ASSEMBLY OF SURFACTANTS: SHAPE TRANSITIONS AND CRITICAL MICELLE CONCENTRATIONS
Asfaw Gezae Daful
ISBN:/DL:T. 1024-2011



the sum of the Boltzmann factor is the Partition Function, $Q$, where the sum is taken over all state values.

$$Q = \sum_{j=1}^{\mathbf{m}} e^{-\epsilon_j / k_B T} \tag{3.4}$$

Suppose that we have two states accessible to a system. Let the energy of the first be given by $E_1$ and the energy of the second be given by $E_2$ . It can be derived that the ratio of the probabilities of occupation of the two states is given by:

$$\frac{P(1)}{P(2)} = \frac{e^{-E_1/k_B T}}{e^{-E_2/k_B T}} \tag{3.5}$$

## 3.4 Free Energy, Entropy and Chemical Potential

An equilibrium ensemble describes the equilibrium probability distribution in phase space of a system subject to some given external constraints. Canonical ensemble is the most practical ensemble with $\mathcal{N}$, $V$, and $T$, fixed. We can imagine a collection of boxes with equal volumes, and equal number of particles. The entire collection is kept in thermal equilibrium. It is a collection of systems (ensembles) with the same number of particles and volume, but the energy is allowed to fluctuate. Energy can be passed from one system to its neighbors, so that the energy of each system fluctuates. Each system is in thermal contact with the remainder, which acts as a heat bath for the system. The ensemble is made up of a collection of cells, each with rigid, impermeable walls (hence constant $\mathcal{N}$ and $V$) that can exchange heat with one another (constant $T$). This ensemble is called the *canonical ensemble*. Most experimental systems are in contact with heat baths, so this is a more natural ensemble than others like the microcanonical ensemble[69, 72–74]. The entire collection is brought to a fixed energy and then the system made adiabatic. Thermal insulation surrounds the entire ensemble and conductive, impermeable walls define each replicated system, thus ensuring constant $T$, $V$, and $\mathcal{N}$ for all members of the ensemble. This guarantees that the ensemble itself can be modeled as an isolated system, thus fulfilling a fundamental requirement for applying the principle of *a priori* probability. On this basis, suitable constraints on mass and energy for the ensemble can be expressed. Assuming that we have $\mathcal{N}$ members of a canonical ensemble. Each member represents the whole macroscopic system of $\mathcal{N}$ molecules in a particular microscopic state. Let $\mathcal{N}_i$ represent the number of ensemble members in state $i$ having energy $E_i$. Then we know that the sum, over all members in each state $i$ will give the total number of members:

UNIVERSITAT ROVIRA I VIRGILI
MICROSCOPIC MODELING OF THE SELF ASSEMBLY OF SURFACTANTS: SHAPE TRANSITIONS AND CRITICAL MICELLE CONCENTRATIONS
Asfaw Gezae Daful
ISBN:/DL:T. 1024-2011



$$\mathcal{N} = \sum_i \mathcal{N}_i \tag{3.6}$$

In addition, the total energy is,

$$E = \sum_i \mathcal{N}_i E_i \tag{3.7}$$

Now we need to determine the number of possible states (ensemble members) among the various microscopic states. We know, for any of these distributions, the probability of finding $\mathcal{N}_j$ ensemble members in the $j^{th}$ state is:

$$\rho_j = \frac{\mathcal{N}_j}{\mathcal{N}} \tag{3.8}$$

As this is just the probability of any distribution $j$, it is needed to replace $\mathcal{N}_j$ with the ensemble average value $\langle \mathcal{N}_j \rangle$ determined from all combinations of the $\mathcal{N}$ ensemble members, $\rho_j = \frac{\langle \mathcal{N}_j \rangle}{\mathcal{N}}$.

From the statistical thermodynamic derivation[69, 70, 72–74] the probability distribution, that can be used to find an ensemble average value of any thermodynamic property that depends upon the microscopic state of the system is:

$$\rho_j = \frac{e^{-\beta E_j}}{\sum_k e^{-\beta E_k}} \tag{3.9}$$

This is the probability distribution where $\beta = \frac{1}{k_B T}$. It can be used to find the expectation value of any thermodynamic property that depends upon the microscopic state of the system. Noting that the denominator of Eq. (3.9) is the normalization term for the distribution of all states. It is an important quantity which will appear in all canonical ensemble averages, and so is given a name, the partition function.

$$Q(N, V, \beta) = \sum_k e^{-\beta E_k} \tag{3.10}$$

$Q$ is the canonical ensemble partition function, so called because it is a sum over all the states partitioned by energy level. The ensemble average of any thermodynamic property, $J$, is then given by:

UNIVERSITAT ROVIRA I VIRGILI
MICROSCOPIC MODELING OF THE SELF ASSEMBLY OF SURFACTANTS: SHAPE TRANSITIONS AND CRITICAL MICELLE CONCENTRATIONS
Asfaw Gezae Daful
ISBN:/DL:T. 1024-2011



$$\langle J \rangle = \sum_k \rho_k J_k = \sum_k \frac{J_k e^{-\beta E_k}}{Q} \tag{3.11}$$

similarly,

$$\langle E \rangle = \sum_k \rho_k E_k = \sum_k \frac{E_k e^{-\beta E_k}}{Q} \tag{3.12}$$

$$\langle P \rangle = \sum_k \rho_k P_k = \sum_k \frac{P_k e^{-\beta E_k}}{Q} \tag{3.13}$$

Here $\langle P \rangle$ corresponds to the thermodynamic pressure and $\langle E \rangle$ corresponds to the thermodynamic energy of the system. Eq. (3.12) gives $E$ in terms of $\beta$, which could in principle be solved for $\beta$ in terms of $E$. In practice, it is more desirable to have $E$ as a function of $\beta$, rather than the other way around, however.

From the classical thermodynamic definition, the Helmholtz free energy, $F$, is given by, $(F = E - TS)$, where $S$ stands for entropy and $T$ for temperature, can be written in terms of the partition function:

$$F = -k_B T \ln Q \tag{3.14}$$

The free energy approach gives a useful starting point for statistical mechanics, as $F$ is a *thermodynamic potential*[70]; *i.e.,* all other thermodynamic functions of the system are obtainable from $F$ by differentiations alone.

The entropy[70] of a system of $N$ particles in a volume of $V$ is given by

$$\begin{aligned} S &= -\left(\frac{\partial F}{\partial T}\right)_{N,V} \\ &= \frac{\partial [k_B T \ln Q]}{\partial T} \\ &= k_B T \left[\ln Q + T \frac{1}{Q} \frac{\partial Q}{\partial T}\right] \end{aligned} \tag{3.15}$$

where, $Q = \sum_i e^{-\frac{E_i}{k_B T}}$, so

$$\frac{\partial Q}{\partial T} = \frac{1}{k_B T^2} \sum_i E_i e^{-\frac{E_i}{k_B T}} \tag{3.16}$$

UNIVERSITAT ROVIRA I VIRGILI
MICROSCOPIC MODELING OF THE SELF ASSEMBLY OF SURFACTANTS: SHAPE TRANSITIONS AND CRITICAL MICELLE CONCENTRATIONS
Asfaw Gezae Daful
ISBN:/DL:T. 1024-2011



Substituting Eq. (3.16) into Eq. (3.15) gives

$$S = k_B \left[ \ln Q + \frac{1}{k_B T} \frac{1}{Q} \sum_i E_i e^{-\frac{E_i}{k_B T}} \right] \tag{3.17}$$

Recalling that $\rho_i = \frac{1}{Q} e^{-\frac{E_i}{k_B T}}$, Eq. (3.17) can be rewritten as

$$S = k_B \left[ \ln Q + \frac{1}{k_B T} \sum_i \rho_i E_i \right] \tag{3.18}$$

The entropy can also be written in terms of the partition function and the ensemble average energy, given that from Eq. (3.12), $\langle E \rangle = \sum_i \rho_i E_i$, the entropy can be defined as:

$$S = k_B \ln Q + \frac{\langle E \rangle}{T} \tag{3.19}$$

Using the definition for the probability distribution the entropy[69, 70, 72–74] can be written as[2]

$$S = -k_B \sum_i \rho_i \ln \rho_i \tag{3.20}$$

The free energy of a system containing different species $i$ has the form:

$$F = \sum_i N_i \mu_i \tag{3.21}$$

here $N_i$ is the number of particles of species $i$ and $\mu_i$ is the chemical potential of that species. Then we can define, $\mu_i$ as,

$$\mu_i = \left( \frac{\partial F}{\partial N_i} \right)_{V,T,N_{j \neq i}} \tag{3.22}$$

2

$$\begin{aligned} S &= k_B \Big[ \ln Q + \frac{1}{k_B T} \sum_i \rho_i E_i \Big] = -k_B \Big[ -\ln Q + \sum_i \rho_i \Big( -\frac{E_i}{k_B T} \Big) \Big] \\ &= -k_B \Big[ -\ln Q + \sum_i \rho_i \ln e^{\Big( -\frac{E_i}{k_B T} \Big)} \Big] = -k_B \Big[ \sum_i \rho_i \ln \Big( \frac{e^{-\frac{E_i}{k_B T}}}{Q} \Big) \Big] \\ &= -k_B \sum_i \rho_i \ln \rho_i \end{aligned}$$

UNIVERSITAT ROVIRA I VIRGILI
MICROSCOPIC MODELING OF THE SELF ASSEMBLY OF SURFACTANTS: SHAPE TRANSITIONS AND CRITICAL MICELLE CONCENTRATIONS
Asfaw Gezae Daful
ISBN:/DL:T. 1024-2011



## 3.5 Partition Function of the Micellar Aggregate

The partition function is a statistical thermodynamic quantity that describes how the particles distribute themselves over the possible quantum states. Considering that a micellar aggregate of $N$ amphiphiles has a well defined geometry, $G$ floating in a micellar solution of $N_w$ water molecules in a volume $V$ and at a temperature $T$. The partition function of such an aggregate can be expressed as[75]:

$$Q(N,V,T,G) = Q_{trans}Q_R(N,T,G)Q_{int}(N,T,G) \tag{3.23}$$

where $Q_{trans}$ is the translational partition function of the whole aggregate, $Q_R$ is the rotational partition function of the aggregate, and $Q_{int}$ is the partition function corresponding the internal degrees of freedom, that is the partition function of an aggregate which is fixed in space. This term includes the internal degrees of freedom of the amphiphiles, their interactions with themselves and their interaction with the surrounding solution. The factorization of the last two factors is valid only if the rotation of the aggregate is much slower than the motion of the molecules within the aggregate, otherwise these rotations are coupled to the internal degree of freedom of its constituent molecules. The free energy is:

$$\begin{aligned} F(N,V,T,G) &= -k_BT\ln Q(N,V,T,G) \\ &= -k_BT\ln\Big(Q_{trans}Q_R(N,T,G)Q_{int}(N,T,G)\Big) \end{aligned} \tag{3.24}$$

The free energy of such a solution is divided into internal and external parts. The external part incorporates terms accounting for the translational (entropy of mixing) and rotational motions of the aggregates as well as intermicellar interaction, while the internal part includes all contributions to the free energy of an isolated aggregate which is fixed in space. The internal free energy depends on intermolecular interactions and conformational energies and entropies, as well as kinetic contributions associated with the motion of the molecules within the aggregate. The internal partition function, $Q_{int}$, of an amphiphilic aggregate involves both kinetic (momentum) and configurational (coordinate) contributions, $Q_{int} = M_N Z_N$, where $Q_N$ is the configurational contributions and $M_N$ is the momentum contributions. The momentum contributions to the total free energy is independent of the aggregate size and shape distribution and therefore plays no role in determining the relative stability of different aggregates[76]. Based on this notation the following discussion is limited to the configurational part of the internal free energy, $F_{int}$

$$F_{int}(N,T,G) = -k_BT\ln Q_n(N,T,G) \tag{3.25}$$

where

$$Q_N(N,T,G) = \sum_{\alpha} exp(-\beta E(\alpha_j, G)) \tag{3.26}$$

which is a sum over all possible configurations of $N$ amphiphilic molecules and $E$ is the energy (Hamiltonian) of the $\alpha_j$ configuration. The contributions to the Hamiltonian energy of the chains, $E$ are:

- the sum of internal free energy of the chains arising from intramolecular attractive interactions. They are taken through the set of the single-chain configurations, i.e. a set of self-avoiding random walk is used.
- the intermolecular interaction between the chain segments

The total conformational free energy of the chain, $E$ can then be written as:

$$E(\alpha_j, G) = E_{intra}(\alpha_j, G) + E_{inter}(\alpha_j, G) \tag{3.27}$$

Therefore we can rewrite Eq.(3.26) as

$$Q_N(N,T,G) = \sum_{\alpha} exp\Big(-\beta E_{intra}(\alpha_j, G) + E_{inter}(\alpha_j, G)\Big) \tag{3.28}$$

and the probability distribution function, *pdf*, of the $N$ chains in configuration $\alpha_j$ is given by

$$P(\alpha_j) = \frac{1}{Q_N} exp(-\beta E(\alpha_j, G)) \tag{3.29}$$

This probability distribution function, $P(\alpha_j)$, gives the probability of finding a given chain in configuration, $\alpha_j$, regardless of the configurations of all other chains. So $P(\alpha_j)$, can be used to calculate the mean-field approximation of any thermodynamic property of interest.

## 3.6 Thermodynamics of Self Assembly of Nonionic Surfactants

The understanding of the thermodynamics of micelle formation is of much theoretical and practical importance. Several thorough discussions of the way to calculate

UNIVERSITAT ROVIRA I VIRGILI
MICROSCOPIC MODELING OF THE SELF ASSEMBLY OF SURFACTANTS: SHAPE TRANSITIONS AND CRITICAL MICELLE CONCENTRATIONS
Asfaw Gezae Daful
ISBN:/DL:T. 1024-2011



changes in thermodynamic properties that accompany micelle formation from experimental data have been described[1–3, 77].

Like all physical processes, self-assembly of surfactants is subject to the laws and limitations of thermodynamics. The micellization process is one of the most important characteristics of surfactant solution and hence it is essential to understand its mechanism and the driving forces of micellization. This requires an analysis of the dynamics of the process as well as the equilibrium aspects whereby the laws of thermodynamics may be applied to obtain the free energy, enthalpy, and entropy of micellization. The general thermodynamic principles of self-assembly have been widely discussed in the literature[1]. The surfactant solution is viewed as a multi-component system consisting of water solvent, singly dispersed surfactant molecules, and aggregates of all possible shapes and aggregation numbers, $N$, (see Fig. 3.1). Let us consider a nonionic surfactant solution consisting of micelles of aggregation number $N$ coexisting with singly dispersed surfactant molecules. The aggregation number $N$ is a single-valued variable in the case of a monodispersed micellar system, whereas $N$ assumes all possible values from 2 to $\infty$, in the case of a polydispersed micellar system. Two general approaches have been employed to tackle micellization problems

1. Phase Separation Model: this approach treats micelles as a separate but soluble phase, which begins to form at the critical micelle concentration, CMC. This model also implies that at the CMC there are discontinuous changes in the properties of the micellar solution

2. Mass Action Model: this approach is consistent with the fact that the properties of the micellar solution change continuously at CMC. Micelles and singly dispersed surfactants molecules are considered to be in an association-dissociation equilibrium.

The mass action approach seams to a give more realistic description of the micelle formation from both thermodynamic and kinetic aspects. In this thesis we used the Mass Action Model approach, as is discussed below.

### 3.6.1 Mass Action Model

This model assumes the association-dissociation equilibrium between free surfactant molecules and micelles. Micelles form spontaneously under the right conditions, which one may refer to as a process of self-assembly. To understand how the micelle formation took place and to apply the mass action law, we will first provide

UNIVERSITAT ROVIRA I VIRGILI
MICROSCOPIC MODELING OF THE SELF ASSEMBLY OF SURFACTANTS: SHAPE TRANSITIONS AND CRITICAL MICELLE CONCENTRATIONS
Asfaw Gezae Daful
ISBN:/DL:T. 1024-2011



a thermodynamic description of the aggregation behavior of surfactant molecules. The formation of an aggregate of size $N$ from the free amphiphiles in solution is governed by a set of equilibria represented as, schematically shown in Fig. 3.1: where, $\mu_1^o$ is the standard chemical potential of the singly dispersed surfactant molecules, $\mu_N^o$ is the standard chemical potential of surfactant molecules in a micelle of aggregation number $N$, $X_1$ is the concentration of the singly dispersed surfactant in solution, and $X_N$, is the concentration of surfactant molecules in micelles of aggregation number $N$. An amphiphilic chain can be considered to belong to an aggregate if any of its tail beads occupies a neighboring site of a tail from another chain. Non-aggregated surfactant chains are called free or single surfactants.

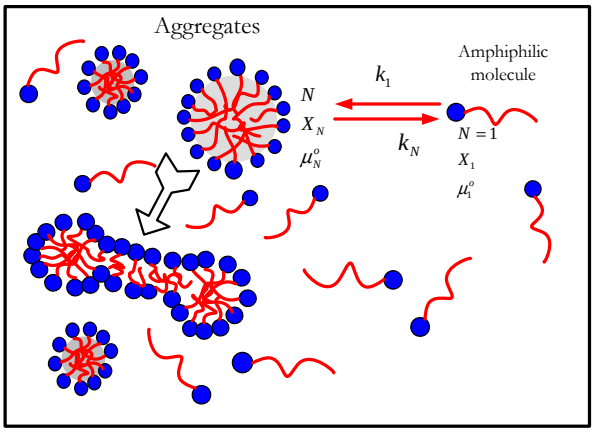


**Figure 3.1:** Schematic representation of self-assembly of amphiphiles into aggregates of different sizes and shapes

The condition of thermodynamic equilibrium requires that the chemical potential of the singly dispersed surfactant molecule must be equal to the chemical potential per surfactant molecule of aggregates of any size, $N$, and any shape. This allows us to write

$$\mu_1 = \mu_2 = \mu_3 = ... = \mu_{N-1} = \mu_N = constant \tag{3.30}$$

where $\mu_1$ is the chemical potential of singly dispersed surfactant molecules in the solution and $\mu_N$ is the chemical potential of the surfactant molecules within micelles of aggregation number $N$.

From a thermodynamics point of view[78–80], if $\Re$ represents the molar (or unit-mass) value of any extensive thermodynamic property, then an excess property,

UNIVERSITAT ROVIRA I VIRGILI
MICROSCOPIC MODELING OF THE SELF ASSEMBLY OF SURFACTANTS: SHAPE TRANSITIONS AND CRITICAL MICELLE CONCENTRATIONS
Asfaw Gezae Daful
ISBN:/DL:T. 1024-2011



$\Re^{excess}$, is defined as the difference between the actual property value of a solution and the value it would have as ideal solution at the same temperature, pressure and concentration, ($\Re^{excess} = \Re - \Re^{ideal}$). Thus, the chemical potential, which is thermodynamic property of interest in this work, of a given system (micelle of size $N$) is given as,

$$\mu_N = \mu_N^{excess} + \mu_N^{ideal} \tag{3.31}$$

which is a function of temperature ($T$), pressure ($P$), and concentration (mole fraction, $X$), defined as:

$$\mu_N = \mu_N^o + \frac{k_B T}{N} \ln \frac{a_N}{N} \tag{3.32}$$

where $a$ is the *activity*, defined as the product of the concentration (mole fraction, $X$) and activity coefficient, $\gamma$, ($a_N = \gamma_N X_N$) of the system; and $\mu_N^o$ is the standard chemical potential. The second term represents the contribution arising from the translational entropy of the micelle. It can be noted that the bigger the micelle, the smaller the importance of this translational entropy. The chemical potential of singly dispersed surfactants is, thus given by

$$\mu_1 = \mu_1^o + k_B T \ln a_1 \tag{3.33}$$

The difference in standard chemical potentials between free surfactants in the bulk solution and surfactants in an aggregate of size $N$, ($\frac{\mu_N^o - \mu_1^o}{k_B T}$), is an important criterion for micelle formation, as will be discussed in the next chapters.

The total chemical potential for an ideal system, *i.e.,* ideal mixing of the surfactants and micelles, is given by

$$\mu_N^{ideal} = \mu_N^o + \frac{k_B T}{N} \ln \frac{X_N}{N} \tag{3.34}$$

The excess chemical potential is then obtained by substituting Eq. (3.34) in to Eq. (3.31)

UNIVERSITAT ROVIRA I VIRGILI
MICROSCOPIC MODELING OF THE SELF ASSEMBLY OF SURFACTANTS: SHAPE TRANSITIONS AND CRITICAL MICELLE CONCENTRATIONS
Asfaw Gezae Daful
ISBN:/DL:T. 1024-2011



$$\begin{aligned}\mu_N^{excess} &= \mu_N - \mu_N^{ideal} \\ &= (\mu_N^o + \frac{k_BT}{N}\ln\frac{a_N}{N}) - (\mu_N^o + \frac{k_BT}{N}\ln\frac{X_N}{N}) \\ &= \frac{k_BT}{N}\ln\frac{a_N}{X_N} \\ &= \frac{k_BT}{N}\ln\gamma_N\end{aligned} \tag{3.35}$$

For a surfactant system, the total chemical potential of surfactant molecules in an aggregate of size $N$, is given by:

$$\begin{aligned}\mu_N &= \mu_N^{ideal} + \mu_N^{excess} \\ &= (\mu_N^o + \frac{k_BT}{N}\ln\frac{X_N}{N}) + (\frac{k_BT}{N}\ln\gamma_N) \\ &= \mu_N^o + \frac{k_BT}{N}\ln\gamma_N\frac{X_N}{N}\end{aligned} \tag{3.36}$$

Here $\mu_N^o$ is the standard chemical potential of surfactants in an aggregate of aggregation number, $N$, and $X_N$ is the mole fraction of surfactants in an aggregate of aggregation number, $N$. The chemical potential of singly dispersed surfactant molecules is

$$\mu_1 = \mu_1^o + k_BT\ln\gamma_1X_1 \tag{3.37}$$

The last two equations, Eqs. (3.36 and 3.37) are combined to give the distribution:

$$\frac{X_N}{N} = \frac{1}{\gamma_N}\left[\gamma_1X_1exp(-\frac{\mu_N^o - \mu_1^o}{k_BT})\right]^N \tag{3.38}$$

This equation, also known as the cluster size distribution, along with the conservation of the total surfactant concentration $X_{total} = \sum_{N=1}^{\infty} X_N$ completely defines the micellar size distribution. If the surfactant system is assumed to behave ideally, the activity coefficients be set to unity, $\gamma_N = 1$, for all $N$, so for an ideal surfactant solution the micellar size distribution is given by:

$$\frac{X_N}{N} = \left[X_1exp\left(-\frac{\mu_N^o - \mu_1^o}{k_BT}\right)\right]^N \tag{3.39}$$

UNIVERSITAT ROVIRA I VIRGILI
MICROSCOPIC MODELING OF THE SELF ASSEMBLY OF SURFACTANTS: SHAPE TRANSITIONS AND CRITICAL MICELLE CONCENTRATIONS
Asfaw Gezae Daful
ISBN:/DL:T. 1024-2011



The implications of this equation are straightforward, recalling that, $\mu_N^o$ is the standard chemical potential of a surfactant molecule in an aggregate of size $N$, and $\mu_1^o$ is the standard chemical potential of a surfactant molecule in the bulk. Aggregates will form only when there is a difference in the free energies between the molecules in the aggregated and dispersed monomer states, (*i.e.* $\mu_N^o < \mu_1^o$). In the case that all $\mu_N^o$ are equal, Eq. (3.39) simplifies to

$$X_N = N X_1^N \tag{3.40}$$

This equation, therefore shows that $X_N \ll X_1$ and most molecules will be in the free surfactant monomer state ($N = 1$). Only when the Gibbs free energy ($G_N^o$), or the standard chemical potential of surfactants in the aggregated states, $\mu_N^o$, is lower than the standard chemical potential of free surfactants ($\mu_N^o < \mu_1^o$), the occurrence of larger aggregates becomes more probable.

If the total surfactant concentration, $X_{total}$ is increased, $X_1$ reaches a critical concentration above which it can increase no further. The conventional term for this concentration is the critical micelle concentration (CMC). Any surfactant added above this concentration will aggregate in larger clusters of a finite size ($N > 1$). Above the CMC the free surfactant concentration remains almost constant, while the concentration of aggregates increases approximately linearly with the total solute concentration $X_{total}$.

From the size distribution equation, Eq. (3.39) many size-dependent properties of the micellar solution can readily be calculated. For instance, the number-average ($\widetilde{N}_n$) and the weight-average ($\widetilde{N}_w$) aggregation numbers can be obtained by

$$\begin{aligned} \widetilde{N}_n &= \frac{\sum_N N X_N}{\sum_N X_N} \\ \widetilde{N}_w &= \frac{\sum_N N^2 X_N}{\sum_N N X_N} \end{aligned} \tag{3.41}$$

## 3.7 Simulation Techniques

The development of computer simulations has provided an alternative mode of research in science. Computer simulations can be used as a linking bridge between theory and experiments. Simulations are not hypothetical remedies for all, and they do not replace theories and experiments[68]. Simulations are best seen as *computer experiments* that serve as adjuncts to theory and real experiments and

UNIVERSITAT ROVIRA I VIRGILI
MICROSCOPIC MODELING OF THE SELF ASSEMBLY OF SURFACTANTS: SHAPE TRANSITIONS AND CRITICAL MICELLE CONCENTRATIONS
Asfaw Gezae Daful
ISBN:/DL:T. 1024-2011



provide otherwise inaccessible or not easily accessible microscopic or macroscopic information that theorists and experimentalists can use. The objective of computer simulation methods of molecular systems is thus to estimate ensemble averages in order to estimate properties of interest of the system.

Such simulations are mainly conducted for the following reasons[81]:

1. they can provide a molecular interpretation of experimental facts, something that can be difficult to gain experimentally
2. they enable the prediction of novel phenomena, emerging structures and properties of materials. In this way simulations can also be used to guide new experiments
3. they can be used to test the approximations, concepts, and predictions made by theories
4. to usefully reproduce or predict properties for a preselected system (*i.e.* one chosen before the simulation results are obtained)
5. to learn about general phenomena; *e.g.* to provide important insights into the physics of fundamental processes
6. in situations in which experiments are impractical, *e.g.* systems at high temperatures or pressures

Simulations can easily examine different theories and visualize the results thus providing valuable insights. Furthermore, they can aid in interpreting experimental results, and in devising new experimental strategies. Computer simulations, for systems of surfactants, frequently use statistical mechanics, that connects the microscopic variables (positions, momenta, and interactions) of a physical system to its macroscopic ones. However, these possibilities and potentials of simulations must deal with the realities of computational demands and resources. More recently, computer simulations have been increasingly used to study the structures and thermodynamics of micelles [37–55].

There are two main classes of simulation models that could be used to study surfactant systems, the detailed atomistic and the coarse-grained models [81]. In the detailed atomistic model, every atom of the simulated system is represented explicitly by an individual potential site. In theory, this atomistic approach would be the most rigorous and accurate approach, but limited by their tremendous computational cost, the simulations generally start from artificial states near equilibrium [81–83]. The whole micellization process is still beyond the reach of such models.

UNIVERSITAT ROVIRA I VIRGILI
MICROSCOPIC MODELING OF THE SELF ASSEMBLY OF SURFACTANTS: SHAPE TRANSITIONS AND CRITICAL MICELLE CONCENTRATIONS
Asfaw Gezae Daful
ISBN:/DL:T. 1024-2011



An alternative to the atomistically detailed model, is the coarse-grained model, in which a number of atoms are grouped together. This model is usually able to describe micellization, although it lacks the detailed structural information that the atomistic model could provide. This model could in turn be divided into continuum and lattice models. The continuum model is more realistic, but the lattice model is computationally more efficient. Numerous simulation studies involving coarse-grained continuum [84] and lattice [46, 47, 49, 52–54, 85] models have been performed. The lattice model has been used extensively to study non-ionic micelles using Monte Carlo simulations [46, 47, 49, 52–54, 85].

The most common lattice model for non-ionic surfactants is probably that of Larson et al. [49, 52, 86]. This model places the surfactant molecules on a fully occupied cubic lattice, and restricts the interactions as well as the direction of growth to the 26 neighboring sites, known as coordination number ($z = 26$). Care [87] used a very similar lattice model, but considered only adjacent sites (no diagonal sites) for chain growth and interactions, ($z = 6$). Using these lattice models, Monte Carlo simulations were performed, and the thermodynamic properties and the size and shape distributions [46, 47, 49, 52–54, 85] of the micelles have been determined. In this section, we discuss a few computational methods that are of great practical importance for an efficient simulation program. Additionally, we discuss some fundamental concepts in computer simulations such as how the Single Chain Mean Field Theory, Monte Carlo and molecular dynamics algorithms work.

### 3.7.1 Periodic Boundary Conditions

In a simulation of a finite number of surfactant molecules, a significant fraction of particles will be at the edges of the system. The environment of these particles will be very different to the environment of a surfactant molecule within the bulk system. In order to reduce this problem, periodic boundary conditions are normally employed [88]. We make copies of the system in all directions, as shown in Fig. 3.2. When a surfactant molecule leaves the central simulation cell at one side, its periodic image enters from the other side, thus conserving the number of surfactant molecules in the central simulation cell.

### 3.7.2 Monte Carlo Simulations

In the Monte Carlo method, statistical thermodynamic properties of a system are estimated by averaging mechanical properties over a large number of configurations or states. Statistical mechanics relates microscopic properties to macrosco-

UNIVERSITAT ROVIRA I VIRGILI
MICROSCOPIC MODELING OF THE SELF ASSEMBLY OF SURFACTANTS: SHAPE TRANSITIONS AND CRITICAL MICELLE CONCENTRATIONS
Asfaw Gezae Daful
ISBN:/DL:T. 1024-2011



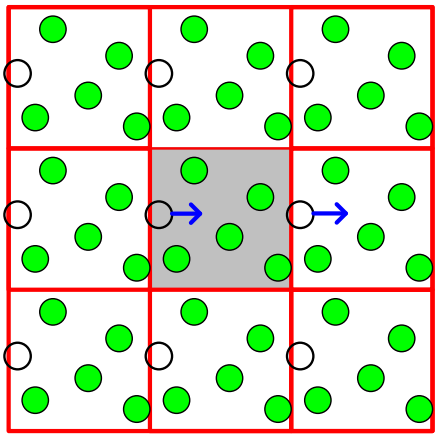

**Figure 3.2:** Schematic illustration of periodic boundary conditions. A surfactant molecule that leaves to the right of the simulation box (center) is replaced by an identical one, moving by the same amount out of a periodic image of the original box

pic behavior of matter. Monte Carlo simulation [46, 49, 52, 54, 59, 85, 89–92] methods are widely used to analyze the physical behavior and the equilibrium properties of many different kinds of macroscopic systems. Larson [49, 52] studied the amphiphile-oil-water phase diagram by integration of the Gibbs-Helmholtz equation. Under this approach, Larson calculated the Helmholtz free energy in the canonical ensemble with an athermal initial condition and then compared these results with zero- and first-order quasi-chemical approximation. In other works, Care et al. [87] and Kurt Binder et al. [93] studied the thermodynamics of cluster formation by calculating the distribution of monomer in clusters. Monte Carlo simulation also allows the change of surfactant characteristics, such as the length of the hydrophilic group or the hydrophobic group, enabling to determine their effects on micelle size, cmc and other thermodynamic properties [46]. Panagiotopoulos et al. [54] determined the phase behavior and micellization of several lattice di-block and tri-block surfactants in Larson type model by histogram-reweighting grand canonical Monte Carlo simulations on a lattice model studied surfactant self-assembly in a supercritical solvent using the Larson model.

In the present work, we studied some thermodynamic parameters such as aggregation number, micellar size distribution and shape transition of micelles through three dimensional lattice Monte Carlo simulation.

The Monte Carlo method is a numerical solution to a problem that models particles (or molecules) interacting with other particles (or molecules) or their environment based upon simple particle-particle or particle-environment interactions. It represents an attempt to model nature through direct simulation of the essential dynamics of the system in question. In this sense the Monte Carlo method is essentially simple in its approach, a solution to a macroscopic system through simulation of its microscopic interactions. Thus, using statistical mechanics the microscopic properties of a system can be related to their macroscopic properties to study the system via Monte Carlo simulation. It is based on the principles of equilibrium statistical mechanics, in which the fundamental premise is that all of the essential information about the system under consideration can be represented by a partition function. Here, the fundamental quantity is the partition function, $Q$, which is the sum of the Boltzmann factors over all possible states, $i$, of a system with $\mathcal{N}$ particles in a volume, $V$, at temperature, $T$. Recalling Eq. (3.10), $Q = \sum_i exp(-\frac{E_i}{k_B T})$, where $\beta = \frac{1}{k_B T}$ and $E_i$ is the total energy of the system in state, $i$, and $k_B$ is Boltzmann's constant. The Boltzmann factors[69, 70, 72–74], $exp(-\frac{E_i}{k_B T})$, are proportional to the probability of finding the system in state $i$. The probability distribution, Eq. (3.9), can be written as

$$P(i) = \frac{1}{Q} exp(-\frac{E_i}{k_B T}) \tag{3.42}$$

and therefore we can calculate the ensemble average of any observable, $\mathcal{A}$, by

$$\langle \mathcal{A} \rangle = \sum_i P(i)\mathcal{A}(i) = \frac{1}{Q} \sum_i \mathcal{A}_i exp(-\frac{E_i}{k_B T}) \tag{3.43}$$

where $\mathcal{A}_i$ is the value of the property $\mathcal{A}$ in a particular state $i$, and $P_i$ is the probability that state $i$ occurs in equilibrium.

As shown in section 3.2 the ensemble average $\langle \mathcal{A} \rangle$ is equal to the time average of $\mathcal{A}$, known as the ergodicity theorem[94]. The importance of the ergodic hypothesis is in the fact that we can completely disregard the time dependent interactions in the system, and still the statistical behavior of the macroscopic system can be evaluated.

Due to the important role that the partition function plays, the aim of many theoretical studies in equilibrium statistical mechanics is to find expressions for the partition function of specific model systems. The macroscopic information of a microscopic system can alternatively be determined from Monte Carlo simulations.

However, the number of accessible states in a large system can be huge thus making the exact evaluation of the average in Eq. (3.43) is unfeasible with current computers. Moreover, some states (those with very small Boltzmann factor)

UNIVERSITAT ROVIRA I VIRGILI
MICROSCOPIC MODELING OF THE SELF ASSEMBLY OF SURFACTANTS: SHAPE TRANSITIONS AND CRITICAL MICELLE CONCENTRATIONS
Asfaw Gezae Daful
ISBN:/DL:T. 1024-2011



contribute very little to the average, and hence should be omitted in an efficient calculation. To overcome these problems, *importance-sampling* is employed. In this scheme the only configurations to be sampled are those that make a significant contribution to the partition function and ensemble averages. This task can be achieved by generating a Markov chain of configurations in which each state is generated by "perturbing" the preceding one in the chain, and accepted as a new configuration only if the detailed balance condition is satisfied.

A sufficient (but not necessary) detailed-balance condition is that for an old, $o$, and a new, $n$, states

$$J(o \to n) = J(n \to o) \tag{3.44}$$

where $J(o \to n)$ is the probability flux from a state, $o$ to a new state, $n$ during a given simulation step. The flux $J(o \to n)$ can be factored into three terms

$$J(o \to n) = p(o)\alpha(o \to n)acc(o \to n) \tag{3.45}$$

where $p(o)$ is the probability of being in state $o$ (which at equilibrium should follow the Boltzmann distibution), $\alpha(o \to n)$ is the probability of generating the trial move from $o$ to $n$, and $acc(o \to n)$ is the probability of accepting the trial move from $o$ and $n$. By combining Eqs. (3.44) and (3.45) the detailed-balance condition can be rewritten as

$$\frac{acc(o \to n)}{acc(n \to o)} = \frac{\alpha(n \to o)}{\alpha(o \to n)} \frac{p(n)}{p(o)} \tag{3.46}$$

where $\frac{p(n)}{p(o)}$ is obtained based on the statistical ensemble we work in. In the case of the $\mathcal{N}VT$ ensemble the ratio can be expressed as the Boltzmann factor of the energy difference:

$$\frac{p(n)}{p(o)} = \frac{Q_{NVT}^{-1} e^{-\beta E(n)}}{Q_{NVT}^{-1} e^{-\beta E(o)}} = e^{-\beta[E(n)-E(o)]} \tag{3.47}$$

where $E(n)$ and $E(o)$ are the system energies for the new and old states, respectively. $Q_{NVT}$ is the partition function defined as the sum of all the energy states, $E_i$, and is given as $Q_{NVT} = \sum e^{-\beta E_i}$. Finally, if we assume that $\alpha(o \to n) = \alpha(n \to o)$ then Eq. (3.46) becomes

$$P_{acc} = acc(o \to n) = min\left(1, e^{-\beta[E(n)-E(o)]}\right) \tag{3.48}$$

UNIVERSITAT ROVIRA I VIRGILI
MICROSCOPIC MODELING OF THE SELF ASSEMBLY OF SURFACTANTS: SHAPE TRANSITIONS AND CRITICAL MICELLE CONCENTRATIONS
Asfaw Gezae Daful
ISBN:/DL:T. 1024-2011



The *min* function returns the smaller of its arguments. A typical importance-sampling Monte Carlo scheme to perform a simulation in the canonical ($\mathcal{N}VT$) ensemble will proceed as follows. The system is prepared in some initial configurations. A chain is chosen randomly and displaced within the simulation cell. If the trial move results in a decrease of the system energy, then the move is accepted and the chain positions updated. If the trial move results in an increase in the energy of the system, instead, the move is accepted with probability, $exp(-\beta\Delta E)$, where $\Delta E$ is the difference in system energy associated with the trial move. This is implemented in a computer simulation by generating a random number in the interval $[0, 1)$ and accepting the move only if the random number is less than the value, $exp(-\beta\Delta E)$. These steps are repeated for the subsequent randomly chosen chains. After a large number of trial moves, simple unweighted averages over the visited states can be calculated since each state is sampled with a probability proportional to its Boltzmann factor.

### 3.7.3 Molecular Dynamics

Molecular dynamics (MD) simulation is a classical technique to compute equilibrium structural and dynamical properties of a many-body system. In this technique each particle moves according to Newton's laws of motion, which are integrated numerically. The positions and velocities of the particles are updated every time-step and the equations of motion integrated to generate a trajectory in phase space. This procedure is repeated for a number of time-steps required to equilibrate the system and calculate accurate time averages. A typical MD simulation will proceed as follows: positions $\mathtt{r}_i$ and velocities $\mathtt{v}_i$ of the particles at time $t$ are stored in the computer. The force acting on each particle is calculated from the potentials ($\mathtt{F}_i = \nabla_i \mathtt{U}$) and then the equation of motion, $\mathtt{F}_i = \mathtt{m}_i\mathtt{a}_i$, is integrated over a finite time-step $\Delta t$. An MD trajectory reproduces the time evolution of the system dynamically. Thermodynamic observables can be obtained by taking the average over this simulation trajectory.

### 3.7.4 Mean Field Theory

Since we don't know the partition function of an arbitrary molecular system (and thus the free energy) scientists have to rely on approximations. The commonly used approximation is the so called mean-field approximation or the assumption of the existence of a mean molecular field which originated in the $19^{th}$ century from the work of Laplace and Rayleigh among others[95]. The assumption made entails

UNIVERSITAT ROVIRA I VIRGILI
MICROSCOPIC MODELING OF THE SELF ASSEMBLY OF SURFACTANTS: SHAPE TRANSITIONS AND CRITICAL MICELLE CONCENTRATIONS
Asfaw Gezae Daful
ISBN:/DL:T. 1024-2011



that the interaction of a molecule experienced by all other molecules is replaced by an effective interaction.

A number of different approaches try to circumvent solving the many-body problem as is done in simulations. The focus is not on the position of every particle in the system, rather it is on the average density at a given position. At each position in space, a given particle interacts with the local average of all other particles, instead of interacting with different individual molecules. Specially for polymer systems in which the exact molecular details are not essential for the overall behavior, this turns out to work rather well.

The Single Chain Mean Field Theory, SCMFT [5, 44–46, 55] and Self Consistent Field, SCF, theory [37, 41–43, 96–100] are used for modeling and studying the surfactant and polymer systems in a lattice and continuous space. In SCMFT a set of all possible conformations of a chain is generated as a Self-Avoiding Random Walk. This set is then weighted in the mean-field. This approach avoids the random-walk statistics used by the SCF theory. SCMFT is a mean-field model which is numerically solved to a self-consistent solution. So, even though the *intramolecular* interactions can be treated 'exactly', the *intermolecular* interactions are treated on a mean-field level. SCMFT deals with the equilibrium distribution of chain molecules in space and the resulting thermodynamic quantities of the system. The theory is formulated in terms of thermodynamic properties and a molecular field, which is associated with the chain molecule. These properties are functions of the molecular fields and vice versa, so at equilibrium these thermodynamic properties and the molecular fields are self-consistent. The molecular fields are varied numerically until the SCMFT solution is found.

### 3.7.5 Self-Avoiding Random Walk

The thermodynamic properties of a polymer chain are determined by its configurations. Configurational analysis is done in dilute solutions. A good solvent in polymer solutions is defined as a solvent in which it is energetically more favorable for the monomers of the polymer to be surrounded by molecules of the solvent than by other monomers. As a consequence, one can imagine that there exists round each monomer a region (the excluded volume) in which the chance of finding another monomer is very small. This leads to a more open and expanded structure of the polymer than if the excluded volume effects were absent. The same is true for surfactant systems too. The most popular model to describe this effect is the self-avoiding random walk (SARW), where we consider only the subset of the random walk which never visit the same site again. During the self-avoiding

UNIVERSITAT ROVIRA I VIRGILI
MICROSCOPIC MODELING OF THE SELF ASSEMBLY OF SURFACTANTS: SHAPE TRANSITIONS AND CRITICAL MICELLE CONCENTRATIONS
Asfaw Gezae Daful
ISBN:/DL:T. 1024-2011



random walk, the random walker has a prefect memory and never returns to a visited site.

There are a number of methods of generating sets of self-avoiding random walks. The simplest method is to generate a random walk on a cubic lattice and check at each step whether the walk is is self avoiding. If not, we throw away the walk we have generated up to that step. Otherwise we continue until we reach the desired length. It clear that due to self trapping it will be difficult to generate long walks. In this thesis we use a variant of this method, introduced by Rosenbluth and Rosenbluth[101] and often goes under the name of the Rosenbluth and Rosenbluth chain growth self-avoiding random walk algorithm. It goes as follows. After making the initial step the walker looks around to determine the number of nearest neighbor sites which up to to that moment it has not visited. It then randomly chooses one of these sites and moves to that site. In this way the walker continues until it has reached a site from where it can no longer continue (dead end) or until it has reached the maximum number of steps one wants to make. In this way we generate a set of self-avoiding random walk. One has to realize that in this way not all self-avoiding random walks of a given length are created with the same probability. Consider the two self-avoiding random walks of five steps shown in Fig. 3.3, in square lattice. The fourth step of the walk on the left can only choose between two possibilities to continue, whereas the walk to the right can choose between three possibilities. For a surfactant molecule, $H_xT_y$,

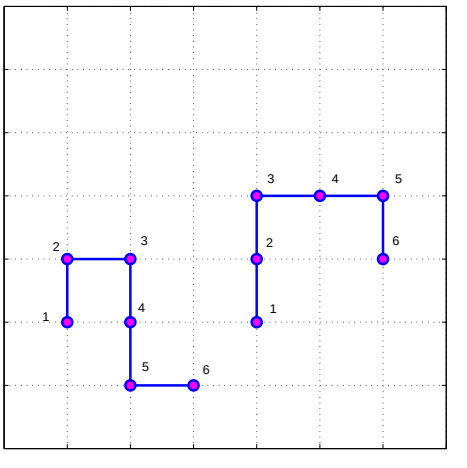


**Figure 3.3:** Growth of a self-avoiding random walk

Where $x$, and $y$ stand for the segment length of the head and tail part of the surfactant. We generate the amphiphile configurations using the Rosenbluth and

UNIVERSITAT ROVIRA I VIRGILI
MICROSCOPIC MODELING OF THE SELF ASSEMBLY OF SURFACTANTS: SHAPE TRANSITIONS AND CRITICAL MICELLE CONCENTRATIONS
Asfaw Gezae Daful
ISBN:/DL:T. 1024-2011



Rosenbluth chain growth algorithm as follows:

1. the first tail bead is randomly inserted in the simulation box
2. a new bead is randomly placed at one of the neighbor sites of the previous bead subjected to the self-avoidance condition and periodic boundary conditions
3. similarly, the next bead is also placed at one of the neighbor sites of the previous bead subject to the self-avoidance condition and periodic boundary conditions. This step is repeated for all beads up to the $(n_T + n_H)^{th}$ head bead

Where $n_T$, and $n_H$ stand for the segment length of the tail and head part of the surfactant, respectively. The overall Rosenbluth weight factor of a chain is calculated from the partial weight of each monomer, obtained in the generation of the chain,

$$W(\alpha) = \prod_{i=1}^{x+y} w_{\alpha,i} \tag{3.49}$$

The partial Rosenbluth weight of each monomer, $i$, is given by the total number of unoccupied neighbor sites of that monomer denoted as $n_u$ divided by the maximum possible number of unoccupied neighbor sites $(z-1)$, where $z$ is the coordination number, $z = 26$

$$w_{\alpha,i} = \frac{n_u}{z-1} \tag{3.50}$$

the Rosenbluth weight of the first monomer is $w_{\alpha,1} = 1$

## 3.8 Micellar Structure and Shape

### 3.8.1 The Packing Parameter

Amphiphilic molecules have both hydrophilic and hydrophobic characteristics. When the concentration of these molecules in a solution is raised above the critical micelle concentration (CMC), the molecules can reduce their free energy by assembling into aggregated structures. Below the CMC, the entropy of mixing dominates

UNIVERSITAT ROVIRA I VIRGILI
MICROSCOPIC MODELING OF THE SELF ASSEMBLY OF SURFACTANTS: SHAPE TRANSITIONS AND CRITICAL MICELLE CONCENTRATIONS
Asfaw Gezae Daful
ISBN:/DL:T. 1024-2011



and the surfactant molecules simply form single dispersed solution. By aggregating, the hydrophobic tail groups are largely able to avoid the unfavorable surface energies associated with contacting the water molecules. Micelles are the simplest form of self-assembled structure. In these structures, the surfactant molecules are arranged with the tail in the center, core, and the head groups around the surface forming a corona of the micelle. The size and shape of the aggregates are determined by the characteristics of the surfactant molecules that form them and their solution conditions[3]. We will briefly show how the optimum head group area and tail length can be expressed as a dimensionless packing parameter.

#### 3.8.1.1 Optimal Head group Area

The driving forces for self-assembly of amphiphilic chains are attractive and repulsive forces [1, 102, 103]. The hydrophobic attraction force at the hydrophobic-water interface, induces the chains to aggregate so as to reduce the tail-water contact. The hydrophilic repulsion between head groups due to various contributions, such as electrostatic, steric, and hydration forces. If the head groups are forced too closely together they will repel each other and on the other hand, if they are too far apart, this forces the hydrophobic tails to come into contact with water, energetically unfavorable. A balance between these two factors gives rise to the optimum head group area, $a_o$.

#### 3.8.1.2 Packing Characteristics

Aggregate structures have a lower energy than the non-aggregated surfactant molecules in solution. The molecular geometry, however, determines the actual shape of the aggregate. The analysis of molecular packing characteristics is facilitated with the use of the dimensionless packing parameter. Israelachvili [1] proposed the concept of molecular packing parameter and demonstrated how the size and the shape of the aggregate at equilibrium can be predicted from a combination of molecular packing considerations and general thermodynamic principles. The molecular packing parameter is defined as

$$P = \frac{v}{al_c} \tag{3.51}$$

where $v$ is the volume of the hydrophilic chain, $a$ is the surface area of the hydrophobic core of the aggregate expressed per molecule in the aggregate (optimal

[3] surfactant concentration, temperature and other physicochemical parameters

UNIVERSITAT ROVIRA I VIRGILI
MICROSCOPIC MODELING OF THE SELF ASSEMBLY OF SURFACTANTS: SHAPE TRANSITIONS AND CRITICAL MICELLE CONCENTRATIONS
Asfaw Gezae Daful
ISBN:/DL:T. 1024-2011



head group area), and $l_c$ is the critical length of the surfactant tail, as shown in Fig. 3.4. The critical length of hydrophobic chain is the longest effective length that the chain can be stretched. It is slightly less than the actual length of the chain due to the bond length and angles[1].

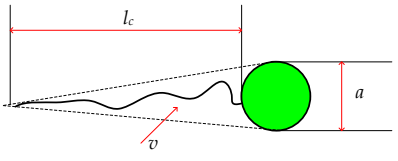


**Figure 3.4:** Schematic representation of surfactant geometry

The packing parameter can be thought of a measure of the curvature of the molecular aggregate. It is the ratio of the tail volume to the volume projected by the optimal head group area. A small packing factor indicates a small tail connected to a large head, and a larger packing parameter indicates a large tail connected to a smaller head. So, small packing paraments lead to highly curved aggregates, like spheres, while larger packing paraments lead to aggregates with less curvature like bilayers. If we consider a spherical micelle with a core radius $r$, made up of $N$ surfactant molecules, then the volume of the core $V = Nv = \frac{4\pi r^3}{3}$, the surface area of the core $A = Na = 4\pi r^2$, and hence,from simple geometrical relations $r = \frac{3v}{a}$. If the core of the micelle is packed with only surfactant tails without any empty space, then the radius $r$ cannot exceed the extended length of the critical length, $l_c$ of the tail. Introducing this constraint in the expression for $r$, one obtains $0 \leq \frac{v}{al_c} \leq \frac{1}{3}$, for spherical micelles.

For spherical, cylindrical or bilayer aggregates made up of $N$ surfactant molecules, the geometrical relations for the volume $V$ and the surface area $A$ are summarized in the following table 3.1. The variables $V$, $A$, and $N$ in the table refer to the entire spherical micelle, unit length of a cylindrical micelle, or unit area of a bilayer aggregate, respectively, for the three shapes. These geometrical relations, together with the constraint that at least one dimension of the aggregate (the radius of the sphere or the cylinder, or the half-bilayer thickness, all denoted by $r$) cannot exceed $l_c$, lead to the following relationship between the packing parameters and aggregate shapes[1, 104]: $0 \leq \frac{v}{al_c} \leq \frac{1}{3}$ for the sphere, $\frac{1}{3} \leq \frac{v}{al_c} \leq \frac{1}{2}$ for the cylinder, and $\frac{1}{2} \leq \frac{v}{al_c} \leq 1$ for the bilayer. Therefore, if we know the molecular packing parameter, the shape and size of the equilibrium aggregate can be readily identified as shown below.

UNIVERSITAT ROVIRA I VIRGILI
MICROSCOPIC MODELING OF THE SELF ASSEMBLY OF SURFACTANTS: SHAPE TRANSITIONS AND CRITICAL MICELLE CONCENTRATIONS
Asfaw Gezae Daful
ISBN:/DL:T. 1024-2011



**Table 3.1:** Geometric relations for Sphere, Cylinder and Bilayer types of aggregates

| Variable | Sphere | Cylinder | Bilayer |
|---|---|---|---|
| Aggregate core Volume $V = Nv$ | $\frac{4\pi r^3}{3}$ | $\pi r^2$ | $2r$ |
| Surface area of the core $A = Na$ | $4\pi r^2$ | $2\pi r$ | 2 |
| area per molecule, $a$ | $\frac{3v}{r}$ | $\frac{2v}{r}$ | $\frac{v}{r}$ |
| packing parameter | $\frac{v}{al_c} \leq \frac{1}{3}$ | $\frac{v}{al_c} \leq \frac{1}{2}$ | $\frac{v}{al_c} \leq 1$ |
| Maximum aggregation number $N_{max}$ | $\frac{4\pi l_c^3}{3v}$ | $\frac{\pi l_c^2}{v}$ | $\frac{2l_c}{v}$ |
| Aggregation number, $N$ | $N_{max}(\frac{3v}{al_c})^3$ | $N_{max}(\frac{2v}{al_c})^2$ | $N_{max}(\frac{v}{al_c})$ |

Noting that it is not possible to form a micelle with $r > l_c$, table 3.1, shows that as long as the packing parameter, $(\frac{v}{a_o l_c})$ is less than $\frac{1}{3}$ for sphere, or less than $\frac{1}{2}$ for cylinder, it will be possible for the actual area, $a$ to be equal to the most optimal areas. For packing parameters greater than $\frac{1}{3}$ (sphere), and greater than $\frac{1}{2}$ (cylinder), the actual area would be larger than optimum and these structures would be energetically unfavored.

UNIVERSITAT ROVIRA I VIRGILI
MICROSCOPIC MODELING OF THE SELF ASSEMBLY OF SURFACTANTS: SHAPE TRANSITIONS AND CRITICAL MICELLE CONCENTRATIONS
Asfaw Gezae Daful
ISBN:/DL:T. 1024-2011

# Chapter 4

# Single Chain Mean Field Theory and Monte Carlo Simulation

## 4.1 Introduction

In this chapter we will show the Lattice model description for model surfactant systems. Two dimensional Single Chain Mean Field Theory (2D-SCMFT) will be presented for Lattice model with no *priori* assumption or restriction on the shape of the micelle followed by a Single Chain Mean Field Theory in continuous space. This 2D-SCMFT along with three dimensional lattice Monte Carlo simulations are used to study the shape transitions of micelles.

## 4.2 Lattice Model Description

Surfactants form micelles in water solution because of the hydrophobic effect [65, 66]. The configurational entropy of water is significantly lowered by contact with hydrophobic solutes because the number of ways the water molecules can make hydrogen bond with neighboring water molecules is reduced in the presence of a solute molecule. This effect can dominate all other contributions to the total free energy of the system. As a result, hydrophobic solutes in water are driven

UNIVERSITAT ROVIRA I VIRGILI
MICROSCOPIC MODELING OF THE SELF ASSEMBLY OF SURFACTANTS: SHAPE TRANSITIONS AND CRITICAL MICELLE CONCENTRATIONS
Asfaw Gezae Daful
ISBN:/DL:T. 1024-2011



to aggregate in order to minimize the surface area of the solutes in contact with water, and hence minimize the total system's free energy. Larson completed the first simulation studies of surfactants on a lattice using an effective Hamiltonian to mimic the consequences of the hydrophobic effect, without having to model the solvent explicitly [49, 52, 86].

In the present work we used a three-dimensional lattice model [46, 49, 52, 86] with periodic boundary conditions to mimic the properties of bulk systems. The same model is used for Monte Carlo simulation and for the Single Chain Means Field Theory simulations in a Lattice model. In this model, space is divided into a cubic lattice of sites that interact equally with their nearest or diagonally-nearest neighbor sites, and do not interact with other sites. This gives a lattice with a coordination number of 26. A lattice site can be occupied by one of the three types of beads: solvent (S); head (H); or tail (T). All beads lie on a cubic lattice, allowing bonds to have any of the 26 following orientations: $(\pm 1, 0, 0)$, $(0, \pm 1, 0)$, $(0, 0, \pm 1)$, $(\pm 1, \pm 1, 0)$, $(\pm 1, 0, \pm 1)$, $(0, \pm 1, \pm 1)$, and $(\pm 1, \pm 1, \pm 1)$. This implies that bond-lengths were not constant in the simulation, but they were allowed to fluctuate between 1, $\sqrt{2}$ and $\sqrt{3}$. We considered an $L \times L \times L$ array of lattice volumes completely occupied by water and surfactant molecules, where $L$ is the box size.

The system studied is a binary mixture of amphiphilic and solvent molecules. We model the amphiphilic molecules as a chain of freely connected segments, each of which occupies one lattice site, whereas the solvent molecules are modeled as single sites. We refer to the amphiphilic molecules as $\mathrm{H}_x\mathrm{T}_y$, where $x$ and $y$ represent the number of segments in the head, H, and tail, T, groups of the surfactant respectively. In this model the amphiphile molecules $\mathrm{H}_x\mathrm{T}_y$ of length $(x + y - 1)$ consists of $x$ hydrophilic heads (H) and $y$ hydrophobic tails (T) connected by $(x + y - 1)$ bonds. We consider $N$ of such amphiphiles which occupy $(x + y)N$ lattice sites. The remaining, $N_w = L^3 - (x+y)N$, sites are occupied by the solvent particles. The excluded volume and periodic boundary conditions are used to mimic bulk conditions and to allow us to fix the number of particles in the canonical, $(NVT)$ ensemble.

The amphiphilic nature of the surfactant molecule is defined by the different types of interactions among H, T, and solvent, S molecules. The interaction between a pair of neighboring units contributes a specified amount of energy to the total energy of the system. For the surfactant-solvent model, the various interaction energies considered are: $\epsilon_{TT}$, $\epsilon_{HH}$, $\epsilon_{SS}$, $\epsilon_{TH}$, $\epsilon_{TS}$ and $\epsilon_{HS}$, for the tail-tail, head-head, solvent-solvent, tail-head, tail-solvent and head-solvent interacting nearest neighbor or diagonal nearest neighbor contacts respectively. The total energy in $k_BT$ of the system is then given by:

UNIVERSITAT ROVIRA I VIRGILI
MICROSCOPIC MODELING OF THE SELF ASSEMBLY OF SURFACTANTS: SHAPE TRANSITIONS AND CRITICAL MICELLE CONCENTRATIONS
Asfaw Gezae Daful
ISBN:/DL:T. 1024-2011



$$E[\Lambda] = N_{TT}(\Lambda)\epsilon_{TT} + N_{HH}(\Lambda)\epsilon_{HH} + N_{SS}(\Lambda)\epsilon_{SS} + N_{TH}(\Lambda)\epsilon_{TH} + N_{TS}(\Lambda)\epsilon_{TS} + N_{HS}(\Lambda)\epsilon_{HS} \tag{4.1}$$

where $N_{TT}$, $N_{HH}$, $N_{SS}$, $N_{TH}$, $N_{TS}$ and $N_{SH}$ are the total number of tail-tail, head-head, solvent-solvent, tail-head, tail-solvent and head-solvent contacts in configuration $\Lambda$.

It is considered that the head part interacts with the same potential as the solvent monomer sites. We suppose that this amount of energy is independent of the orientation of the pair, and the value is same for all nearest and diagonally nearest neighbor contact. Thus, as the solvent and the hydrophilic head part of the surfactant interacts with the same potential. We considered here both (the hydrophilic head and the solvent) as essentially H-type monomers. The interaction energy of an H-type site belonging to a solvent or the hydrophilic head of a surfactant interacts with another H-type site is denoted by $\epsilon_{HH}$. So equation Eq. (4.1) can be rewritten as

$$E[\Lambda] = N_{TT}(\Lambda)\epsilon_{TT} + N_{HH}(\Lambda)\epsilon_{HH} + N_{TH}(\Lambda)\epsilon_{TH} \tag{4.2}$$

The relationships between the number of interactions $N_{TT}$, $N_{HH}$, $N_{TH}$, of a total, $N_a$, amphiphilic molecules of connected sites of $n_H$ hydrophilic head beads and $n_T$ hydrophobic tail beads, and $N_s$ solvent molecules can be described as

$$N_{HH} = \frac{zN_H - N_{TH}(\Lambda)}{2} \tag{4.3}$$

$$N_{TT} = \frac{zN_T - N_{TH}(\Lambda)}{2} \tag{4.4}$$

where $z$ is the coordination number, ($z = 26$), of the lattice; and the total number of sites of H-type monomer is, ($N_H = N_a n_H + N_s$), and that of tail bead is, ($N_T = N_a n_T$). Substituting these equations, Eqs. (4.3 and 4.4) into equation Eq.(4.2), gives the total energy of the configuration,

$$E[\Lambda] = \frac{z}{2}\Big(N_T\epsilon_{TT} + N_H\epsilon_{HH}\Big) + N_{TH}[\Lambda]\Big(\epsilon_{HT} - \frac{1}{2}(\epsilon_{HH} + \epsilon_{TT})\Big) \tag{4.5}$$

The partition function, $Q$, of the canonical ensemble, ($NVT$) can then be defined by summing the Boltzmann factor of the set of energies for the system of, ($N_a(n_H + n_T) + N_s$), lattice sites

UNIVERSITAT ROVIRA I VIRGILI
MICROSCOPIC MODELING OF THE SELF ASSEMBLY OF SURFACTANTS: SHAPE TRANSITIONS AND CRITICAL MICELLE CONCENTRATIONS
Asfaw Gezae Daful
ISBN:/DL:T. 1024-2011



$$Q(N,V,T) = \sum_{\{\Lambda\}} exp\Big(-\beta E[\Lambda]\Big) \tag{4.6}$$

where $\beta = \frac{1}{k_B T}$, $k_B$ and $T$, being the Boltzmann's constant and temperature respectively. Substituting Eq. (4.5) in to Eq. (4.6), gives

$$Q(N,V,T) = \sum_{\{\Lambda\}} exp\Bigg(-\beta\bigg[\frac{z}{2}(N_T\epsilon_{TT}+N_H\epsilon_{HH})+N_{TH}[\Lambda](\epsilon_{HT}-\frac{1}{2}(\epsilon_{HH}+\epsilon_{TT}))\bigg]\Bigg) \tag{4.7}$$

From Eq.(4.7), we can see that only the second term depends on the conformation, and the first term is constant for a system considered and can be taken out of the summation

$$Q(N,V,T) = Constant \times \sum_{\{\Lambda\}} exp\Big(-\beta N_{TH}[\Lambda][\epsilon_{HT} - \frac{1}{2}(\epsilon_{HH} + \epsilon_{TT})]\Big) \tag{4.8}$$

In this type of models, there is only one independent, relevant, interaction energy parameter for each pair of interaction, Eq. 4.9.

$$\varepsilon = \epsilon_{HT} - \frac{1}{2}\epsilon_{HH} - \frac{1}{2}\epsilon_{TT} \tag{4.9}$$

Furthermore, we define the dimensionless temperature, $T^* = \frac{k_B T}{\varepsilon}$. In this work $\epsilon_{TT}$ is set to $-2$ (resulting in attractive interactions for nearest-neighbor tail-tail contact) [5, 46, 47, 54, 55] , and $\epsilon_{HH}$ and $\epsilon_{HT}$ are arbitrarily set to zeroin order to simplify the single chain mean field theory equations given in the following section. The total energy can therefore be expressed as follows

$$E[\Lambda] = \frac{z}{2}\Big(N_T\epsilon_{TT} + N_H\epsilon_{HH}\Big) + N_{TH}[\Lambda]\varepsilon \tag{4.10}$$

Since the number of each bead (S, H, and T) in the lattice is constant the first term is also constant, thus only the second term represents a thermodynamically relevant change in the energy.

UNIVERSITAT ROVIRA I VIRGILI
MICROSCOPIC MODELING OF THE SELF ASSEMBLY OF SURFACTANTS: SHAPE TRANSITIONS AND CRITICAL MICELLE CONCENTRATIONS
Asfaw Gezae Daful
ISBN:/DL:T. 1024-2011



## 4.3 Single Chain Mean Field Theory

A Single Chain Mean Field Theory, SCMFT [5, 44–46, 55] is used for modeling and studying the surfactant and polymer systems in a lattice and continuous space. In SCMFT, a set of all possible chain conformations are generated as a self-avoiding random walk. This set is then weighted in the molecular mean-field. This approach avoids the random-walk statistics used by the Self Consistent Field, SCF, theory [37, 41–43, 96–100]. SCMFT is a molecular mean-field model which is numerically solved as a self-consistent solution. So, even though the *intra-molecular* interactions can be treated '*exactly*', the *intermolecular* interactions are treated on a *mean-field* level. SCMFT deals with the equilibrium distribution of chain molecules in space and the resulting thermodynamic quantities of the system. The theory is formulated in terms of thermodynamic properties and a molecular field, which is associated with the chain molecule. These properties are functions of the molecular fields and vice versa, so at equilibrium these thermodynamic properties and the molecular fields are self-consistent. The molecular fields are varied numerically until a SCMF solution is found.

The Single Chain Mean Field Theory is a chain based technique where explicit molecular conformations and the mean field variables are considered, *i.e.*, it exactly accounts for the configurations of a single microscopically detailed chain at the molecular level. It was originally developed to study the molecular organization of amphiphilic tails in dry core aggregates and later generalized to include solvent molecules [44, 45]. The implementation of the theory for surfactant self-assembly without the dry core restriction was presented for lattice chains by Mackie et al. [46]. In SCMFT simulation we regard the evolution of an ensemble of chains in external fluctuating field. These external fields mimic the instantaneous interactions of the chains with their surroundings. The interactions between different chains are described through a mean molecular field which is found self-consistently. Thus SCMFT is based on looking at a central chain with all its intramolecular interactions explicitly taking into account, while the interactions of this chain with the other surrounding amphiphilic and solvent molecules (intermolecular interactions) are taken within a mean-field approximation. The intermolecular mean-field interactions are inhomogeneous as the micellar aggregate is clearly inhomogeneous. It is derived by determining the probability distribution function of the chain conformations and the distribution of solvent molecules within the aggregate by functional minimization of the aggregate's total free energy. The calculation of the probability distribution function, $P(\alpha_j)$, (Eq. (3.29)) is thus, the central objective of the Single Chain Mean Field Theory. Once the probability distribution function is known, any thermodynamic property of interest of the micellar aggregate can

UNIVERSITAT ROVIRA I VIRGILI
MICROSCOPIC MODELING OF THE SELF ASSEMBLY OF SURFACTANTS: SHAPE TRANSITIONS AND CRITICAL MICELLE CONCENTRATIONS
Asfaw Gezae Daful
ISBN:/DL:T. 1024-2011



be obtained. The starting point of the SCMFT is to consider that all amphiphilic molecules are equivalent so that the state of the system is completely characterized by the knowledge of the singlet configurational probability distribution. In the next two sections we will describe the SCMFT in lattice and continuous space.

### 4.3.1 SCMFT in Lattice Space

A Single Chain Mean Field Theory have been used to study micellization process and its equilibrium properties in one dimensional lattice system[5, 46, 55], where the mean-field lattice discretization into concentric spherical or cylindrical shells (see sections (5.2.1) and (5.3.1)) by which micelles of spherical and infinitely long cylindrical micelles were dealt with.

Here we present the two dimensional description of Single Chain Mean Field Theory, with no pre-assumption on the micellar shapes to be formed. This gives the freedom for the system, not only to form aggregates of any geometric shape that satisfies the thermodynamic conditions of the micellar solution, but also to undergo morphological transformations upon changing solution conditions.

The mean field is divided into $Z_l$ slices (layers) along the $z$-*axis* and $N_c$ concentric shells of radii $r$ in the $x$-$y$ plane (see Fig.4.1). The packing constraints (single occupancy, *i.e.*, no two beads or segments of the surfactant or solvent molecule can occupy the same lattice site), or repulsive interactions, are given by the fact that the sum of average volume fractions of the head, tail and the solvent is unity.

$$\langle\phi_S(r,z)\rangle + \langle\phi_T(r,z)\rangle + \langle\phi_H(r,z)\rangle = 1 \tag{4.11}$$

where $\phi_S$, $\phi_H$ and $\phi_T$ are volume fractions of solvent, head and tail part of the surfactant respectively. The mean field average volume fractions of head and tail segments are obtained from their mean field average distributions, given by equations Eqs. (4.12 and 4.13).

$$\langle\phi_H(r,z)\rangle = \frac{N}{V(r,z)}\langle n_H(r,z)\rangle \tag{4.12}$$

$$\langle\phi_T(r,z)\rangle = \frac{N}{V(r,z)}\langle n_T(r,z)\rangle \tag{4.13}$$

where $V(r,z)$ is the total volume of layer $z$ and shell $r$, $N$ is the number of chains in the system, and the angle brackets, $\langle ...\rangle$, indicate mean field properties

UNIVERSITAT ROVIRA I VIRGILI
MICROSCOPIC MODELING OF THE SELF ASSEMBLY OF SURFACTANTS: SHAPE TRANSITIONS AND CRITICAL MICELLE CONCENTRATIONS
Asfaw Gezae Daful
ISBN:/DL:T. 1024-2011



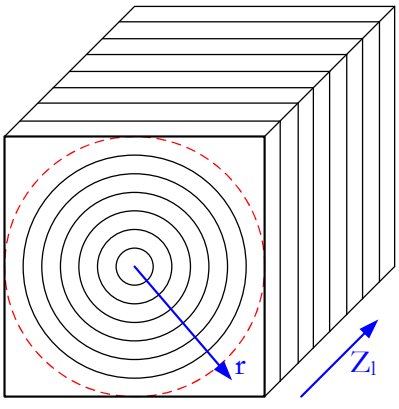


**Figure 4.1:** Discretization of the mean field into $N_c$ concentric circular shells of radius $r$ and $Z_l$ layers or slices in a 2D cylindrical fields. Lattice sites in the corners of the box are included with those of the last shell.

over the probability distribution function, $P(\alpha)$, of the chain conformations. The mean field approximation of the distribution of tail and head segments on shell $r$ and layer $z$ are respectively given by, Eq. (4.14) and Eq. (4.15)

$$\langle n_T(r,z)\rangle = \sum_{\alpha} P(\alpha) n_T(\alpha,r,z) \tag{4.14}$$

$$\langle n_H(r,z)\rangle = \sum_{\alpha} P(\alpha) n_H(\alpha,r,z) \tag{4.15}$$

where $n_T(\alpha,r,z)$ and $n_H(\alpha,r,z)$ are the number of tail and head group distributions per amphiphile per shell $r$ and layer $z$ respectively. $P(\alpha)$ is the probability distribution of a chain conformation, $\alpha$.

The attractive contribution to the interaction energy is considered to be the intramolecular attractive interaction per chain in the aggregate, Eq. (4.16)

$$\langle E_{intra}\rangle = \epsilon_{TT} \sum_{\alpha} P(\alpha) n_{TT}^{intra}(\alpha) \tag{4.16}$$

where $n_{TT}^{intra}(\alpha)$ is the intramolecular nonbonded tail-tail interactions of conformation $\alpha$, that is calculated exactly in the generation of the set of single chain

UNIVERSITAT ROVIRA I VIRGILI
MICROSCOPIC MODELING OF THE SELF ASSEMBLY OF SURFACTANTS: SHAPE TRANSITIONS AND CRITICAL MICELLE CONCENTRATIONS
Asfaw Gezae Daful
ISBN:/DL:T. 1024-2011



configurations and the average number of intramolecular tail-tail contacts per chain can be written as

$$\left\langle n_{TT}^{intra} \right\rangle = \sum_{\alpha} P(\alpha) n_{TT}^{intra}(\alpha) \tag{4.17}$$

where the summation is taken over the set of all possible chain configurations.

The intermolecular interaction term, the interaction of the central chain with its surrounding, is written in a mean-field approximation. Namely, we take the probability of having a neighboring site to a tail segment of the central chain occupied by a tail segment of another chain, be given by the average local density of tail segments. This is nonlocal since the average density of segments is inhomogeneous in both $r$ and $z$ directions. Thus, the intermolecular attractive contribution can be written as Eq. (4.18)

$$\langle E_{inter} \rangle = \frac{\epsilon_{TT}}{2} \sum_{z} \sum_{r} \langle n_{n,T}(r,z) \rangle \langle \phi_T(r,z) \rangle \tag{4.18}$$

where $\langle n_{n,T}(r,z) \rangle$ is the average number of empty nearest neighbor contacts in a given layer $z$ and shell $r$, *i.e.*, the mean field approximation for the average number of solvent molecules in contact with a tail bead. The division by a factor of 2 in Eq. (4.18) fixes the double counting in the chain-chain contacts.

The entropy of the aggregate is needed to determine the aggregates free energy. It contains two contributions, the conformational entropy of the amphiphiles and the translational entropy of the solvent molecules, and is given by Eq. (4.19).

$$\frac{S}{k_B} = -N \sum_{\alpha} P(\alpha) \ln P(\alpha) - \sum_{z} \sum_{r} n_S(r,z) \ln \phi_S(r,z) \tag{4.19}$$

where $\phi_S(r,z)$ is the volume fraction of the solvent and $n_S$ is the number of solvent sites at layer $z$ and shell $r$. The configurational free energy of the aggregate is then given by, Eq. (4.20).

$$\frac{F}{k_B T} = \beta N \Big[ \langle E_{inter} \rangle + \langle E_{intra} \rangle \Big] - \frac{S}{k_B} - \beta \sum_{z} \sum_{r} n_S(r,z) \mu_S \tag{4.20}$$

The aggregate is considered to be in contact with a bath of pure solvent of chemical potential $\mu_S$. The first two terms of Eq. (4.20) are the energetic and entropic contributions, whose sum is the Helmholtz free energy. The probability

UNIVERSITAT ROVIRA I VIRGILI
MICROSCOPIC MODELING OF THE SELF ASSEMBLY OF SURFACTANTS: SHAPE TRANSITIONS AND CRITICAL MICELLE CONCENTRATIONS
Asfaw Gezae Daful
ISBN:/DL:T. 1024-2011



distribution function, $P(\alpha)$, and solvent density profile, $\phi_S(r,z)$, are found by functional minimization of the free energy Eq. (4.20), subject to the packing constraints, Eq. (4.11). This functional minimization is carried out by introducing the set of Lagrange multipliers, $\pi(r,z)$, to give the probability distribution function, $P(\alpha)$,

$$P(\alpha) = \frac{e^{-\mathcal{H}[\alpha]}}{\sum_\alpha e^{-\mathcal{H}[\alpha]}} \tag{4.21}$$

Where $\mathcal{H}[\alpha]$ is the mean field Hamiltonian, given by

$$\begin{aligned}\mathcal{H}[\alpha] = &\sum_z \sum_r \pi(r,z)\Big[n_H(\alpha,r,z) + n_T(\alpha,r,z)\Big] \\ &+ \chi_{TT} n_{TT}^{intra}(\alpha) \\ &+ \frac{\chi_{TT}}{2}\sum_z\sum_r \frac{N-1}{V(r,z)}\Big[n_{n,T}(\alpha,r,z)\langle n_T(r,z)\rangle \\ &+ \langle n_{n,T}(r,z)\rangle n_T(\alpha,r,z)\Big]\end{aligned} \tag{4.22}$$

We define the dimensionless interaction parameter $\chi_{TT} = \beta\epsilon = \frac{\epsilon}{T^*}$, where $\beta = 1/k_BT$ and $\epsilon$ is the relevant interaction energy parameter given by Eq. (4.9), and $T^*$ is the dimensionless temperature parameter. The SCMFT gives rules for how to compute the probability distribution function of the chain conformations and the distribution of solvent molecules within the aggregate by functional minimization of the aggregate's free energy subject to the lattice single site occupancy constraint, for all $r$ and $z$, Eq. (4.11). Once the probability distribution function is known, any thermodynamic property of interest of the micellar aggregate can be obtained from the $P(\alpha)$ values, as well as the structure of the micelle can be determined from the volume fraction profiles.

The solvent volume fraction profile is given by

$$\phi_S(r,z) = exp\left[-\pi(r,z) + \mu_S\right] \tag{4.23}$$

where the thermodynamic equilibrium condition that the chemical potential of the solvent, $\mu_S$, must be constant at all $r$ and $z$ has been introduced. The expression for the solvent density profile gives us the physical interpretation of the

Lagrange multipliers. They are the osmotic pressures necessary to keep the chemical potential of the solvent constant at all shells $r$ and layers $z$. The expressions for the solvent volume fraction profile and the probabilities can be substituted back into the free energy expression, Eq. (4.20), to obtain

$$\begin{aligned}\frac{F}{k_BT} = &-\chi_{TT}\frac{(N-1)}{2}\sum_z\sum_r \langle n_{n,T}(r,z)\rangle \langle n_T(r,z)\rangle - N\ln q \\ &-\sum_z\sum_r \pi(r,z)V(r,z)\end{aligned} \tag{4.24}$$

where $q$ is the normalization constant, the single chain partition function given by

$$q = \sum_\alpha e^{-\mathcal{H}[\alpha]} \tag{4.25}$$

that ensures $\sum_\alpha P(\alpha) = 1$ in Eq. (4.21), where the sum is taken over the set of all possible chain configurations. What remains is to determine the Lagrange multipliers $\pi(r,z)$. In order to do this, we substitute the explicit form of the probability distribution function, Eq. (4.21), and that of the solvent density profile, Eq. (4.23), into the constraint equations, Eq. (4.11), and obtain:

$$\sum_\alpha \left\{ P(\alpha)\frac{N}{V(r,z)}\left[n_H(\alpha,r,z) + n_T(\alpha,r,z)\right]\right\} + e^{-\pi(r,z)} = 1 \qquad \forall_{r,z} \tag{4.26}$$

which is a set of nonlinear self-consistent equations that can be solved by standard numerical methods.

The thermodynamic parameter that determines the equilibrium between micelles and free amphiphiles in solution, and the distribution between micelles of different sizes is the difference between the standard chemical potential of a amphiplile molecule in a micellar aggregate of size $N$, $\mu_N^o$, and the corresponding quantity for the free amphiphiles in the bulk solution, $\mu_1^o$. The difference in standard chemical potential between free amphiphilic chains and those self-assembled into aggregates of size $N$, is given by:

UNIVERSITAT ROVIRA I VIRGILI
MICROSCOPIC MODELING OF THE SELF ASSEMBLY OF SURFACTANTS: SHAPE TRANSITIONS AND CRITICAL MICELLE CONCENTRATIONS
Asfaw Gezae Daful
ISBN:/DL:T. 1024-2011



$$exp\left(-\frac{\mu_N^o-\mu_1^o}{k_BT}\right)\approx\frac{V}{N}\frac{\sum_\alpha exp\left(-\frac{\mathcal{H}_N[\alpha]}{k_BT}\right)/W(\alpha)}{\sum_\alpha exp\left(-\frac{\mathcal{H}_1[\alpha]}{k_BT}\right)/W(\alpha)} \tag{4.27}$$

where $\mathcal{H}_N[\alpha]$ and $\mathcal{H}_1[\alpha]$ are the mean field Hamiltonian of surfactants in a micelle of size $N$ and free surfactants in the bulk solution, $k_B$ is the Boltzmann constant, $T$ is the temperature, $V$ is total volume of simulation box, and $N$ is total number of surfactant molecules in the system. The sum is over a given sample with conformations distributed with statistical weight, $W(\alpha)$, which here is the weight associated with the Rosenbluth and Rosenbluth algorithm[101] used in generating the chain, as shown in Eq. (3.49).

The Single Chain Mean Field Theory is applied to study the thermodynamic and structural properties of micellar aggregates. The information obtained is then used in the mass action model to determine the properties of the solution.

Solving the Single Chain Mean Field equations relies on a discretization scheme. The field is discretized according to the geometry of the system and the symmetry considerations. The mean field is discretized into $N_c$ concentric circular shells of radius $r$ in $x$-$y$ plane and $Z_l$ layers or slices along the $z$-$axiz$, as show in Fig. 4.1. Any property will be described in coordinates $(r, z)$. Lattice sites in the corners of the box are included with those of the last shell.

Same equations, Eqs. (4.11 – 4.26) are used for the one dimensional Single Chain Mean Field Theory case, except that all properties are considered only along their radial distribution. The mean field is discretized into concentric spherical shells of radii $r$ for spherical micelles, and into concentric cylindrical shells of radii $r$, see Fig. 4.2.

### 4.3.2 SCMFT in Continuous Space

The SCMFT for a lattice molecular model has proven to be able to quantitatively describe the self-assembly of amphiphilic systems. The predictions of the theory for equilibrium and thermodynamic properties were compared with Monte Carlo simulations and show an excellent quantitative agreements[46]. Here we want to develop the SCMFT in continuous space and compared the predicted results with experiments.

The first step of the SCMF calculations is the definition of a coarse-grained model of a molecule and the interaction of the coarse grained beads with the fields.

UNIVERSITAT ROVIRA I VIRGILI
MICROSCOPIC MODELING OF THE SELF ASSEMBLY OF SURFACTANTS: SHAPE TRANSITIONS AND CRITICAL MICELLE CONCENTRATIONS
Asfaw Gezae Daful
ISBN:/DL:T. 1024-2011



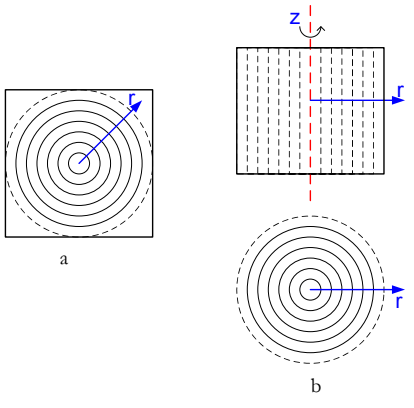


**Figure 4.2:** One dimensional discretization of the mean field into (a) concentric spherical shells and (b) concentric cylindrical shells of radius $r$.

The proper chain statistics is attained through the direct generation of the representative sampling of conformations $\Gamma$ of a single molecule. These conformations take into account the angles between the bonds, the orientations and positions of conformations in the simulation box. The free energy, $F$, of the system in a simulation box volume, $V$, containing, $N$, surfactants in the mean field approximation is given by

$$\frac{F}{Vk_BT} = \int c(\Gamma) \ln \frac{c(\Gamma)}{e} \Lambda^{3N} d\Gamma + \int \frac{d\mathbf{r}}{V} c_s(\mathbf{r}) \ln \frac{c_s(\mathbf{r})}{e} \Lambda_s^3 + \int c(\Gamma) u(\Gamma) d\Gamma \tag{4.28}$$

where $c_s(\mathbf{r})$ is the concentration of solvent molecules, the spatial integration is over the volume of the box $V$, while $\Lambda$ and $\Lambda_s$ are the de Broglie lengths of the beads of surfactant molecules and solvent, correspondingly. Since the correlations between the chains are decoupled, the distribution function of conformations $c(\Gamma)$ is related to the probability of a single molecule conformation $P(\Gamma)$, *via* $c(\Gamma) = NP(\Gamma)/V$. The function $u(\Gamma)$ represents the interaction potential of the conformation $\Gamma$ with the fields. The interactions of the beads inside a given conformation, $u_{intra}(\Gamma)$, can be decoupled from the interactions with the fields. Thus, $u(\Gamma)$ can be written as

$$u(\Gamma) = u_{intra}(\Gamma) + \frac{N-1}{2}\int \frac{d\mathbf{r}}{V} P(\Gamma')\widehat{u}(\Gamma,\Gamma',\mathbf{r})d\Gamma' + \int \frac{d\mathbf{r}}{V} c_s(\mathbf{r})\widetilde{u}(\Gamma,\mathbf{r}) \tag{4.29}$$

where $\widehat{u}(\Gamma,\Gamma',\mathbf{r})$ describes the interactions with the beads of other molecules of conformation $\Gamma'$ and $\widetilde{u}(\Gamma,\mathbf{r})$ describes the interactions with the solvent. The factor $1/2$ avoids double counting and $(N-1)$ is due to the separate intra-molecular part.

In the following, we consider a surfactant molecule comprised of only two types of beads: hydrophilic, H and hydrophobic, T. In the case of more complex structure, the equations are easily generalized. Introducing three interaction parameters: between hydrophobic beads and solvent, $\varepsilon_{TW}$, between hydrophilic beads and solvent, $\varepsilon_{HW}$ and between hydrophilic beads and hydrophobic beads, $\varepsilon_{HT}$, the interaction energy yields

$$\begin{aligned} u(\Gamma) = {} & u_{intra}(\Gamma) \\ & + \frac{N-1}{2}\varepsilon_{HT}\int d\mathbf{r}\left[\phi^H_{int}(\Gamma,\mathbf{r})\left\langle c_T(\mathbf{r})\right\rangle + \phi^T_{int}(\Gamma,\mathbf{r})\left\langle c_H(\mathbf{r})\right\rangle\right] \\ & + \varepsilon_{TW}\int d\mathbf{r}\phi^T_{int}(\Gamma,\mathbf{r})c_s(\mathbf{r}) + \varepsilon_{HW}\int d\mathbf{r}\phi^H_{int}(\Gamma,\mathbf{r})c_s(\mathbf{r}) \end{aligned} \tag{4.30}$$

where $\phi^H_{int}(\Gamma,\mathbf{r})$ and $\phi^T_{int}(\Gamma,\mathbf{r})$ are the interaction fields of each conformation in a given position in space. Since the conformations are generated prior to calculations, these properties, as well as the excluded volume of the conformation $\Gamma$ in a given position of space, $\phi_{ex}(\Gamma,\mathbf{r})$, are known exactly for each conformation. $\langle c_T(\mathbf{r})\rangle$ and $\langle c_H(\mathbf{r})\rangle$ are the average fields of concentrations of T and H, respectively. Average concentrations of each type of bead and the average volume fraction $\phi(\mathbf{r})$ are calculated as averages of the corresponding concentrations of the conformations as

$$\langle c_T(\mathbf{r})\rangle = \int P(\Gamma)c_T(\Gamma,\mathbf{r})d\Gamma \tag{4.31}$$

$$\langle c_H(\mathbf{r})\rangle = \int P(\Gamma)c_H(\Gamma,\mathbf{r})d\Gamma \tag{4.32}$$

$$\langle \phi(\mathbf{r})\rangle = \int P(\Gamma)\phi_{ex}(\Gamma,\mathbf{r})d\Gamma \tag{4.33}$$

UNIVERSITAT ROVIRA I VIRGILI
MICROSCOPIC MODELING OF THE SELF ASSEMBLY OF SURFACTANTS: SHAPE TRANSITIONS AND CRITICAL MICELLE CONCENTRATIONS
Asfaw Gezae Daful
ISBN:/DL:T. 1024-2011



In turn, the volume fraction of solvent is calculated from the incompressibility condition, applied locally as

$$\phi_s(\mathbf{r}) = 1 - N \langle \phi(\mathbf{r}) \rangle \tag{4.34}$$

The probabilities of the conformations $P(\Gamma)$ are found from the minimization of the free energy Eq. (4.28)

$$\frac{\delta F\{P(\Gamma)\}}{\delta P(\Gamma)} = 0 \tag{4.35}$$

subject to the incompressibility condition Eq. (4.34) by the way of the Lagrange multiplier, $\pi(\mathbf{r})$. This gives

$$P(\Gamma) = \frac{1}{Q} e^{-\mathcal{H}_{MF}(\Gamma)} \tag{4.36}$$

where $Q$ is the normalization factor, insuring

$$\int P(\Gamma) d\Gamma = 1 \tag{4.37}$$

and $\mathcal{H}_{MF}(\Gamma)$ is the Hamiltonian given by

$$\begin{aligned} \mathcal{H}_{MF}(\Gamma) &= u_{intra}(\Gamma) \\ &+ (N-1)\varepsilon_{HT} \int d\mathbf{r} \left[ \phi^H_{int}(\Gamma, \mathbf{r}) \langle c_T(\mathbf{r}) \rangle + \phi^T_{int}(\Gamma, \mathbf{r}) \langle c_H(\mathbf{r}) \rangle \right] \\ &+ \varepsilon_{TW} \int d\mathbf{r} \phi^T_{int}(\Gamma, \mathbf{r}) \frac{\phi_s(\mathbf{r})}{v_s} + \varepsilon_{HW} \int d\mathbf{r} \phi^H_{int}(\Gamma, \mathbf{r}) \frac{\phi_s(\mathbf{r})}{v_s} \\ &- \int d\mathbf{r} \frac{\phi_{ex}(\Gamma, \mathbf{r})}{v_s} \ln \phi_s(\mathbf{r}) \end{aligned} \tag{4.38}$$

Here we assume that the volume of the beads and the solvent are equal to $v_s$, (where $v_s$ is the molar volume of solvent water), hence, $\phi_s(\mathbf{r}) = c_s(\mathbf{r}) v_s$. The minimization with respect to the concentration of the solvent, $\delta F / \delta c_s(\mathbf{r}) = 0$, gives the Lagrange multiplier in the form $\pi(r) \approx -1/v_s \ln \phi_s(\mathbf{r})$. Since we assume the beads T and H are of the same size, the interactions T-H and H-T are symmetrical,

thus we have omitted $\int d\mathbf{r}(c_T(\Gamma,\mathbf{r})\left\langle\phi^H_{int}(\mathbf{r})\right\rangle + c_H(\Gamma,\mathbf{r})\left\langle\phi^T_{int}(\mathbf{r})\right\rangle)$ and multiplied the second term by 2.

The Equations, Eqs. (4.31 – 4.38) represent a closed set of non-linear equations, which can be solved iteratively. The mean molecular fields Eqs. (4.31 – 4.33) define the probability of each conformation Eq. (4.36) in the fields, while the values of mean fields are calculated as averages over the probabilities of conformations, closing the self-consistency loop. The solution of these equations gives the equilibrium distribution of the molecular fields, probabilities of the conformations, the molecular structure of the equilibrium aggregates, the average size of the aggregates and the equilibrium free energy.

## 4.4 Lattice Monte Carlo Simulation

### 4.4.1 Introduction

In the present work we used a three dimensional Monte Carlo simulation in a lattice model, as discussed in sections 3.7.2 and 4.2. The Metropolis Monte Carlo algorithm will be described followed by and Monte Carlo moves used in this work.

### 4.4.2 Metropolis Monte Carlo algorithm

A large number of chain configurations are generated using Rosenbluth and Rosenbluth chain growth algorithm [101]. From all of the possible configurations of the system, a starting configuration is randomly selected. The total energy of this initial configuration, denoted by $E_{old}$, is then calculated according to the previous energy parameters Eq. (4.10). This initial configuration is then altered by selecting a random surfactant chain and then moving it by Monte Carlo moves. The excluded volume interaction requires no more than one bead per lattice site. If any attempted move violates either the excluded volume or the bond length restriction (the bond length can have values of 1, $\sqrt{2}$ and $\sqrt{3}$), it is rejected. The acceptance or rejection of one attempted move, which satisfies both the excluded volume and the bond length conditions, is further governed by the Metropolis rule[46, 49, 86, 105]. The energy of the new, trial configuration, $E_{new}$, is calculated and it is accepted if the energy change ($\Delta E = E_{new} - E_{old}$) is negative; otherwise, it is accepted with a probability, $P_{acc}$ given by Eq. (3.48).

This procedure is continued until equilibrium is reached as it is necessary to ensure that the system is equilibrated before the sampling is started. The system

UNIVERSITAT ROVIRA I VIRGILI
MICROSCOPIC MODELING OF THE SELF ASSEMBLY OF SURFACTANTS: SHAPE TRANSITIONS AND CRITICAL MICELLE CONCENTRATIONS
Asfaw Gezae Daful
ISBN:/DL:T. 1024-2011



is considered to be in equilibrium when the total interaction energy of the system is almost constant over repeated Monte Carlo steps.

The simulations were initiated with a random configuration and $10^9$ Monte Carlo steps were applied in order to make sure that the systems were equilibrated (see Fig. 4.3). An additional $10^{11}$ steps were then used in order to calculate the average properties of the system.

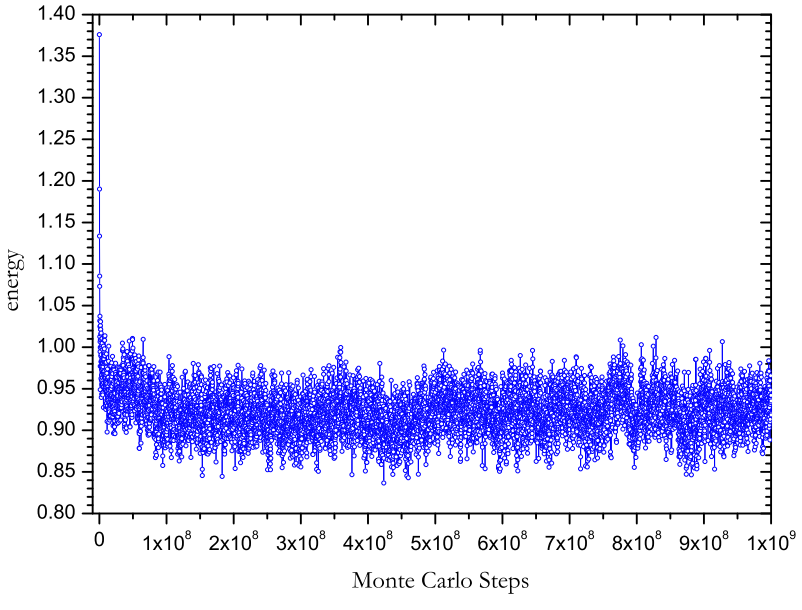


**Figure 4.3:** Equilibrated energy, in $k_BT$

### 4.4.3 Monte Carlo Moves

To implement the Metropolis Monte Carlo procedure described in section 4.4.2, for a particular system, one must decide how new system configurations will be generated from existing configurations. In the case of a Larson-type model [94, 106, 107] of a surfactant system, this means deciding how the surfactant chains will move on the lattice. Different chain moves have been reported for lattice and off lattice simulations. In this section we will describe the Monte Carlo moves used in this work.

UNIVERSITAT ROVIRA I VIRGILI
MICROSCOPIC MODELING OF THE SELF ASSEMBLY OF SURFACTANTS: SHAPE TRANSITIONS AND CRITICAL MICELLE CONCENTRATIONS
Asfaw Gezae Daful
ISBN:/DL:T. 1024-2011



#### 4.4.3.1 Chain Reptation

Reptation is based on a *slithering snake* algorithm where: (i) the terminal head or tail unit randomly moves to a nearest neighbor site. (ii) the second unit (attached to the terminal head or tail unit) moves forward to replace the original lattice position of the terminal head or tail unit. (iii) the third unit in the chain moves forward to replace the original lattice position of the second unit and the process repeats itself as it propagates along the length of the surfactant molecule. (iv) the displaced solvent molecule takes the place of the old terminal tail or head unit site. The end result is a one-lattice-site move by the whole surfactant in the randomly chosen direction. Through reptation, all statistically significant configurations of the system can be obtained.

#### 4.4.3.2 Configurational Bias Monte Carlo Move

There are many situations in which the acceptance probabilities of trial moves in Monte Carlo simulations drop to almost zero, resulting in a very inefficient simulation. In these circumstances, we bias the generation of trial moves such that they stand a greater probability of being accepted, *i.e.*, a trial move is selected from a set of trial positions with a probability proportional to the Boltzmann distribution, favoring the position having the lowest energy. It turns out we can do this without affecting the equilibrium distribution provided we change our acceptance probabilities. The bias has to be corrected after the trial move to obey detailed balance, but the acceptance probability of the new configuration is much higher than just some randomly inserted configuration.

To illustrate how the procedure works, consider a set of self-avoiding configurations of surfactant chains on a lattice with coordination number 26:

1. One surfactant chain is chosen at random for removal
2. The Rosenbluth weight, for this chain is then calculated by counting the number of unoccupied sites, $z_u(i)$, around the next bead to be removed. For the chain that is being removed the Rosenbluth weight is represented by, $W_{old}$, which is defined as the product of these weights divided by the lattice coordination number, $z$:

$$W_{old} = \prod_{i=n-1}^{1} \frac{z_u(i)}{z} \tag{4.39}$$

where $n$ is the chain length

UNIVERSITAT ROVIRA I VIRGILI
MICROSCOPIC MODELING OF THE SELF ASSEMBLY OF SURFACTANTS: SHAPE TRANSITIONS AND CRITICAL MICELLE CONCENTRATIONS
Asfaw Gezae Daful
ISBN:/DL:T. 1024-2011



3. To replace the chain back into the cell a lattice site is chosen at random, and the chain is regrown starting from that site.

4. The chain is regrown. After setting each site in its place on the lattice, the possible ways that the next site can be placed are calculated. By this method the Rosenbluth weight, $W_{new}$, for this chain is calculated:

$$W_{new} = \prod_{i=1}^{n-1} \frac{z_u(i)}{z} \tag{4.40}$$

As the lattice is completely filled with surfactant chains and the solvent (water), the chain is regrown in place of water sites, and the sites where this chain is taken have to be filled by the sites removed during the chain regrowth.

If $z_u(i)$ becomes zero for any of the sites, then the system is returned to its old state and the configuration is not altered. Detailed balance is maintained using the ratio of the two Rosenbluth weights in the acceptance criterion:

$$P_{acc} = \min\{1, \frac{W_{new}}{W_{old}} exp(-\beta \Delta E)\} \tag{4.41}$$

where $\Delta E$ is the energy change in performing the move and $P_{acc}$ is the probability of accepting the move.

#### 4.4.3.3 Cluster Move

Single surfactant molecules can be moved by the aforementioned Monte Carlo moves. Surfactants self-assemble into micelles above their CMC. It is of considerable interest to study the equilibrium properties of such micellar system, yet, to sample the equilibrium properties of micellar solutions, the micelles must be able to move and exchange surfactants as well. Thus we implement a Monte Carlo Cluster move that makes it possible to group surfactant molecules together into clusters and displace the entire micelles with respect to each other[106].

1. First we decide which molecules will be allowed to bond together. A bond is formed between every pair of nearest neighbors

2. We define a bond probability, $p$, which is the probability that two neighboring sites form a cluster bond. If one segment of a chain is bonded to a cluster then the whole chain is included

UNIVERSITAT ROVIRA I VIRGILI
MICROSCOPIC MODELING OF THE SELF ASSEMBLY OF SURFACTANTS: SHAPE TRANSITIONS AND CRITICAL MICELLE CONCENTRATIONS
Asfaw Gezae Daful
ISBN:/DL:T. 1024-2011



3. The probability of creating a given configuration of clusters $\mathcal{C}$ from a configuration of $\Lambda$ of molecules is

$$P[\mathcal{C}(\Lambda)] = \sum_{\{B\}\epsilon C} p^{n_b(B)}(1-p)^{n_{nb}(B)} \tag{4.42}$$

where the summation is taken over the set of different bond configurations, $\{B\}$, that gives the same cluster configuration $\mathcal{C}$, and $n_b$ and $n_{nb}$ are the numbers of possible cluster bonds that are made or not made, respectively. The cluster configuration is now changed to obtain a new configuration $\mathcal{C}'$ and $\Lambda'$. If we denote the old cluster configuration, *old*, and the new as *new*, and the energy of the new and the old configuration denoted as $U_{new}$ and $U_{old}$ respectively, then the detailed balance condition requires that

$$\begin{aligned} &exp[-\beta U_{old}][p^{n_b(old)}(1-p)^{n_{nb}(old)}]acc(old \to new) = \\ &exp[-\beta U_{new}][p^{n_b(new)}(1-p)^{n_{nb}(new)}]acc(new \to old) \end{aligned} \tag{4.43}$$

Eq. (4.43) can be written as the ratio of the acceptance probabilities:

$$\frac{acc(old \to new)}{acc(new \to old)} = \frac{exp[-\beta U_{new}][p^{n_b(new)}(1-p)^{n_{nb}(new)}]}{exp[-\beta U_{old}][p^{n_b(old)}(1-p)^{n_{nb}(old)}]} \tag{4.44}$$

To generate these cluster configurations, we use the cluster multiple labeling technique [106], which allows a cluster configuration to be generated using only one pass through the lattice by using multiple labels for one cluster and keeping note of the labels which belong to each cluster. A random chain is picked and the cluster to which it belongs is moved one lattice site in a random direction. The number of non-bonded contacts between the displaced cluster and all other clusters is noted before and after the move. The move is then accepted or rejected based on the Metropolis acceptance criterion for Eq. (4.44),

$$P_{acc}(old \to new) = \min\left[1, \frac{[p^{n_b(new)}(1-p)^{n_{nb}(new)}]exp[-\beta U_{new}]}{[p^{n_b(old)}(1-p)^{n_{nb}(old)}]exp[-\beta U_{old}]}\right] \tag{4.45}$$

Various micellar properties are calculated during the Monte Carlo simulation. Among many interesting results of the simulations, we present a brief description of the radii of gyration tensor, so as to show how the micellar shape transition occurs.

UNIVERSITAT ROVIRA I VIRGILI
MICROSCOPIC MODELING OF THE SELF ASSEMBLY OF SURFACTANTS: SHAPE TRANSITIONS AND CRITICAL MICELLE CONCENTRATIONS
Asfaw Gezae Daful
ISBN:/DL:T. 1024-2011



## 4.5 Principal Moments of Inertia and Radius of Gyration Tensor

In order to study the shape transition of micelles at the molecular level, we define a micelle as follows; when one of hydrophobic tail bead of a surfactant molecule is in contact with at least one tail bead of another surfactant molecule in a micelle, then the surfactant molecule belongs to the cluster.

### 4.5.1 Principal Moments of Inertia

An approximate idea of the shape of the aggregates can be obtained from the interpretation of the principal moments of inertia. We use the principal moments of inertia of surfactants with respect to the center of mass, to obtain information about the shape and size of the micellar aggregate in our simulations. The moment of inertia is used to describe rotational motion, but is also an indicator for the micellar shape. The moments of inertia, as a function of the mean field probability distribution, are given by

$$\begin{aligned}
I_{xx} &= \sum_{\alpha} P(\alpha) \sum_{i=1}^{n_T+n_H} \Big( [y(\alpha,i)-y_o]^2 + [z(\alpha,i)-z_o]^2 \Big) \\
I_{yy} &= \sum_{\alpha} P(\alpha) \sum_{i=1}^{n_T+n_H} \Big( [x(\alpha,i)-x_o]^2 + [z(\alpha,i)-z_o]^2 \Big) \\
I_{zz} &= \sum_{\alpha} P(\alpha) \sum_{i=1}^{n_T+n_H} \Big( [x(\alpha,i)-x_o]^2 + [y(\alpha,i)-y_o]^2 \Big) \\
I_{xy} &= -\sum_{\alpha} P(\alpha) \sum_{i=1}^{n_T+n_H} \Big( [x(\alpha,i)-x_o] \times [y(\alpha,i)-y_o] \Big) \\
I_{xz} &= -\sum_{\alpha} P(\alpha) \sum_{i=1}^{n_T+n_H} \Big( [x(\alpha,i)-x_o] \times [z(\alpha,i)-z_o] \Big) \\
I_{yz} &= -\sum_{\alpha} P(\alpha) \sum_{i=1}^{n_T+n_H} \Big( [y(\alpha,i)-y_o] \times [z(\alpha,i)-z_o] \Big)
\end{aligned} \tag{4.46}$$

where $(n_T + n_H)$ is the total length of the surfactant with $n_T$ tail and $n_H$ head beads; $x_o$, $y_o$, $z_o$ represent the center of mass of the aggregate; and $x(\alpha, i)$, $y(\alpha, i)$,

UNIVERSITAT ROVIRA I VIRGILI
MICROSCOPIC MODELING OF THE SELF ASSEMBLY OF SURFACTANTS: SHAPE TRANSITIONS AND CRITICAL MICELLE CONCENTRATIONS
Asfaw Gezae Daful
ISBN:/DL:T. 1024-2011



$z(\alpha, i)$ are the positions of the $i^{th}$ bead of conformation $\alpha$. Where $I_{xy} = I_{yx}$, $I_{xz} = I_{zx}$, and $I_{yz} = I_{zy}$, thus I is a symmetric tensor. Here $I_{xx}$ denotes the moment of inertia around the *x-axis* when the micelles are rotated around the *x-axis*, and $I_{xy}$ denotes the moment of inertia around the *y-axis* when the micelles are rotated around the *x-axis*, and so on.

Other parameters that are sensitive to the micelle structure are the ratios of the three principal moments of inertias of aggregates, changes in these ratios at different concentrations indicate the morphological changes, *i.e.* the shape transition of a micelle. The ratio of two pairs of these three values can then be used to describe the shape of the given aggregate.

A measure of the aggregate asphericity can be obtained from the calculation of ratios of the three principal moments of inertia of the aggregate $I_{xx}/I_{yy}$, $I_{xx}/I_{zz}$, and $I_{yy}/I_{zz}$ as functions of the aggregate size. Thus, for instance, for a spherical aggregate all the three moments of inertias are equal, resulting in $I_{xx}/I_{yy} \approx I_{xx}/I_{zz} \approx I_{yy}/I_{zz} \approx 1$, and for a cylindrical micelle, $I_{zz}$ is smaller than the other two, that gives $I_{xx}/I_{zz} \approx I_{yy}/I_{zz} \gg 1$ and $I_{xx}/I_{yy} \approx 1$ and for discoidal aggregates $I_{zz}$ is larger than the other two thus $I_{xx}/I_{zz} \approx I_{yy}/I_{zz} \ll I_{xx}/I_{yy} \approx 1$.

### 4.5.2 Radius of Gyration Tensor

To quantitatively investigate the shapes and the structure of the micelles the principal radii of gyration was calculated for the aggregates by first calculating the squared radius of gyration tensor of each aggregate.

$$R^2_{xx} = \begin{pmatrix} R^2_{x_1x_1} & R^2_{x_1x_2} & R^2_{x_1x_3} \\ R^2_{x_2x_1} & R^2_{x_2x_2} & R^2_{x_2x_3} \\ R^2_{x_3x_1} & R^2_{x_3x_2} & R^2_{x_3x_3} \end{pmatrix} \tag{4.47}$$

The matrix elements, $R^2_{x_ix_j}$, are defined as

$$R^2_{x_ix_j} = \frac{1}{N_m}\sum_{k=1}^{N_m}(x_{i,k} - x_{i,cm})(x_{j,k} - x_{j,cm}) \tag{4.48}$$

where $N_m$ is the total number of sites in the aggregate, and $x_{i,k}$ and $x_{j,k}$ are the $i^{th}$ and $j^{th}$ components of the positions of the $k^{th}$ monomer of the surfactant. The coordinates of the center of mass of the aggregate are

$$x_{i,cm} = \frac{1}{N_m}\sum_{k=1}^{N_m} x_{i,k} \tag{4.49}$$

UNIVERSITAT ROVIRA I VIRGILI
MICROSCOPIC MODELING OF THE SELF ASSEMBLY OF SURFACTANTS: SHAPE TRANSITIONS AND CRITICAL MICELLE CONCENTRATIONS
Asfaw Gezae Daful
ISBN:/DL:T. 1024-2011



We next find the eigenvalues of each of the matrices defined by $R_1$, $R_2$ and $R_3$, and diagonalized into the form

$$R^2 = \begin{pmatrix} R_1^2 & 0 & 0 \\ 0 & R_2^2 & 0 \\ 0 & 0 & R_3^2 \end{pmatrix} \tag{4.50}$$

where the diagonal elements are ordered so that $R_1 > R_2 > R_3$. This transformation is a rotation of the micelle so that the principal axes of the radius of gyration tensor will be coinciding with the Cartesian coordinate axes, and $R_1^2$, $R_2^2$, and $R_3^2$ are the ordered eigenvalues of the mean-square radius of gyration tensor. These values characterize the size and shape of the micelles in each of the principal directions. The values of the radius of gyration tensor for model surfactant $\mathrm{H}_x\mathrm{T}_y$ are recorded during the Monte Carlo simulation. For comparison, note that for a perfect cylinder of length $\ell$ and radius $r$, $R_2$ and $R_3$ are equal to each other and proportional to $r$, and $R_1$ is proportional to $\ell$, *i.e.*, $R_2^2 \approx R_3^2 \ll R_1^2$; for prefect sphere $R_1^2 = R_2^2 = R_3^2$, and for disk like micelles$R_2^2 \approx R_3^2 \gg R_1^2$. Another parameter that is sensitive to the micelle structure is the ratio of the radii of gyration tensors. The shape of aggregates is analyzed by introducing ratios of the radii of gyration tensor defined as $R_2^2/R_1^2$ and $R_3^2/R_1^2$.

For each snapshot, $i$, the values of $R_1^2$, $R_2^2$, and $R_3^2$ are recorded, and the ratios,

$$\begin{aligned} \alpha(i) &= \left(\frac{R_2}{R_1}\right)^2 \\ \beta(i) &= \left(\frac{R_3}{R_1}\right)^2 \end{aligned} \tag{4.51}$$

are calculated. A distribution function is defined as $PD\Big(\alpha(i), \beta(i)\Big)$ that is calculated for all snapshots to get how many times we encounter an aggregate having the ratios of the radii of gyration tensor $\alpha(i)$ and $\beta(i)$. Note that these $\alpha(i)$ and $\beta(i)$ can have values in the interval, $(0, 1)$, therefore $i$ is a vector of length $m$ of values between $(0, 1)$. If $\alpha(i)$ and $\beta(i)$ are close to unity this implies that the three radii of gyration tensor are almost equal, so the aggregate has a spherical shape. If $\alpha(i)$ and $\beta(i)$ are close to zero implies that first radius of gyration tensor, $R_1^2$, much bigger than the other two, so the aggregate has cylindrical shape. If $\beta(i) \approx 0$ and $\alpha(i) \approx 1$ the aggregate will be disk. The different geometric shapes of the aggregates can approximately be distinguished as follows (see Fig. 4.4 and Table 4.1).

UNIVERSITAT ROVIRA I VIRGILI
MICROSCOPIC MODELING OF THE SELF ASSEMBLY OF SURFACTANTS: SHAPE TRANSITIONS AND CRITICAL MICELLE CONCENTRATIONS
Asfaw Gezae Daful
ISBN:/DL:T. 1024-2011



**Table 4.1:** Approximate representations of variations of shapes of aggregates with $\alpha$ and $\beta$

| | | |
|---|---|---|
| $\alpha \approx \beta \approx 0$ | $R_1 >> R_2 \approx R_3$ | Cylinder |
| $\alpha \approx \beta \approx 1$ | $R_1 \approx R_2 \approx R_3$ | Sphere |
| $\alpha \approx 1$ and $\beta \approx 0$ | $R_1 \approx R_2 > R_3$ | Disk |

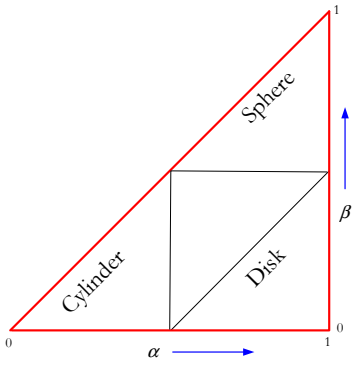


**Figure 4.4:** Schematic representation of different geometric shape of micelles as a function of the ratios of the radii of gyration tensors, $\alpha$ and $\beta$; $(a)$. if $\alpha \approx \beta \approx 0$ that is $R_1 >> R_2 \approx R_3$ then the aggregate is finite size cylindrical micelle $(b)$. if $\alpha \approx \beta \approx 1$ that is $R_1 \approx R_2 \approx R_3$ then the aggregate is spherical micelle $(c)$. if $\alpha \neq \beta$ (or $\alpha$ close to 1 and $\beta$ close to 0) that is $R_1 \approx R_2 > R_3$ the aggregate is can be of disk micelle $(d)$. for $0 \ll \alpha \approx \beta \ll 1$, spherical and finite size cylindrical micelles exist together with micelles of intermediate shapes in the system, indicating the shape transition of spherical micelles into finite size cylindrical micelles.

UNIVERSITAT ROVIRA I VIRGILI
MICROSCOPIC MODELING OF THE SELF ASSEMBLY OF SURFACTANTS: SHAPE TRANSITIONS AND CRITICAL MICELLE CONCENTRATIONS
Asfaw Gezae Daful
ISBN:/DL:T. 1024-2011

UNIVERSITAT ROVIRA I VIRGILI
MICROSCOPIC MODELING OF THE SELF ASSEMBLY OF SURFACTANTS: SHAPE TRANSITIONS AND CRITICAL MICELLE CONCENTRATIONS
Asfaw Gezae Daful
ISBN:/DL:T. 1024-2011

# Chapter 5

# Shape Transitions of Micelles

## 5.1 Introduction

Above the critical micellar concentration, amphiphilic molecules in aqueous solutions spontaneously self-assemble into aggregates or microstructures known as micelles, driven by the hydrophobicity of the tails and the hydrophilic nature of the head groups of the surfactant. They are capable to spontaneously self-assemble into aggregates of different geometric shapes such as spheres, ellipsoids, cylinders, disks, bilayers, vesicles etc. Normally, at low concentrations close to the critical micelle concentration, small spherical micelles are formed; however changes in the solution conditions such as surfactant concentration, temperature and other physicochemical parameters can cause changes in the micellar morphology[1–6, 63, 71, 100, 102, 108–113], which is termed as a shape transition of micelles. At higher surfactant concentrations, the spherical micelles can undergo one-dimensional growth into cylindrical micelles, or two-dimensional growth into discoidal micelles, for instance.

A number of experimental studies have revealed the rich diversity of micellar morphologies displayed by amphiphilic systems that play an increasingly important role in many biological and industrial processes, for instance, in drug loading and delivery, catalysis, cosmetics, separation processes in engineering and environmental science and technology etc. Interestingly, all these applications depend

UNIVERSITAT ROVIRA I VIRGILI
MICROSCOPIC MODELING OF THE SELF ASSEMBLY OF SURFACTANTS: SHAPE TRANSITIONS AND CRITICAL MICELLE CONCENTRATIONS
Asfaw Gezae Daful
ISBN:/DL:T. 1024-2011



on the capability to tune and control the shape and size of the aggregates that surfactants form in solution. The size, shape, and structure of micelles are thus important characteristics in determining their main properties and areas of application [1–4, 6, 7], for example the shape and size of micelles are directly related to the viscosity [2, 56] and other rheological features of the micellar solution, which are important in many applications involving surfactants.

The question of the shape of the micelle has received a considerable interest from many investigators. An empirical relation for micellar structure, based upon the geometry of various micellar shapes and the space occupied by the hydrophilic and hydrophobic groups of the surfactant molecules, has been developed by Israelachvili [1] (see section 3.8 of chapter 3).

As various morphologies were observed, the transition between different morphologies became an active research area. An increasing attention has been paid to micelles that undergo a sphere to cylinder transition [5, 8, 9, 15, 30, 32, 100, 109, 114–116] in theoretical and simulation studies. At concentrations slightly above the critical micelle concentration, micelles are usually spherical. Changes in temperature, surfactant concentration, or the addition of some additives (like electrolytes or salts) in the solution may change the size, shape, aggregation number, and stability of the micelles [1–4, 6, 108, 109].

Based on static light scattering experiments on ionic surfactants at high salt concentrations, Debye et al. [8] and Eriksson [9] showed that the micelles can undergo a transition from spherical to rod-like aggregates upon increasing surfactant concentration above the critical micelle concentration. This idea has been supported by many other experimental works by using measurements, of pulse gradient spin-echo NMR (Nuclear Magnetic Resonance) [10–12], viscosity [13, 14], turbidity [15, 16, 117], dynamic light scattering [16, 17], static light scattering [18, 19, 118, 119], Cryogenic-Temperature (cryo-TEM) [20–23], transmission electron microscopy (TEM) [117, 120, 121]and Small-Angle Neutron Scattering [24–27, 122].

Some experimental studies also showed a shape transition from sphere to rod-like micelles by increasing the length of the alkyl chain of the hydrophobic group or decreasing the length of the hydrophilic group of the surfactant [25, 28, 29], by synthesizing surfactants of different tail and head segment lengths. The micellar shape strongly depends on the hydrophobic and hydrophilic chain lengths of the surfactant molecules. Surfactant molecules with relatively shorter hydrophobic chain than their hydrophilic chain are suggested to form spherical micelles, whereas those with longer hydrophobic chain than their hydrophilic chain form rod-like micelles. Hitoshi Yamaoka et al. [25] have investigated the behavior of amphiphilic

UNIVERSITAT ROVIRA I VIRGILI
MICROSCOPIC MODELING OF THE SELF ASSEMBLY OF SURFACTANTS: SHAPE TRANSITIONS AND CRITICAL MICELLE CONCENTRATIONS
Asfaw Gezae Daful
ISBN:/DL:T. 1024-2011



block copolymers synthesized by living cationic polymerization in aqueous solution of amphiphilic block copolymers of vinyl ethers containing 2-hydroxyethyl vinyl ether (HOVE) and partially deuterated n-butyl vinyl ether (NBVE), and have determined the size and shape of the micelles by the SANS technique. They report the transition of the micellar shape from sphere to rod with increasing molar fraction of the hydrophobic part of the polymer. Pavletta et al. [12] showed the sphere to rod shape transition of two surfactants in aqueous solution, the anionic surfactant SDP-2S (sodium dodecyl dioxyethylene-2 sulfate) and the nonionic surfactant Triton X-100 (octylphenol-polyoxyethylene ether with 9.5 ethoxy groups), investigated by NMR spectroscopy. Shoichi Ikeda [30] introduced a theory of the salt-induced and temperature-induced sphere to rod transition of surfactant micelles and the reversible linear aggregation of surfactant into rod-like micelles on the basis of a simple treatment of the mass action law and statistical thermodynamics.

Theories have been developed to predict the micellization properties of surfactants [31–36], and computer simulations[37–47, 47–55] have also been increasingly used to study the structures and thermodynamics of micelles.

Molecular dynamic simulation attempts have been made in order to address structural properties of micelles [29, 38–40, 48, 50, 51, 123–131]. Despite the fact that they imposed a given shape of the micelle, the simulations of Haile et al. [124] provided useful information about the segment density distributions and conformational statistics. O'Connell et al. [29] studied the effect of chain length and head group properties on the internal micelle structure, micellar shape, and chain conformation inside the micelle. They found that the average aggregate shape is somewhat nonspherical, regardless of head group size and surfactant chain length. The molecular dynamics simulations of Palmer and Lui [127] incorporated an additional bending energy term using a quasi-realistic model. Smit et al. [128, 129] and Fodi et al. [130] carried out molecular dynamics simulations of the spontaneous aggregation of surfactants for a simple oil, water and surfactant system and analyzed the detailed structure of a water/oil interface in the presence of micelles. Marrink et al. [38] studied the kinetics of spontaneous micelle formation by means of molecular dynamic simulations of dodecylphosphocholine (DPC) surfactant molecules in water. They showed the spontaneous aggregation of the DPC surfactant into a spherical micelles at low concentrations and that at higher concentrations worm-like micelles appear to be more stable than the spherical micelle. Fujiwara et al. [59] studied how the micellar shape changes depending on the hydrophilicity and hydrophobicity of the amphiphilic molecule, $H_1T_2$, using molecular dynamic simulations of coarse-grained rigid amphiphilic molecules with explicit solvent molecules. They observe three kinds of isolated micelles, disk, cy-

UNIVERSITAT ROVIRA I VIRGILI
MICROSCOPIC MODELING OF THE SELF ASSEMBLY OF SURFACTANTS: SHAPE TRANSITIONS AND CRITICAL MICELLE CONCENTRATIONS
Asfaw Gezae Daful
ISBN:/DL:T. 1024-2011



lindrical, and spherical micelles by changing the intensity of the hydrophilicity and hydrophobicity.

Monte Carlo simulations of amphiphilic solutions in lattices have also been used extensively to study the micellar properties, such as critical micelle concentration, structure of aggregates and micellar shape and size, aggregation number, etc. for different types of amphiphiles in solution [46, 49, 52, 87, 89, 90, 132, 133]. These methods are generally based on lattice models in which a surfactant molecule is represented as a chain of chemical groups occupying certain lattice sites on a two or three-dimensional lattice. Extensive work has been done by Larson [49, 52] showing that surfactant self-assembly can be achieved by Monte Carlo simulations without having to resort to any preassembled micellar structure or shape. However, the majority of Larson's works have focused on three component surfactant-oil-water systems. Care [87] applied Monte Carlo simulation in a two-dimensional square lattice and studied the thermodynamics of cluster formation by calculating the distribution of surfactant monomers in clusters. Xuehao et al.[90] applied Monte Carlo method to simulate the process of the self-assembling of amphiphilic diblock copolymers in a selective solvent. They illustrated the dependence of the aggregate morphologies of diblock copolymers in solution on the length of corona-forming segments (hydrophilic part in case of surfactants), *i.e.*, with the decrease of the corona-forming segments, the transition of spherical micelles to rod-like aggregates occurs. Equilibrium properties of micellar solutions of nonionic surfactant, $H_4T_4$, were also studied by Mackie et al. [46] using three dimensional lattice Monte Carlo simulations. Equilibrium size and shape distributions of self-assembled micelles of $H_2T_2$ were investigated by Hatton et al. [85]. They found that the spherical micelles grow in one dimension to form spherically capped cylinders. Panagiotopoulos et al. [54] determined the phase behavior and micellization of several diblock, $H_xT_y$, and triblock, $H_xT_yH_x$ and $T_yH_xT_y$, surfactants in a Larson-type model by histogram-reweighting grand canonical Monte Carlo simulations on a lattice model.

Monte Carlo simulation by Termonia [91], shows the effect of the length, $x$, of the hydrophilic block on the final aggregate morphology in pure water of an amphiphile $H_xT_y$. For $y = 40$, higher values of $x$ ($x = 80$ and $x = 40$) lead to the formation of spherical micelles with a core of hydrophobic segments surrounded by a corona of the hydrophilic block. At smaller values ($x = 20$), however, cylindrical micelles are formed. A typical explanation [91] for the transition from spherical micelles to cylindrical micelles is based on an increase in the radius of the core with a decrease in the size of the hydrophilic H block at a constant length of the T block. The latter implies a corresponding increase in the degree of stretching of the T block that, because of a loss in entropy, eventually leads to an instability

UNIVERSITAT ROVIRA I VIRGILI
MICROSCOPIC MODELING OF THE SELF ASSEMBLY OF SURFACTANTS: SHAPE TRANSITIONS AND CRITICAL MICELLE CONCENTRATIONS
Asfaw Gezae Daful
ISBN:/DL:T. 1024-2011



and a transition from spherical to cylindrical morphology.

Ben-Shaul et al. [32] and den Otter et al. [134] made a first order approach for the sphere to cylinder transition by adopting as a premise the fact that large aggregation numbers are associated with a preference for cylindrical or bilayer packing of amphiphilic molecules. The effect of this premise on the equilibrium size distribution of micellar aggregates and its dependence on the concentration were explored. Hoeve et al. [135] derived possible distributions of micellar sizes with a fairly sharp maximum. They assumed that a spherical shape persisted until the micelle became so large that further growth was impossible without having polar heads in the interior of the micelle. However, the predicted shape was plate-like rather than rod-like, when large micelles were formed.

Although these Monte Carlo and Molecular Dynamic simulation techniques have been used to study the self assembly of micellar systems, obtaining the free energy of formation of the micelle, size and shape distribution and many other important equilibrium properties like critical micelle concentration, are computationally expensive.

Scheutjens and Fleer [96, 97] proposed mean field calculations, to study the polymer adsorption in a self-consistent mean field approximation and later Leermakers et al. [37, 41–43] applied a self-consistent field (SCF) theory to study the self-assembly of surfactant molecules into micelles. Thus, they were able to compute the volume fraction profiles of the hydrophilic head and hydrophobic tail groups in the micelle which correspond to the minimum in the free energy of the system. Leermakers [37] generalized the SCF to treat surfactant solutions. Böhmer and Koopal [98] applied this theory to study the micellization of nonionic surfactants and their adsorption from aqueous solution on hydrophilic and hydrophobic surfaces. They also showed that the critical micelle concentration increases and the aggregation number decreases if the hydrophilic block becomes longer. The SCF considers the surfactant to be a Gaussian chain in an inhomogeneous mean field.

The Single Chain Mean Field Theory (SCMFT), where configurations of full chains are used in a mean field calculations, developed for dry core micelles by Szleifer et al. [44, 45, 136], and then generalized for polymer solvent systems. Mackie et al. [46] applied SCMFT without the assumption of a sharp interface and dry core for spherical micelles. The lattice based SCMFT [46, 55] has been solved to get a detailed microscopic information on the configurations and their distribution in the system, the standard chemical potential difference between free surfactants and surfactants associated in the micelle, the critical micelle concentration as well as the aggregation number and the size distributions of micelles.

They were found to be in an excellent agreement with Monte Carlo simulations except for a significantly smaller aggregation number for SCMFT.

Recently, the SCF model has been extended to study the shape transition in micellar solutions for nonionic surfactants [99]. The preliminary results support the coexistence of spherical and dumbbell-like micelles, that is, finite size cylindrical micelles with swollen end-caps. This type of structure was proposed by Eriksson et al. [9] on the basis of a detailed analysis of the mechanical equilibrium state of the micelle. May and Ben-Shaul [32] have also determined the equilibrium shape and energy of the micelle by functional minimization of the total free energy, which is expressed as an integral over local molecular packing free energies in different regions of the micelle. Despite the fact that they consider this theory as a molecular-level one, the local packing free energy per molecule is expressed in terms of macroscopic quantities such as the surface tension or the elastic stretching modulus. Dumbbell-like micelles have also been seen by transmission electron microscopy at cryogenic temperatures (cryo-TEM) with a dimeric (gemini) surfactant by Bernheim-Groswasser et al. [20].

May and Ben-Shaul [32] modeled the sphere to cylinder transition as a sphero-cylinder model, where they assumed the packing free energy of the micelle is a sum of contributions from amphiphile molecules packed in the cylindrical body and the two hemi-spherical end caps. Zaid et al. [5] used a similar, sphero-cylindrical, model in SCMFT, assuming a linear combination of the standard chemical potentials of independent spherical and infinite cylindrical micelles. The standard chemical potential differences in the latter were chosen as the minimums as a function of the number of chains in the aggregate, both in the spherical and the infinite cylindrical geometry. The SCMFT finds that the symmetric surfactant, $H_4T_4$, favors the formation of spherical micelles independent of amphiphile concentrations, while the asymmetric $H_3T_6$ amphiphile prefers cylindrical micelle at higher amphiphile concentration. Jódar-Reyes et al.[100] used a self-consistent field theory to analyze the micellar shape transition in nonionic surfactants of the type $C_nE_m$, and describe as a sudden shape transition from sphere to cylinder upon an increase in surfactant concentration. The grand potential[100] and packing free energy [32] of the cylindrical micelle were reported to have an oscillatory behavior with an amplitude that decays with the length of the cylinder. According to these models [5, 32, 100] of the micellar growth, the sphere to rod transition is a continuous process, with the average micellar size increasing monotonically as a function of the surfactant concentration.

On the other hand, besides spherical and cylindrical or rod-like micelles, micelles with various special topologies have been experimentally [137–139] observed, such as disk micelles, toroidal micelles, unilamellar and multilamellar vesicles etc.

UNIVERSITAT ROVIRA I VIRGILI
MICROSCOPIC MODELING OF THE SELF ASSEMBLY OF SURFACTANTS: SHAPE TRANSITIONS AND CRITICAL MICELLE CONCENTRATIONS
Asfaw Gezae Daful
ISBN:/DL:T. 1024-2011



These structures provide new opportunities for designing soft materials with enhanced functionalities for various applications, and understanding the thermodynamic aspects of micellar self-assembly and the shape transition they undergo is pivotal in their applications.

Many experiments, theoretical studies and simulations indicated that the micellar structures and size distributions not only depend on molecular parameters, *i.e.*, the chain length of the amphiphilic molecules, the hydrophilic-to-hydrophobic ratio, and the intermolecular interactions, but also on system parameters such as the concentration, and temperature. According to the conventional pathway[1], the amphiphilic molecules first self-assemble into small spherical micelles, then elongate (coalesce) to rod-like micelles, the rod-like micelles transform themselves to bilayers, and finally, the bilayers bend around and close up to vesicles. But recent studies have expanded the variety of micellar shapes to an unconventional forms that include disks[137, 140–143], toroids[138, 140, 144], tubes[145], helices[146], etc.

Despite the large amount of work, experimentally, theoretically, and simulations, devoted to the shape transition of micelles, a comprehensive microscopic understanding of the concentration induced shape transition is still missing. Micelles of different geometric shape have drawn considerable interest over the past few decades, both from a theoretical viewpoint as well as for industrial and technological applications, the range of which keeps expanding. Understanding how micellar structure is connected to the chemical composition and geometry of the surfactant, and in turn, how the structural features of the aggregates can be tuned by specific control parameters, and how these dictate the bulk properties, offers a considerable challenge.

The purpose of this work is two-fold:

1. exploring how the concentration induced sphere to cylinder transition takes place. Addressing questions like, how do finite size cylindrical micelles evolve from spherical micelles? and how do the morphological transformations look like?

2. answering questions like, can the spherical micelle transform to aggregates of other geometric structures like disk and donut like micelles? Investigating how the spherical micelles transforms to disk like micelles

In this chapter we study the micelle formation and stability analysis for model nonionic surfactants, $H_xT_y$ using a one dimensional Single Chain Mean Field Theory, where spherical and infinite cylindrical micelles are studied separately. We

UNIVERSITAT ROVIRA I VIRGILI
MICROSCOPIC MODELING OF THE SELF ASSEMBLY OF SURFACTANTS: SHAPE TRANSITIONS AND CRITICAL MICELLE CONCENTRATIONS
Asfaw Gezae Daful
ISBN:/DL:T. 1024-2011



then present a two dimensional Single Chain Mean Field Theory, 2D-SCMFT, and Monte Carlo Simulations to systematically study the sphere to cylinder transition of micelles, and get answers for the above posed questions. We also show the existence of an alternative pathway of disk and donut like micelle formation for a model nonionic surfactant, *i.e.,* concentration induced sphere to disk transition.

## 5.2 Simulation Methodology

The simulations of this work are performed in a cubic box of volume $V$ containing $N$ amphiphilic molecules fixed at a temperature $T$. The amphiphile configurations are obtained using the Rosenbluth and Rosenbluth chain growth self-avoiding random walk algorithm[101] and periodic boundary conditions are used. We generate the amphiphile configurations using the Rosenbluth and Rosenbluth chain growth algorithm, see section 3.7.5. The overall Rosenbluth weight factor of a chain is calculated from the partial weight of each monomer, obtained in the generation of the chain given by Eq. (3.49) and the partial Rosenbluth weight, $w_{\alpha,i}$, of each monomer, $i$, of configurations, $\alpha$, is given by Eq. (3.50).

It is important to note at this point that the set of configurations $\alpha$, include all possible bond sequences and the positions of the chain with respect to the center of the aggregate. Once we have a set of configurations, they can be placed onto the lattice and the chain distributions counted as a function of radial distribution from the aggregate center in 1D SCMFT and the radial and axial distributions for the 2D SCMFT cases.

### 5.2.1 1D SCMFT

The micelle formation and stability analysis for model nonionic surfactants, $H_x T_y$ is studied using a one dimensional Single Chain Mean Field Theory, 1D SCMFT. Spherical micelles and infinite cylindrical micelles are considered, where a symmetry of the field is pre-assumed, and as a consequence, the topology of the micelles is to some extent dictated. The field discretization for spherical and infinite cylinder models are shown in Fig. 4.2.

We generated one million amphiphile configurations using the Rosenbluth and Rosenbluth chain growth algorithm [101] and placed them on a lattice divided into concentric spherical and cylindrical shells, so that the distribution of tails, heads, and nearest neighbor contacts can be obtained for each configuration. For

UNIVERSITAT ROVIRA I VIRGILI
MICROSCOPIC MODELING OF THE SELF ASSEMBLY OF SURFACTANTS: SHAPE TRANSITIONS AND CRITICAL MICELLE CONCENTRATIONS
Asfaw Gezae Daful
ISBN:/DL:T. 1024-2011



each configuration, $\alpha$, intramolecular tail-tail interactions, $n_{TT}^{intra}(\alpha)$, are calculated exactly and the chain segment distribution of tails $n_T(\alpha, r)$, heads $n_H(\alpha, r)$, and nearest neighbor contacts of the tail segment $n_{n,T}(\alpha, r)$, are counted along with their radial distribution from the aggregate center and the *z-axis*. The SCMFT gives a set of nonlinear self-consistent equations to determine the Lagrange multiplier field $\pi(r)$ and the mean field properties $\langle n_T(r)\rangle$ and $\langle n_{n,T}(r)\rangle$, which in turn are used to compute the structure of the micelle and any thermodynamic property of interest via the probability distribution function of the configuration, $P(\alpha)$. In both cases, spherical and infinite cylindrical systems, the primary results are the standard chemical potential difference, $(\mu_N^o - \mu_1^o)/k_BT$, an important thermodynamic parameter that determines the equilibrium between singly dispersed surfactants in the solution and surfactants in the micellar aggregate. The radial volume fraction profiles of the solvent $\phi_S(r)$, tail $\phi_T(r)$, and head $\phi_H(r)$ are also obtained, where the center of the lattice corresponds to $r = 0$.

### 5.2.2 2D SCMFT

A two dimensional Single Chain Mean Field Theory, (2D-SCMFT), is used to study the shape transition of micelles of different geometric shapes. The 2D-SCMFT is checked by reproducing the spherical and infinite size cylindrical micelle properties obtained from 1D-SCMFT, like the standard chemical potential differences. 2D-SCMFT in a two dimensional cylindrical geometry of the mean field is used to study the shape transition from the spherical micelle to wards the finite size cylindrical micelle, and the disk (donut like) micelles. In this 2D-SCMFT, surfactants can form a micelle of a range of any geometric shapes, no pre-assumption of the shape of the micelle is made. We study the shape transition of micelles via the 2D-SCMFT with no *a priori* restrictions on the form of the micelle.

The simulation box is divided into $Z_l$ slices (layers) along the *z-axis* and in each layer there are $N_{circ}$ concentric shells along the $x$ and $y$ plane specified by radii $r$, where $Z_l = L$ and $N_c = \frac{L-1}{2} + 1$, $L$ being the cubic box size, see Fig 4.1. The shell volume, $V(r, z)$, is defined by counting the number of sites included in each circular shell of radius $r$, of a given layer, $z$. A site is considered to be included in a shell if its center falls within the shell as defined in continuous space. The lattice sites at the corners of the simulation box are included in the last shell. We generate the amphiphile configurations using the Rosenbluth and Rosenbluth chain growth algorithm [101] and placed them on a lattice divided into circular shells of slices, so that the distribution of tails, heads, and nearest neighbor contacts can be obtained for each configuration. The system is allowed to form a micelle without pre-assumption of its shape.

UNIVERSITAT ROVIRA I VIRGILI
MICROSCOPIC MODELING OF THE SELF ASSEMBLY OF SURFACTANTS: SHAPE TRANSITIONS AND CRITICAL MICELLE CONCENTRATIONS
Asfaw Gezae Daful
ISBN:/DL:T. 1024-2011



For each conformation, $\alpha$, the first tail of the amphiphile is placed in the simulation box randomly and then the chain is grown using self avoiding random walk, subjected to periodic boundary conditions. Intramolecular tail-tail interactions, $n_{TT}^{intra}(\alpha)$, are calculated exactly for all the configurations. The chain distribution of tails $n_T(\alpha, r, z)$, heads $n_H(\alpha, r, z)$, and nearest neighbor contacts $n_{n,T}(\alpha, r, z)$, are counted along with their radial and axial distribution from the aggregate center. To find the Lagrange multipliers (osmotic pressure), $\pi(r, z)$, the volume fraction profiles $\phi_S(r, z)$, $\phi_T(r, z)$, and $\phi_H(r, z)$, whose averages depend on the probability distribution $P(\alpha)$, are substituted into the packing constraint equation Eq. (4.11). The SCMFT gives a set of nonlinear self-consistent equations to determine the Lagrange multiplier field $\pi(r, z)$ and the mean field properties $\langle n_T(r, z)\rangle$ and $\langle n_{n,T}(r, z)\rangle$, which in turn are used to compute the structure of the micelle and any thermodynamic property of interest.

A Fortran program has been developed, in F90, to solve the set of nonlinear self-consistent equations from the SCMFT. The program runs in parallel using OpenMP parallel architecture. The necessary input data that are needed to solve this set of nonlinear self-consistent equations are the chain conformations, the number of chains in the aggregate, box size, and the dimensionless temperature, $T^*$. The simulations are conducted in cubic boxes of volume, $25^3$, $27^3$ and $35^3$ with $2 \times 10^6$, $4 \times 10^6$ and $6 \times 10^6$ configurations respectively. The outputs are the set of values of the lagrange multiplier $\pi(r, z)$ and the mean field properties, *i.e* the mean field values for the distributions of tail $\langle n_T(r, z)\rangle$ and the nearest neighbor contacts $\langle n_{n,T}(r, z)\rangle$. From the self-consistent solution, the structure of the micelle is obtained and the probability distribution function, $P(\alpha)$, is fully determined, and any desired conformational average involved in any thermodynamic property of the micellar aggregate can thus be obtained.

### 5.2.3 Monte Carlo

In addition to the SCMFT we have also used Monte Carlo simulations. The model used for the Monte Carlo simulations is exactly the same as for the SCMFT, namely the Larson model[52] described in section 4.2. Details of the Monte Carlo simulations and calculations of some important properties are given in section 3.7.2 of chapter 3 and sections 4.4 and 4.5.2 of chapter 4. A box of volume $100^3$ with periodic boundary conditions was chosen and the following Monte Carlo moves[147] were used where the probability of choosing the move is given in brackets, chain reptation (80 %), CBMC chain growth (19.99 %), cluster move (0.01 %). In the case of the cluster moves and for the analysis of the cluster size distributions, a surfactant is taken to be part of a cluster when one of the hydrophobic tail beads

UNIVERSITAT ROVIRA I VIRGILI
MICROSCOPIC MODELING OF THE SELF ASSEMBLY OF SURFACTANTS: SHAPE TRANSITIONS AND CRITICAL MICELLE CONCENTRATIONS
Asfaw Gezae Daful
ISBN:/DL:T. 1024-2011



is in contact with at least one tail bead of another surfactant molecule.

The simulations were initiated with a random configuration and $10^9$ Monte Carlo steps were applied in order to make sure that the systems were equilibrated. An additional $10^{11}$ steps were then used in order to calculate the average properties of the system.

## 5.3 Results and Discussions

We present essential results to better understand and study the micelle formation process and stability analysis in one dimensional Single Chain Mean Field Theory (1D SCMFT) for spherical and infinite cylindrical micelles of model surfactants, $H_xT_y$. The plots of chemical potential difference, $(\mu_N^o - \mu_1^o)/k_BT$, and volume fraction profiles of spherical and infinite cylindrical are compared and discussed. Based on these results a candidate surfactant is chosen to study the shape transition process and we present the 2D SCMFT results of the morphological transformations. In the second part (section 5.3.2), we turn our attention to micellar morphological transformations. We address the question, of how the shape of the micelle changes from sphere to cylinder or disk on increasing surfactant concentration in the system.

### 5.3.1 1D Spherical and Infinite Cylindrical Micelles

The one dimensional Single Chain Mean Field Theory (1D SCMFT) was applied in the canonical (NVT) ensemble to describe the micellization process and for the calculation of the micellar aggregate chemical potential and other important micellar properties. Chains are grown on the lattice using the Rosenbluth and Rosenbluth [101] chain growth algorithm to avoid overlap of configurations and periodic boundary conditions were also used. The self-assembly behaviors of linear model surfactants, $H_3T_6$, $H_2T_6$, and $H_4T_4$were studied at different dimensionless temperature, $T^*$, in a simulation box of $L^3$. Two independent simulations were performed to simulate the spherical and infinite cylindrical micelles, where a comparative analysis of the two systems sheds light on the sphere to cylinder transition. These surfactants are selected to study the stability of micelles they form. Panagiotopoulos et al. [54] determined the phase behavior and micellization of several lattice diblock and triblock surfactants in a Larson-type model. All the above chosen surfactants, are micelle forming, even though $H_3T_6$ and $H_2T_6$ are close to the boundary between micelle forming systems and systems undergoing microscopic phase separation[54]. In the infinitely long cylindrical micelles, we consider all

UNIVERSITAT ROVIRA I VIRGILI
MICROSCOPIC MODELING OF THE SELF ASSEMBLY OF SURFACTANTS: SHAPE TRANSITIONS AND CRITICAL MICELLE CONCENTRATIONS
Asfaw Gezae Daful
ISBN:/DL:T. 1024-2011



relevant properties per unit length of the cylinder and radial components of all properties of interest in the system.

#### 5.3.1.1 $H_3T_6$

To study the micellization behavior of this linear model surfactant, $H_3T_6$, $10^6$ chain configurations were randomly generated on a lattice divided into (1) spherical shells and (2) infinite cylindrical shells, using the Rosenbluth and Rosenbluth chain growth algorithm[101] in a simulation box of volume, $V = 19^3$. The predictions of the SCMFT for the standard chemical potential difference, $(\mu_N^o - \mu_1^o)/k_BT$, of micelles of aggregation number, $N$, at dimensionless temperature, $T^* = 9.5$, are shown in Fig. 5.1 for spherical and infinite cylindrical micellar system. The infinite cylindrical micelle has lower standard chemical potential difference, $(\mu_N^o - \mu_1^o)/k_BT$, compared to that of the spherical micelles. This indicates that the infinite cylindrical micelle is more stable than the spherical micelle for this model surfactant.

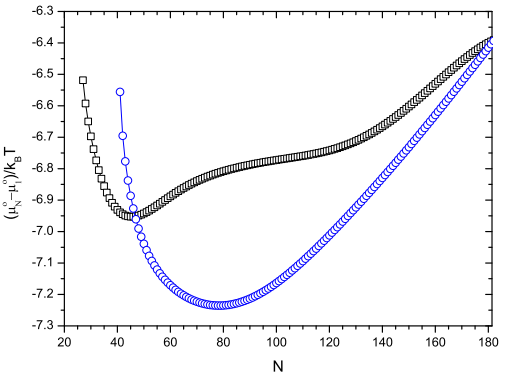


**Figure 5.1:** The standard chemical potential difference $(\mu_N^o - \mu_1^o)/k_BT$, of $H_3T_6$ versus micellar aggregation number $N$ of the spherical micelle (square) and the infinite cylindrical micelle (circles), at $T^* = 9.5$. In the case of the infinite cylindrical geometry, the *x-axis* gives the number of surfactants for a 19 lattice site section of the infinite cylinder.

In Figure 5.2 we show the radial distribution of volume fraction of stable spherical micelles that corresponds to the aggregation number of the minimum standard chemical potential difference (see Fig. 5.1), $N = 50$ and the infinite cylindrical micelle for, $N = 80$. The volume fraction profiles of the head and tail of the surfactant along with the solvent of the micelles are as expected; the core of the

UNIVERSITAT ROVIRA I VIRGILI
MICROSCOPIC MODELING OF THE SELF ASSEMBLY OF SURFACTANTS: SHAPE TRANSITIONS AND CRITICAL MICELLE CONCENTRATIONS
Asfaw Gezae Daful
ISBN:/DL:T. 1024-2011



micelle is predominantly packed by the tail segments, at small $r$ values, and the head groups are concentrated on the outside of the micelle, forming the corona of the micelle. The volume fraction profiles of the infinite cylindrical micelle are comparable to that of the spherical ones; the cores and coronas have the same characteristics. The hydrophobic core radius of the infinite cylindrical micelle is observed to be smaller than the spherical micelle. Qualitatively, this difference arises from the fact that in spherical micelles only a small number of chains are stretched to the limit, as the available volume in a sphere decreases quadratically with the distance from the interface, whereas most chains are relaxed and enjoy nearly maximal conformational freedom [5, 20, 32, 99]. In contrast, in a cylindrical micelle, the available volume decreases only linearly with the distance from the interface, implying that a larger fraction of the chains must be fully stretched when the radius of the hydrophobic core is equal to the chain length.

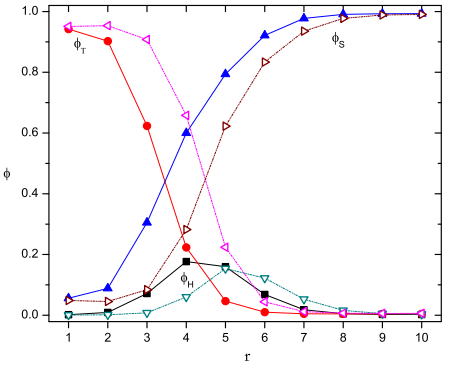


**Figure 5.2:** Radial variation of volume fraction profiles of tail $\phi_T(r)$, head $\phi_H(r)$, and solvent $\phi_S(r)$, versus radius $r$, of the spherical micelle (dash dot dot lines with opened symbols) and infinite cylindrical micelle (solid lines with filled symbols) for $H_3T_6$

The micellization process studied with SCMFT, is observed to be independent of the box size, provided that the simulation box volume is big enough, so that the micelle does not touch the periodic image, and sufficient configurations are generated. The standard chemical potential difference, $(\mu_N^o - \mu_1^o)/k_BT$, of $H_3T_6$ in different box sizes are plotted against the micellar aggregation number. The micellar aggregation number, $N_m$, is obtained by subtracting the free surfactants in the bulk solution from the total number of surfactants in the system. These plots of standard chemical potential differences versus $N_m$, from simulations in different box sizes overlaps, as shown in Fig. 5.3. The box sizes and the number of configurations, $\alpha$, used in each box, are shown in Table 5.1.

UNIVERSITAT ROVIRA I VIRGILI
MICROSCOPIC MODELING OF THE SELF ASSEMBLY OF SURFACTANTS: SHAPE TRANSITIONS AND CRITICAL MICELLE CONCENTRATIONS
Asfaw Gezae Daful
ISBN:/DL:T. 1024-2011



**Table 5.1:** Configurations $\alpha$ for different simulation boxes of volume $V$

| V | $19^3$ | $21^3$ | $23^3$ | $25^3$ | $31^3$ |
|---|---|---|---|---|---|
| $\alpha$ | $10^6$ | $1.5 \times 10^6$ | $2.0 \times 10^6$ | $2.5 \times 10^6$ | $4.5 \times 10^6$ |

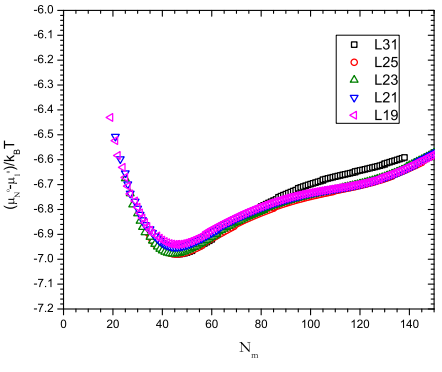


**Figure 5.3:** Standard chemical potential differences, $(\mu_N^o - \mu_1^o)/k_BT$, of $H_3T_6$ versus micellar aggregation number $N_m$ of the spherical micelles at $T^* = 9.5$ for different simulation box sizes

From the chemical potential differences, we determine the CMC of $H_3T_6$ at $T^* = 9.5$ using the mass-action model as described previously in section 3.6.1. According to the Israelachvilli [1] definition of the CMC, we plot the free surfactant concentration, $X_1$, as a function of total surfactant concentration, $X_t$ in Fig. 5.4. The free surfactant concentration reaches a plateau, indicating that any new surfactant molecule added to the system preferably undergoes micellation instead of remaining as a free surfactant chains in the bulk solution. Since the concentration of free amphiphiles remains almost constant after the CMC is reached, we can use the value of $X_1$ of micellar solutions as a good estimate for the value of the CMC at low surfactant concentrations. The CMC value is $\approx 7.0 \times 10^{-4}$ in mole fraction.

#### 5.3.1.2 $H_2T_6$

We study the micellization behavior of $H_2T_6$, both in spherical and infinite size cylindrical geometries. $10^6$ chain configurations were randomly generated on a lattice divided into spherical shells and infinite cylindrical shells, using the Rosenbluth and Rosenbluth chain growth algorithm[101], in a simulation box of volume $V = 19^3$. The predictions of the SCMFT for the standard chemical potential difference, $(\mu_N^o - \mu_1^o)/k_BT$, of micelles of aggregation number, $N$, at dimensionless temperature, $T^* = 9.5$, are shown in Fig. 5.5 for both spherical and infinite

UNIVERSITAT ROVIRA I VIRGILI
MICROSCOPIC MODELING OF THE SELF ASSEMBLY OF SURFACTANTS: SHAPE TRANSITIONS AND CRITICAL MICELLE CONCENTRATIONS
Asfaw Gezae Daful
ISBN:/DL:T. 1024-2011



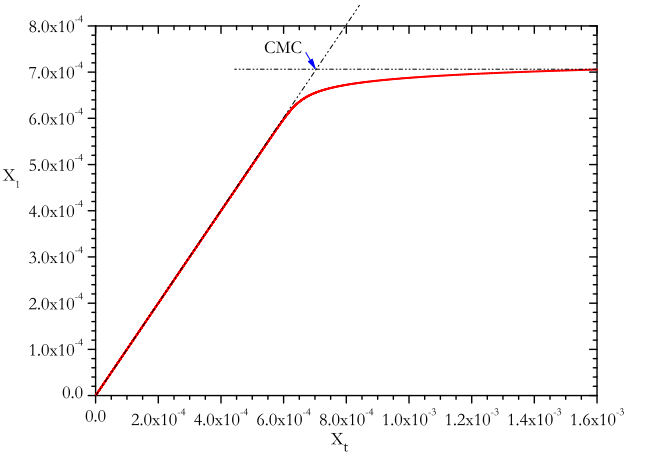


**Figure 5.4:** Free surfactant mole fraction ($X_1$) as a function of the total surfactant concentration ($X_N$) for $H_3T_6$, at $T^* = 9.5$. CMC$\approx 7.0 \times 10^{-4}$ in mole fraction

cylindrical micelles. In this case, the infinite cylindrical micelle has a lower standard chemical potential difference compared to that of the spherical micelles. Like $H_3T_6$, the infinite cylindrical micelle of $H_2T_6$ is more stable than the spherical micelle with lower standard chemical potential differences.

The radial distribution of volume fraction profiles of stable micelles that corresponds to the aggregation number of the minimum free energy of formation of the spherical and the infinite cylindrical micelles are shown in Fig. 5.6. As in the case of $H_3T_6$, the core is predominantly packed by the hydrophobic tail of the surfactant and the head groups are concentrated on the outside of the micelle, forming the corona of the micelle. The volume fraction profiles of the infinite cylindrical micelle are comparable to that of the spherical ones; the cores and coronas have the same characteristics. The hydrophobic core radius of the infinite cylindrical micelle is observed to be smaller than the spherical micelle, as discussed in section 5.3.1.1. The CMC value is calculated as shown in Fig. 5.7.

#### 5.3.1.3 $H_4T_4$

The self-assembly behavior of symmetric linear non ionic model surfactant, $H_4T_4$, has been studied. The equilibrium size and shape of the this model surfactant is studied by SCMFT and is observed that $H_4T_4$ prefers to form spherical mi-

UNIVERSITAT ROVIRA I VIRGILI
MICROSCOPIC MODELING OF THE SELF ASSEMBLY OF SURFACTANTS: SHAPE TRANSITIONS AND CRITICAL MICELLE CONCENTRATIONS
Asfaw Gezae Daful
ISBN:/DL:T. 1024-2011



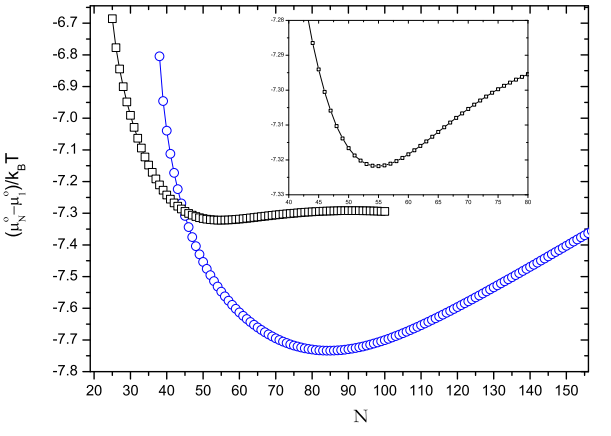


**Figure 5.5:** Standard chemical potential differences, $(\mu_N^o - \mu_1^o)/k_BT$, of $H_2T_6$, versus micellar aggregation number $N$ of the micelle at $T^* = 9.5$. Spherical micelle (squares)and infinite cylindrical micelle(circles). In the case of the infinite cylindrical geometry, the *x-axis* gives the number of surfactants for a 19 lattice site section of the infinite cylinder. The inset shows the standard chemical potential differences plot for the range of $N = 40$ to $N = 80$ for the spherical micelle

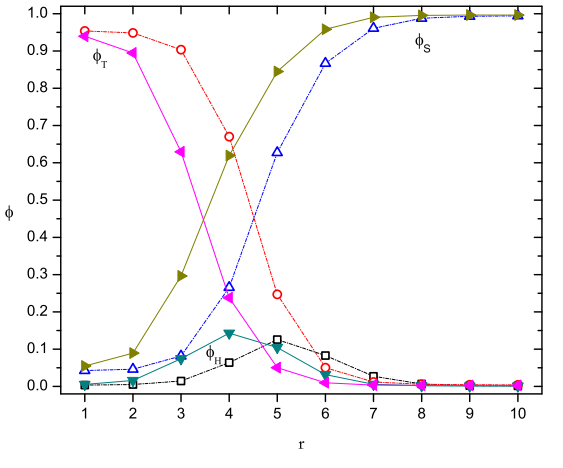


**Figure 5.6:** Radial variation of volume fraction profile of tail $\phi_T(r)$, head $\phi_H(r)$, and solvent $\phi_S(r)$, versus radius $r$, of the spherical micelle (dash dot dot lines with opened symbols) and infinite cylindrical micelle (solid lines with filled symbols) for $H_2T_6$ at $T^* = 9.5$

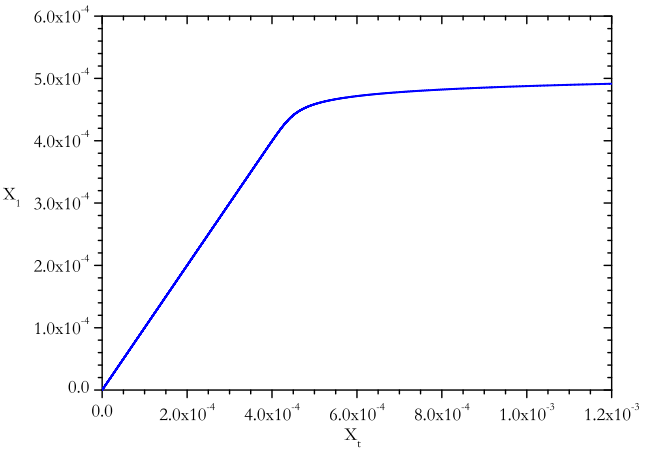


**Figure 5.7:** Free surfactant mole fraction ($X_1$) as a function of the total surfactant concentration ($X_N$) for $H_2T_6$. CMC$\approx 4.90 \times 10^{-4}$ in mole fraction

celles. $10^6$ chain configurations were randomly generated on a lattice divided into spherical shells, the same result were obtained when $10^7$ configurations were used. The standard chemical potential differences from of the SCMFT calculations at dimensionless temperatures, $T^* = 7.25$, $T^* = 7.0$ and $T^* = 6.5$ are shown in Fig. 5.8.

The standard chemical potential difference for spherical and infinite cylindrical micelles at $T^* = 6.5$ for $H_4T_4$ are presented in Fig. 5.9. It shows that the spherical micelle has a lower standard chemical potential difference than the infinite cylindrical micelle, implying that $H_4T_4$ prefers forming spherical micelles. The radial distribution of volume fraction profiles of stable micelles that corresponds to the aggregation number of the minimum free energy of formation of the spherical and the infinite cylindrical micelles are shown in Fig. 5.10. The total number of surfactants in the bulk is $N_{bulk} \approx 16$ for the spherical micelles and $N_{bulk} \approx 6$ for the infinite cylindrical micelles. As in the case of $H_2T_6$ and $H_3T_6$, the core is predominantly packed by the hydrophobic tail of the surfactant and the head groups are concentrated on the outside of the micelle, forming the corona of the micelle. The volume fraction profiles of the infinite cylindrical micelle are comparable to that of the spherical ones; the cores and coronas have the same characteristics. The hydrophobic core radius of the infinite cylindrical micelle is observed to be smaller than the spherical micelle, as discussed in section 5.3.1.1.

UNIVERSITAT ROVIRA I VIRGILI
MICROSCOPIC MODELING OF THE SELF ASSEMBLY OF SURFACTANTS: SHAPE TRANSITIONS AND CRITICAL MICELLE CONCENTRATIONS
Asfaw Gezae Daful
ISBN:/DL:T. 1024-2011



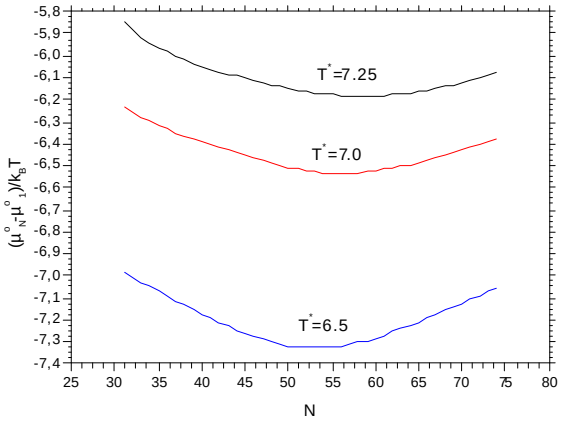


**Figure 5.8:** Standard chemical potential difference, $(\mu_N^o - \mu_1^o)/k_BT$, of spherical micelles of $H_4T_4$ versus micelles aggregation number, $N$, for dimensionless temperatures $T^* = 7.25$, $T^* = 7$ and $T^* = 6.5$, in a simulation box of size $19^3$

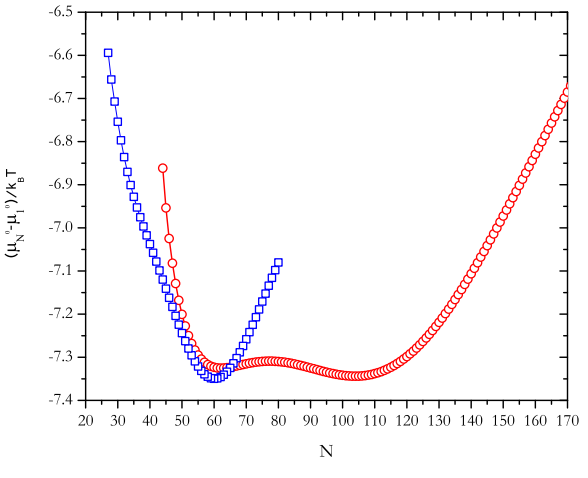


**Figure 5.9:** Standard chemical potential difference, $(\mu_N^o - \mu_1^o)/k_BT$, for spherical micelle (squares) and for infinite cylindrical micelle (circles), of $H_4T_4$, at dimensionless temperature $T^* = 6.5$. In the case of the infinite cylindrical geometry, the *x-axis* gives the number of surfactants for a 19 lattice site section of the infinite cylinder.

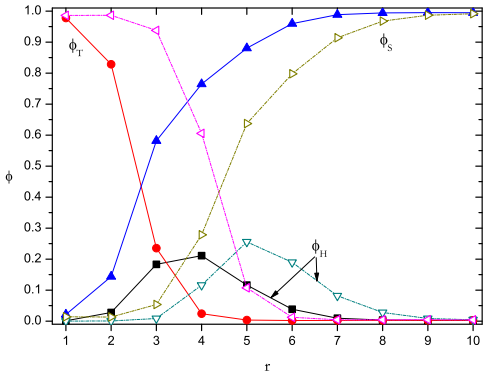


**Figure 5.10:** Radial variation of volume fraction profile of tail $\phi_T(r)$, head $\phi_H(r)$, and solvent $\phi_S(r)$, versus radius $r$, of the spherical micelle (dash dot dot lines with opened symbols) and infinite cylindrical micelle (solid lines with filled symbols) for $H_4T_4$

#### 5.3.1.4 $H_3T_3$, $H_4T_5$, $H_4T_6$ and $H_4T_{16}$

Similarly, the micellization process of $H_3T_3$ at $T^* = 7.0$, $H_4T_5$ at $T^* = 9.5$, $H_4T_6$ at $T^* = 9.5$ and $H_4T_{16}$ at $T^* = 16.0$ are studied using SCMFT and stable spherical micelles are obtained. We present the standard chemical potential difference, $(\mu_N^o - \mu_1^o)/k_BT$, between the free surfactant chains in the bulk solution and surfactants associated with the micelles of aggregation number, $N$; and the volume fraction profiles of the hydrophobic tail, hydrophilic head and solvent corresponding to the micelles with minimum free energy of formation, in Figs. (5.12 – 5.15). The minimum in the standard chemical potential difference corresponds to the optimal aggregation number.

Our microscopic model captures the main aspects of the sphere to cylinder transition. After studying the micellization behavior and stability of the selected model surfactants. We chose $H_4T_4$ and $H_3T_6$ as candidates to study the shape transitions of micelles which are dealt with two dimensional Single Chain Mean Field Theory, as will be discussed in the following section (section 5.3.2).

UNIVERSITAT ROVIRA I VIRGILI
MICROSCOPIC MODELING OF THE SELF ASSEMBLY OF SURFACTANTS: SHAPE TRANSITIONS AND CRITICAL MICELLE CONCENTRATIONS
Asfaw Gezae Daful
ISBN:/DL:T. 1024-2011



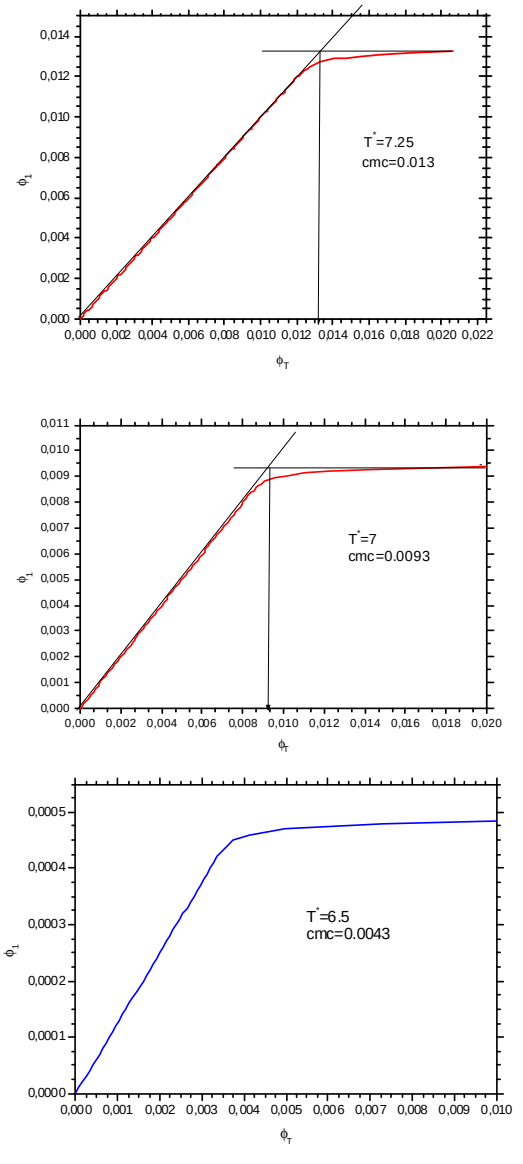


**Figure 5.11:** Free surfactant volume fraction $\phi_1$ versus the total surfactant volume fraction $\phi_t$ for $H_4T_4$ at dimensionless temperatures, $T^*$ of 6.5, 7.0 and 7.25

UNIVERSITAT ROVIRA I VIRGILI
MICROSCOPIC MODELING OF THE SELF ASSEMBLY OF SURFACTANTS: SHAPE TRANSITIONS AND CRITICAL MICELLE CONCENTRATIONS
Asfaw Gezae Daful
ISBN:/DL:T. 1024-2011



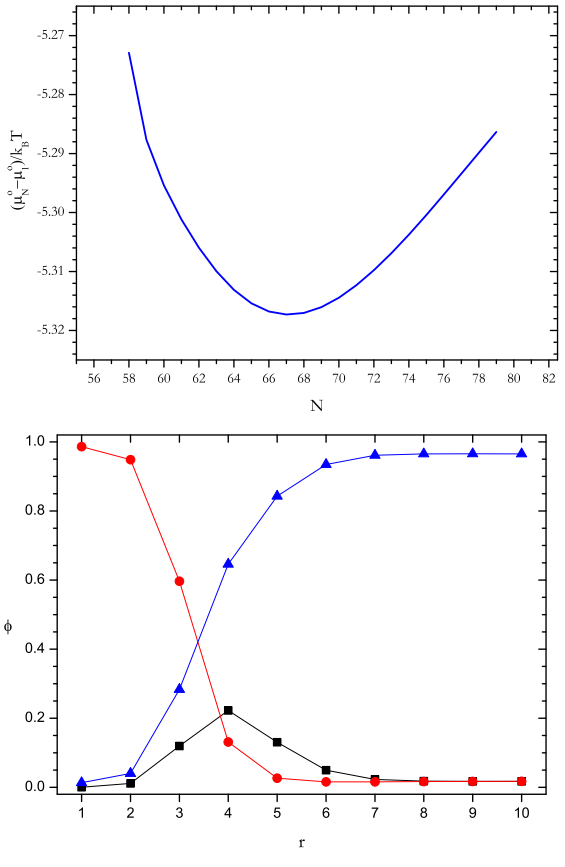


**Figure 5.12:** Standard chemical potential difference of $H_3T_3$ versus micelles aggregation number, $N$ (left); radial variation of volume fraction profile of tail, $\phi_T(r)$ head $\phi_H(r)$, and solvent $\phi_S(r)$, versus radius $r$, of the spherical micelle ($N = 67$) (right); for dimensionless temperature $T^* = 7.0$, box size $19^3$

UNIVERSITAT ROVIRA I VIRGILI
MICROSCOPIC MODELING OF THE SELF ASSEMBLY OF SURFACTANTS: SHAPE TRANSITIONS AND CRITICAL MICELLE CONCENTRATIONS
Asfaw Gezae Daful
ISBN:/DL:T. 1024-2011



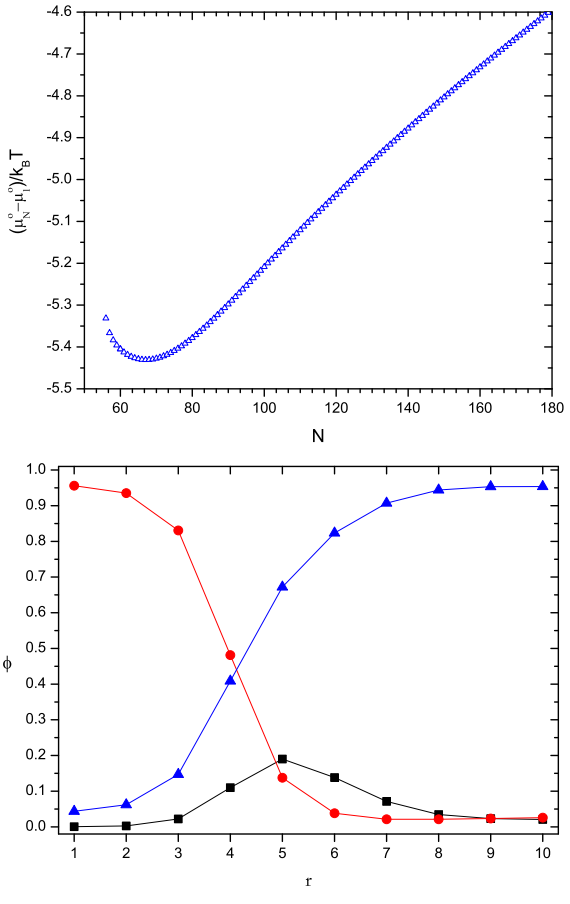


**Figure 5.13:** Standard chemical potential difference of $H_4T_5$ versus micelles aggregation number, $N$ (left); radial variation of volume fraction profile of tail, $\phi_T(r)$ head $\phi_H(r)$, and solvent $\phi_S(r)$, versus radius $r$, of the spherical micelle ($N = 70$) (right); for dimensionless temperature $T^* = 9.5$, box size $19^3$

UNIVERSITAT ROVIRA I VIRGILI
MICROSCOPIC MODELING OF THE SELF ASSEMBLY OF SURFACTANTS: SHAPE TRANSITIONS AND CRITICAL MICELLE CONCENTRATIONS
Asfaw Gezae Daful
ISBN:/DL:T. 1024-2011



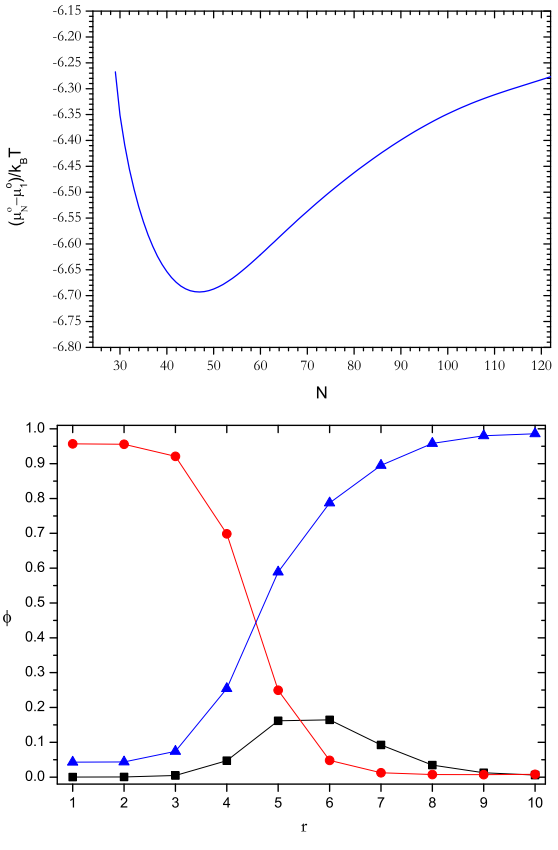


**Figure 5.14:** Standard chemical potential difference of $H_4T_6$ versus micelles aggregation number, $N$ (left); radial variation of volume fraction profile of tail, $\phi_T(r)$ head $\phi_H(r)$, and solvent $\phi_S(r)$, versus radius $r$, of the spherical micelle ($N = 50$) (right); for dimensionless temperature $T^* = 9.5$, box size $19^3$

UNIVERSITAT ROVIRA I VIRGILI
MICROSCOPIC MODELING OF THE SELF ASSEMBLY OF SURFACTANTS: SHAPE TRANSITIONS AND CRITICAL MICELLE CONCENTRATIONS
Asfaw Gezae Daful
ISBN:/DL:T. 1024-2011



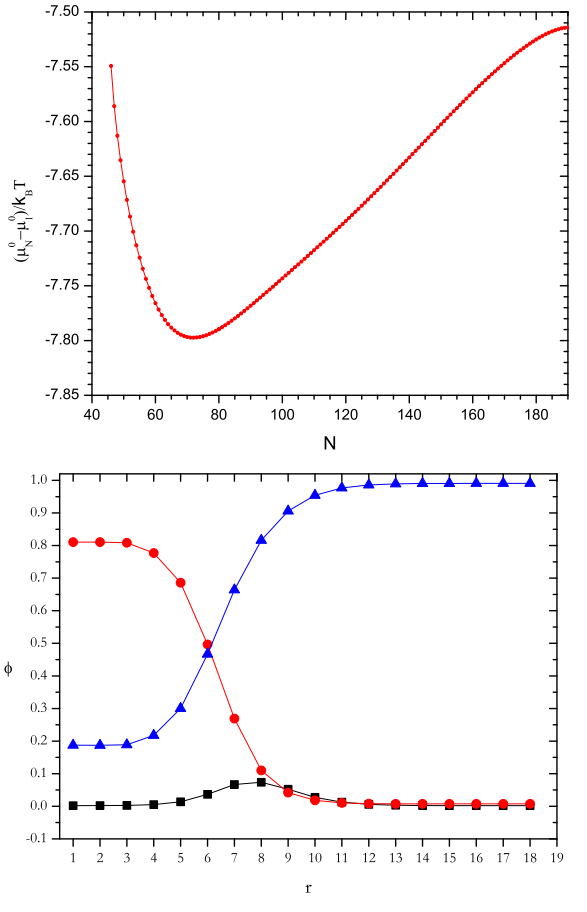


**Figure 5.15:** Standard chemical potential difference of $H_4T_{16}$ versus micelles aggregation number, $N$ (left); radial variation of volume fraction profile of tail, $\phi_T(r)$ head $\phi_H(r)$, and solvent $\phi_S(r)$, versus radius $r$, of the spherical micelle ($N = 70$) (right); for dimensionless temperature $T^* = 16.0$, box size $35^3$

UNIVERSITAT ROVIRA I VIRGILI
MICROSCOPIC MODELING OF THE SELF ASSEMBLY OF SURFACTANTS: SHAPE TRANSITIONS AND CRITICAL MICELLE CONCENTRATIONS
Asfaw Gezae Daful
ISBN:/DL:T. 1024-2011



**Table 5.2:** CMC values of model nonlinear surfactants in mole fraction ($X$) and volume fraction ($\phi$)

| | | CMC | |
|---|---|---|---|
| | $T^*$ | X | $\phi$ |
| $H_2T_6$ | 9.5 | $4.90 \times 10^{-04}$ | $3.92 \times 10^{-03}$ |
| $H_3T_3$ | 7.0 | $4.10 \times 10^{-03}$ | $2.46 \times 10^{-02}$ |
| $H_3T_6$ | 9.5 | $7.00 \times 10^{-04}$ | $6.30 \times 10^{-03}$ |
| | 11.5 | $3.70 \times 10^{-04}$ | $3.33 \times 10^{-02}$ |
| $H_4T_4$ | 6.5 | $4.95 \times 10^{-04}$ | $3.96 \times 10^{-03}$ |
| | 7.0 | $1.15 \times 10^{-03}$ | $9.20 \times 10^{-03}$ |
| | 7.25 | $1.63 \times 10^{-03}$ | $1.30 \times 10^{-02}$ |
| $H_4T_5$ | 9.5 | $3.65 \times 10^{-03}$ | $3.29 \times 10^{-02}$ |
| $H_4T_6$ | 9.5 | $9.5 \times 10^{-04}$ | $9.5 \times 10^{-03}$ |
| $H_4T_{16}$ | 16 | $3.30 \times 10^{-04}$ | $6.6 \times 10^{-03}$ |

### 5.3.2 2D Spherical and Finite Size Cylindrical Micelles

At surfactant concentrations below the critical micelle concentration, mainly singly dispersed molecules are present in the solution. In contrast, at concentrations above the critical micelle concentration, micelles containing a large number of surfactant molecules are formed in the solution, that can assume a variety of shapes such as spherical, ellipsoidal micelles, large cylindrical micelles which may be rigid or flexible, and spherical bilayer vesicles, etc. One does expect that the hydrophobic tails of the surfactants that aggregate together to form a micelle will concentrate in the center of the micelle, to maximize the number of tail-tail contacts, so that the hydrophilic heads be expelled to the outer regions forming the corona of the micelle. This fundamental micellar behavior has been shown for simple spherical and infinite cylindrical micelles in section 5.3.1 using one dimensional Single Chain Mean Field Theory. Such behavior of micellization process and the concentration induced shape transition, that the micelle may undergo, have quantitatively been produced for micelles of different geometric shapes using the two dimensional Single Chain Mean Field Theory (2D SCMFT). We present 2D SCMFT, and Monte Carlo simulation results, that shed light on the morphological transformation of micelles; and answers to the questions, what is the aggregate shape at low concentration, and how the shape of this aggregate changes upon increasing concentration. Particularly, the shape transition from spherical to finite size cylindrical micelles (or disk like micelles) by increasing the surfactant concen-

UNIVERSITAT ROVIRA I VIRGILI
MICROSCOPIC MODELING OF THE SELF ASSEMBLY OF SURFACTANTS: SHAPE TRANSITIONS AND CRITICAL MICELLE CONCENTRATIONS
Asfaw Gezae Daful
ISBN:/DL:T. 1024-2011



tration in the system will be shown. As pointed out in section 5.3.1, we chose the linear surfactants $H_4T_4$ and $H_3T_6$ to study the morphological transformations of micelles with concentration in 2D SCMFT and Monte Carlo simulations.

The 2D SCMFT is checked to reproduce the standard chemical potential difference and other relevant properties obtained in the 1D SCMFT. As it is shown in Fig. 5.16 and Fig. 5.17 the minumum in the standard chemical potentials coincide for the 1D-SCMFT and 2D-SCMFT.

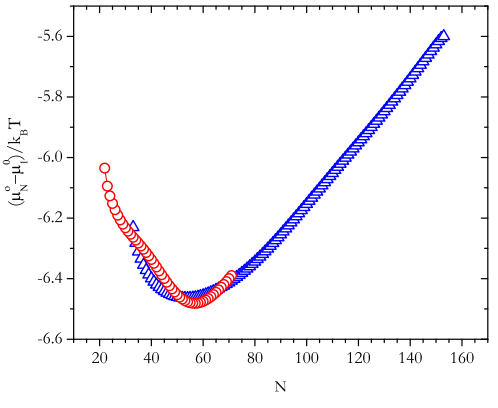


**Figure 5.16:** Standard chemical potential differences, $(\mu_N^o - \mu_1^o)/k_BT$, vs. $N$, from 1D-SCMFT (circles) and 2D-SCMFT (triangles) for $H_4T_4$ at $T^* = 7.0$

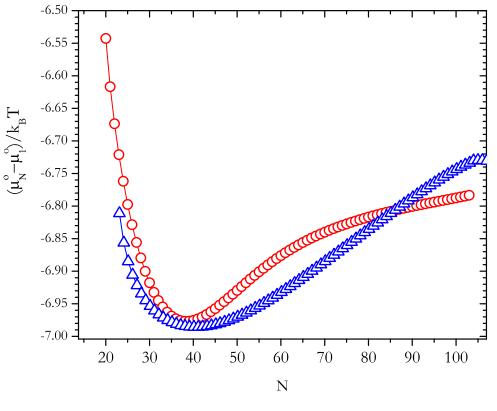


**Figure 5.17:** Standard chemical potential differences, $(\mu_N^o - \mu_1^o)/k_BT$, vs. $N$, from 1D-SCMFT (circles) and 2D-SCMFT (triangles) for $H_3T_6$ at $T^* = 9.5$

UNIVERSITAT ROVIRA I VIRGILI
MICROSCOPIC MODELING OF THE SELF ASSEMBLY OF SURFACTANTS: SHAPE TRANSITIONS AND CRITICAL MICELLE CONCENTRATIONS
Asfaw Gezae Daful
ISBN:/DL:T. 1024-2011



## $H_4T_4$

A stable spherical micelle is formed at low concentration with a minimum in the standard chemical potential difference, Fig. 5.18. A typical two dimensional contour plot of volume fraction profiles of tail, head of the surfactant for spherical as well as the solvent for a system with $N = 60$ is shown in Fig. 5.19. Fig. 5.20, shows the contour plots for the volume fraction profiles of the hydrophilic tail group for selected systems with total number of $N$ surfactants. Increasing surfactant number increases the size of the spherical micelle without changing its geometric shape. This behavior of $H_4T_4$ is also shown using Monte Carlo simulations, by calculating the ratios radii of gyration tensors. Fig. 5.22, shows that the shape of the micelles remain spherical as the surfactant concentration increases. As the surfactant concentration increases, the number of spherical micelles increase. Similar to the 1D-SCMFT results shown in section 5.3.1.3, the 2D-SCMFT and Monte Carlo simulation results also show that this symmetric linear surfactant, $H_4T_4$ prefers to form spherical micelles. The total number of surfactants in the bulk is $N_{bulk} \approx 10$.

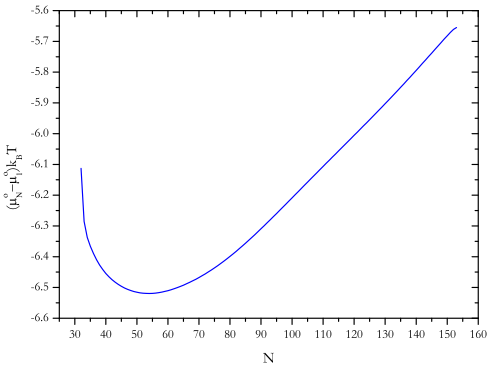


**Figure 5.18:** Standard chemical potential differences, $(\mu_N^o - \mu_1^o)/k_BT$, vs. $N$, for spherical micelles of $H_4T_4$ at $T^* = 7.0$, from 2D-SCMFT simulation, $N_{bulk} \approx 10$

We also present a three-dimensional *isosurface*, that is a surface representing points of constant value from the volume fraction profiles of the hydrophobic tail. The 3D-*isosurface* plots shown in Fig. 5.21 correspond to the layer (surface) of the core of the micelle at which $\phi_T(r, z) \approx \phi_T^{bulk}$, where $\phi_T^{bulk}$ is the bulk concentration of the hydrophobic tail (volume fraction).

The equilibrium micelle size distribution Monte Carlo simulation for the same system with volume fractions 0.016, 0.024, and 0.032, is shown in Fig. 5.23. The

UNIVERSITAT ROVIRA I VIRGILI
MICROSCOPIC MODELING OF THE SELF ASSEMBLY OF SURFACTANTS: SHAPE TRANSITIONS AND CRITICAL MICELLE CONCENTRATIONS
Asfaw Gezae Daful
ISBN:/DL:T. 1024-2011



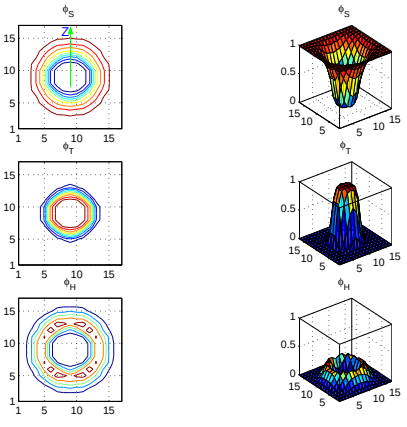

**Figure 5.19:** Volume fraction profile of the solvent ($\phi_S$), hydrophobic tail ($\phi_T$), and hydrophilic head ($\phi_H$) from top to bottom. 2D contour plots (left) and 3D surface plots (right) of spherical micelle of $N = 60$, in a cubic box of $V = 17^3$. For the linear surfactant $H_4T_4$ at $T^* = 7.0$. $N_{bulk} \approx 10$

micellar size distributions are smooth with a single peak. The peaks at an aggregation number of about 80, correspond to the spherical micelle. One can see that only spherical micelles are formed by the linear symmetric surfactant $H_4T_4$.

## $H_3T_6$

In section 5.3.1.1, we have shown that the infinite cylindrical micelle of $H_3T_6$ has a lower standard chemical potential difference than the spherical micelle, unlike that of $H_4T_4$ (see section 5.3.1.3). In this section, we will present 2D-SCMFT and Monte Carlo simulation results that can help to understand the micellization process and the concentration induced shape transition. A spherical micelle is formed at low concentration, then it is observed that the micelle can undergo one dimensional growth into finite size cylindrical micelle or a two dimensional growth into disk micelles. These morphological transformations are also seen to pass through some intermediate shapes such as prolate and oblate spheroids. Two dimensional contour plots of volume fraction profiles for spherical, prolate micelle and finite size cylindrical micelles as well as infinitely long cylindrical micelles are shown in Figs. 5.24 and 5.25.The volume fraction profiles of spherical and finite size cylindrical micelles are presented in terms of equal density contour plots as well as 3D surface plots, where the higher values of volume fraction are given by red

UNIVERSITAT ROVIRA I VIRGILI
MICROSCOPIC MODELING OF THE SELF ASSEMBLY OF SURFACTANTS: SHAPE TRANSITIONS AND CRITICAL MICELLE CONCENTRATIONS
Asfaw Gezae Daful
ISBN:/DL:T. 1024-2011



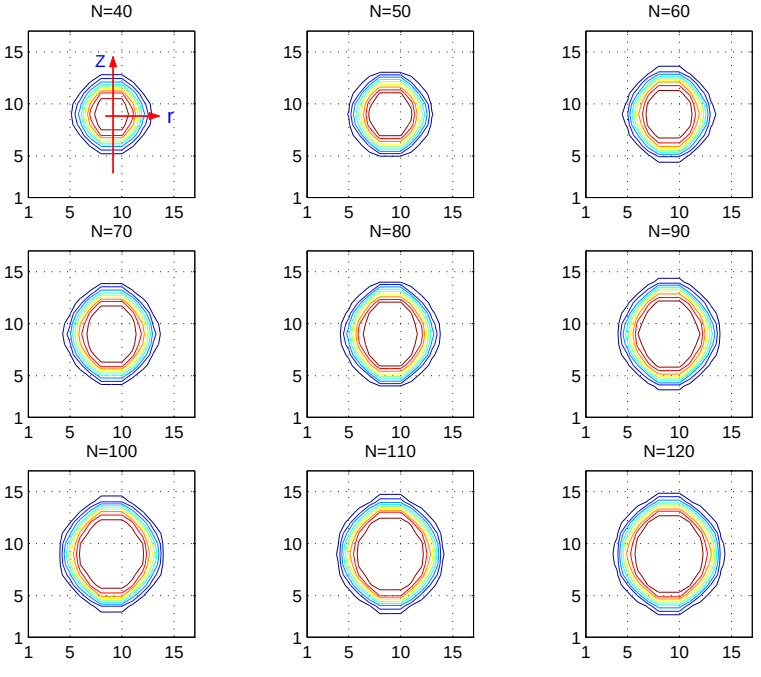


**Figure 5.20:** Volume fraction profile of the hydrophobic tails ($\phi_T$), showing that the spherical micelle of $H_4T_4$ surfactant keeps on growing without changing its spherical shape. These micelles are presented for selected systems with total number of surfactants, $N$, from a simulation box of volume, $V = 17^3$. For linear surfactant $H_4T_4$ at $T^* = 7.0$.

UNIVERSITAT ROVIRA I VIRGILI
MICROSCOPIC MODELING OF THE SELF ASSEMBLY OF SURFACTANTS: SHAPE TRANSITIONS AND CRITICAL MICELLE CONCENTRATIONS
Asfaw Gezae Daful
ISBN:/DL:T. 1024-2011



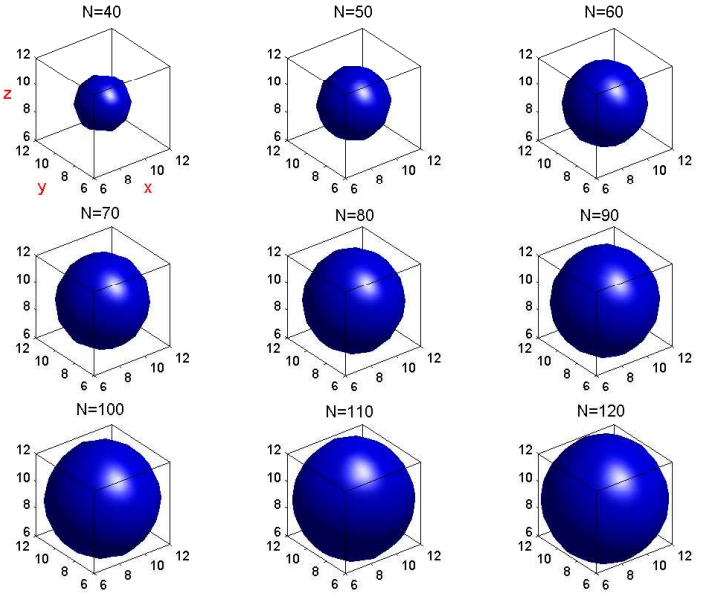


**Figure 5.21:** The 3D-*isosurface* plots of the hydrophobic core of micelles of different aggregation number, $N$. The *isosurfaces* correspond to the layer (surface) of the core of the micelle where $\phi_T(r,z) \approx \phi_T^{bulk}$. For linear surfactant $H_4T_4$ at $T^* = 7.0$

UNIVERSITAT ROVIRA I VIRGILI
MICROSCOPIC MODELING OF THE SELF ASSEMBLY OF SURFACTANTS: SHAPE TRANSITIONS AND CRITICAL MICELLE CONCENTRATIONS
Asfaw Gezae Daful
ISBN:/DL:T. 1024-2011



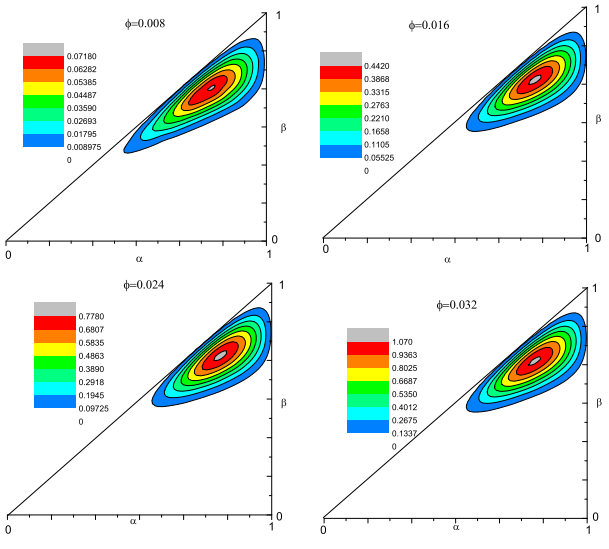


**Figure 5.22:** Contour plots of the distribution function $PD(\alpha, \beta)$ (sec. 4.5.2), plotted as a function of $\alpha$ and $\beta$, for systems with volume fraction, $\phi$ of 0.008, 0.016, 0.024, and 0.032,(containing 1000, 2000, 3000, and 4000 surfactants) in a simulation box of volume $V = 100^3$ for $H_4T_4$ at $T^* = 6.5$

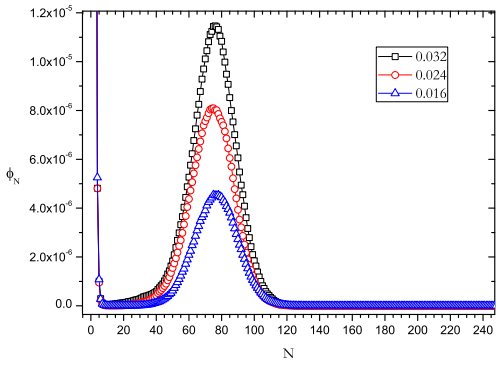


**Figure 5.23:** Micellar size distribution for systems with volume fractions 0.016, 0.024, and 0.032 in a simulation box of volume $100^3$, for $H_4T_4$ at $T^* = 6.5$.

and the lower as blue. Volume fraction profiles of both the tail and head groups as well as the solvent are presented. A contour plot representing the volume fraction profiles in color scaling for a spherical micelle of aggregation number, $N = 60$, prolate spheroid, $N = 130$ and finite size cylindrical micelle, $N = 240$ are shown in Figs. 5.24 and 5.25. The structure of the cylindrical micelle has many features in common with simple spherical micelles. The core of the micelle is composed of hydrophobic tails of the surfactant and the hydrophilic heads are on the surface forming hydrophilic corona. From the 2D contour and the 3D surface plots of the volume fraction profiles it is clearly seen that the two ends of the cylindrical micelle have a slightly larger diameter than the cylindrical body. The total number of surfactant in the bulk, $N_{bulk}$, are also calculated, as will be shown in Fig. 5.33.

#### 5.3.2.1 Micelle Shape and Size: Volume Fraction Profiles

The shapes of the have been shown through 2D contour and 3D-*isosurface* plots of the volume fraction profiles of the solvent, the head and tail parts of the amphiphilic surfactant, as a function of total number of surfactants in the system, $N$. The volume fraction profile of the hydrophobic tail parts of the surfactants is presented for micelles of selected systems with total number of surfactants $N$, so as to show how the shape of the micelle changes upon increase of $N$. Volume fraction profiles of selected systems with $N$ equal to 60, 80, 90, 100, 110, 120, 130, 140 and 150 in a simulation box of volume $V = 27^3$ are shown in Fig. 5.26. Similarly the volume fraction profiles of selected micelles of higher number of surfactants, $N$ equal to 163, 175, 180, 190, 200, 210, 220, 230, 240, 250, 255 and 260 in a bigger simulation box of volume $V = 35^3$ are shown in Fig. 5.27. One can see how the finite size cylindrical micelle evolves from the spherical micelle as $N$ increases. As can clearly be seen in Fig. 5.26, at lower concentrations distinctly spherical micelles are formed. Increasing surfactant concentration increases the size of the micelle up to a point, where it can no longer grow keeping its spherical shape. The spherical micelle first starts to elongate in the *z-axis* at about $N \approx 80$ forming an ellipsoidal spheres, (about $N \approx 90$ up to $N \approx 120$). The micelle keeps on elongating in the *z-axis* and finally changes to a prolate spheroid shape micelle (see Fig. 5.26) for $N$ around 120 up to about 130. The prolate spheroid micelle continues growing into *croquette* like structure (*e.g.* $N \approx 140$). The *croquette* like structure of the micelle elongates and evolves to a rod micelle (*e.g.* $N = 150$).

Due to finite size effects, (the micelle size gets bigger and starts to touch the wall of the simulation box at about $N = 160$, not included here), we used a simulation box of bigger volume, $V = 35^3$, to completely see how the shape of the aggregate transforms for higher aggregation numbers. The prolate micelles (say

UNIVERSITAT ROVIRA I VIRGILI
MICROSCOPIC MODELING OF THE SELF ASSEMBLY OF SURFACTANTS: SHAPE TRANSITIONS AND CRITICAL MICELLE CONCENTRATIONS
Asfaw Gezae Daful
ISBN:/DL:T. 1024-2011



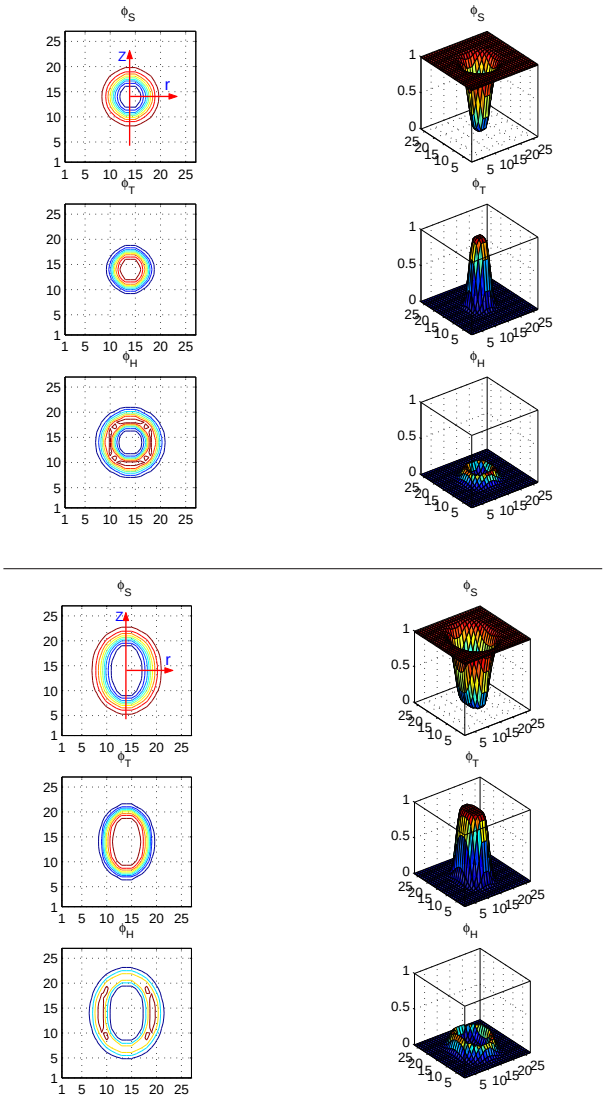


**Figure 5.24:** Volume fraction profile of the solvent, hydrophobic tail, and hydrophilic head from top to bottom. 2D contour plots (left) and 3D surface plots (right); of spherical micelle of $N = 60$ (above) and a prolate spheroid micelle of $N = 130$ (below), in a simulation box of $V = 27^3$ for the linear surfactant $H_3T_6$ at $T^* = 9.5$, $N_{bulk} \approx 22$ in both cases.

UNIVERSITAT ROVIRA I VIRGILI
MICROSCOPIC MODELING OF THE SELF ASSEMBLY OF SURFACTANTS: SHAPE TRANSITIONS AND CRITICAL MICELLE CONCENTRATIONS
Asfaw Gezae Daful
ISBN:/DL:T. 1024-2011



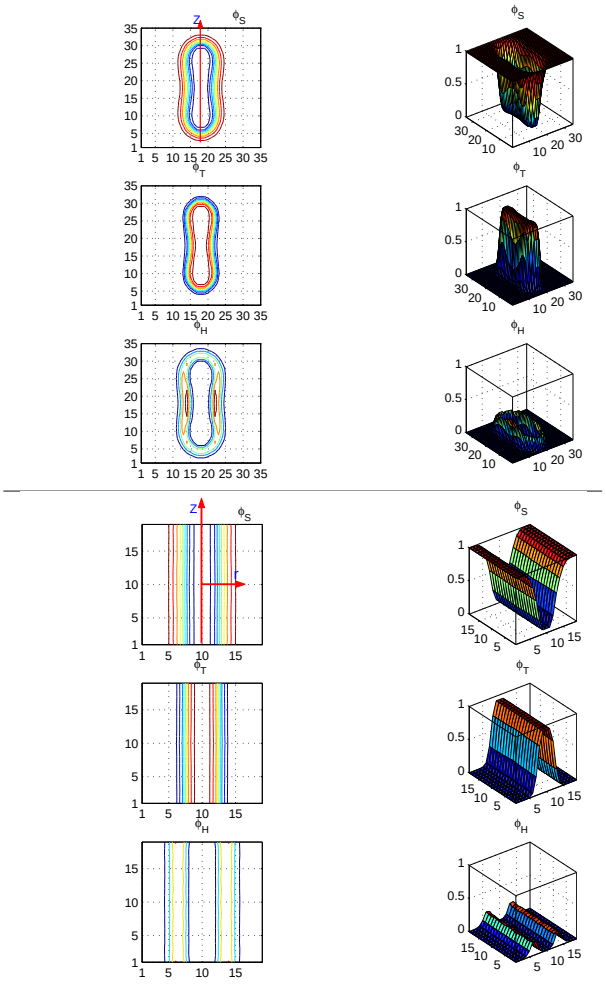


**Figure 5.25:** Volume fraction profile of the solvent, hydrophobic tail, and hydrophilic head from top to bottom. 2D contour plots (left) and 3D surface plots (right); for a finite size cylindrical micelle of $N = 240$, in a simulation box of $V = 35^3$ (above) and an infinitely long cylindrical micelle of $N = 90$ in a simulation box of $V = 19^3$ (below) for a linear surfactant $H_3T_6$ at $T^* = 9.5$, $N_{bulk} \approx 52$

UNIVERSITAT ROVIRA I VIRGILI
MICROSCOPIC MODELING OF THE SELF ASSEMBLY OF SURFACTANTS: SHAPE TRANSITIONS AND CRITICAL MICELLE CONCENTRATIONS
Asfaw Gezae Daful
ISBN:/DL:T. 1024-2011



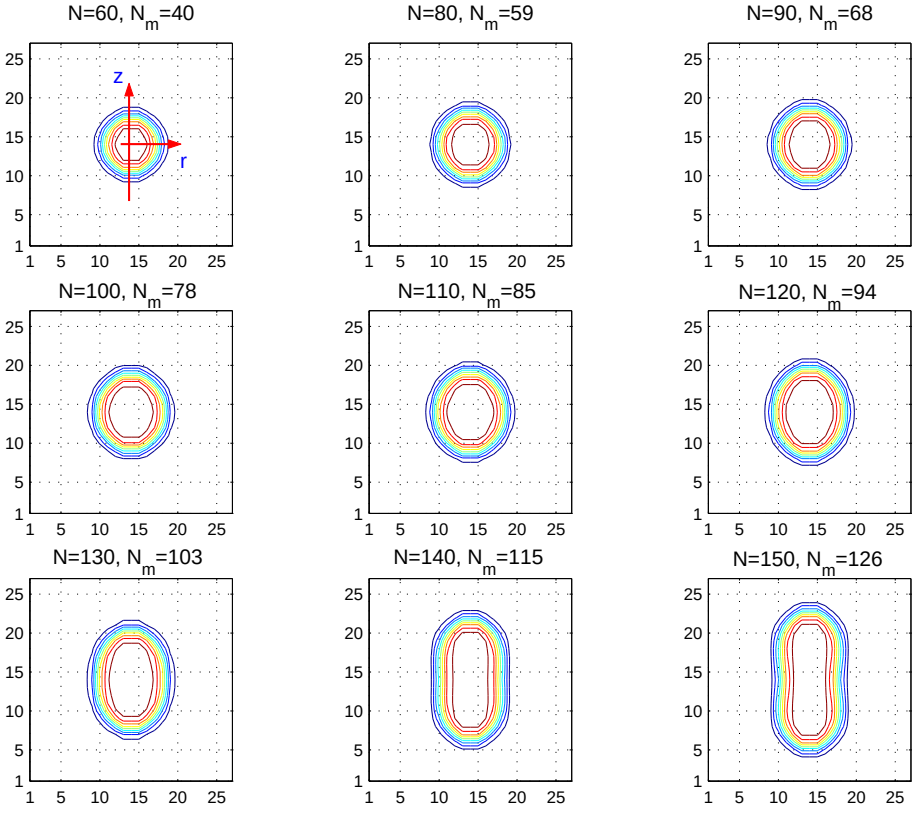


**Figure 5.26:** Volume fraction profile of the hydrophobic tails, showing the shape transition of micelles. Spherical, ellipsoidal, prolate spheroids and croquette like micelles are presented for systems of selected number of surfactants, $N$, from simulations in a cubic box of volume, $V = 27^3$. For linear surfactant $H_3T_6$ at $T^* = 9.5$.

UNIVERSITAT ROVIRA I VIRGILI
MICROSCOPIC MODELING OF THE SELF ASSEMBLY OF SURFACTANTS: SHAPE TRANSITIONS AND CRITICAL MICELLE CONCENTRATIONS
Asfaw Gezae Daful
ISBN:/DL:T. 1024-2011



for $N = 163$) change to croquette like structure ($N = 175$) upon increase of $N$, and then finite size cylindrical micelles are observed to evolve at about $N = 190$, see Fig. 5.27.

The finite size cylindrical micelle has two parts, the cylindrical part and the hemispherical end caps. This was convincingly argued by Eriksson [9] and others [32, 100] that the end caps of cylindrical micelles must have a larger diameter than their cylindrical body. Since the limit of the spherical packing of the hydrophobic parts of the surfactant is already achieved in the hemispherical end caps, further addition of surfactants to such a micelle does not lead to the reconstruction of the end caps rather only elongates the cylindrical part of the micelle. One can clearly see that the cylindrical part of the micelle increases in length with $N$, where with an addition of approximately 8 extra surfactants to the system, the cylindrical micelle lengths increases by one lattice site.

Similarly, we present a three-dimensional *isosurface*, that is a surface representing points of constant value from the volume fraction profiles of the hydrophobic tail. The 3D-*isosurface* plots shown in Fig. 5.28 correspond to the layer (surface) of the core of the micelle at which $\phi_T(r, z) \approx \phi_T^{bulk}$, where $\phi_T^{bulk}$ is the bulk concentration of the hydrophobic tail (volume fraction). Fig. 5.28 shows the evolution in the shape of micelles that are formed in aqueous solution of $H_3T_6$ surfactant on increasing the surfactant concentration. The spherical micelle( say $N = 60$) first becomes an ellipsoidal and prolate spheroid ($N = 120$, $N = 130$ and $N = 163$) with increasing concentration. On further increasing of the concentration of the surfactant, the prolate spheroid micelles is converted into croquette shaped micelle. The end caps of finite size cylindrical micelle are observed to form on the croquette like micelle with increasing the concentration. Once the end cap and the cylindrical body are formed, the length of the cylindrical body increases upon increasing the surfactant concentration. It is quite interesting that the two dimensional SCMFT used in the present work successfully shows the concentration induced sphere to cylinder transition of the micelle.

UNIVERSITAT ROVIRA I VIRGILI
MICROSCOPIC MODELING OF THE SELF ASSEMBLY OF SURFACTANTS: SHAPE TRANSITIONS AND CRITICAL MICELLE CONCENTRATIONS
Asfaw Gezae Daful
ISBN:/DL:T. 1024-2011



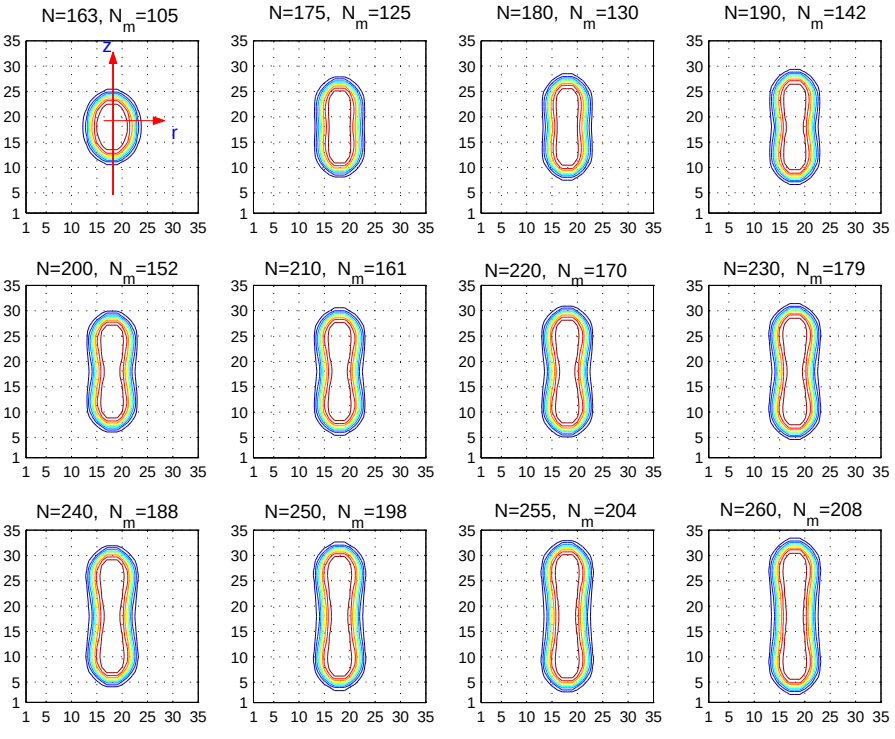


**Figure 5.27:** Volume fraction profile of the hydrophobic tails, showing the shape transition of micelles. Ellipsoidal, prolate spheroids, croquette like micelles and finite size cylindrical micelles are presented for selected systems with $N$ surfactants, from simulations in a cubic box of volume $V = 35^3$. For linear surfactant $H_3T_6$ at $T^* = 9.5$.

UNIVERSITAT ROVIRA I VIRGILI
MICROSCOPIC MODELING OF THE SELF ASSEMBLY OF SURFACTANTS: SHAPE TRANSITIONS AND CRITICAL MICELLE CONCENTRATIONS
Asfaw Gezae Daful
ISBN:/DL:T. 1024-2011



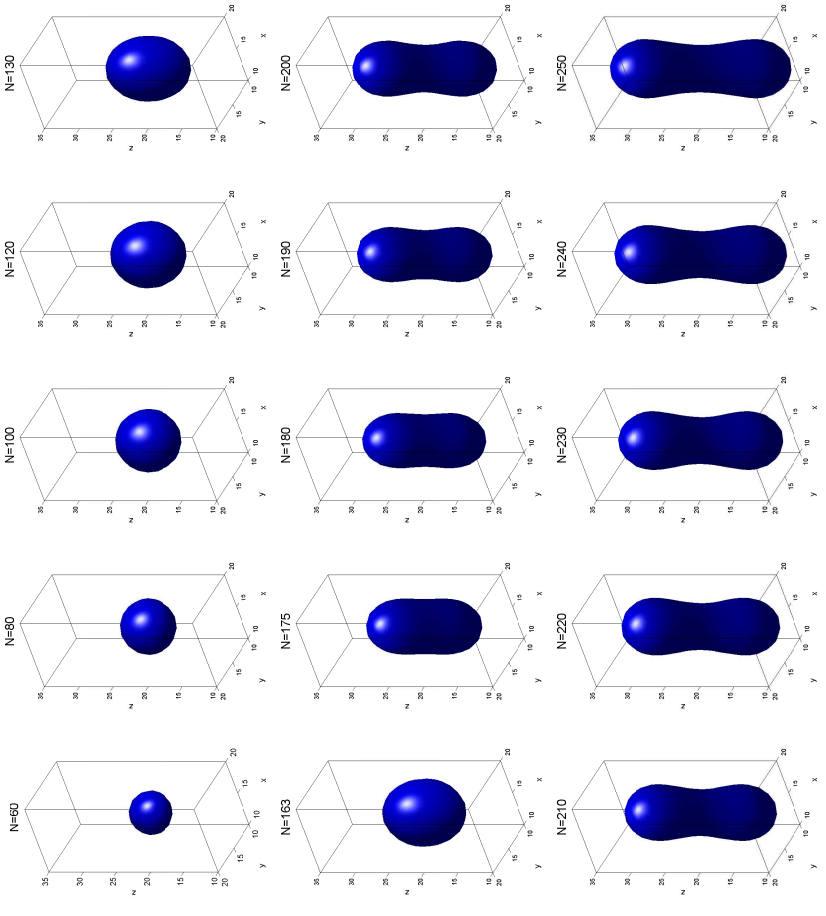


**Figure 5.28:** The 3D-*isosurface* plots of the hydrophobic core of micelles of different $N$. The *isosurfaces* correspond to the layer (surface) of the core of the micelle where $\phi_T(r,z) \approx \phi_T^{bulk}$. For linear surfactant $H_3T_6$ at $T^* = 9.5$

UNIVERSITAT ROVIRA I VIRGILI
MICROSCOPIC MODELING OF THE SELF ASSEMBLY OF SURFACTANTS: SHAPE TRANSITIONS AND CRITICAL MICELLE CONCENTRATIONS
Asfaw Gezae Daful
ISBN:/DL:T. 1024-2011



#### 5.3.2.2 Principal Moments of Inertia

Notwithstanding the visual evidences of the volume fraction profiles of the micelles, we also calculate the ratios of the principal moments of inertia of the aggregates. Fig. 5.29 shows the ratios $I_{xx}/I_{zz}$ versus the total number of surfactants in the system, $N$. The micelle shape is perfectly spherical when the ratios the three moments of inertia equal to 1 , and $I_{xx}$ and $I_{yy}$ increase as the micelle elongates along the $z$-axis, while $I_{zz}$ remains constant. From Fig. 5.29, we can also see that the value of $I_{xx}/I_{zz}$, increases with the size of the micelle, especially for $N \geq 70$ indicating that the micelle elongates along the $z$-axis. At the same time, the ratio $I_{xx}/I_{yy} = 1$ by definition and for the whole simulation series and $I_{xx}/I_{zz} = I_{yy}/I_{zz}$, (not shown) again indicating that the micelle elongates preferentially in the *z-axis*. As already mentioned in the previous section, the simulation has been continued in a large simulation box and the ratios of the three principal moments of inertia. Similarly, it is observed that the ratio $I_{xx}/I_{zz}$ increase with surfactant concentration indicating that the micelle elongates preferentially in the *z-axis*. This supports, the visual evidences from the volume fraction profiles, that the spherical micelle elongates to prolate spheroid, and then to coquette like structure which finally elongates into finite size cylindrical micelle upon increasing surfactant concentration.

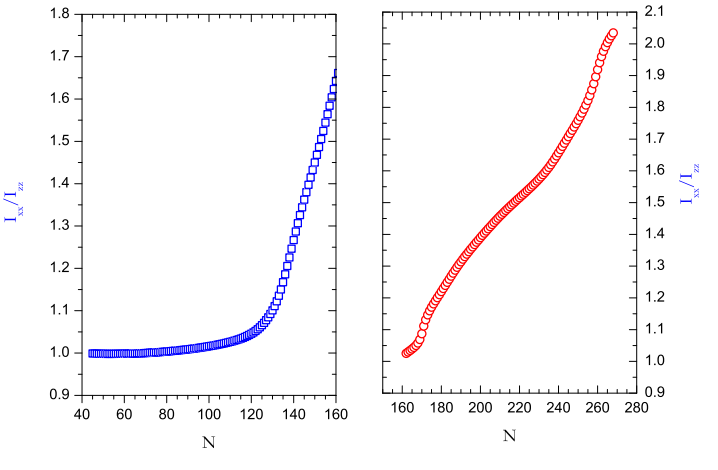


**Figure 5.29:** Variation of the ratio of the principal moments of inertia, $I_{xx}/I_{zz}$, with the total number of surfactants in the system, $N$, for simulation boxes of volume sizes $V = 27^3$ (squares) and $V = 35^3$ (circles)

UNIVERSITAT ROVIRA I VIRGILI
MICROSCOPIC MODELING OF THE SELF ASSEMBLY OF SURFACTANTS: SHAPE TRANSITIONS AND CRITICAL MICELLE CONCENTRATIONS
Asfaw Gezae Daful
ISBN:/DL:T. 1024-2011



#### 5.3.2.3 Standard Chemical Potential Differences

The thermodynamic parameter that determines the equilibrium between singly dispersed surfactants in the solution and surfactants associated in micelles of different size and shape is the difference between their standard chemical potentials. The Single Chain Mean Field Theory presents us a direct access to the standard chemical potentials differences which shows the free energy of formation change when one surfactant molecule is added to an aggregate. The prediction of the SCMFT for the standard chemical potential differences, $(\mu_N^o - \mu_1^o)/k_BT$ of micelles as a function of the total number of surfactants $N$ is presented in Fig. 5.30 for simulation boxes of volumes $27^3$ and $35^3$. As discussed in section 5.3.2.1 the micellar morphology can transform between geometric shapes on increasing surfactant concentration. In this section we will see how the standard chemical potential differences varies with $N$ and identify stable and unstable geometric shapes of the micelle. At low aggregation numbers a stable spherical micelle is formed, in a simulation box of volume $27^3$. The size of the spherical micelle increases with $N$, and reaches an optimum aggregation number where the standard chemical potential difference, $(\mu_N^o - \mu_1^o)/k_BT$, is minimum ($N_{min} = 60$). Increasing the aggregation number increases the size of the micelle up to a point, where it can no longer grow keeping within its spherical shape. Further addition of surfactants, forces the micelle to undergo morphological transformations (see Figs. 5.26, 5.27 and 5.28), into geometric shapes compatible with the new thermodynamic conditions and packing parameters. The micelle elongates into a prolate spheroid and the standard chemical potential difference increases and reaches a maximum at ($N = 130$). Further increases in $N$ leads the prolate micelle to transform to a croquette like micelle and the standard chemical potential difference starts to decreases. The simulation is continued in a bigger box of volume $V = 35^3$ with total number of surfactants $N = 163$ which is equivalent to that of $N = 130$ for $V = 27^3$ ( 25 and 55 surfactants are in the bulk for $V = 27^3$ with $N = 130$ and for $V = 35^3$ with $N = 163$ respectively), and the standard chemical potential difference decreases with $N$, forming the croquette like micelle, and reaches another minimum when a finite size cylindrical micelle with two end caps is formed ($N \approx 190$). Further increase of $N$ increases the length of the cylindrical part of the micelle and the standard chemical potential difference increases reaching maximum at $N = 255$. This is in agreement with May and Ben-Shaul[32] and Jódar-Reyes et al.[100] and Leermakers et.al [99], who pointed out that the grand potential[99, 100] and packing energy[32] of the cylindrical micelle is reported to have an oscillatory behavior with an amplitude that decays with the length of the cylinder, showing that the cylindrical part must have a minimum length to avoid strongly unfavorable interferences between the end caps.

UNIVERSITAT ROVIRA I VIRGILI
MICROSCOPIC MODELING OF THE SELF ASSEMBLY OF SURFACTANTS: SHAPE TRANSITIONS AND CRITICAL MICELLE CONCENTRATIONS
Asfaw Gezae Daful
ISBN:/DL:T. 1024-2011



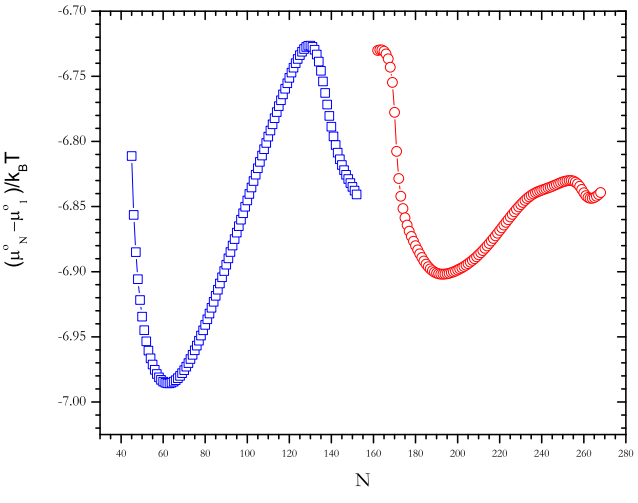


**Figure 5.30:** Standard chemical potential differences $(\mu_N^o - \mu_1^o)/k_BT$ versus the total number of surfactants in the system, $N$, at dimensionless temperature, $T^* = 9.5$; for simulation boxs of $27^3$ (squares) and $35^3$ (circles)

Values, for instance the standard chemical potential differences, for 2D infinite cylinder and spheres in the 2D calculations are in agreement with the infinite cylinder and sphere from 1D calculations, Fig. 5.17. Similar to the 1D SCMFT (section 5.3.1.1), the 2D SCMFT is found to be simulation box size independent. The standard chemical potential difference plots versus the aggregation number of the micelle, (after subtracting surfactants in the bulk, $N_m = N - N_{bulk}$) overlaps independently of the box size. Fig. 5.31 shows the standard chemical potential difference, $(\mu_N^o - \mu_1^o)/k_BT$ vs. $N_m$, of simulations boxes of $27^3$ and $35^3$ at a dimensionless temperature, $T^* = 9.5$ for $H_3T_6$.

The energy barrier accompanying the sphere to cylinder transition is shown in Fig. 5.32.

UNIVERSITAT ROVIRA I VIRGILI
MICROSCOPIC MODELING OF THE SELF ASSEMBLY OF SURFACTANTS: SHAPE TRANSITIONS AND CRITICAL MICELLE CONCENTRATIONS
Asfaw Gezae Daful
ISBN:/DL:T. 1024-2011



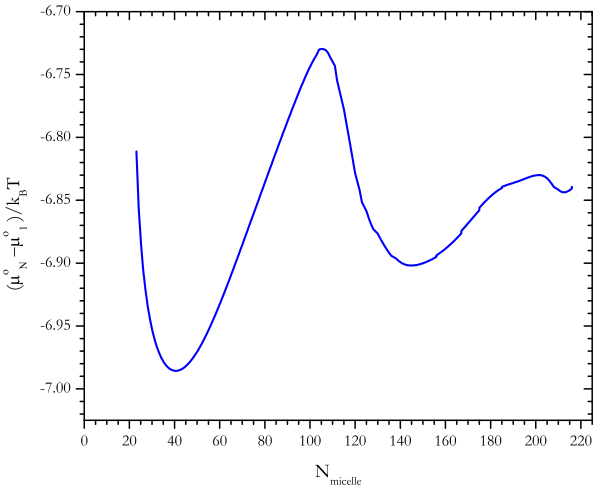


**Figure 5.31:** Standard chemical potential differences $(\mu_N^o - \mu_1^o)/k_BT$ versus the micellar aggregation number of the micelle, $N_m$, from simulations of $27^3$ and $35^3$.

UNIVERSITAT ROVIRA I VIRGILI
MICROSCOPIC MODELING OF THE SELF ASSEMBLY OF SURFACTANTS: SHAPE TRANSITIONS AND CRITICAL MICELLE CONCENTRATIONS
Asfaw Gezae Daful
ISBN:/DL:T. 1024-2011



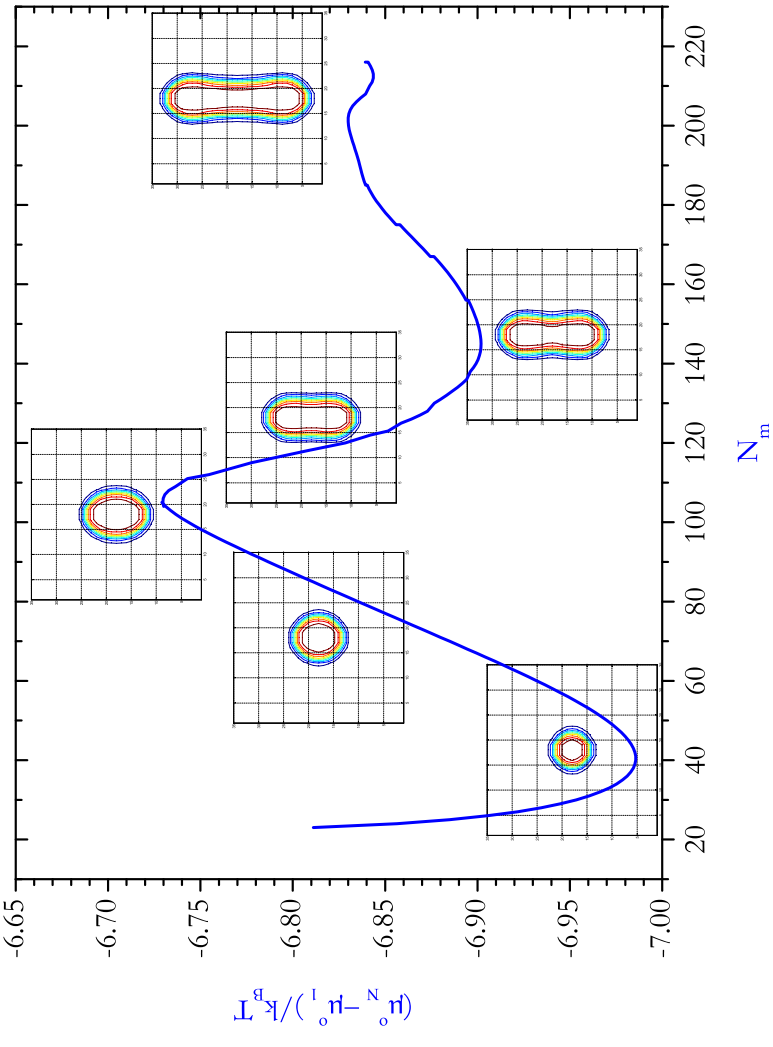


**Figure 5.32:** Micellar shape transition along with the standard chemical potential differences $(\mu_N^o - \mu_1^o)/k_BT$ versus the micellar aggregation number of the micelle, $N_m$, for $N_m = 40$, $N_m = 80$, $N_m = 110$, $N_m = 125$, $N_m = 140$ and $N_m = 200$

UNIVERSITAT ROVIRA I VIRGILI
MICROSCOPIC MODELING OF THE SELF ASSEMBLY OF SURFACTANTS: SHAPE TRANSITIONS AND CRITICAL MICELLE CONCENTRATIONS
Asfaw Gezae Daful
ISBN:/DL:T. 1024-2011



Porte et al.[148] have suggested that there should be a gap in the size distribution of wormlike micelles, between the spherical micelles and the long micelles, because of the more unfavorable state of the surfactants that are at the junction between the cylindrical body and the end caps, i.e., at the neck of the micelle. In agrement with Porte, the standard chemical potential differences $(\mu_N^o - \mu_1^o)/k_BT$ versus the micellar aggregation number of the micelle, $N_m$ shown in Fig. 5.31, one can easily see that there is a maximum in free energy of formation between the spherical and finite size cylinder, that is the energy barrier involved in the elongation process.

Upon surfactant micellization, the concentration of free surfactant monomers in aqueous solution becomes independent, or only weakly dependent, on the total concentration of added surfactant molecules [1, 2, 149]. This is because from an enthalpic and entropic point of view, it is more favorable that the added surfactant molecules contribute either to the growth of existing micelles or to the increase in the population of similarly-sized micelles. The variation of the standard chemical potential difference with total surfactant concentration shown in Figs. 5.30 and 5.31, is accompanied with the variation of bulk concentration of the surfactant too. The Single Chain Mean Field theory results show that the free surfactant concentration varies with the total surfactant concentration. We present the variation of the number of free surfactants in the bulk solution as a function of the total number of surfactants in the system, see Fig. 5.33. The number of free surfactants in the bulk, $N_{bulk}$, is observed to follow the same trend as the standard chemical potential difference. When the standard chemical potential difference decreases, $N_{bulk}$ decreases too and increases when the standard chemical potential difference increases. The lower the standard chemical potential difference, the more stable will be the micelle, and more surfactants prefer to self assemble into a micelle thus reducing the free surfactants in the bulk solution. In other words, the higher the standard chemical potential difference, the less stable will be the micelle and thus more surfactant molecules will be in the bulk solution.

### 5.3.3 Disk and Donut like Micelles

Besides the standard or the conventional pathway, that the amphiphilic molecules first self-assemble into small spherical micelles, then elongate to cylindrical micelles as discussed above (section 5.3.2), SCMFT simulation shows the existence of an alternative pathway, where the spherical micelles transform to disk and donut like micelles. The spherical micelle on growing transforms into oblate like structure that evolves to a disk then to donut like micelles with increasing $N$, as shown in Figs. 5.34 and 5.35. The standard chemical potential difference versus $N$ is also

UNIVERSITAT ROVIRA I VIRGILI
MICROSCOPIC MODELING OF THE SELF ASSEMBLY OF SURFACTANTS: SHAPE TRANSITIONS AND CRITICAL MICELLE CONCENTRATIONS
Asfaw Gezae Daful
ISBN:/DL:T. 1024-2011



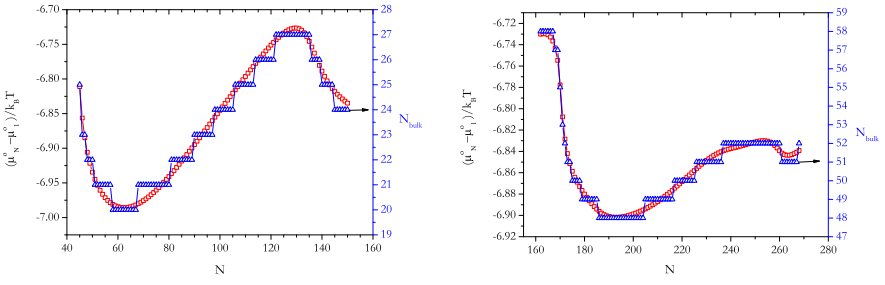


**Figure 5.33:** Variation of the number of free surfactants in the bulk solution, $N_{bulk}$, versus the total number of surfactants in the system, $N$, in simulation boxes of $V = 27^3$ (left) and $V = 35^3$ (right), along with their respective standard chemical potential difference, $(\mu^o_N - \mu^o_1)/k_BT$

presented in Fig. 5.37.

As can be seen in Fig. 5.38, the energy barrier between the spherical and disk micelles is smaller than between the spherical and finite cylindrical micelles. However, the disk and donut like micelles are indeed less favorable energetically than the cylindrical and spherical micelles.

A two dimensional contour and 3D surface plots of a donut micelle is presented in Fig. 5.36. Like the micelles of other geometric shapes, the hydrophilic tail is shielded from the solvent by the head group. The head group is observed to concentrate more on the top and bottom of the donut. This may lead the donut micelle to transform to a toroidal micelle on further increase of the number of surfactants.

### 5.3.4 Monte Carlo Simulation

Monte Carlo simulations show the concentration induced shape transitions of micelles of model surfactant $H_3T_6$, unlike $H_4T_4$ (see section 5.3.2). The shape transition occurs from spherical micelle to cylindrical micelles through a region where both spheres and cylinders coexist together. The coexistence of spherical and cylindrical micelles has also been supported with experimental results using cryo-TEM and pulse gradient spin-echo NMR[22] and simulations[85, 99, 150].

To illustrate this discussion, we present simulation results for systems with volume fractions ($\phi$) 0.00675, 0.009, 0.0135, 0.018, 0.0225, 0.027, 0.0333 and 0.036 (containing 750, 1000, 1500, 2000, 2500, 3000, 3700, 4000 surfactants) in a simulation box of volume $100^3$. The contour plots of the distribution function $PD(\alpha, \beta)$,

UNIVERSITAT ROVIRA I VIRGILI
MICROSCOPIC MODELING OF THE SELF ASSEMBLY OF SURFACTANTS: SHAPE TRANSITIONS AND CRITICAL MICELLE CONCENTRATIONS
Asfaw Gezae Daful
ISBN:/DL:T. 1024-2011



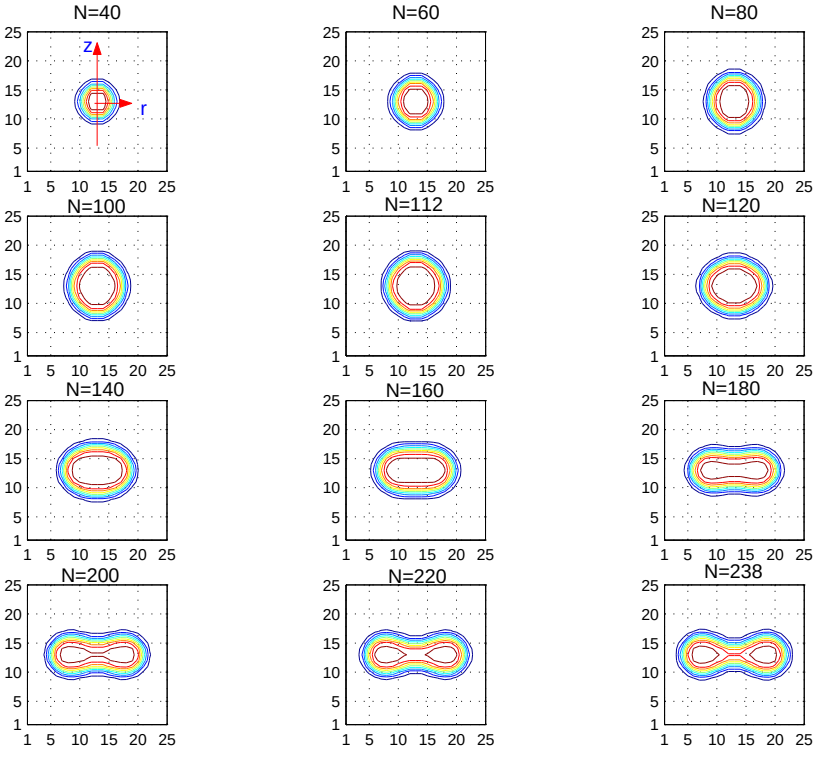


**Figure 5.34:** Volume fraction profiles of the hydrophobic tail are presented for selected systems of $N$ surfactants showing the sphere to disk transition of micelles of $H_3T_6$ at $T^* = 9.5$, in a cubic box of $V = 25^3$

UNIVERSITAT ROVIRA I VIRGILI
MICROSCOPIC MODELING OF THE SELF ASSEMBLY OF SURFACTANTS: SHAPE TRANSITIONS AND CRITICAL MICELLE CONCENTRATIONS
Asfaw Gezae Daful
ISBN:/DL:T. 1024-2011



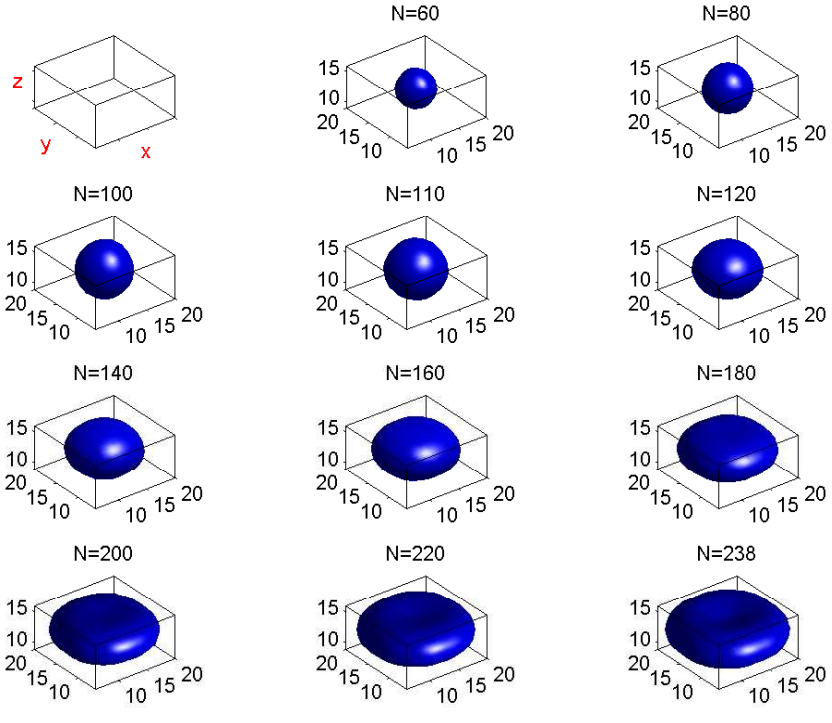


**Figure 5.35:** The 3D-*isosurface* plots of the hydrophobic core of micelles for different, $N$, to show the sphere to disk shape transition. The *isosurfaces* correspond to the layer (surface) of the core of the micelle where $\phi_T(r,z) \approx \phi_T^{bulk}$.

UNIVERSITAT ROVIRA I VIRGILI
MICROSCOPIC MODELING OF THE SELF ASSEMBLY OF SURFACTANTS: SHAPE TRANSITIONS AND CRITICAL MICELLE CONCENTRATIONS
Asfaw Gezae Daful
ISBN:/DL:T. 1024-2011



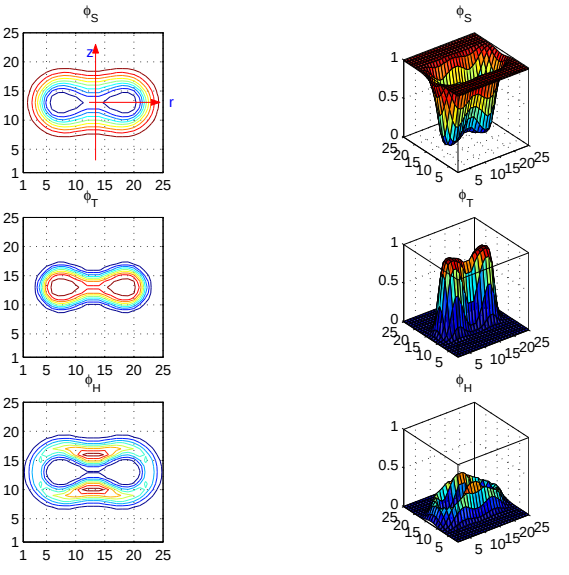


**Figure 5.36:** Volume fraction profile of the solvent, hydrophobic tail, and hydrophilic head from top to bottom. 2D contour plots (left) and 3D surface plots (right) of donut micelle of $N = 230$, in a cubic box of $V = 25^3$. For linear surfactant $H_3T_6$ at $T^* = 9.5$.

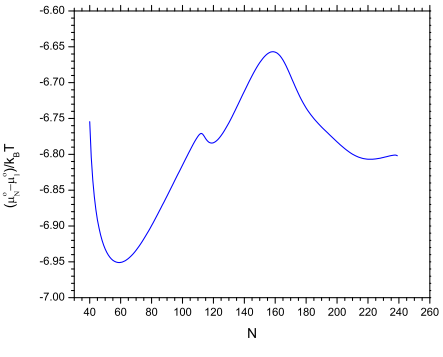


**Figure 5.37:** Standard chemical potential differences, $(\mu_N^o - \mu_1^o)/k_BT$, vs. $N$, of disk micelle, for $H_3T_6$

UNIVERSITAT ROVIRA I VIRGILI
MICROSCOPIC MODELING OF THE SELF ASSEMBLY OF SURFACTANTS: SHAPE TRANSITIONS AND CRITICAL MICELLE CONCENTRATIONS
Asfaw Gezae Daful
ISBN:/DL:T. 1024-2011



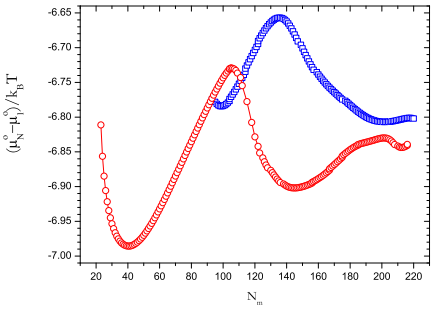


**Figure 5.38:** Standard chemical potential differences, $(\mu_N^o - \mu_1^o)/k_BT$, vs. $N_m$, of disk micelles(squares) and finite size cylindrical micelles(circles).

plotted as a function of $\alpha$ and $\beta$, as described in section 4.5.2, are shown in Fig. 5.39. At low concentration predominantly spherical micelles are formed, say for $N = 750$ or $\phi = 0.00675$. Increasing the concentration moves the peak values of the contour plots from the sphere to the cylinder region, where the spherical and cylindrical micelles coexist along with some aggregates of intermediate shapes, see for $N = 1000$ ($\phi = 0.009$) and $N = 1500$ ($\phi = 0.0135$). On further increase of surfactant concentration, the cylindrical region has the highest peak values, above $N = 2000$ ($\phi = 0.018$). One can see from Fig. 5.39 that, though the peak moves to the cylindrical micelle region as concentration increases, there are still a large number of spherical micelles coexisting with the cylindrical ones. The coexistence of the spherical and cylindrical micelles together in the system, is indicative that the transition of spherical micelles to cylindrical micelles occurs by saturating the concentration of spherical micelles before forming the cylindrical ones.

The equilibrium micelle size distribution for the same systems discussed above, is shown in Fig. 5.40. The micellar size distributions are smooth with a peak and shoulder. The peaks at an aggregation number of about 90, correspond to the spherical micelle. As the surfactant concentration is increased the micellar size distribution becomes wider, forming a shoulder in the distribution curve that shows the existence of the cylindrical micelle. It is clearly seen that the shoulder increases with concentration, where the excess surfactants are moving to the long cylindrical micelle. This indicates that the density of cylindrical micelles increases with concentration for large $N > 1000$, in agreement with the contour plots in Fig. 5.39.

Fig. 5.41 shows the aggregate morphologies of the $H_3T_6$ where the spherical micelles and cylindrical aggregates coexist together in the system, indicating that

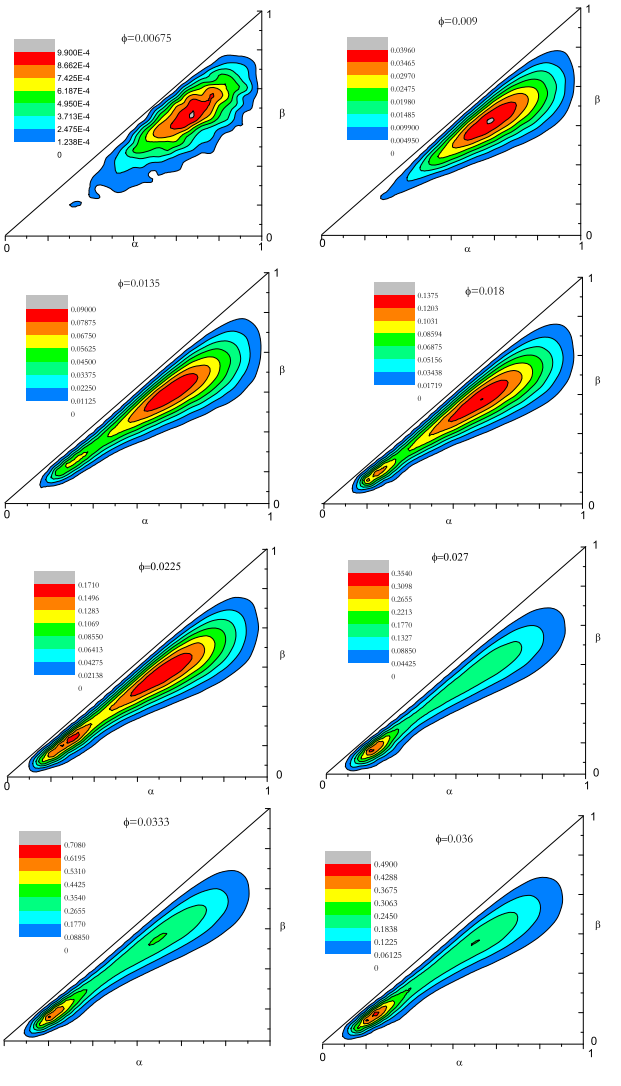


**Figure 5.39:** Contour plots of the distribution function $PD(\alpha, \beta)$ (sec. 4.5.2), plotted as a function of $\alpha$ and $\beta$, for systems with volume fractions ($\phi$) 0.00675, 0.009, 0.0135, 0.018, 0.0225, 0.027, 0.0333 and 0.036 (containing 750, 1000, 1500, 2000, 2500, 3000, 3700, 4000 surfactants) in a simulation box of volume $100^3$

UNIVERSITAT ROVIRA I VIRGILI
MICROSCOPIC MODELING OF THE SELF ASSEMBLY OF SURFACTANTS: SHAPE TRANSITIONS AND CRITICAL MICELLE CONCENTRATIONS
Asfaw Gezae Daful
ISBN:/DL:T. 1024-2011



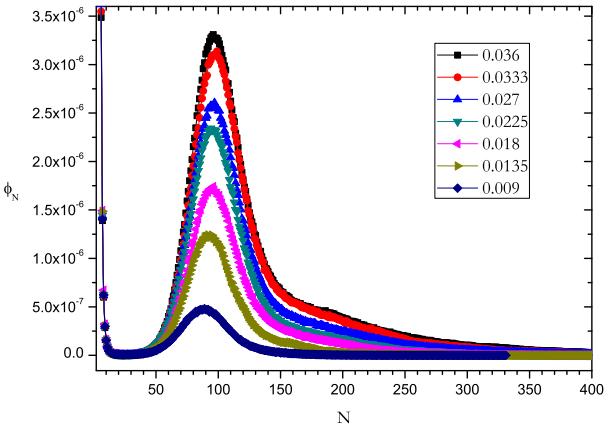


**Figure 5.40:** Micellar size distribution for systems containing with volume fractions 0.009, 0.0135, 0.018, 0.0225, 0.027, 0.0333 and 0.036 in a simulation box of volume $100^3$, for $H_3T_6$ at $T^* = 9.5$

the transition of spherical micelles to cylindrical micelles occurs.

A number of configurations were studied from all the systems, (shown for systems of $N = 1000$, $N = 2000$, $N = 3000$ and $N = 4000$), and show that the larger micelles are not only due to the coalescence of spherical micelles but they are instead fully developed long cylindrical micelles.

The details of the morphological transformations of micelles shown in sections 5.3.2 and 5.3.3, from the Single Chain Mean Field Theory, are supported by our Monte Carlo simulations. In what follows we present three dimensional configurational plots from the Monte Carlo simulation, showing micelles of different geometric shapes. Spheres, ellipsoidal, short cylindrical micelles and long finite size cylindrical micelles with bigger end caps are observed, see Fig. 5.42 to Fig. 5.46. Similar to the SCMFT our Monte Carlo simulation reveals the disk like micelles, see Fig. 5.47 to Fig. 5.49

UNIVERSITAT ROVIRA I VIRGILI
MICROSCOPIC MODELING OF THE SELF ASSEMBLY OF SURFACTANTS: SHAPE TRANSITIONS AND CRITICAL MICELLE CONCENTRATIONS
Asfaw Gezae Daful
ISBN:/DL:T. 1024-2011



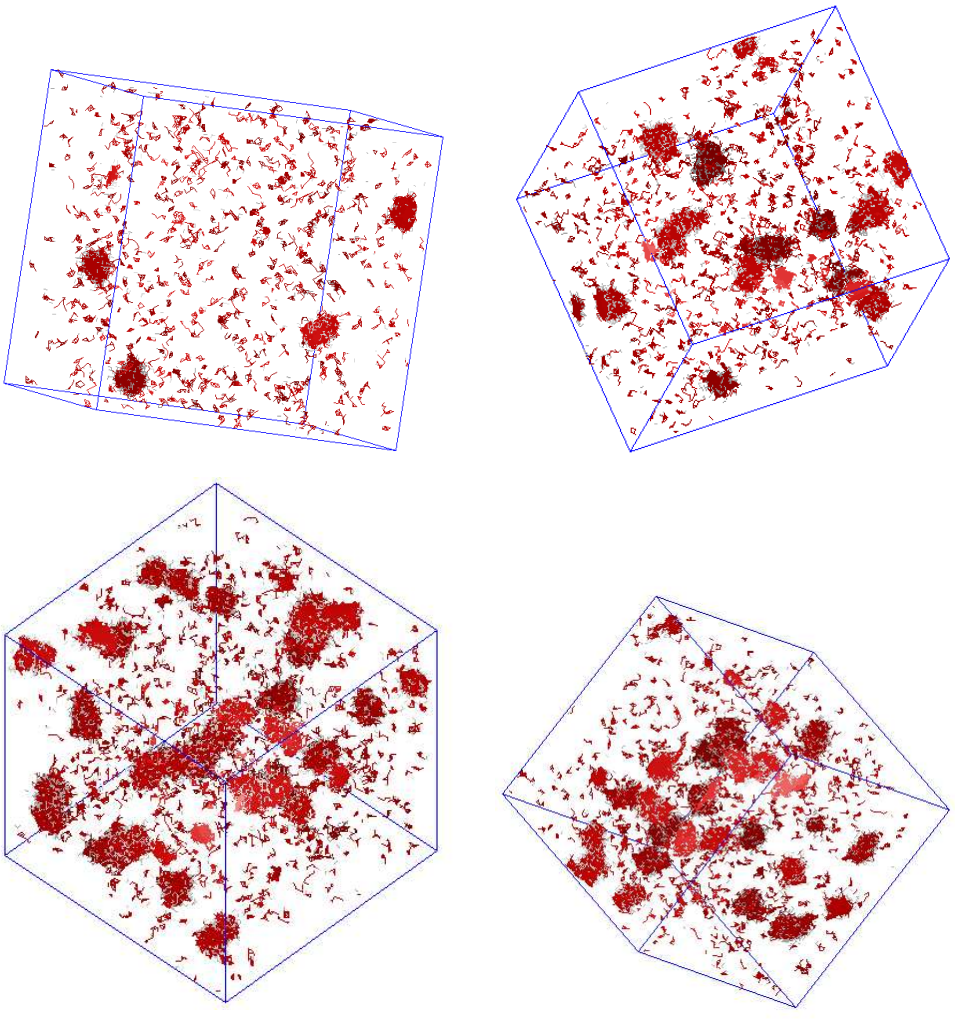

**Figure 5.41:** Snapshots of aggregate morphologies of $H_3T_6$ for $N = 1000$, $N = 2000$, $N = 3000$ and $N = 4000$ surfactants in the solution; starting from top left and proceeding clockwise

UNIVERSITAT ROVIRA I VIRGILI
MICROSCOPIC MODELING OF THE SELF ASSEMBLY OF SURFACTANTS: SHAPE TRANSITIONS AND CRITICAL MICELLE CONCENTRATIONS
Asfaw Gezae Daful
ISBN:/DL:T. 1024-2011



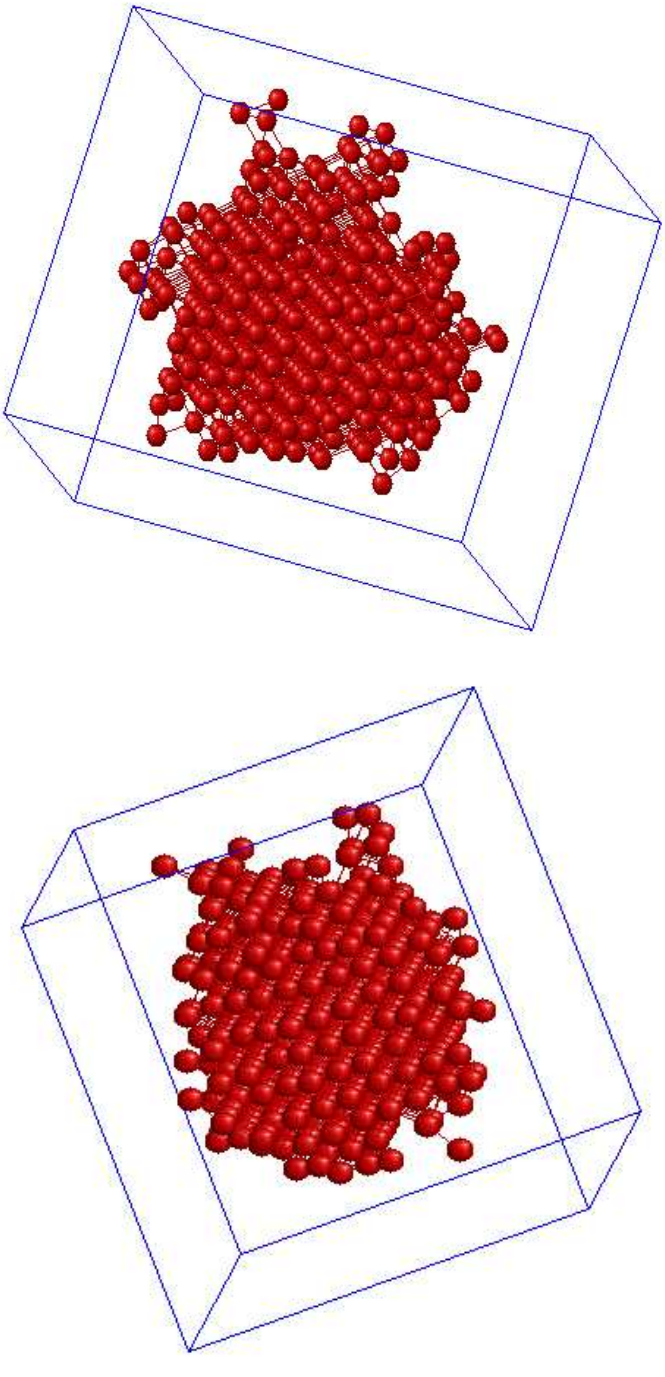

**Figure 5.42:** Snapshots obtained from Monte Carlo simulations illustrate the spherical micelles of aggregation numbers $N = 91$ (above) and $N = 89$ (below)

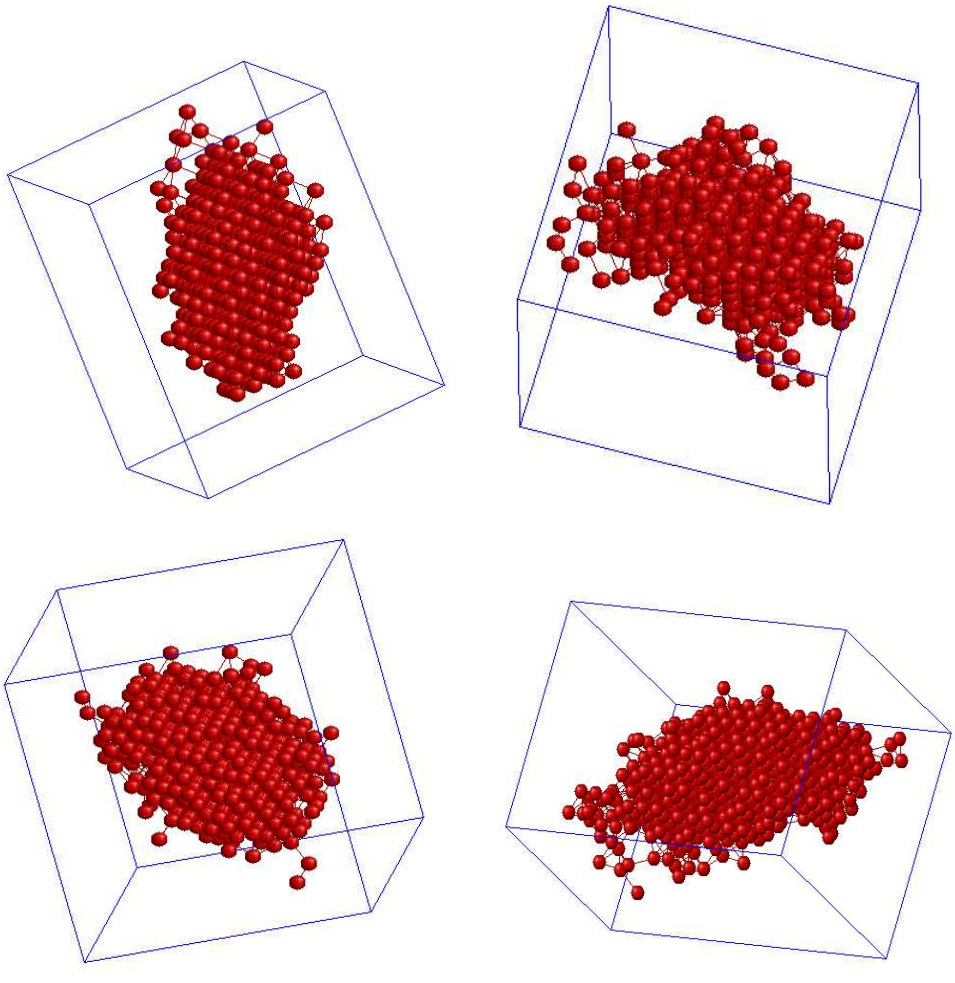

**Figure 5.43:** Snapshots of ellipsoidal micelles obtained from Monte Carlo simulations for aggregation numbers $N = 73$, $N = 75$, $N = 110$ and $N = 87$ starting from top left and proceeding clockwise

UNIVERSITAT ROVIRA I VIRGILI
MICROSCOPIC MODELING OF THE SELF ASSEMBLY OF SURFACTANTS: SHAPE TRANSITIONS AND CRITICAL MICELLE CONCENTRATIONS
Asfaw Gezae Daful
ISBN:/DL:T. 1024-2011



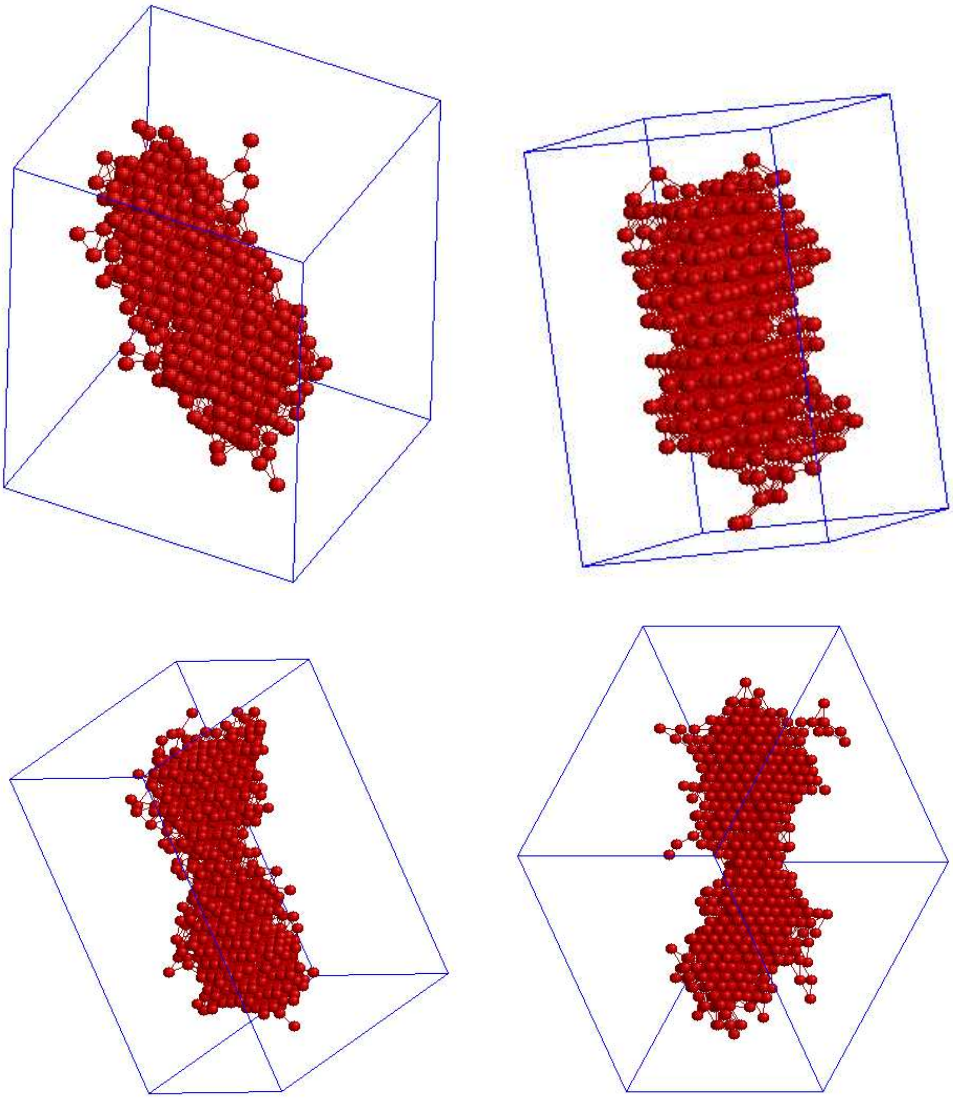

**Figure 5.44:** Snapshots of short cylindrical micelle (croquette like micelle) and long cylindrical micelles with spherical end caps of larger diameters than the cylindrical body, obtained from Monte Carlo simulations for aggregation numbers $N = 88$, $N = 94$, $N = 130$ and $N = 150$.

UNIVERSITAT ROVIRA I VIRGILI
MICROSCOPIC MODELING OF THE SELF ASSEMBLY OF SURFACTANTS: SHAPE TRANSITIONS AND CRITICAL MICELLE CONCENTRATIONS
Asfaw Gezae Daful
ISBN:/DL:T. 1024-2011



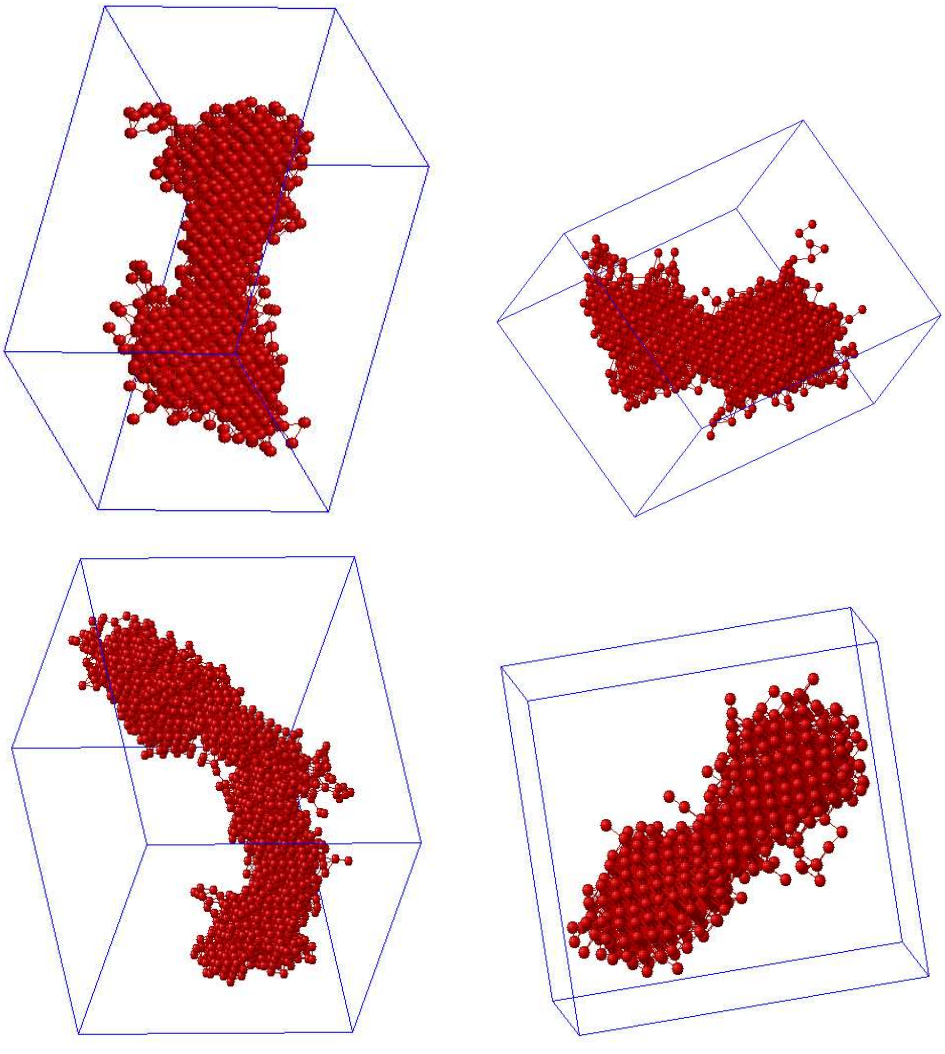

**Figure 5.45:** Snapshots of long cylindrical micelles with spherical end caps of larger diameters than the cylindrical body, obtained from Monte Carlo simulations for aggregation numbers $N = 170$, $N = 209$, $N = 160$ and $N = 350$.

UNIVERSITAT ROVIRA I VIRGILI
MICROSCOPIC MODELING OF THE SELF ASSEMBLY OF SURFACTANTS: SHAPE TRANSITIONS AND CRITICAL MICELLE CONCENTRATIONS
Asfaw Gezae Daful
ISBN:/DL:T. 1024-2011



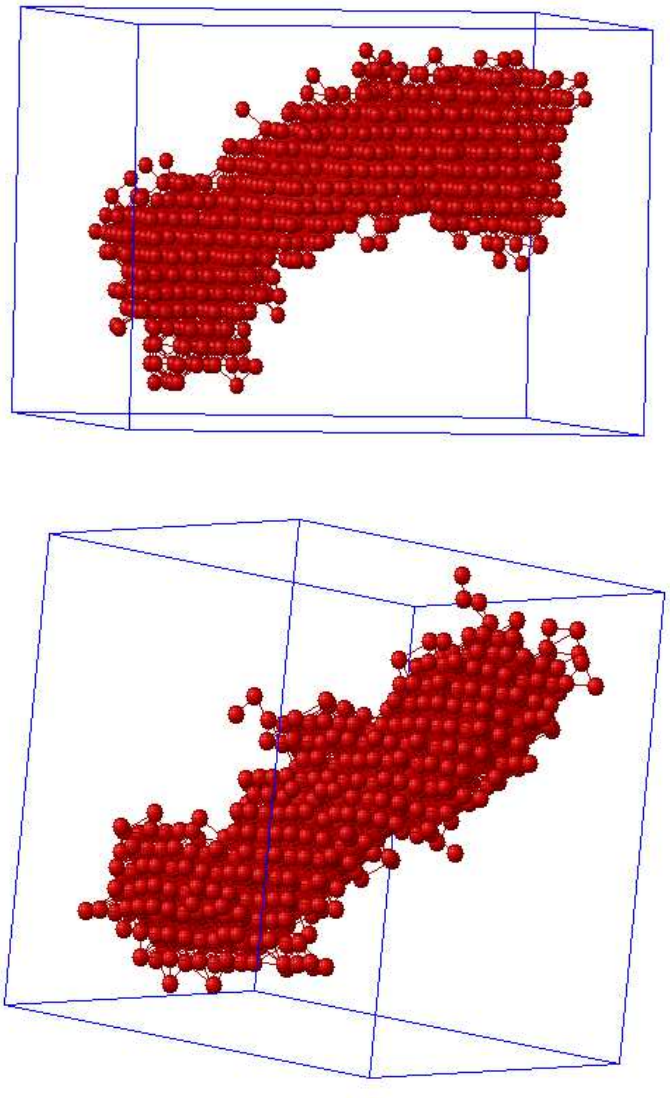

**Figure 5.46:** Snapshots of long cylindrical micelles with spherical end caps of larger diameters than the cylindrical body, obtained from Monte Carlo simulations for aggregation numbers $N = 212$, (above) and $N = 170$ (below)

UNIVERSITAT ROVIRA I VIRGILI
MICROSCOPIC MODELING OF THE SELF ASSEMBLY OF SURFACTANTS: SHAPE TRANSITIONS AND CRITICAL MICELLE CONCENTRATIONS
Asfaw Gezae Daful
ISBN:/DL:T. 1024-2011



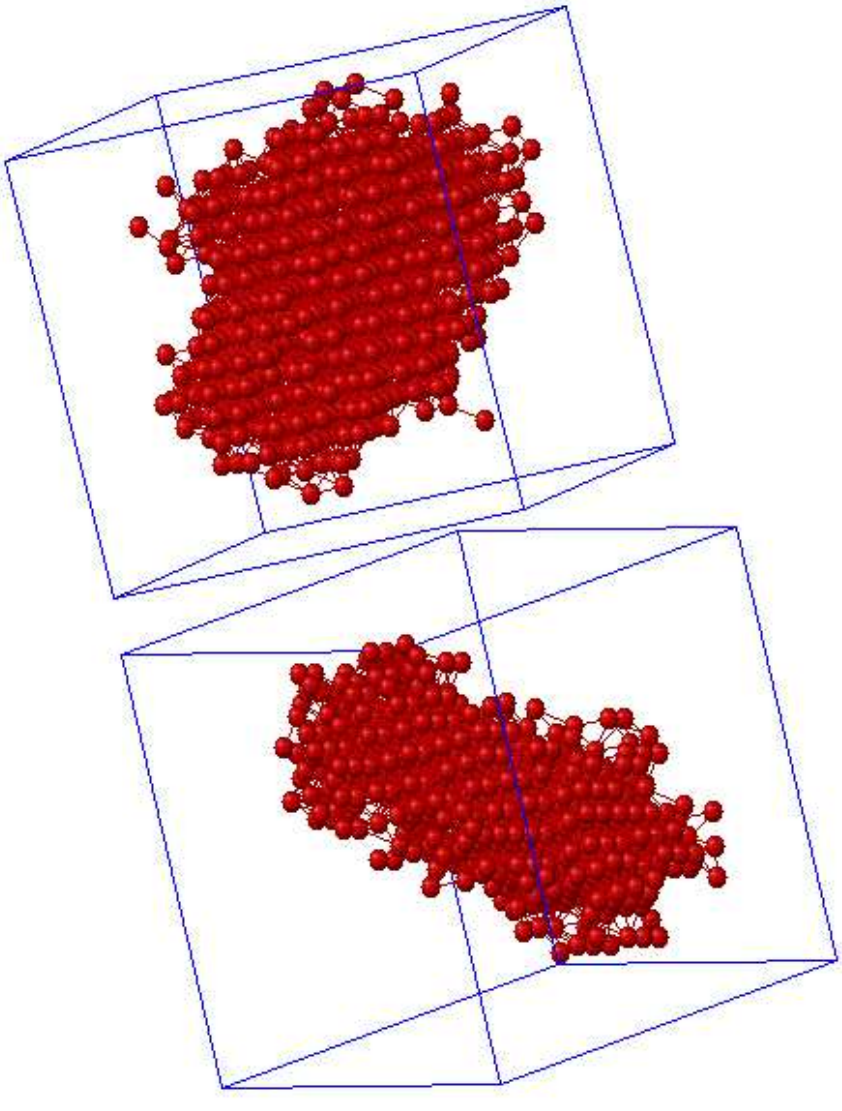

**Figure 5.47:** Snapshots of disk micelles, obtained from Monte Carlo simulations for aggregation numbers $N = 121$, presented with top and side views

UNIVERSITAT ROVIRA I VIRGILI
MICROSCOPIC MODELING OF THE SELF ASSEMBLY OF SURFACTANTS: SHAPE TRANSITIONS AND CRITICAL MICELLE CONCENTRATIONS
Asfaw Gezae Daful
ISBN:/DL:T. 1024-2011



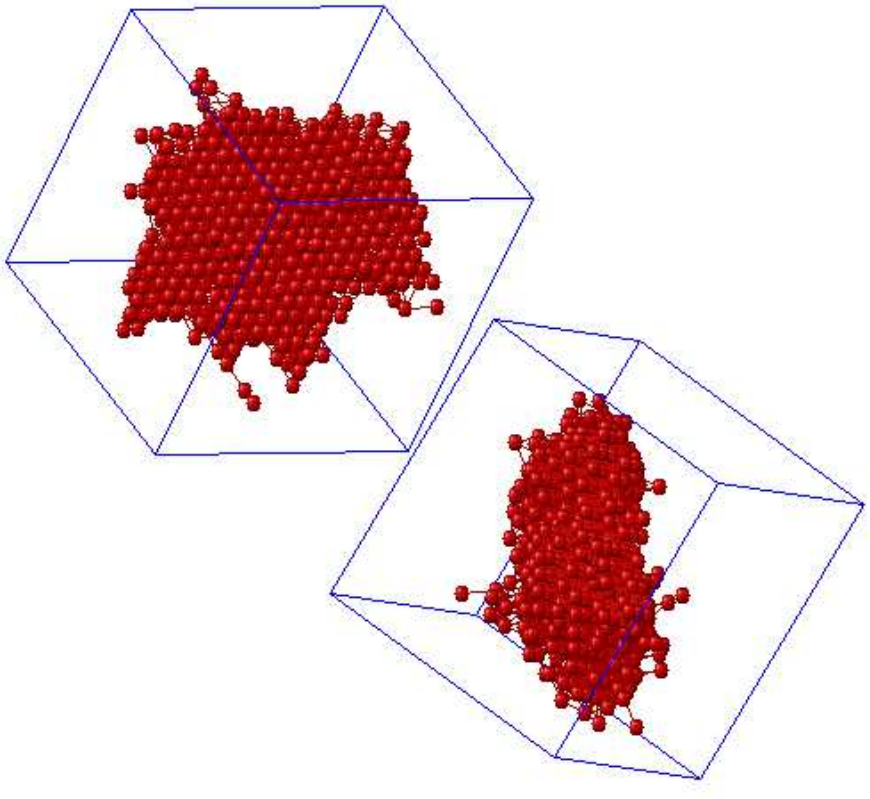

**Figure 5.48:** Snapshots of disk micelles, obtained from Monte Carlo simulations for aggregation numbers $N = 124$, presented with top and side views

UNIVERSITAT ROVIRA I VIRGILI
MICROSCOPIC MODELING OF THE SELF ASSEMBLY OF SURFACTANTS: SHAPE TRANSITIONS AND CRITICAL MICELLE CONCENTRATIONS
Asfaw Gezae Daful
ISBN:/DL:T. 1024-2011



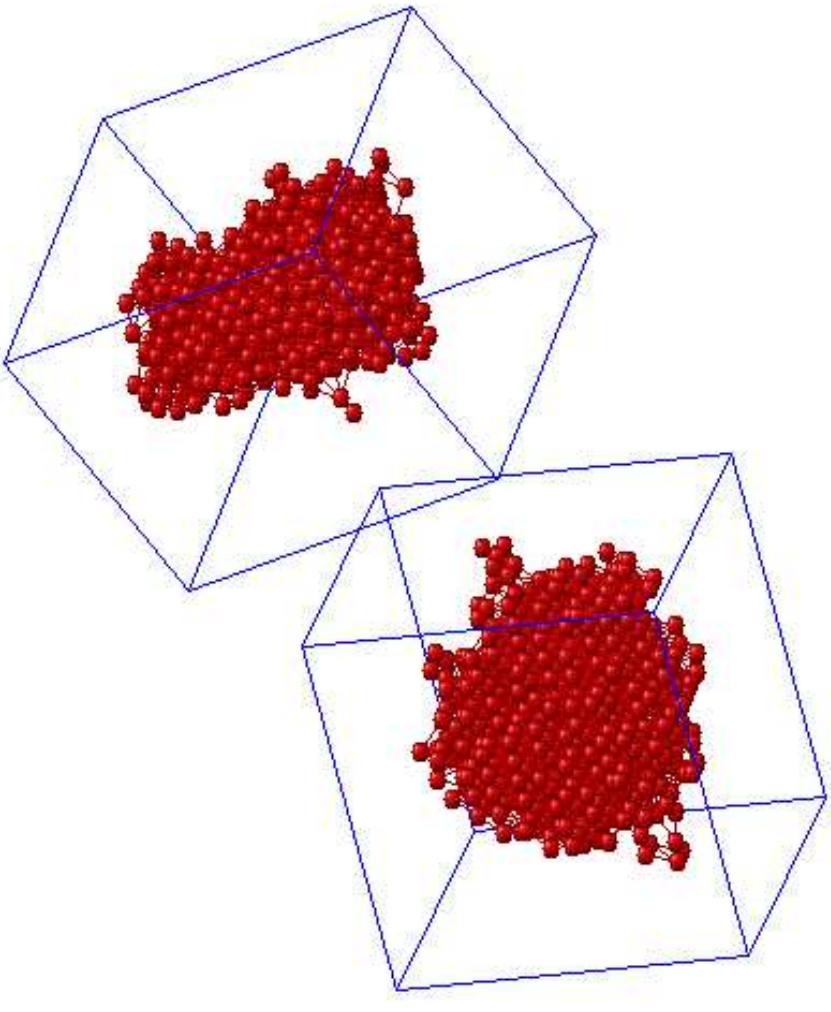

**Figure 5.49:** Snapshots of disk micelles, obtained from Monte Carlo simulations for aggregation numbers $N = 107$ , presented with top and side views

UNIVERSITAT ROVIRA I VIRGILI
MICROSCOPIC MODELING OF THE SELF ASSEMBLY OF SURFACTANTS: SHAPE TRANSITIONS AND CRITICAL MICELLE CONCENTRATIONS
Asfaw Gezae Daful
ISBN:/DL:T. 1024-2011



## 5.4 Conclusions

We applied the Single Chain Mean Field Theory and Monte Carlo Simulations to systematically study the concentration induced shape transition of linear model surfactants. We studied the micelle formation and stability using a one dimensional Single Chain Mean Field Theory (1D-SCMFT), where spherical and infinitely long cylindrical micelles were considered. The 1D-SCMFT reveals that symmetric surfactants and asymmetric surfactants, with tail segments longer than the head segments, prefers to form cylindrical micelles at higher concentration.

A two dimensional Single Chain Mean Field Theory (2D-SCMFT) is used with no *priori* assumption on the shape of the micelle. This 2D-SCMFT allowed us to determine the standard chemical potential, volume fraction profiles and other structural properties of micelles of any geometric shape. Our 2D-SCMFT reveals all the essential growth characteristics of micelles, particularly the concentration induced shape transition as a gradual and continuous evolution of micellar shape with increasing surfactant concentration. At low concentration, the micelles are mainly spherical. As the aggregate size is increased, we show that the micelle can undergo a one-dimensional growth into finite size cylindrical micelle or a two-dimensional growth into a discoidal micelle.

In case of the one-dimensional growth of the micelle, the spherical micelle starts to grow along the *z-axis* to ellipsoidal spheroid and prolate spheroid micelle which gradually changes into croquette like structure. The croquette like micelle then finally changes into a finite cylindrical micelle with two spherical end caps and cylindrical body. The volume fraction profiles show that the diameter of the end caps is larger than that of the cylindrical body. Further increase of total surfactant concentration, increases only the length of the cylindrical body. The energy barrier between the spherical and finite cylindrical micelles is manifested by a maximum in the standard chemical potential difference plots. Similarly, our Monte Carlo simulation show the sphere to cylinder shape transition occurs through a region where spherical and cylindrical micelles coexist, *i.e.,* at low concentration only spherical micelles are obtained, but as the concentration increases the coexistence of both spherical and cylindrical micelles is observed. Further increase of surfactant concentration leads to predominantly long cylindrical micelles.

In addition to the sphere to cylinder transition, the 2D-SCMFT shows the existence of an alternative pathway of a disk and donut like micelles, *i.e.,* the spherical micelle grows into an oblate spheroid which in turn evolves into a disk and then into a donut like micelle. The process of the morphological change from sphere to disk is interesting and attractive in itself.

UNIVERSITAT ROVIRA I VIRGILI
MICROSCOPIC MODELING OF THE SELF ASSEMBLY OF SURFACTANTS: SHAPE TRANSITIONS AND CRITICAL MICELLE CONCENTRATIONS
Asfaw Gezae Daful
ISBN:/DL:T. 1024-2011



We have also shown the interplay among total surfactant concentration, micellar shape and the standard chemical potential differences. The early stage of the shape transition of the spherical micelle into prolate or oblate spheroid involve a large energetic barrier. Finally we conclude that our two dimensional Single Chain Mean Field Theory calculations reveal all the essential growth characteristics of linear micelles.

UNIVERSITAT ROVIRA I VIRGILI
MICROSCOPIC MODELING OF THE SELF ASSEMBLY OF SURFACTANTS: SHAPE TRANSITIONS AND CRITICAL MICELLE CONCENTRATIONS
Asfaw Gezae Daful
ISBN:/DL:T. 1024-2011

# Chapter 6

# Accurate Critical Micelle Concentrations from a Single Chain Mean Field theory

In this chapter a Single Chain Mean Field Theory is applied together with an explicit, but simple continuous space, microscopic model to quantitatively describe the micellization process of surfactants. The mass action model used to the CMC calculation is presented following a brief introduction. The model of the nonionic polyethylene oxide alkyl ether, $C_nE_m$ surfactants is followed by discussion about the interaction parameters used. Finally, resulting values of the CMC and other micellar properties are presented. The chapter finishes with conclusions.

## 6.1 Introduction

Surfactants are short amphiphilic molecules containing hydrophilic and hydrophobic groups, referred to as the head and tail respectively. As already discussed in chapter 2, the surfactant head can be anionic, cationic, zwitterionic, or nonionic. The surfactant tail can consist of linear or branched hydrocarbons. In addition, aromatic groups, such as benzene rings, and alkyl halides, such as fluorocarbons, may be present in the surfactant tail. At low concentrations, surfactants form a dilute homogeneous solution of individual molecules, while at high concentrations, above a threshold concentration, the amphiphilic molecules self-assemble into ag-

UNIVERSITAT ROVIRA I VIRGILI
MICROSCOPIC MODELING OF THE SELF ASSEMBLY OF SURFACTANTS: SHAPE TRANSITIONS AND CRITICAL MICELLE CONCENTRATIONS
Asfaw Gezae Daful
ISBN:/DL:T. 1024-2011



gregates or microstructures known as micelles [1–4]. These micelles coexist with singly dispersed surfactant molecules, knows as free surfactants in the bulk solution. The surfactant molecules comprising the micelle have their hydrophobic tails shielded from water in the aggregate interior, the core of the micelle, and their hydrophilic heads exposed to water at the aggregate surface, the micelle core-water interface referred as corona. The micellization process is governed by the balance of interactions of hydrophobic and hydrophilic groups with the solvent. The onset of the aggregation into micelles usually occurs within a narrow range of surfactant concentration, and is quantified by a single concentration value, the critical micelle concentration (CMC)[1]. The CMC designates the onset of aggregation of free surfactants into micelles in the spontaneous micellization process emerging over this narrow concentration range. Although the micellization is not a thermodynamic transition, solutions containing surfactants exhibit at the CMC drastic changes in physical and chemical properties such as surface tension, turbidity, conductivity, self diffusion, osmotic pressure, solubilization, and detergent activity [2, 3]. Thus, the knowledge of precise values of the CMC and an accurate description of the micellization process at a molecular level may be crucial both from a fundamental point of view as well as for practical applications.

The CMC can be determined experimentally by a number of methods, usually from the inflection point of some physical property of the solution as a function of surfactant concentration, including capillary electrophoresis [151, 152], tensiometry [153, 154], conductometry [155], fluorescence anisotropy probe[156], light scattering [157, 158], fluorimetry [159, 160], calorimetry [161], spectrophotometry [162], ion-selective electrodes [163], and nuclear magnetic resonance (NMR) spectroscopy [164]. It can also be defined as the total surfactant concentration at which the concentration of single surfactant molecule in the simulation box saturates with increasing total surfactant concentration. Further addition of surfactants to the solution leads to an increasing number of micelles.

The micellization of surfactants has been intensively studied theoretically with a number of analytical models and computer simulations. Nagarajan et al. [31, 35, 36] and Blankschtein et al. [33, 34] introduced a molecular thermodynamic modeling approach that allows for the prediction of several thermodynamic properties of self-assembled systems, including the CMC and phase behavior. In this approach, the free energy of formation of the micelle, that is, the free-energy change associated with transferring a free surfactant in aqueous solution to a micellar aggregate, is obtained as the sum of several phenomenological free energy contributions[36] such as the transfer free energy, interfacial free energy, packing free energy contribution, the steric free energy and the electrostatic free energy. An *a priori* estimate needs to be made about how the surfactant molecules will

UNIVERSITAT ROVIRA I VIRGILI
MICROSCOPIC MODELING OF THE SELF ASSEMBLY OF SURFACTANTS: SHAPE TRANSITIONS AND CRITICAL MICELLE CONCENTRATIONS
Asfaw Gezae Daful
ISBN:/DL:T. 1024-2011



position and orient themselves within the preassembled micellar aggregate and a knowledge of the chemical structure of the surfactant is required to get the free energy contributions. Blankschtein et al.[165] applied molecular dynamics (MD) simulations at an oil/water interface to identify what portions of the surfactant should be modeled as the head and what portions should be modeled as the tail in the context of the molecular-thermodynamic theories of micelle formation.

Monte Carlo (MC) simulations of amphiphilic solutions in lattices have also been used extensively to study the micellization behavior of different types of amphiphiles in solution[46, 47, 49, 52–54, 85]. Panagiotopoulos et al.[54] determined the phase behavior and micellization of several lattice diblock and triblock surfactants using the Larson model[49, 52] by histogram-reweighting grand canonical MC simulations. Mackie et al.[46] studied the micelle size, CMC and other thermodynamic properties of a model linear surfactants, $H_4T_4$ using Monte Carlo simulation and a Single Chain Mean Field (SCMF) theory[55]. Apart from MC simulations, MD simulations [38–40, 48, 50, 51] have proven to be very effective for simulating all-atom and coarse grained models, offering a direct link between chemical structures of surfactants and the micellization process. However, obtaining the free energy of formation of the micelle and many other important equilibrium properties like the CMC from MC and MD simulations is computationally expensive.

Scheutjens and Fleer proposed a mean field approach [96, 97] to study polymer adsorption in a self-consistent mean field approximation and later Leermakers et al. [37, 41–43] applied this self-consistent field (SCF) theory in order to study the self-assembly of surfactant molecules into micelles. The SCF approach considers the surfactant to be a Gaussian chain in an inhomogeneous mean field.

One of the theoretical methods that can *quantitatively* describe the thermodynamics of the micellization process and provide detailed microscopic information about the structure of the micelles is the Single Chain Mean Field (SCMF) theory. This method solves for a model of surfactant molecules at a coarse grained level similar to MC or MD simulations and reproduce the structure of the micelles, the configurations of surfactants and their distribution in the system, the free energy of formation of the micelle and hence, the CMC, the aggregation number and the size distributions of the micelles. Molecular models such as the one used in this work have strong advantages over thermodynamic approaches and we can expect higher transferability not just to other molecules but also to other properties, as well as direct access to all the microscopic information. The SCMF theory was originally developed to study the molecular organization of short amphiphilic molecules in micelles and bilayers assuming dry core aggregates [44, 45, 136] or allowing also solvent molecules in the core [46]. The predictions of lattice based SCMF theory

UNIVERSITAT ROVIRA I VIRGILI
MICROSCOPIC MODELING OF THE SELF ASSEMBLY OF SURFACTANTS: SHAPE TRANSITIONS AND CRITICAL MICELLE CONCENTRATIONS
Asfaw Gezae Daful
ISBN:/DL:T. 1024-2011



[46, 55] are in good agreement with MC simulations.

Recently, the SCMF methodology was generalized to study the self-assembly of a mixture of an arbitrary number of types of molecules of an arbitrary structure interacting with each other through mean fields [166]. The SCMF theory and its numerical implementation allows for direct quantitative comparison of equilibrium properties of self-assembled structures with experimental data [166].

In this chapter, we apply this methodology to the micellization problem and show how the SCMF theory together with an explicit microscopic model for surfactant molecules can be used to *quantitatively* model the micellization process of surfactants. In particular, we have chosen to model polyoxyethylene alkyl ether, $C_nE_m$, a non-ionic surfactant, in order to evaluate the predictive power, precision and capabilities of our method due to the large amount of experimental data available for this surfactant. Polyoxyethylene alkyl ethers, $C_nE_m$, are nonionic surfactants with low critical micelle concentrations (CMC) in water, compatible with other surfactants, and of a mild nature. These surfactants are widely used in personal care products, detergency, paint formulations, controlled drug delivery, *etc*. We show that the SCMF theory produces with high accuracy the values of the CMC and allows for a description of the micellization thermodynamics at the molecular level.

We start with the basic equations of the SCMF theory and the micellization process, given in section 4.3.2 of chapter 4. Furthermore, we present the model that we have used for the $C_nE_m$ surfactant and the manner in which the parameters of this model have been selected. We continue with the discussion of the main results and the predictions of this model for the family of $C_nE_m$ surfactants with different head and tail lengths and compare against experimental results from the literature. Both the ability of the SCMF theory to reproduce the experimental CMC values as well as microscopic details such as the average micellar size and the predicted density profiles of the micelles are discussed. The temperature dependence of the CMC and aggregation numbers are analyzed. The chapter finishes with the conclusions of the most relevant results.

### 6.1.1 Calculation of the CMC

The micellization process is not a thermodynamic transition and the micelles coexist with free surfactants over a range of concentrations. That is why there are several definitions for the CMC. We use the Israelachvili definition[1] and the CMC is taken to be the surfactant concentration at which a line of unit slope passing through the origin intersects the asymptote of the free chain concentration beyond

UNIVERSITAT ROVIRA I VIRGILI
MICROSCOPIC MODELING OF THE SELF ASSEMBLY OF SURFACTANTS: SHAPE TRANSITIONS AND CRITICAL MICELLE CONCENTRATIONS
Asfaw Gezae Daful
ISBN:/DL:T. 1024-2011



the onset of micellization, in a plot of free surfactants mole fraction versus total surfactant mole fraction.

The mass action model is used in order to calculate the free chain and micellar concentrations for CMC estimations from the SCMFT (see section 3.6.1). In particular, the mass action model can be given as

$$X_N = N\left\{X_1 exp[-\frac{\mu_N^o - \mu_1^o}{k_B T}]\right\}^N \tag{6.1}$$

where $\mu_N^o$, and $\mu_1^o$ are respectively the standard chemical potentials for amphiphiles in an aggregate of size, $N$ and for a free chain; $X_N$ is the mole fraction of surfactant molecules in aggregates of size $N$, and $X_1$ is the mole fraction of free surfactant chains; $k_B$ is the Boltzmann constant, and $T$ is the temperature.

We calculate the standard chemical potential by way of the SCMFT, which leads us to the expression for the difference in standard chemical potential between free chains and micelles of size $N$, given by Eq. (4.27).

## 6.2 Model of the $C_nE_m$ Surfactant

Most nonionic surfactants are ethylene oxide adducts where the polyoxyethylene (PEO) moiety is the hydrophilic part of the surfactant molecule. The hydrophobic part can be a variety of apolar moieties including alkyl chains, alkyl benzene and their fluorinated counterparts, silicone derivatives or polyoxypropylene chains. Because many of the experimental CMC values refer to polyoxyethylene alkyl ether surfactants, we chose this surfactant family. Polyoxyethylene alkyl ethers have the general formula, $(C_nH_{2n+1}(OCH_2CH_2)_mOH)$ and are referred to as $C_nE_m$ with $n$ indicating the number of carbons in the alkyl chain and $m$ being the number of ethylene oxide units in the hydrophilic part.

The surfactant molecule is modeled as a linear chain of beads, all of the same size. The distance between the centers of the beads is chosen to correspond to the average distance between the lattice sites in a cubic lattice of coordination 26, *i.e.* 1.42 of the diameter of the beads ($\approx \frac{6\times1+12\times\sqrt{2}+8\times\sqrt{3}}{26}$). Each tail or T bead represents a $CH_2$ group of the hydrophobic tail while each head or H bead represents an $OCH_2CH_2$ group of the hydrophilic head (see Fig. 6.1). We assume that the chain is completely rigid within each Kuhn segment, while the junctions between the segments are free to rotate. The Kuhn segment length [167–170] of polyethylene (alkyl chain) is taken to be 8[167, 170] and that of

UNIVERSITAT ROVIRA I VIRGILI
MICROSCOPIC MODELING OF THE SELF ASSEMBLY OF SURFACTANTS: SHAPE TRANSITIONS AND CRITICAL MICELLE CONCENTRATIONS
Asfaw Gezae Daful
ISBN:/DL:T. 1024-2011



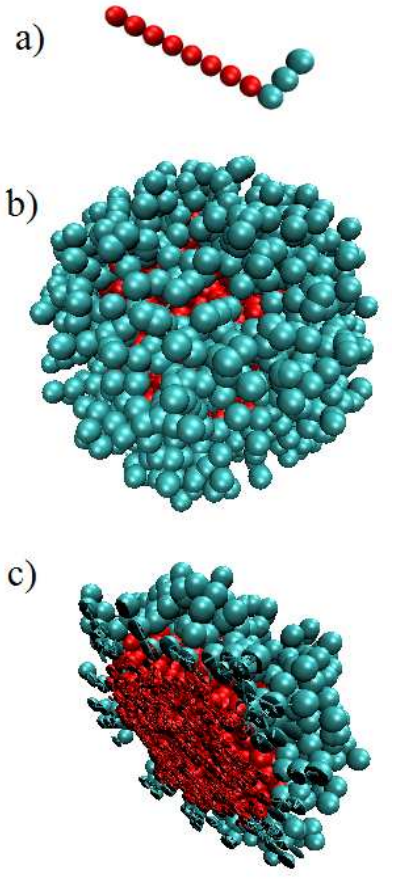


**Figure 6.1:** a) Coarse-grained model of the $C_8E_3$ surfactant and the resulting mean-field "snapshot" (plot of most probable conformations) of a spherical micelle comprising of $N = 382$ surfactants, b) perspective view and c) cross-section view. The hydrophobic part is shown as red and the hydrophilic part as light blue. The chain is completely rigid within each Kuhn segment.

UNIVERSITAT ROVIRA I VIRGILI
MICROSCOPIC MODELING OF THE SELF ASSEMBLY OF SURFACTANTS: SHAPE TRANSITIONS AND CRITICAL MICELLE CONCENTRATIONS
Asfaw Gezae Daful
ISBN:/DL:T. 1024-2011



the oxyethelene chain is set to be 4[168–170]. Such a model of chain rigidity is justified since we are interested in equilibrium properties at the mean field level. The conformations of our model surfactant, are obtained using the Rosenbluth and Rosenbluth chain growth algorithm [101], which insures self-avoidance of the generated conformations.

The configurations of the molecule of type, $C_nE_m$, are obtained using the Rosenbluth and Rosenbluth chain growth algorithm [101]. Unlike sections 3.7.5 and 3.7.5, the rigidity of the chain within the Kuhn segment makes its chain generation to be slightly different, as follows.

1. the first tail bead is randomly inserted in the simulation box
2. a new bead is randomly placed at one diameter distance from the previous bead subjected to the self-avoidance condition
3. similarly, the next bead is also placed at one diameter distance from the previous bead subject to the self-avoidance condition and an additional rigidity restriction that this bead be on a straight line with respect to the two previous beads.
4. step 3 is repeated for all beads up to the $(N_k^{th})$ bead where $N_k$ is the Kuhn segment length of the alkyl chain
5. step 2 is be applied to place the $(N_k + 1)^{th}$ bead, followed by steps 3 and 4, till the end of the alkyl chain.
6. the oxyethelene head group is then grown similarly, starting from the last bead of the alkyl chain and applying steps 2-5 with respect to its own Kuhn segment length, $N_k$

The resulting bias in the distribution of conformations is corrected with the corresponding weights in the probability of each conformation. From one to four million configurations were used, depending on the simulation volume, in order to properly sample the single chain configurational space. This sampling was checked by repeating the calculations with double the number of configurations to ensure that the resulting free energy was consistent.

In such a simple model, only three interaction parameters are required: tail-solvent, $\varepsilon_{TW}$, tail-head, $\varepsilon_{TH}$, and head-solvent, $\varepsilon_{HW}$, (see Eq. (4.38)). Furthermore, we estimate the values of the interaction parameters from available experimental data, in order to adjust the parameters as little as possible. Most of the literature data of the interaction parameters of polymers are given in terms of Flory

$\chi$-parameters [171] defined for a lattice model or related solubility parameters [172]. In our continuous space model, the surfactant beads have an explicit intramolecular hard core repulsion within the bead diameter. The enthalpic contribution is modeled by way of a square well potential which is described by a well interaction energy and additional interaction radius $r_{int}$[166]. Thus, we need to relate our square well potential parameters from continuous space conformations with the lattice model parameters, although this correspondence is not exact due to large difference in the conformational space of the chains between the two models. Interaction volume, $v_{int}$, of chains in continuous space depends on the conformation, while on a lattice it is a constant. However, we can make a rough approximation by relating the average interaction volume over continuous space conformations with that of a lattice. The interaction volume of a cell in a cubic lattice is equal to its coordination number, $z = 26$. In our continuous space model, the beads of diameter $\sigma = 1$ interact with the neighbors over the interaction range. For an isolated bead the interaction volume $v_{int} = \frac{4\pi}{3}(r_{int}^3 - \sigma^3)$, however, if the beads of the chain are close enough, their interaction ranges can overlap, thus making the interaction in the overlapping zones stronger. In order to get a rough correspondence to the lattice model, we have adjusted numerically the value of the interaction radius $r_{int} = 1.61$ of the continuous model to give an average interaction number per bead $z = 26$. With this, the interaction parameters are related as $\chi = z\varepsilon/kT$. In addition, the excluded volumes of real space conformations and the chains on the lattice do not match. By matching the free energy for a linear chain composed of $n = 8$ monomers $H_4T_4$ between lattice and continuous models gives the ratio between the excluded volumes $(\sum_\Gamma \int v_{ex}(\Gamma, \mathbf{r})d\mathbf{r})/(\Gamma_{tot} n v_s) = 0.885$, where $\Gamma_{tot}$ is the total number of conformations in the sampling. Hence, the excluded volume contribution (last term in 4.38) should be corrected by the corresponding factor.

### 6.2.1 Interaction Parameters

All systems studied in this work are binary mixtures of amphiphilic chains, composed of head and tail monomers, and solvent. Since there are three species, only three interaction parameters are required, the tail-solvent, $\chi_{TW}$; tail-head, $\chi_{TH}$; and head-solvent, $\chi_{HW}$. A first approximation for the tail-solvent interaction parameter $\chi_{TW}$, is taken from equilibrium solubility data of alkanes in water. The activity coefficient[79] of a solvent $a_1$ is given by

$$\ln a_1 = \ln(1 - \phi_2) + (1 - 1/r)\phi_2 + \chi_{TW}\phi_2^2 \tag{6.2}$$

where $\phi_2$ is the volume fraction of the polymer and $r$ is the chain segment number (ratio of polymer to solvent molar volume). Assuming that the alkyl ether tails

UNIVERSITAT ROVIRA I VIRGILI
MICROSCOPIC MODELING OF THE SELF ASSEMBLY OF SURFACTANTS: SHAPE TRANSITIONS AND CRITICAL MICELLE CONCENTRATIONS
Asfaw Gezae Daful
ISBN:/DL:T. 1024-2011



of the polyoxyethylene alkyl ether surfactants are similar to alkane molecules, we calculated the activity coefficient of alkane chains from the water-$n$-ethane, water-$n$-propane, water-$n$-butane, water-$n$-pentane, water-$n$-hexane, water-$n$-heptane, water-$n$-octane, water-$n$-nonane and the water-$n$-decane systems, (alkanes of $C_2$ to $C_{10}$), at infinite dilution in water at $25°C$, from liquid-liquid equilibrium data of alkane-water system[173, 174]. This activity coefficient in turn is used to calculate the $\chi_{TW}$ parameters for each alkane extrapolating the values to infinite dilution of the solvent. These calculations indicated that the $\chi_{TW}$ should have a value of approximately 2.5. The interaction parameter of the EO group with water, $\chi_{HW}$, in terms of the Flory lattice model, has a strong concentration dependence[175]. This reflects the conformational dependence of interactions with water and the formation of hydrogen bonds. However, the heads of the surfactant $C_nE_m$ are relatively short and the interactions of the heads groups with water are much weaker than the tail-water interactions. We found a weak dependence of the CMC values for this parameter and no concentration gradient in the corona of micelles. Thus, we used a constant value $\chi_{HW} = 0.5$ to model interactions of EO units with water at $25°C$ and did not adjust it further.

In order to refine the approximate value of the tail-solvent parameter,$\chi_{TW}$, and to adjust the value of the $\chi_{TH}$, for which we were unable to find any experimental data, we used an optimization technique, so as to reproduce the experimental CMC value of the the following surfactants $C_{10}E_3$, $C_{10}E_6$, $C_{10}E_8$, $C_8E_3$, $C_8E_6$, $C_8E_8$, $C_6E_3$, $C_6E_6$, $C_6E_8$, $C_{16}E_9$. In particular, a series of simulations was conducted for different values of $\chi_{TW}$ and $\chi_{TH}$, i.e. keeping one of these parameters fixed and running simulations with a range of values of the other parameter. The optimization gave us $\chi_{TW} = 2.40$ and $\chi_{TH} = 0.34$. During this process we observed that the CMC is highly sensitive to $\chi_{TW}$ and less sensitive to $\chi_{TH}$. For instance a 3% change in $\chi_{TW}$ can result in a 100% change of the CMC, while a 25% change in $\chi_{TH}$ can result in only a 13% change of the CMC.

To summarize, the following parameters, $\chi_{HW} = 0.5$, $\chi_{TW} = 2.40$ and $\chi_{TH} = 0.34$, only two of which are adjusted, have been used to model the CMC and the equilibrium properties of the full family of $C_nE_m$ surfactants given in the following section.

## 6.3 Results and Discussion

The CMC values obtained from the SCMF theory and the equilibrium sizes of the micelles for a wide range of polyoxyethylene alkyl ether surfactants, $C_nE_m$ are compared with experimental values from the literature at $25°C$ in 6.1, which

UNIVERSITAT ROVIRA I VIRGILI
MICROSCOPIC MODELING OF THE SELF ASSEMBLY OF SURFACTANTS: SHAPE TRANSITIONS AND CRITICAL MICELLE CONCENTRATIONS
Asfaw Gezae Daful
ISBN:/DL:T. 1024-2011



also includes the molar volume, $V_M$, and molar weight $M_W$ of the surfactants. The relative errors for the CMCs and aggregation numbers have been calculated for several of the surfactants and are found to be between 1% and 4% for the CMCs and about 1% for the aggregation number. This means that the CMCs and aggregation numbers given in 6.1 are accurate to two significant figures. The CMC in mole fraction, $X$, is related to the CMC in [mol/L] $C$ from the following relationship,

$$C = \frac{1}{V_M + V_S(\frac{1}{X} - 1)} \tag{6.3}$$

where $V_S$ and $V_M$ are the molar volumes of the solvent and surfactant, respectively. As can be seen, the CMC values of the present work are in good agreement with the experimental values.

We present the standard chemical potential by way of the SCMFT, as shown for some surfactants in Fig. 6.2.

which leads us to the expression for the difference in standard chemical potential between free chains and micelles of size $N$, given by Eq. (4.27).

UNIVERSITAT ROVIRA I VIRGILI
MICROSCOPIC MODELING OF THE SELF ASSEMBLY OF SURFACTANTS: SHAPE TRANSITIONS AND CRITICAL MICELLE CONCENTRATIONS
Asfaw Gezae Daful
ISBN:/DL:T. 1024-2011



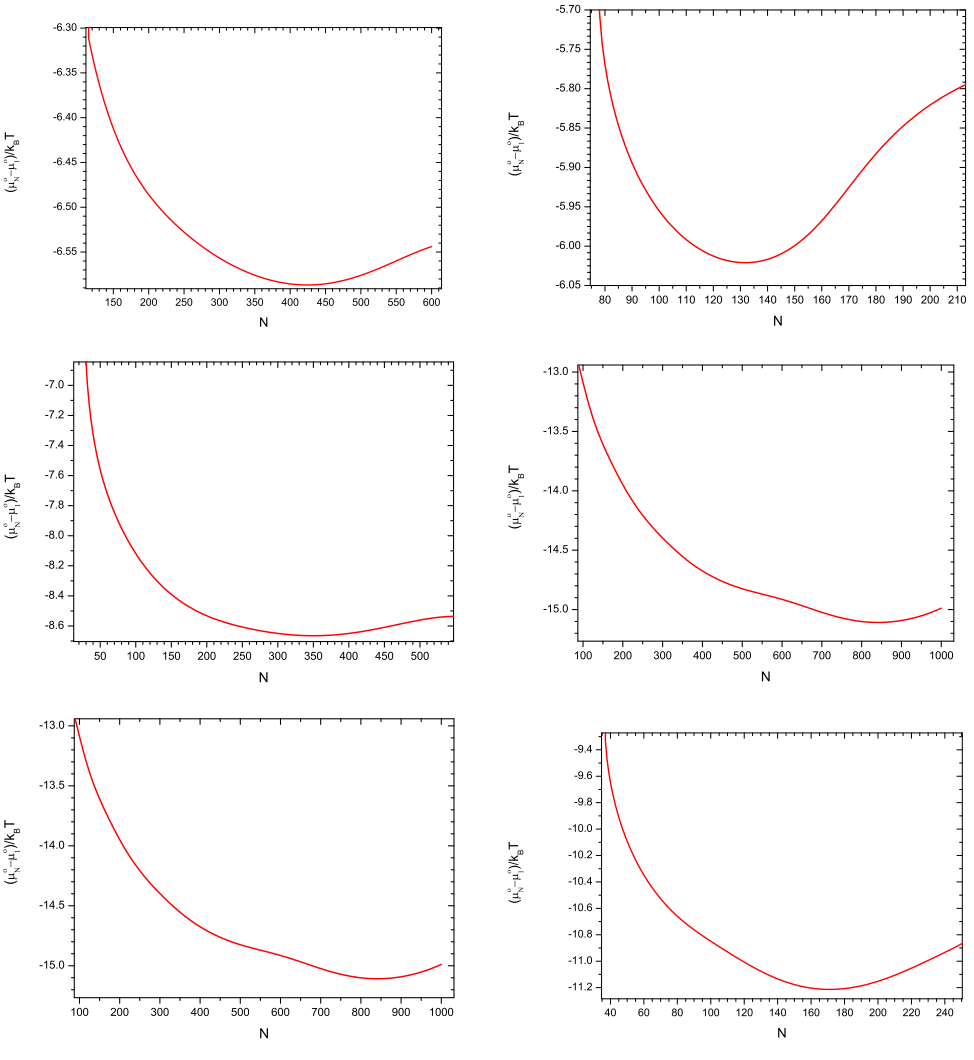


**Figure 6.2:** Standard chemical potential differences $\frac{\mu_N^o - \mu_1^o}{k_B T}$ versus the total number of surfactants in the system, $N$, for surfactants $C_6E_3$, $C_6E_6$, $C_{14}E_3$, $C_{12}E_{25}$, $C_{16}E_6$, and $C_8E_4$ starting from top left and proceeding clockwise

**Table 6.1:** Calculated and experimental critical micelle concentrations and micelle aggregation numbers of polyoxyethylene alkyl ether surfactants, $C_nE_m$, at 25°$C$.

| Nonionic Surfactant | $M_W$ [g/mol] | $V_M$ [mol/L] | Experiment CMC [mol/L] | mol.frac | $N$ | Simulation CMC [mol/L] | mol.frac | $N$ |
|---|---|---|---|---|---|---|---|---|
| $C_nE_3$ | | | | | | | | |
| $C_6E_3$ | 234 | 0.227 | 0.09 [176, 177] | 0.00185 | | 0.075 | 0.0013 | 380 |
| $C_7E_3$ | 248 | 0.245 | 0.02[176] | 3.62E-04 | | 0.017 | 3.1E-04 | 375 |
| $C_8E_3$ | 262 | 0.27 | 0.0075[3, 176, 177] | 1.36E-04 | | 0.0051 | 9.2E-05 | 370 |
| $C_{12}E_3$ | 318 | 0.32 | 1.00E-04[3, 176] | 9.40E-07 | | 9.5E-05 | 1.7E-06 | 975 |
| $C_{14}E_3$ | 346 | 0.374 | 1.00E-05[176] | 1.80E-07 | | 1.2E-05 | 2.1E-07 | 870 |
| $C_{16}E_3$ | 374 | 0.41 | 1.20E-06[176] | 2.16E-08 | | 1.6E-06 | 2.8E-08 | 820 |
| $C_nE_4$ | | | | | | | | |
| $C_6E_4$ | 278 | 0.266 | 0.09 | 0.00167[178] | | 0.085 | 0.0016 | 210 |
| $C_8E_4$ | 306 | 0.31 | 0.008[176] | 1.56E-04 | | 0.0090 | 1.6E-04 | 333 |
| $C_{12}E_4$ | 363 | 0.376 | 6.40E-05[3, 176, 179] | 1.2E-06 | | 8.8E-05 | 1.6E-06 | 905 |
| $C_nE_5$ | | | | | | | | |
| $C_6E_5$ | 322 | 0.305 | 0.09[176] | 0.00173 | | 0.099 | 0.0018 | 140 |
| $C_8E_5$ | 350 | 0.32 | 0.009[3, 176] | 1.77E-04 | | 0.010 | 1.8E-04 | 260 |
| $C_{10}E_5$ | 378 | 0.39 | 8.40E-04[176, 180] | 1.46E-05 | | 8.8E-04 | 1.6E-05 | 908 |
| $C_{12}E_5$ | 406 | 0.41 | 6.20E-05[3, 176, 181] | 1.2E-06 | | 8.8E-05 | 1.6E-06 | 855 |
| $C_{14}E_5$ | 434 | 0.47 | 1.00E-05[176] | 1.80E-07 | | 1.2E-05 | 1.8E-07 | 840 |
| $C_nE_6$ | | | | | | | | |
| $C_6E_6$ | 366 | 0.345 | 0.0695[180] | 0.00127 | | 0.12 | 0.0021 | 123 |
| $C_8E_6$ | 395 | 0.39 | 0.0098[3, 176, 177, 180, 181] | 1.80E-04 | | 0.012 | 2.0E-04 | 200 |
| $C_{10}E_6$ | 423 | 0.418 | 9.00E-04[3, 177, 180, 181] | 1.63E-05 | | 0.0011 | 2.0E-05 | 470 |
| $C_{12}E_6$ | 451 | 0.45 | 8.70E-05[3, 176, 177, 179–181] | 1.6E-06 | 400 | 1.0E-04 | 1.9E-06 | 775 |
| $C_{16}E_6$ | 507 | 0.528 | 1.00E-06[3, 180] | 2.35E-08 | 2430 | 1.3E-06 | 2.3E-08 | 750 |
| $C_nE_7$ | | | | | | | | |
| $C_{10}E_7$ | 467 | 0.457 | 9.62E-04 | 1.74E-05[178] | | 0.0013 | 2.4E-05 | 250 |
| $C_{12}E_7$ | 495 | 0.49 | 8.20E-05[3, 176] | 1.5E-06 | | 1.3E-04 | 2.4E-06 | 520 |
| $C_{16}E_7$ | 551 | 0.567 | 1.70E-06[3] | 3.07E-08 | 594 | 1.5E-06 | 2.6E-08 | 720 |
| $C_nE_8$ | | | | | | | | |
| $C_8E_8$ | 482 | 0.459 | 0.01[176] | 1.81E-04 | | 0.015 | 2.8E-04 | 270 |
| $C_9E_8$ | 497 | 0.517 | 0.003[181] | 5.43E-05 | | 0.0045 | 8.2E-05 | 215 |
| $C_{10}E_8$ | 511 | 0.51 | 1.00E-03[3, 176, 181] | 1.81E-05 | | 0.0015 | 2.7E-05 | 250 |
| $C_{11}E_8$ | 524 | 0.52 | 3.00E-04[176, 181] | 5.42E-06 | | 4.9E-04 | 8.8E-06 | 310 |
| $C_{12}E_8$ | 538 | 0.54 | 1.00E-04[3, 176, 179, 180] | 1.28E-06 | 123 | 1.7E-04 | 3.0E-06 | 380 |
| $C_{13}E_8$ | 553 | 0.571 | 3.00E-05[176] | 4.88E-07 | | 5.1E-05 | 9.2E-07 | 670 |
| $C_{14}E_8$ | 567 | 0.569 | 9.00E-06[3, 176, 181] | 1.63E-07 | | 1.6E-05 | 2.9E-07 | 780 |
| $C_{15}E_8$ | 581 | 0.588 | 3.50E-06[176, 181] | 6.32E-08 | | 5.2E-06 | 9.2E-08 | 760 |
| $C_{16}E_8$ | 595 | 0.606 | 5.00E-07[176] | 2.17E-08 | | 1.8E-06 | 3.2E-08 | 660 |
| $C_nE_9$ | | | | | | | | |

Continued on next page

UNIVERSITAT ROVIRA I VIRGILI
MICROSCOPIC MODELING OF THE SELF ASSEMBLY OF SURFACTANTS: SHAPE TRANSITIONS AND CRITICAL MICELLE CONCENTRATIONS
Asfaw Gezae Daful
ISBN:/DL:T. 1024-2011



**Table 6.1 – continued from previous page**

| Nonionic Surfactant | $M_W$ [g/mol] | $V_M$ [mol/L] | Experiment CMC [mol/L] | mol.frac | $N$ | Simulation CMC [mol/L] | mol.frac | $N$ |
|---|---|---|---|---|---|---|---|---|
| $C_8E_9$ | 527 | 0.53 | 0.013[176, 177, 181] | 2.37E-04 | | 0.016 | 2.9E-04 | 170 |
| $C_{10}E_9$ | 555 | 0.535 | 0.00138[177, 180, 181] | 2.35E-05 | | 0.0018 | 3.1E-05 | 240 |
| $C_{12}E_9$ | 583 | 0.58 | 8.00E-05[3, 176] | 1.81E-06 | | 1.8E-04 | 3.3E-06 | 283 |
| $C_{16}E_9$ | 639 | 0.645 | 2.12E-06[3, 181] | 3.79E-08 | 219 | 2.2E-06 | 3.9E-08 | 570 |
| $C_{12}E_m$ | | | | | | | | |
| $C_{12}E_{10}$ | 626 | 0.62 | 9.00E-05[176] | 1.63E-06 | | 2.0E-04 | 3.6E-06 | 270 |
| $C_{12}E_{11}$ | 670 | 0.665 | | | | 2.5E-04 | 4.5E-06 | 244 |
| $C_{12}E_{12}$ | 714 | 0.71 | 1.00E-04[3, 176] | 1.80E-06 | 81 | 2.8E-04 | 5.0E-06 | 293 |
| $C_{12}E_{13}$ | 758 | 0.767 | 2.00E-04[176] | 3.60E-06 | | 3.0E-04 | 5.5E-06 | 284 |
| $C_{12}E_{23}$ | 1198 | 1.12 | 6.00E-05[176] | 1.08E-06 | 40 | 7.6E-04 | 1.4E-05 | 215 |
| $C_{12}E_{25}$ | 1286 | 1.2 | 1.00E-04[176] | 1.80E-06 | | 6.5E-04 | 1.2E-05 | 170 |

UNIVERSITAT ROVIRA I VIRGILI
MICROSCOPIC MODELING OF THE SELF ASSEMBLY OF SURFACTANTS: SHAPE TRANSITIONS AND CRITICAL MICELLE CONCENTRATIONS
Asfaw Gezae Daful
ISBN:/DL:T. 1024-2011



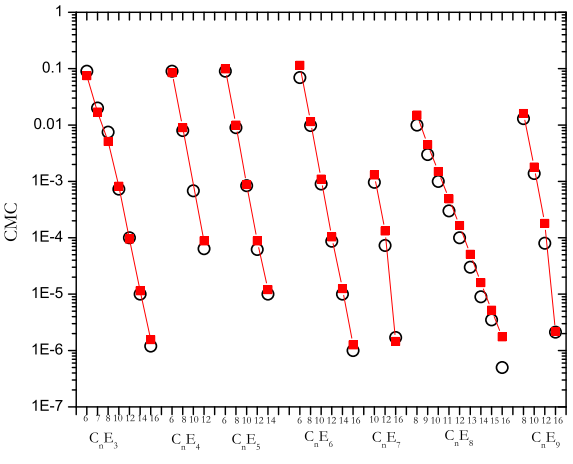


**Figure 6.3:** Critical micelle concentration in [mol/L] versus the length of the hydrophobic tail group $n$ for surfactants $C_nE_3$, $C_nE_4$, $C_nE_5$, $C_nE_6$, $C_nE_7$, $C_nE_8$, and $C_nE_9$. Open circles are experimental data from the literature, while filled squares are values calculated from the SCMF theory values, lines are included to help guide the eye.

Fig.6.3 and Fig. 6.4 show the dependence of the CMC on the number of ethylene oxide (head) groups, $m$, and methylene (tail) groups, $n$. It is found that varying the length of the tail group for a constant length of the head group causes the CMC to decrease exponentially, as can be seen by the linear decrease in the CMC in the log-linear plot in Fig. 6.3. A longer hydrophobic tail length indicates that it is thermodynamically more favorable for the molecule to leave the aqueous solution, i.e. increasing the chain length of the hydrophobic alkyl segment $n$, enhances the repulsive hydrocarbon-water interaction. This increases the tendency to push the hydrocarbons out of the aqueous medium. Therefore, this results in the formation of micelles at lower concentrations, and hence reduces the critical micelle concentration.

On the other hand, a longer hydrophilic head length gives the contrary result. The longer the hydrophilic chain the surfactant has, the more soluble it is in aqueous solution, thus reducing the surfactant's tendency to migrate from the bulk to the interface and aggregate into a micelle. For the cases in which the length of the hydrophobic tail remains constant and the length of the hydrophilic head increases, the CMC values increases slightly with increasing the head group length. Fig. 6.4 shows experimental and SCMFT simulation CMC values of the surfactants $C_nE_m$, where the length of the tail $n$ is kept constant and the length of the head, $m$ increases. As can be seen, the CMC increases with the length

UNIVERSITAT ROVIRA I VIRGILI
MICROSCOPIC MODELING OF THE SELF ASSEMBLY OF SURFACTANTS: SHAPE TRANSITIONS AND CRITICAL MICELLE CONCENTRATIONS
Asfaw Gezae Daful
ISBN:/DL:T. 1024-2011



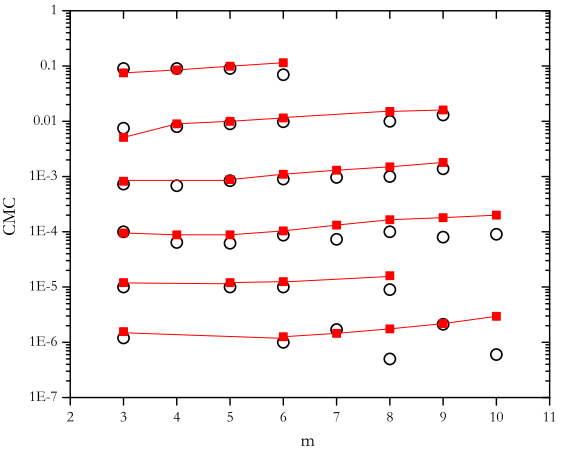


**Figure 6.4:** Critical micelle concentration in [mol/L] versus the length of the head group, $m$ for $C_nE_m$ surfactants for given tail lengths, $n$ ($n$=6, 8, 10, 12, 14, and 16 from top to bottom). Open circles are experimental values from the literature, while filled squares are values calculated from the SCMF theory, lines are included to help guide the eye.

of the head group $m$ for all $C_nE_m$. The SCMFT simulation predicts a smoother trend for the CMC with increasing number of hydrophilic monomers as compared with the literature experimental values, this is particularly the case for the long hydrophobic tails ($C_{12}$, $C_{14}$, $C_{16}$). In addition we observe that the change of the CMC value per oxyethylene unit in the hydrophilic head is much smaller than that per methylene unit in the hydrophobic tail.

Amphiphiles with an increase in the number of methylene groups, $n$ of the alkyl chain of the hydrophobic tail leads to a decrease in the CMC [3, 182]. A linear relationship is found between the log CMC and the number of methylene (tail) groups, in the tail chain, $n$, for surfactants with the same number of head groups, as shown in Fig. 6.3. The dependence of CMC on $n$ may be expressed as:

$$\log \mathrm{CMC} = \mathrm{a} - \mathrm{bn} \tag{6.4}$$

The constants a and b are calculated from the simulation results, and in the following table for series of surfactants $C_nE_m$, for a given $m$.

UNIVERSITAT ROVIRA I VIRGILI
MICROSCOPIC MODELING OF THE SELF ASSEMBLY OF SURFACTANTS: SHAPE TRANSITIONS AND CRITICAL MICELLE CONCENTRATIONS
Asfaw Gezae Daful
ISBN:/DL:T. 1024-2011



**Table 6.2:** Constants for relating a and b in Eq. (6.4), for surfactants $C_nE_m$

| m | a | b |
|---|---|---|
| 3 | 1.43923 | -0.4512 |
| 4 | 1.92709 | -0.4982 |
| 5 | 1.93697 | -0.4944 |
| 6 | 2.01844 | -0.4959 |
| 7 | 2.02769 | -0.4918 |
| 8 | 2.09321 | -0.4912 |
| 9 | 2.08146 | -0.4842 |

Fig. 6.5, shows the variation of free surfactant concentration($X_1$) as a function of the total amphiphilic concentration $X_t$ for $C_nE_3$, where $n$ is equal to 6, 7, 8, 10, 12, 14 and 16. The intersection of the line $X_1 = X_t$ and an asymptotic line of the second part of the curve gives the critical micelle concentration. After this concentration (CMC) $X_1$ saturates to a nearly constant value, indicating that any new surfactant molecule added to the system preferably undergoes micellation instead of remaining as a free surfactant in the bulk phase, as energetically it becomes increasingly favorable to the formation of larger clusters. Notice that the plots of $X_1$ as a function of $X_t$ for different length of the hydrophilic head group ( i.e. keeping $m$ constant for $C_nE_m$ at 4, 5, 6, 7, 8, and 9, and changing hydrophobic tail length $n$ for each $m$) show similar trends (not shown) as Fig. 6.5. One can easily see that the longer the hydrophobic chain segment the lower is its CMC value.

The equilibrium micelle size distribution for the some selected surfactants are shown in Fig. 6.6. The micellar size distributions are smooth with a peak, corresponding to the average aggregation number of the micelle.

In agreement with geometric considerations[3], the aggregation numbers in aqueous solution increase with an increase in the length of the hydrophobic group, and decrease with respect to an increase in the number of hydrophilic units[1]. Fig. 6.7 shows the variation of the aggregation number with the length of the hydrophilic segment, $m$, of the surfactant, $C_{12}E_m$, where it can be seen that the longer the hydrophilic segment, the lower the aggregation number is. It can also be seen that the decrease in the aggregation number per unit length of the hydrophilic segment is faster for short hydrophilic segment lengths.

It is of course expected that the hydrophobic part of the surfactant will concen-

[1] For example, in a spherical micelle in aqueous media, the surface area, $n \times a_o = 4\pi(l_c+\Delta)^2$, or $n = 4\pi(l_c+\Delta)^2/a_o$ where $\Delta$ is the added length of the radius of the sphere due to the hydrophilic group. Similarly, the volume of the hydrophobic core $n \times V_H = \frac{4}{3}\pi l_c^3$ or $n = \frac{4}{3}\pi l_c^3/V_H$, (see section 3.8)

UNIVERSITAT ROVIRA I VIRGILI
MICROSCOPIC MODELING OF THE SELF ASSEMBLY OF SURFACTANTS: SHAPE TRANSITIONS AND CRITICAL MICELLE CONCENTRATIONS
Asfaw Gezae Daful
ISBN:/DL:T. 1024-2011



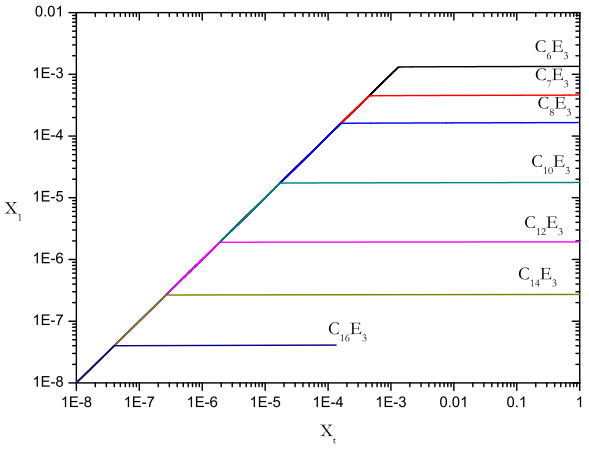


**Figure 6.5:** Variation of the free surfactant concentration $X_1$ as a function of the total concentration $X_t$ for $C_nE_3$.

trate in the center of the micelle, to maximize the number of tail-tail contacts, so that the hydrophilic parts be expelled to the outer regions of the micelle. Such a behavior has indeed been observed in previous simulations, and is also found in this work. As already mentioned, micelles consist of a core of hydrophobic chains shielded from contact with water by hydrophilic head groups. The hydrophilic units of surfactants form a micellar corona. This can be seen in the configuration plot of a spherical micelle of $C_8E_3$ with aggregation number $N = 382$, and its cross-sectional view in Fig. 6.1. Please note that this is plotted by selecting the most probable conformations so as to give a general idea of the micelle and although the individual chain configurations are correct, it does not include excluded volume interactions between surfactants.

In Fig. 6.8 and Fig. 6.9 the radial volume fraction profiles of a micelle of size $N = 100$ and $N = 1000$ respectively are given for the $C_{16}E_3$ surfactant. As can be seen from the plots, the core of the micelle is predominantly occupied by the tail segments, with the hydrophilic head segments at the interface between the tail segments and the bulk water where it has a maximum. Fig. 6.8 is typical of micellar distribution plots for spherical micelles found in this and other simulation studies and has an approximately constant value of the different tail and head segments away from the interfacial zone inside the micelle core. However, in the case of the larger micelles found in this work for aggregation sizes greater than ($N \sim 400$) a different behavior is observed. In particular, the volume fraction of

UNIVERSITAT ROVIRA I VIRGILI
MICROSCOPIC MODELING OF THE SELF ASSEMBLY OF SURFACTANTS: SHAPE TRANSITIONS AND CRITICAL MICELLE CONCENTRATIONS
Asfaw Gezae Daful
ISBN:/DL:T. 1024-2011



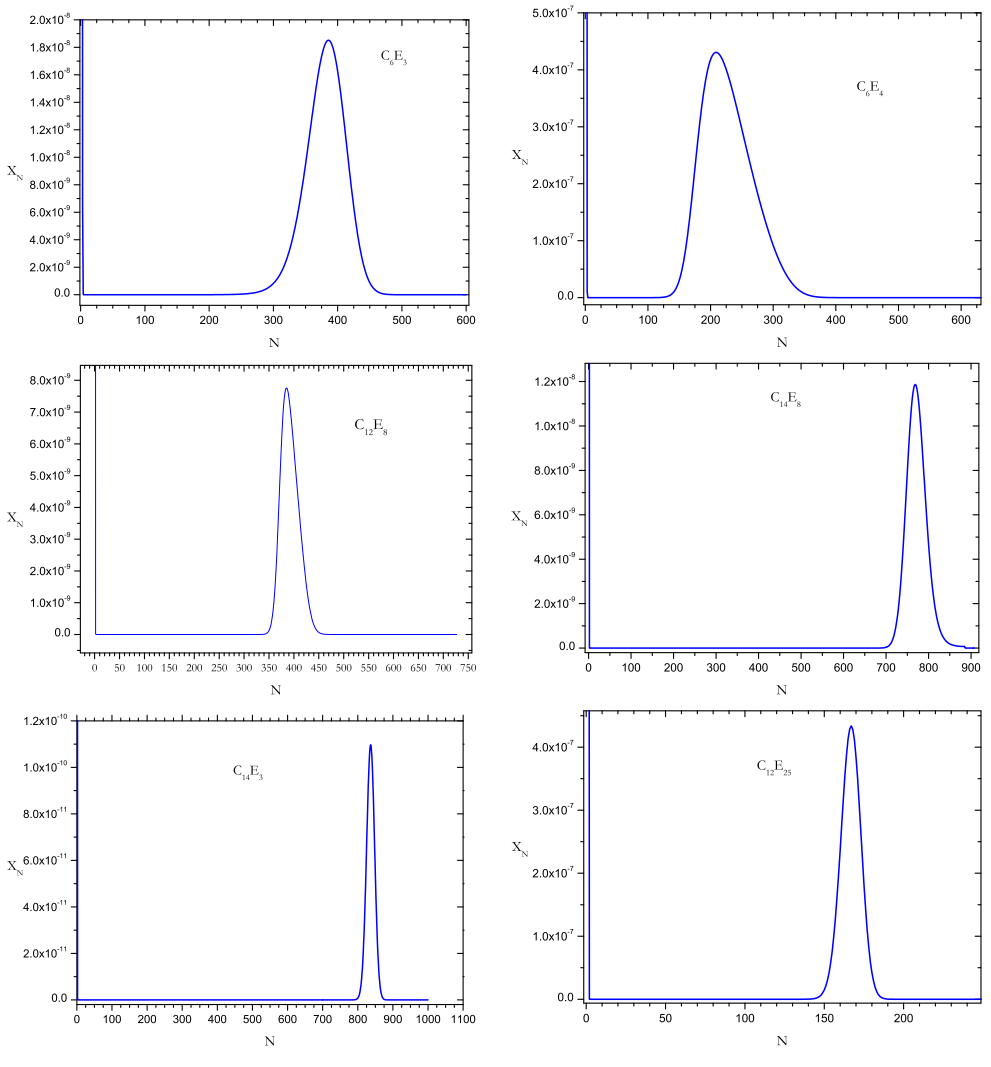


**Figure 6.6:** Micellar concentration, $X_N$, versus aggregation number $N$ for selected surfactants

UNIVERSITAT ROVIRA I VIRGILI
MICROSCOPIC MODELING OF THE SELF ASSEMBLY OF SURFACTANTS: SHAPE TRANSITIONS AND CRITICAL MICELLE CONCENTRATIONS
Asfaw Gezae Daful
ISBN:/DL:T. 1024-2011



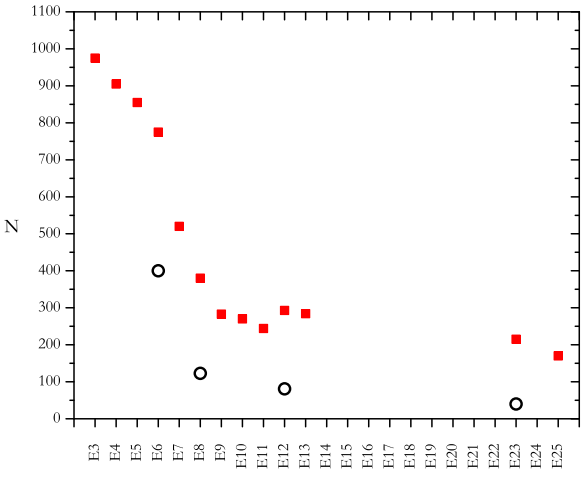


**Figure 6.7:** Effect of the number of oxyethylene monomers, $m$, on the aggregation number for the polyoxyethylene alkyl ether surfactants of hydrophobic length 12, $C_{12}E_m$, in a log-linear plot. Open circles represent literature experimental values while filled squares represent SCMFT simulation values from this work.

UNIVERSITAT ROVIRA I VIRGILI
MICROSCOPIC MODELING OF THE SELF ASSEMBLY OF SURFACTANTS: SHAPE TRANSITIONS AND CRITICAL MICELLE CONCENTRATIONS
Asfaw Gezae Daful
ISBN:/DL:T. 1024-2011



tail segments drops towards the center of the micelle and that of the head segments increases. This is no doubt due to fact that as the volume and hence diameter of the micelle core becomes larger, at some point the tails are not able to reach the center while maintaining the head at the surface. Normally this forces the free energy of the micelle to increase and makes the larger micelles unfavorable. However, due to the interaction parameters used in this work, namely that the tail-head interaction is more favorable than the tail-water one, it is found that an even more stable conformation can be found in some cases by placing the heads in the center as well as at the interface. This can be seen from the plots of the volume fraction profiles given in Fig. 6.9 for a micelle of size $N = 1000$ where the head volume fraction reaches a second maximum in the center of the micelle, a "prevesicular" micelle.

With regards to the experimental data available, a wide range of micelle aggregation numbers from less than a hundred to several thousand have been reported for these surfactants (see Table 6.1), however it is not clear what geometrical form these micelles have. The SCMFT calculations carried out here assume a spherical geometry which may not be consistent with the experimental system. It is also possible to carry out calculations for other one or two dimensional geometries in the SCMFT, however these calculations have not been carried out in this work since the main focus here is on reproducing the CMC values. In addition, variations in the interaction parameters may affect the relative stability of these large micelles, where the balance between the tail-head and tail-water interaction is certainly important. The tail-head interaction is not available experimentally and is difficult to fix. These effects can change the size of the preferred aggregation number as small changes of the order of a fraction of a $kT$ are important, and so the simulation data for aggregation number should be treated with caution. However, the CMC is controlled by free energy differences of several $kT$ and is not expected to be significantly affected.

We have also investigated the temperature dependence of the CMC and aggregation number for several of the surfactants. Here we assume that the model $\chi$ parameters should have an inverse temperature dependence. In Fig. 6.10 a plot of the CMC for $C_8E_6$ is given as a function of temperature along with the available experimental data where we have modified our original $\chi$ parameters accordingly. As can be seen, we obtain a similar behavior with a decrease in the CMC with temperature as expected. However, the model over predicts the rate of this change. We also find the correct qualitative behavior for the increase in aggregation number with temperature. In fact, it is well known that such an inverse dependence is adequate only for simple solvents and that the hydrogen bonding characteristics of water make it more difficult to model. Experimental data for the temperature

UNIVERSITAT ROVIRA I VIRGILI
MICROSCOPIC MODELING OF THE SELF ASSEMBLY OF SURFACTANTS: SHAPE TRANSITIONS AND CRITICAL MICELLE CONCENTRATIONS
Asfaw Gezae Daful
ISBN:/DL:T. 1024-2011



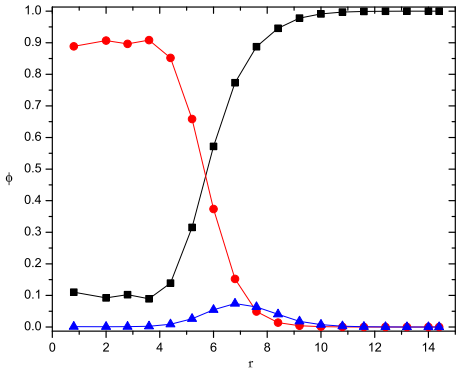


**Figure 6.8:** Radial distribution of volume fraction profiles for the $C_{16}E_3$ surfactant for a micelle of size $N = 100$: tail (circles), head (triangles) and solvent(squares)

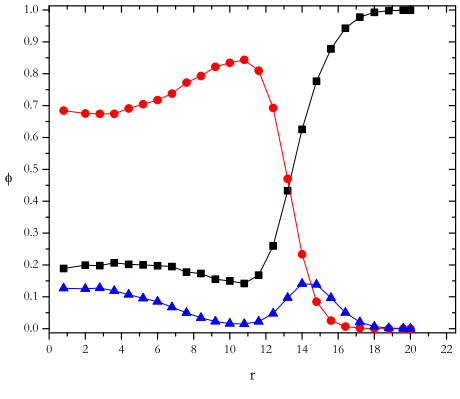


**Figure 6.9:** Radial distribution of volume fraction profile for the $C_{16}E_3$ surfactant for a micelle of size $N = 1000$: tail (circles), head (triangles) and solvent(squares)

UNIVERSITAT ROVIRA I VIRGILI
MICROSCOPIC MODELING OF THE SELF ASSEMBLY OF SURFACTANTS: SHAPE TRANSITIONS AND CRITICAL MICELLE CONCENTRATIONS
Asfaw Gezae Daful
ISBN:/DL:T. 1024-2011



dependence of hydrocarbons in water is available[173] and, together with additional information for the temperature dependence of the head water and head tail interaction, it should be possible to obtain an improved temperature dependence. This effective model gives a similar qualitative temperature dependence of the Aggregation number of micelles see Fig. 6.11. Similarly, the temperature dependence of the CMC values of $C_{12}E_4$ and its corresponding aggregation numbers are shown in Fig. 6.12.

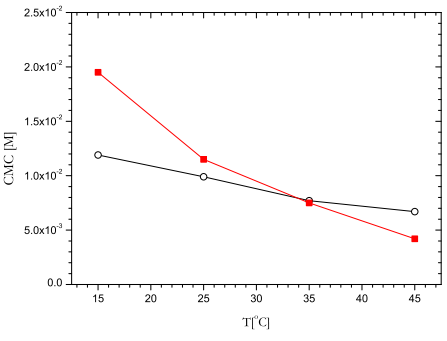


**Figure 6.10:** CMC of $C_8E_6$ as a function of temperature: experimental value (circles), simulation value (squares)

UNIVERSITAT ROVIRA I VIRGILI
MICROSCOPIC MODELING OF THE SELF ASSEMBLY OF SURFACTANTS: SHAPE TRANSITIONS AND CRITICAL MICELLE CONCENTRATIONS
Asfaw Gezae Daful
ISBN:/DL:T. 1024-2011



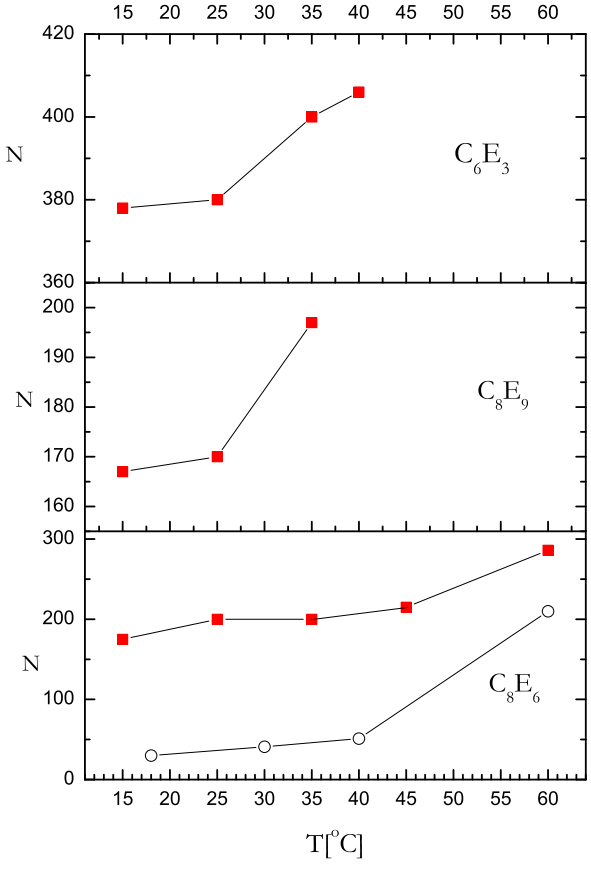


**Figure 6.11:** Aggregation number of as a function of temperature:experimental value (circles), simulation value (squares)

UNIVERSITAT ROVIRA I VIRGILI
MICROSCOPIC MODELING OF THE SELF ASSEMBLY OF SURFACTANTS: SHAPE TRANSITIONS AND CRITICAL MICELLE CONCENTRATIONS
Asfaw Gezae Daful
ISBN:/DL:T. 1024-2011



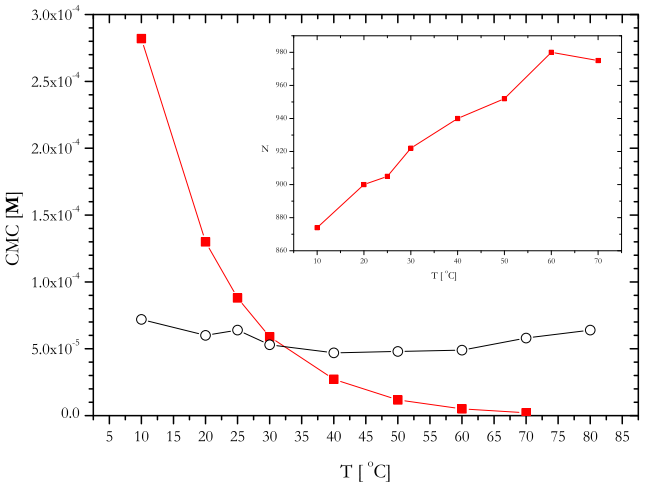


**Figure 6.12:** CMC values of $C_{12}E_4$ as a function of temperature: experimental value (circles), simulation value (squares). The inset shows its aggregation number, $N$, of as a function of temperature from the the SCMFT calculations

## 6.4 Conclusions

In this work, the Single Chain Mean Field Theory has been applied to quantitatively reproduce the critical micelle concentration values of a wide range of nonionic polyoxyethylene alkyl ether surfactants, $C_nE_m$. The main objective was to develop an explicit but simple microscopic model within our SCMFT simulation methodology in order to capture the micellization process. In particular, a three interaction parameter continuous space model has been chosen. The head-water interaction was taken from literature experimental work, whereas the tail-water interaction was estimated from alkane-water solubility data. An optimization method was then applied to fine tune the tail-water interaction and fit the head-tail interaction, for which no experimental information could be found. The resulting SCMFT model has been shown to successfully reproduce the experimental critical micelle concentrations of polyoxyethylene alkyl ether surfactants in water. As expected, the cmc values decrease exponentially with increasing surfactant tail length while it slightly increases with an increase of the head length of the surfactant.

In addition, certain microscopic properties were also calculated and analyzed. These include the micellar volume fraction profiles as well as the preferred aggregation number, where it was found that increasing the alkyl chain (tail) length

UNIVERSITAT ROVIRA I VIRGILI
MICROSCOPIC MODELING OF THE SELF ASSEMBLY OF SURFACTANTS: SHAPE TRANSITIONS AND CRITICAL MICELLE CONCENTRATIONS
Asfaw Gezae Daful
ISBN:/DL:T. 1024-2011



or decreasing the poly(oxyethylene) chain (head) length causes an increase in the micelle aggregation number. The aggregation number may be sensitive to the approximations used in this work and further work requires to be carried out to check assumptions such as the assumed spherical geometry or the particular values of the head-tail interaction parameters, particularly for the larger micelles of more than approximately four hundred surfactants. To conclude, this work offers interesting perspectives for the use of an explicit microscopic model with the Single Chain Mean Field Theory to quantitatively model the micellization process and give accurate values for the critical micelle concentrations.

UNIVERSITAT ROVIRA I VIRGILI
MICROSCOPIC MODELING OF THE SELF ASSEMBLY OF SURFACTANTS: SHAPE TRANSITIONS AND CRITICAL MICELLE CONCENTRATIONS
Asfaw Gezae Daful
ISBN:/DL:T. 1024-2011

UNIVERSITAT ROVIRA I VIRGILI
MICROSCOPIC MODELING OF THE SELF ASSEMBLY OF SURFACTANTS: SHAPE TRANSITIONS AND CRITICAL MICELLE CONCENTRATIONS
Asfaw Gezae Daful
ISBN:/DL:T. 1024-2011

# Bibliography

[1] J. Israelachvili, *Intermolecular and Surface Forces*, 7th ed. (Academic Press, California, USA, 1998).

[2] K. Holmberg, B. Jonsson, B. Kronberg, and B. Lindman, *Surfactants and Polymers in Aqueous Solution*, 2nd ed. (John Wiley & Sons, Ltd, 2002).

[3] M. J. Rosen, *Surfactants and Interfacial Phenomena* (John Wiley & Sons, LTD, 2004).

[4] I. W. Hamley, *Introduction to Soft Matter: Synthetic and Biological Self-Assembling Materials* (John Wiley & Sons, Ltd, 2007).

[5] Z. A. Al-Anber, J. Bonet-Avalos, M. A. Floriano, and A. D. Mackie, J. Chem. Phys., **118**, 3816 (2003).

[6] K. L. Mittal and D. O. Shah, *Adsorption and aggregation of surfactants in solution* (Marcel Dekker, Inc., New York, USA, 2003).

[7] T. Goel, M. Kumbhakar, T. Mukherjee, and H. Pal, Journal of Photochemistry and Photobiology A: Chemistry, **209**, 41 (2010).

[8] P. Debye and E. W. Anacker, J. phy. Colloid Chem., **55**, 644 (1951).

[9] J. C. Eriksson and S. Ljunggren, J. Chem. Soc. Faraday Trans., **2**, 1209 (1985).

[10] J. Molina-Bolívar, J. Aguiar, J. M. Peula-García, and C. C. Ruiz, J. Phys. Chem. B, **108**, 12813 (2004).

[11] A. Rodriguez, M. del Mar Graciani, K. Bitterman, A. T. Carmona, and M. L. Moya, Journal of Colloid and Interface Science, **13**, 542 (2007).

UNIVERSITAT ROVIRA I VIRGILI
MICROSCOPIC MODELING OF THE SELF ASSEMBLY OF SURFACTANTS: SHAPE TRANSITIONS AND CRITICAL MICELLE CONCENTRATIONS
Asfaw Gezae Daful
ISBN:/DL:T. 1024-2011



[12] S. P. Denkova, L. V. Lokeren, I. Verbruggen, and R. Willem, J. Phys. Chem., **112**, 10935 (2008).

[13] D. Stigter, J. Phys. Chem., **70**, 1323 (1966).

[14] M. Miura and M. Kodama, Bulletin of the Chemical Society of Japan, **45**, 2265 (1972).

[15] S. Hayashi and S. Ikeda, J. Phys. Chem. (1980).

[16] K. W. Herrmann, J. Phys. Chem., **68**, 1540 (1964).

[17] D. Attwood., A. Terreros, E. Lopez-Cabarcos, and P. A. Galera-Gomezy, Journal of Colloid and Interface Science, **235**, 247 (2001).

[18] M. Kodama, Y. Kubota, and M. Miura, Bulletin of the Chemical Society of Japan, **45**, 2953 (1972).

[19] T. Kato, M.-A. Kanada, and T. Seimiya, journal of colloid and interface science, **181**, 149 (1996).

[20] A. Bernheim-Groswasser, R. Zana, and Y. Talmon, J. Phys. Chem. B, **104**, 4005 (2000).

[21] A. Bernheim-Groswasser, E. Wachtel, and Y. Talmon, Langmuir, **16**, 4131 (2000).

[22] A. Khan, A. Kaplun, Y. Talmon, and M. Hellsten, Journal of Colloid and Interface Science, **181**, 191 (1996).

[23] Y. Zheng, W. You-Yeon, F. S. Bates, H. T. Davis, L. E. Scriven, and Y. Talmon, J.phys.chem. B, **103**, 10331 (1999).

[24] P. Cummins, E. Staples, J. Penfold, and R. K. Heenan, Langmuir, **5**, 1195 (1989).

[25] M. Nakano, H. Matsuoka, H. Yamaoka, A. Poppe, and D. Richter, Macromolecules, **32**, 697 (1999).

[26] P. Kaewsaiha, K. Matsumoto, and H. Matsuoka, Langmuir, **23**, 9162 (2007).

[27] H. Heerklotz, A. Tsamaloukas, K. Kita-Tokarczyk, P. Strunz, and T. Gutberlet, J. Am. Chem. Soc., **126**, 16544 (2004).

[28] R. G. Alargova, K. D. Danov, J. T. Petkov, P. A. Kralchevsky, G. Broze, and A. Mehreteab, Langmuir, **13**, 5544 (1997).

UNIVERSITAT ROVIRA I VIRGILI
MICROSCOPIC MODELING OF THE SELF ASSEMBLY OF SURFACTANTS: SHAPE TRANSITIONS AND CRITICAL MICELLE CONCENTRATIONS
Asfaw Gezae Daful
ISBN:/DL:T. 1024-2011



[29] S. Karaborni and J. O'Connell, J. Phys. Chem., **94**, 2624 (1990).

[30] S. Ikeda, J. Chem. Phys., **88**, 2144 (1984).

[31] E. Ruckenstein and R. Nagarajan, J. Phys. Chem., **85**, 3010 (1981).

[32] S. May and A. Ben-Shaul, J. Phys. Chem., **105**, 630 (2001).

[33] N. Zoeller, L. Lue, and D. Blankschtein, Langmuir, **13**, 5258 (1997).

[34] I. Reif, M. Mulqueen, and D. Blankschtein, Langmuir, **17**, 5801 (2001).

[35] R. Nagarajan, Langmuir, **1**, 331 (1985).

[36] R. Nagarajan, Langmuir, **7**, 2934 (1991).

[37] F. A. M. Leermakers and J. M. H. M. Scheutjens, J. Phys. Chem, **93**, 7417 (1989).

[38] S. J. Marrink, D. P. Tieleman, and A. E. Mark, J. Phys. Chem. B, **104**, 12165 (2000).

[39] N. Yoshii, K. Iwahashi, and S. Okazakia, J. Chem. Phys, **124**, 184901 (2006).

[40] B. Z. Shang, Z. Wang, and R. G. Larson, J. Phys. Chem. B, **112**, 2888 (2007).

[41] F. A. M. Leermakers, C. M. Wijmans, and G. J. Fleer, Macromolecules, **28**, 3434 (1995).

[42] V. de Bruijn, L. J. P. van den Broeke, F. A. M. Leermakers, and J. T. F. Keurentjes, Langmuir, **18**, 10467 (2002).

[43] Y. Lauw, F. A. M. Leermakers, and M. A. C. Stuart, J. Phys. Chem., **107**, 10912 (2003).

[44] A. Ben-Shaul, W. M. Gelbart, and I. Szleifer, J. Chem. Phys, **83**, 3597 (1985).

[45] I. Szleifer, A. Ben-Shaul, and W. M. Gelbart, J. Chem. Phys, **83**, 3612 (1985).

[46] A. D. Mackie, A. Z. Panagiotopoulos, and I. Szleifer, Langmuir, **13**, 5022 (1997).

[47] A. M. Floriano, E. Caponetti, and A. Z. Panagiotopoulos, Langmuir, **15**, 3143 (1999).

UNIVERSITAT ROVIRA I VIRGILI
MICROSCOPIC MODELING OF THE SELF ASSEMBLY OF SURFACTANTS: SHAPE TRANSITIONS AND CRITICAL MICELLE CONCENTRATIONS
Asfaw Gezae Daful
ISBN:/DL:T. 1024-2011



[48] M. Sammalkorpi, M. Karttunen, and M. Haataja, J. phy. chem. B, **111**, 11722 (2007).

[49] R. G. Larson, J. Chem. Phys., **89**, 1642 (1988).

[50] E. Khurana, S. O. Nielsen, , and M. L. Klein, J. Phys. Chem. B, **110**, 22136 (2006).

[51] G. Jian, R. Ying, and G. Wei, Chinese Journal of Chemical Engineering, **17**, 654 (2009).

[52] R. G. Larson, L. E. Scriven, and H. T. Davis, J. Chem. Phys., **83**, 2411 (1985).

[53] H. Gharibi, S. Hashemianzadeh, and B. Razavizadeh, Physicochemical and Engineering Aspects, **196**, 31 (2002).

[54] A. Z. Panagiotopoulos, M. A. Floriano, and S. K. Kumar, Langmuir, **18**, 2940 (2002).

[55] Z. A. Al-Anber, J. Bonet-Avalos, and A. D. Mackie, J. Chem. Phys., **122**, 104910 (2005).

[56] S. Ozeki and S. Ikeda, Journal of Colloid and Interface Science, **77**, 219 (1980).

[57] T. F.Tadros, *Applied Surfactants: Principles and Applications* (Wiley -Vich Verlag GmbH & Co. KGaA, 2005).

[58] R. Anthony and L. Jones, *Soft Condensed Matter*, 1st ed., edited by O. U. Press (Oxford University Press, USA, 2002).

[59] S. Fujiwara, T. Itoh, M. Hashimoto, and R. Horiuchi, J. Phys. Chem., **130**, 144901 (2009).

[60] A. Bhattacharya and S. D. Mahanti, J. Phys.: Condens. Matter, **12**, 6141 (2000).

[61] A. V. Sineva, A. M. Parfenova, and A. A. Fedorova, Colloids and Surfaces A: Physicochemical and Engineering Aspects, **306**, 68 (2007).

[62] T. Polubesova, S. Nir, D. Zadaka, O. Rabinovitz, C. Serban, L. Groisman, and B. Rubin, Environmental Science & Technology, **39**, 2343 (2005).

[63] L. L. Schramm, *Surfactants: Fundamentals and Applications in the Petroleum Industry* (Cambridge University Press, 2000).

UNIVERSITAT ROVIRA I VIRGILI
MICROSCOPIC MODELING OF THE SELF ASSEMBLY OF SURFACTANTS: SHAPE TRANSITIONS AND CRITICAL MICELLE CONCENTRATIONS
Asfaw Gezae Daful
ISBN:/DL:T. 1024-2011



[64] S. A. Hagan, A. G. A. Coombes, M. C. Garnett, S. E. Dunn, M. C. Davies, L. Illum, and S. S. Davis, Langmuir, **12**, 2153 (1996).

[65] C. Tanford, *The Hydrophobic Effect: Formation of Micelles and Biological Membranes* (John Wiley & Sons, Inc., 1973).

[66] L. Maibaum, A. R. Dinner, and D. Chandler, J. Phys. Chem. B, **108**, 6778 (2004).

[67] D. Chandler, Nature, **437**, 640 (2005).

[68] R. Rajagopalan, Current Opinion in Colloid & Interface Science, **6**, 357 (2001).

[69] S. A. Safran, *Statistical Thermodynamics of Surfaces, Interfaces, and Membranes* (Westview Press, 2003).

[70] B. Widom, *Statistical Mechanics: A Concise Introduction for Chemists*, 1st ed. (Cambridge University Press, 2002).

[71] J. Ulmius, H. Wennerstroem, L. B. A. Johansson, G. Lindblom, and S. Gravsholt, J. Phys. Chem., **83**, 2232 (1979).

[72] T. L. Hill, *An introduction to statistical thermodynamics* (Dover Publications, 1987).

[73] N. Laurendeau, *Statistical thermodynamics: fundamental and applications* (Cambridge University Press, New York, 2005).

[74] McQuarry and A. Donald, *Statistical Thermodynamics* (University Science Books, 1973).

[75] I. Szleifer, *Statestical thermodynamics of amphiphilic aggregates*, Ph.D. thesis, Hebrew University, Israel (1988).

[76] Z. A. Al-Anber, *Statistical Thermodynamics of Surfactants, Micelles and Microemulsions*, Ph.D. thesis, Universitat Rovira i Virgili (2003).

[77] Y. Moroi, *Micelles: Theoretical and Applied Aspects* (Plenum Press, New York, 1992).

[78] J. Smith, H. V. Ness, and M. Abbott, *Introduction to Chemical Engineering Thermodynamics*, 6th ed. (McGraw-Hill Science, 2000).

[79] J. M. Prausnitz, R. N. Lichtenthaler, and E. G. de Azevedo, *Molecular thermodynamics of fluid-phase equilibria*, 3rd ed. (Prentice-Hall PTR, 1999).

UNIVERSITAT ROVIRA I VIRGILI
MICROSCOPIC MODELING OF THE SELF ASSEMBLY OF SURFACTANTS: SHAPE TRANSITIONS AND CRITICAL MICELLE CONCENTRATIONS
Asfaw Gezae Daful
ISBN:/DL:T. 1024-2011



[80] B. Linder, *Thermodynamics and Introductory Statistical Mechanics* (Wiley-Interscience, 2004).

[81] J. C. Shelley and M. Y. Shelley, current opinion in colloid and Interface Science, **5**, 101 (2000).

[82] C. D. Bruce, M. L. Berkowitz, L. Perera, , and M. D. E. Forbes, J. Phys. Chem. B, **106**, 3788 (2002).

[83] J. Maillet, V. Lachet, and P. V. Coveney, Phys. Chem. Chem. Phys., **1**, 5277 (1999).

[84] A. Milchev, A. Bhattacharya, and K. Binder, Macromolecules, **34**, 1881 (2001).

[85] P. H. Nelson, G. C. Rutledge, and T. A. Hatton, J. Chem. Phys., **107**, 10777 (1997).

[86] R. G. Larson, J. Chem. Phys., **83**, 2411 (1985).

[87] C. M. Care, J. Chem. SOC.FaradayTrans. 1, **83**, 2905 (1987).

[88] M. Allen and D. Tildesley, *Computer Simulation of Liquids* (Clarendon, Oxford, 1991).

[89] B. Owenson and L. R. Pratt, J. Phys. Chem., **88**, 2905 (1984).

[90] H. Xuehao, H. Liang, and C. Pan, Physical Review E, **63** (2001).

[91] Y. Termonia, Journal of Polymer Science, **40**, 890 (2002).

[92] S. K. Talsania, R.-G. L. A, K. K. Mohanty, and R. Rajagopalan, Langmuir, **15**, 437 (1999).

[93] D. Viduna, A. Milchev, and K. Binder, Macromol. Theory Simul., **7**, 649 (1998).

[94] D. Frenkel and B. Smit, *Understanding Molecular Simulation: From Algorithms to Applications*, 2nd ed. (Academic Press, 2001).

[95] M. Opper and D. Saad, *Advanced mean field methods: theory and practice* (The MIT Press, 2001).

[96] J. M. H. M. Scheutjens and G. J. Fleer, American Chemical Society, **83**, 1619 (1979).

UNIVERSITAT ROVIRA I VIRGILI
MICROSCOPIC MODELING OF THE SELF ASSEMBLY OF SURFACTANTS: SHAPE TRANSITIONS AND CRITICAL MICELLE CONCENTRATIONS
Asfaw Gezae Daful
ISBN:/DL:T. 1024-2011



[97] J. M. H. M. Scheutjens and G. J. Fleer, J. Phys. Chem., **84**, 178 (1980).

[98] M. R. Böhmer and L. K. Koopal, Langmuir, **6**, 1478 (1990).

[99] F. A. M. Leermakers, P. R. Majhi, P. L. Dubin, X. Feng, X. Guo, and C. Tribet, J. Phys. Chem. B, **108**, 5980 (2004).

[100] A. B. Jódar-Reyes and F. A. M. Leermakers, J. Phys. Chem. B, **110**, 6300 (2006).

[101] M. N. Rosenbluth and A. W. Rosenbluth, Journal of chemical physics, **23**, 356 (1955).

[102] S. Puvvada and D. Blankschtein, The Journal of Physical Chemistry, **96**, 5579 (1992).

[103] S. Puvvada and D. Blankschtein, Langmuir, **90**, 894 (1990).

[104] R. Nagarajan, Langmuir, **18**, 31 (2002).

[105] N. Metropolis and S. Ulam, Journal of the American Statistical Association, **44**, 335 (1949).

[106] A. D. Mackie, *Aggregation and Phase behavior for Lattice Polymer and Amphiphile Models*, Ph.D. thesis, Cornell University (1996).

[107] D. P. Landau and K. Binder, *A Guide to Monte Carlo Simulations in Statistical Physics*, 2nd ed. (Cambridge University Press, 2005).

[108] F. Sterpone, G. Briganti, and C. Pierleoni, Langmuir, **25**, 8960 (2009).

[109] A. Gonzalez-Perez, L. Varela, M. Garcia, and J. Rodriguez, Journal of Colloid and Interface Science, **293**, 213 (2006).

[110] A. González-Pérez and J. M. Ruso, Colloids and Surfaces A: Physicochemical and Engineering Aspects, **356**, 84 (2010).

[111] M. Chauhan, G. Kumar, A. Kumar, K. Sharma, and S. Chauhan, Colloids and Surfaces, **180**, 111 (2001).

[112] K. N. Panchal, A. Desai, and T. Nagar, Journal of Dispersion Science and Technology, **27**, 963 (2006).

[113] H. H. Kohler and J. Strnad, J. Phys. Chem, **94**, 7628 (1990).

[114] G. Porte, Y. Poggi, J. Appell, and G. Maret, J. Phys. Chem., **88**, 5713 (1984).

UNIVERSITAT ROVIRA I VIRGILI
MICROSCOPIC MODELING OF THE SELF ASSEMBLY OF SURFACTANTS: SHAPE TRANSITIONS AND CRITICAL MICELLE CONCENTRATIONS
Asfaw Gezae Daful
ISBN:/DL:T. 1024-2011



[115] A. Gonzalez-Perez, J. Czapkiewicz, G. Prieto, and J. Rodriguez, Colloid Polym Sci, **281**, 1191 (2003).

[116] J. Zhang, Z. Ge, X. Jiang, P. Hassan, and S. Liu, Journal of Colloid and Interface Science, **316**, 796 (2007).

[117] S. E. Burke and A. Eisenberg, Langmuir, **17**, 6705 (2001).

[118] P. A. Cirkel and G. J. M. Koper, Langmuir, **14**, 7095 (1998).

[119] H. von Berlepsch, H. Dautzenberg, G. Rother, and J. Jäger, Langmuir, **12**, 3631 (1996).

[120] W. Lin, C. Zheng, X. Wan, D. Liang, and Q. Zhou, Macromolecules, **43**, 5405 (2010).

[121] S. J. Lee and M. J. Park, Langmuir, **26**, 17827 (2010).

[122] L. He, V. M. Garamus, S. S. Funari, M. Malfois, R. Willumeit, and B. Niemeyer, The journal of physical chemistry. B, **106**, 7596 (2002).

[123] B. Widom, J. Phys. Chem., **88**, 6508 (1984).

[124] J. M. Haile, M. C. Woods, and J. . P. O'Connell, J. Phys. Chem., **90**, 1875 (1986).

[125] K. Watanabe, M. Ferrario, and M. L. Klein, J. Phys. Chem., **92**, 819 (1988).

[126] D. R. Rector, F. V. Swol, and J. R. Henderson, Molecular Physics, **82**, 1009 (1994).

[127] B. J. Palmer and J. Liu, LangmuirI, **12**, 6015 (1996).

[128] B. Smit, P. A. J. Hilbers, K. Esselink, L. Rupert, N. van Os, and A. Schlijper, J. Phys. Chem., **95**, 6361 (1991).

[129] B. Smit, K. Esselink, P. A. J. Hilbers, N. M. V. Os, L. A. M. Rupert, and I. Szleifer, J. Phys. Chem., **9**, 9 (1993).

[130] B. Fodi and R. Hentschke, LangmuirI, **16**, 1626 (2000).

[131] G. Jian, G. Wei, and L. Jinghai, Science in China Ser. B Chemistry, **48**, 470 (2005).

[132] T. Zehl, M. Wahab, H. J. Mögel, and P. Schiller, Langmuir, **22**, 2523 (2006).

UNIVERSITAT ROVIRA I VIRGILI
MICROSCOPIC MODELING OF THE SELF ASSEMBLY OF SURFACTANTS: SHAPE TRANSITIONS AND CRITICAL MICELLE CONCENTRATIONS
Asfaw Gezae Daful
ISBN:/DL:T. 1024-2011



[133] T. Zehl, M. Wahab, R. Schmidt, P. Schiller, and H. Mögel, Journal of Molecular Liquids, **147**, 178 (2009).

[134] W. K. den Otter, S. A. Shkulipa, and W. J. Briels, J. Phys. Chem., **119**, 2363 (2003).

[135] C. A. J. Hoeve and G. C. Benson, J. Phys. Chem., **61**, 1149 (1957).

[136] A. Ben-Shaul, W. M. Gelbart, and I. Szleifer, Proc. Natl. Acad. Sci., **81**, 4601 (1984).

[137] W. F. Edmonds, Z. Li, M. A. Hillmyer, and T. P. Lodge, Macromolecules, **39**, 4526 (2006).

[138] H. Xuehao and F. Schmid, phys. Rev. Lett., **100**, 137802 (2008).

[139] H. Huang, B. Chung, J. Jung, H.-W. Park, and T. Chang, Angew. Chem. Int. Ed., **48**, 4594 (2009).

[140] Z. Chen, H. Cui, K. Hales, K. Qi, K. L. Wooley, and D. J.Pochan, Science, **306**, 94 (2004).

[141] M. Swanson-Vethamuthu, E. Feitosa, and W. Brown, Langmuir, **14**, 1590 (1998).

[142] D. J.Pochan, Langmuir, **21**, 7533 (2005).

[143] T. Uneyama, J. Chem. Phys., **126**, 114902 (2007).

[144] J. Zhu, Y. Liao, and W. Jiang, Langmuir, **20**, 3809 (2004).

[145] J. Raez, I. Manners, and M. A. Winnik, J. Am. Chem. Soc., **124**, 10381 (2002).

[146] J. J. L. M. Cornelissen, M. Fischer, N. A. J. M. Sommerdijk, and R. J. M. Nolte, Science, **280**, 1427 (1998).

[147] A. D. Mackie, K. Onur, and A. Z. Panagiotopoulos, J. Chem. Phys., **104**, 3718 (1996).

[148] G. Porte and J. Appell, American Chemical Society, **85**, 2511 (1981).

[149] R. Zana, Colloids and Surfaces A: Physicochemical and Engineering Aspects, **123-124**, 27 (1997).

[150] M. Kenward and M. D. Whitmore, J. Chem. Phys., **116**, 3455 (2002).

UNIVERSITAT ROVIRA I VIRGILI
MICROSCOPIC MODELING OF THE SELF ASSEMBLY OF SURFACTANTS: SHAPE TRANSITIONS AND CRITICAL MICELLE CONCENTRATIONS
Asfaw Gezae Daful
ISBN:/DL:T. 1024-2011



[151] C.-E. Lin, I.-J. Fang, Y.-J. Deng, W.-S. Liao, H.-T. Cheng, and W.-P. Huang, Journal of Chromatography A, **1051**, 85 (2004).

[152] F. Stanley, A. Warner, E. Schneiderman, and A. Stalcup, Journal of Chromatography A, **1216**, 8431 (2009).

[153] Z. Zheng and J. P. Obbard, Water Research, **36**, 2667 (2002).

[154] E. Calvo, R. Bravo, A. Amigo, and J. Gracia-Fadrique, Fluid Phase Equilibria, **282**, 14 (2009).

[155] H. Sifaoui, K. Lugowska, U. Domanska, A. Modaressi, and M. Rogalski, Journal of Colloid and Interface Science, **314**, 643 (2007).

[156] M. V. Thorsteinsson, J. Richter, A. L. Lee, and P. DePhillips, Analytical Biochemistry, **340**, 220 (2005).

[157] S. Paillet, B. Grassl, and J. Desbrieres, Analytica Chimica Acta, **636**, 236 (2009).

[158] S. Reis, C. G. Moutinho, C. Matosa, B. de Castro, P. Gameiro, and J. L. Lima, Analytical Biochemistry, **334**, 117 (2004).

[159] X. Zhang, J. K. Jackson, and H. M. Burt, J. Biochem. Biophys. Methods, **31**, 145 (1996).

[160] K. Hara, H. Kuwabara, O. Kajimoto, and K. Bhattacharyya, Journal of Photochemistry and Photobiology A: Chemistry, **124**, 159 (1999).

[161] Z. Li, E. Mintzer, and R. Bittman, Chemistry and Physics of Lipids, **130**, 197 (2004).

[162] N. Li, H. Luo, and S. Liu, Spectrochimica Acta Part A, **60**, 1811 (2004).

[163] J. L. López-Fontan, A. Gonzalez-Perez, J. Costa, J. M. Ruso, G. Prieto, P. C. Schulz, and F. Sarmiento, Journal of Colloid and Interface Science, **294**, 458 (2006).

[164] U. R. M. Kjellin, J. Reimer, and P. Hansson, Journal of Colloid and Interface Science, **262**, 506 (2003).

[165] C. B. Stephenson, K. Beers, and D. Blankschtein, Langmuir, **22**, 1500 (2006).

[166] S. Pogodin and V. A. Baulin, Soft Matter, **6**, 2216 (2010).

UNIVERSITAT ROVIRA I VIRGILI
MICROSCOPIC MODELING OF THE SELF ASSEMBLY OF SURFACTANTS: SHAPE TRANSITIONS AND CRITICAL MICELLE CONCENTRATIONS
Asfaw Gezae Daful
ISBN:/DL:T. 1024-2011



[167] A. I. Leonov and M. Siline, polymer, **43**, 5521 (2002).

[168] K. Mortensen, J. Phys.: Condens. Matter, **8**, A103 (1996).

[169] S. M. Aharoni, Macromolecules, **16**, 1722 (1983).

[170] R. Kimmich and N. Fatkullin, Advances in polymer science, **170**, 1 (2004).

[171] P. F. Flory, *Principles of Polymer Chemistry* (Cornell University Press, 1953).

[172] J. Brandrup, E. H. Immergut, E. A. Grulke, A. Abe, and D. R. Bloch, *Polymer Handbook*, 4th ed. (John Wiley & Sons, 2005).

[173] S. Mokraoui, C. Coquelet, A. Valtz, P. E. Hegel, and D. Richon, Ind. Eng. Chem. Res., **46**, 9257 (2007).

[174] S. Zhang, T. Hiaki, and K. Kojima, Fluid Phase Equilibria, **149**, 27 (1998).

[175] V. A. Baulin and A. Halperin, Macromolecules, **35**, 6432 (2002).

[176] A. Berthod, S. Tomer, and J. G. Dorsey, Talanta, **55**, 69 (2001).

[177] J. Corkill, J. Goodmaann, and D. S. P. Harrod, Trans. Faraday Soc., **60**, 202 (1963).

[178] J.-S. Cheng and Y.-P. Chen, Fluid Phase Equilibria, **232**, 37 (2005).

[179] L.-J. Chen, S.-Y. Lin, C.-C. Huang, and E.-M. Chen, Physicochemical and Engineering Aspects, **135**, 175 (1998).

[180] C. Chen, AIChE Journal, **42**, 3231 (1996).

[181] X.-S. Li, J.-F. Lu, Y.-G. Li, and J.-C. Liu, Fluid Phase Equilibria, **153**, 215 (1998).

[182] M. Corrin, Journal of Colloid Science, **3**, 333 (1948).

UNIVERSITAT ROVIRA I VIRGILI
MICROSCOPIC MODELING OF THE SELF ASSEMBLY OF SURFACTANTS: SHAPE TRANSITIONS AND CRITICAL MICELLE CONCENTRATIONS
Asfaw Gezae Daful
ISBN:/DL:T. 1024-2011